5

10

THE UNIVERSITY OF OKLAHOMA

GRADUATE COLLEGE

THERMAL ISOMERIZATION OF CYCLOPROPANE AT ELEVATED PRESSURES

A DISSERTATION

SUBMITTED TO THE GRADUATE FACULTY

in partial fulfillment of the requirements for the degree of

DOCTOR OF PHILOSOPHY

BY

OMER ALLEN PIPKIN

Norman, Oklahoma

1964

THERMAL ISOMERIZATION OF CYCLOPROPANE AT ELEVATED PRESSURES

APPROVED BY

C. M. Sheppard

R. L. Huntington

Raymond D. Daniels

S. E. Babb, Jr.

F. M. Townend

DISSERTATION COMMITTEE

ACKNOWLEDGEMENTS

While a few brief expressions of acknowledgement are hardly adequate for conveying ones real feeling of gratitude, certainly the many persons who have contributed in various ways toward the preparations for, performance of, and reporting of this study are entitled to no less than this.

The writer is especially indebted to his committee chairman, Dr. C. M. Sliepcevich, and to the other members of his committee, Dr. R. L. Huntington, Dr. R. D. Daniels, Dr. F. M. Townsend and Dr. S. E. Babb, Jr.

In construction of the experimental apparatus, the skilled craftsmanship of Mr. J. C. Hood and his associates, Mr. G. J. Scott and Mr. J. Edmundson, of the Physics Department instrument shop, has been invaluable. Important contributions were also made by Mr. F. W. White and his associates of the University Physical Plant welding department, and by Mr. J. J. Fox of the Chemical Engineering maintenance department.

Mr. E. L. Johnson provided very capable assistance with assembly of the apparatus and in carrying-out the experiments. The excellent illustrations in this manuscript were prepared by Mr. G. H. Droescher.

Most especially, I wish to thank my colleague Mr. J. L. Lott of the high pressure laboratory for many helpful discussions.

The author is grateful to several organizations which provided financial assistance during his course of graduate study and the period of this investigation. The generous organizations were: Monsanto Chemical Company, Cities Service Research and Development Company, National Science Foundation, and The University of Oklahoma. Continental Oil Company provided helpful advice on chromatographic analysis, and furnished the chromatograph columns without charge.

Omer Allen Pipkin

TABLE OF CONTENTS

Page

LIST OF ILLUSTRATIONS vii

LIST OF TABLES x

Chapter

I. INTRODUCTION 1

II. THEORETICAL CONSIDERATIONS 4

General
Unimolecular Reaction Theory
Thermodynamic Activities versus Concentrations

III. REVIEW OF PREVIOUS WORK 31

General Background
Reaction Mechanism and Kinetics
Thermodynamics and Composition at Equilibrium
Ranges of Pressure and Temperature
Types of Apparatus
Catalysis

IV. DESCRIPTION OF EXPERIMENTAL APPARATUS 49

Feed System
Preheater Section
Reactor Section
Product Section
Auxiliaries

V. EXPERIMENTAL PROCEDURE 79

Preliminary Procedures
Startup Procedure
Run Procedure
Shutdown Procedure
Calibrations and Measurement of Variables
Difficulties Encountered

Chapter Page

VI. ANALYTICAL PROCEDURE AND APPARATUS..... 99

Previous Methods of Analysis
Principles of Chromatographic Analysis
Chromatograph Equipment Description
Chromatograph Operation and Calibration

VII. METHOD OF DATA ANALYSIS..... 114

Development of Expression for Calculation of k_c from Experimental Data
Calculation of Reaction Energy of Activiation
Estimation of Maximum Departure from Isothermal Behavior
Estimation of Maximum Error in the Calculation of k_c
Calculation of k_a Values
Estimation of Net Propylene Yield with Simultaneous Isomerization and Polymerization
Pressure Dependence of the Rate Constant k_c

VIII. DISCUSSION OF RESULTS..... 130

IX. CONCLUSIONS..... 167

NOMENCLATURE..... 170

LITERATURE CITED..... 177

APPENDICES..... 185

A. ANALYTICAL SECTION..... 185

B. THERMODYNAMICS OF CYCLOPROPANE ISOMERIZATION.... 195

C. EQUIPMENT DESIGN FOR HIGH TEMPERATURE AND PRESSURE..... 201

D. EVALUATION OF DIFFUSIONAL EFFECTS..... 212

E. IGNITOR AND BASO DEVICE ELECTRICAL CIRCUITS..... 225

F. BURNER AND SAND BATH HEATER DRAWINGS..... 227

G. SUMMARY OF EXPERIMENTAL DATA..... 232

H. SAMPLE DATA SHEETS AND CALCULATIONS..... 241

I. REACTION RATES NEAR EQUILIBRIUM..... 248

LIST OF ILLUSTRATIONS

Figure		Page
1.	Plot of $1/k_c$ against $1/C_A$ and Extrapolation for k_∞	12
2.	Plot of log k_c/k_∞ against log p	14
3.	Cyclopropane Isomerization Process Flow Diagram.	50
4.	Photograph of High-Pressure Cell Front Panel	54
5.	Photograph of Equipment Inside the High-Pressure Cell	57
6.	Modified Kuentzel Bomb Preheater	58
7.	Photograph of Reactor Section of Sand Bath Heater	64
8.	Reactor Welded Coupling	69
9.	Photograph of Chromatograph	106
10.	Gas Chromatograph Schematic Diagram	107
11.	Axial Temperature Variation (Isocline Solution).	123
12.	Observed Boundary between the Isomerization Design and Region of Significant Polymerization.	132
13.	Cyclopropane Isomerization First-Order Behavior (900°F.)	134
14.	Cyclopropane Isomerization First-Order Behavior (950°F.)	136
15.	Arrhenius Correlation for Cyclopropane Isomerization (250 p.s.i.)	139
16.	Arrhenius Correlation for Cyclopropane Isomerization (500 p.s.i.)	140

Figure Page

17. Arrhenius Correlation for Cyclopropane Isomerization (1000 p.s.i.)..... 141

18. Arrhenius Correlation for Cyclopropane Isomerization (1500 p.s.i.)..... 142

19. Arrhenius Correlation for Cyclopropane Isomerization (2000 p.s.i.)..... 143

20. Rate Constant Temperature Dependence at Various Pressures..... 144

21. Effect of Polymerization on Net Propylene Yield. 146

22. Polymerization Effect (Run V-875°F.)..... 147

23. Comparison of Actual and Predicted Net Propylene Yield for Run V..... 148

24. Preheater Conversion (Stainless Steel Coil) Run XX-950°F..... 151

25. Preheater Conversion (Kuentzel Bombs) Run XII-900°F..... 153

26. Preheater Conversion (Kuentzel Bombs) Run XVII-900°F..... 154

27. Plot of $1/k_c$ against 1/p (850°F.)..... 156

28. Plot of $1/k_c$ against 1/p (900°F.)..... 157

29. Rate Constant Variation with Pressure (900°F.).. 160

30. Rate Constant Variation with Pressure (950°F.).. 162

31. Effect of Nonideal Behavior at High Pressure on the Unimolecular Reaction Rate Constant..... 164

32. Chromatograph Calibration Curve..... 192

33. Typical Chromatogram..... 193

34. Chromatograph Electrical Circuit Diagram..... 194

35. $\Delta G°$ for Cyclopropane Isomerization..... 199

36. Cyclopropane and Propylene Viscosity Data..... 224

37. Burner Ignition System Electrical Circuit Diagrams..... 226

Figure Page

38. Details of Sand Bath Heater Construction..... 228

39. Details of Sand Bath Heater Grid Construction... 229

40. Sectional Elevation of Burner for Sand Bath Heater..... 231

LIST OF TABLES

Table		Page
1.	Temperature and Pressure Ranges of Cyclopropane Thermal Isomerization	46
2.	Summary of Data for Figure 13	135
3.	Summary of Data for Figure 14	137
4.	Summary of Data for Figures 29 and 30	163
5.	Standard Sample Composition and Peak Height Ratios	189
6.	Peak Ratio 95 Per Cent Confidence Range for Single, Duplicate and Triplicate Sampling	190
7.	Range of Error in Prediction of Composition from Figure 32 (with 95 Per Cent Confidence)	191
8.	ΔG° for Cyclopropane Isomerization	198
9.	Reynolds Number Calculations	218
10.	Parameters for Evaluation of Significance of Longitudinal and Radial Diffusion	220
11.	Parameter for Evaluation of Validity of Plug Flow Assumption	222
12.	Summary of Experimental Results	233
13.	Summary of Runs Used in Arrhenius Correlations	240

THERMAL ISOMERIZATION OF CYCLOPROPANE AT ELEVATED PRESSURES

CHAPTER I

INTRODUCTION

Homogeneous gas-phase reactions, in general, have not been studied extensively at high pressure because, in most cases of practical interest, the reactions can be performed more efficiently in the presence of catalysts. Unimolecular, homogeneous gas-phase reactions, in particular, have received little attention at high pressure. For the most part, these reactions have only been investigated in the "more interesting" region of subatmospheric pressure.

Pressure is an important variable to be considered in the design of reaction systems. There are two fundamental pressure effects which must be analyzed: (1) the effect of pressure on the equilibrium relationship, and hence the maximum reaction yield, and (2) the effect of pressure on the reaction rate itself. It is the second effect which is of primary interest in the present study.

It is widely held that thermodynamic activities should replace concentrations in rate expressions for non-

ideal systems. This view has its origin from the manner in which the thermodynamic equilibrium constant expression may be obtained for elementary reversible reactions by applying the principle of mass action, in terms of thermodynamic activities, to both the forward and reverse reaction rates. With such a formulation, both the forward and reverse specific rate constants are presumed to be independent of concentration. Opposing this view are the results of absolute reaction rate theory. According to this theory, the reaction rate cannot be in constant proportion to the reactant activities, owing to the presence of a term which represents the activity coefficient of an activated complex.

A unimolecular reaction study at high pressures appears to offer a clear-cut method for choosing between the two viewpoints discussed in the previous paragraph. For a unimolecular reaction, in which the activated complex is not expected to have properties widely different from those of the reactant molecule, the specific rate constant, as defined in terms of concentrations, should be independent of pressure. On the other hand, if this condition is true, then the specific rate constant, as defined in terms of thermodynamic activities, cannot remain constant, since for a first-order reaction the two "constants" are related to each other by the activity coefficient of the reactant.

Thermal isomerization of cyclopropane was selected as the unimolecular reaction to be studied for several reasons. First, the reaction, except under severe conditions,

yields only propylene as a product; thus, the reaction product is a simple binary mixture of cyclopropane and propylene, readily analyzed by gas chromatography. Second, the absence of a change in the number of moles upon reaction, plus the similarily of physical properties for propylene and cyclopropane, greatly simplifies hydrodynamic analysis. Third, reliable data are available for the reaction at atmospheric pressure and below to provide some basis for a check of results.

Apart from seeking to show whether or not thermodynamic activities are preferred over concentrations in reaction rate expressions, this work involved other goals: viz., (1) to obtain, for the first time, cyclopropane thermal isomerization rate data at pressures substantially above atmospheric, (2) to observe how closely the high pressure rate constants are in agreement with the k_∞ values obtained in the literature by extrapolation of low pressure data, and (3) to design, build, and demonstrate the workability of a high-pressure, high-temperature, noncatalytic, continuous flow-type reaction system.

The reaction was carried-out in a gold-lined, coiled, tubular reactor of stainless steel located in an isothermal bath of fluidized sand. Data were obtained at temperatures ranging from 850 to 1100°F., while pressures were varied from 250 to 2000 p.s.i.

CHAPTER II

THEORETICAL CONSIDERATIONS

The material of this chapter is divided into three sections. In the first section, the general principles of reaction kinetics are briefly reviewed; while in the second section, attention is directed to unimolecular theory, and to the aspects of that theory which are pertinent to the present investigation. The last section is concerned with establishing whether or not a theoretical foundation exists for replacement of concentration variables in rate expressions by thermodynamic activities.

General

> "There is no theory of rates which stands, so to speak, on its own feet; all existing theories depend, in one form or another, on ideas carried over from the study of matter at equilibrium, which is to say in an unchanging condition."
>
> Denbigh (16, p. 437)

This comment by Denbigh seems appropriate for obtaining the proper perspective in any discussion of reaction rate theory. While the thermodynamics of matter in the equilibrium state is well established, the foundations of rate theories are far less firm, and deducing kinetic principles from the behavior of systems at equilibrium involves "boot strap"

operations which must be carried-out with caution. Without doubt, the most singularly successful development of this type was by Arrhenius who rationalized the temperature dependence of the specific rate constant from van't Hoff's equation for the effect of temperature on the concentration equilibrium constant. The result deduced by Arrhenius was

$$k = Ae^{-E_A/RT} \qquad \text{II-1}$$

where k is the specific rate constant, E_A is the energy activation, and A is the frequency factor. The Arrhenius equation remains as one of the most generally useful results in kinetic theory today. In fact, for elementary unimolecular and bimolecular homogeneous gas-phase reactions, the Arrhenius equation is so well established that deviations from the predicted temperature effect can usually be attributed to experimental error.

It should be remarked that while Equation II-1 was deduced from a thermodynamic relationship, it is not implied that rates are predictable from thermodynamics, as both A and E_A are functions of other than thermodynamic variable (e.g. values of E_A may be substantially reduced with selection of the proper catalyst). Subsequently, it will be shown that near equilibrium the net reaction rate is proportional to the free energy change; but once again, thermodynamics does not determine the rate of reaction because the constant of proportionality is a function of catalyst activity and other nonthermodynamic quantities.

Interestingly enough, the initial formulation of the principle of mass action by Guldberg and Waage was for the prediction of reaction rates. It was not until they later applied the rate expressions to reversible reactions that the equilibrium constant relationship was derived (21). Now it is well known that the principle of mass action, as originally formulated, is not of general utility, since seldom is the reaction mechanism revealed by the stoichiometric equation of a reaction. However, in elementary reactions, and in elementary steps of complex reactions, the principle applies and is supported by collision theory. The principle of mass action, as applied to the thermodynamic equilibrium constant expression, is of general usefulness where thermodynamic activities are the "active masses". This suggests that, perhaps, at least for elementary reactions, rate expressions should be formulated in terms of thermodynamic activities. More attention is given to this subject in the last section of this chapter.

To this point, reaction rates have been discussed without reference to a formal definition. In this work, the term reaction rate will always refer to the time rate of change in the number of moles of a component per unit volume; state mathematically

$$r_i = -\frac{1}{V}\frac{dn_i}{dt} \qquad \text{II-2}$$

Equation II-2 is not ambiguous when applied to both batch and flow processes; however, in the latter, it is necessary to

associate the volume V with a fixed mass. Thus, V will usually be a function of time in the flow process; whereas, in the batch process V is the constant volume of the system. As defined, the rate is always positive for the component transformed. Formally, the reaction rate may be expressed as

$$-\frac{1}{V}\frac{dn_i}{dt} = k_c f(C_1, C_2 \cdots C_n) = k_a f(a_1, a_2 \cdots a_n) \qquad \text{II-3}$$

where the specific rate constant k_c is defined in terms of concentration variables and k_a is defined in terms of activities. The relationship between these specific rate constants is explored in the last section of this chapter.

Returning once more to the Arrhenius development, as pointed out by Eyring and Eyring (18), the real significance of the treatment lies not so much in the remarkable success of the mathematical result, but instead in the interpretation of the results by Arrhenius in terms of "active" molecules. The proposal by Arrhenius, that equilibrium exists between normal molecules and the "active" molecules which have sufficient energy for reaction, embodies the two concepts which are fundamental to both the collision theory of reaction rates and the absolute reaction rate theory: viz., (1) the presence of an equilibrium condition and (2) the presence of an activated state.

In the collision theory of chemical reactions, reaction occurs upon collision provided the reactants possess a certain minimum activation energy E_A. The number of colli-

sions z_o is determined from the kinetic theory of gases, while the fraction of molecules possessing energy in excess of E_a is found through statistical mechanics and the Maxwell-Boltzmann distribution of energy to be $e^{-E_A/RT}$. In using the Maxwell-Boltzmann distribution it is assumed that the reaction rate is not so fast that the equilibrium distribution of energy is significantly disturbed (62, p. 155). z_o is given by the expression

$$z_o = C_1 C_2 \ (r_1+r_2)^2 \sqrt{\frac{8\pi RT(M_1+M_2)}{M_1 M_2}} \qquad \text{II-4}$$

for double collisions (24), where C, r and M signify concentration, molecular radius and molecular weight. Thus the specific rate constant from collision theory can be written as

$$k = z_o e^{-E_A/RT} \qquad \text{II-5}$$

In comparing this result with the Arrhenius Equation, it is seen that collision theory indicates a dependence of A on $\sqrt{T}$, since A and z_o are equal and z_o is proportional to $\sqrt{T}$ from Equation II-4.

Since the absolute reaction rate theory will be discussed in some detail in connection with the theory of unimolecular reactions in the next section, only the derived expression for the specific reaction rate will be given here to permit a comparison with Equations II-1 and II-5; i.e., from absolute reaction rate theory (23)

$$k = \frac{k_B T}{h} K_c^* \qquad \text{II-6}$$

where k_B is the Boltzmann constant, h is Planck's constant and K_c^* is the concentration equilibrium constant for reactants and the activated complex.

Unimolecular Reaction Theory

Unimolecular reactions are those reactions which proceed through a transition state consisting of a single, activated molecule. Few unimolecular reactions are elementary; most are complex and involve the formation of free radicals. Only certain isomerization and decomposition reactions are known to take place in a single elementary step; cyclopropane isomerization is such a reaction.

When first discovered, unimolecular reactions were not understood. Their first-order behavior was not readily reconciled with the second-order collision process. This difficulty prompted Perrin (60) in 1919 to propose that activation was brought about by the absorption of radiation. Perrin's theory had its difficulties, and was totally discredited when it was discovered that unimolecular reactions became of second-order at reduced pressures. In 1922, Lindemann (52) proposed a unimolecular reaction mechanism which was compatible with both experimental results and collision theory. His mechanism, with some refinements, remains the accepted one today.

With the Lindemann mechanism, three processes are visualized to occur simultaneously: (1) normal molecules collide to produce activated molecules, (2) activated mole-

cules collide with normal molecules and are deactivated, and (3) activated molecules decompose to form products. The mechanism is given more concisely with the equations

$$(1)\quad A + A \xrightarrow{k_f} A^* + A$$

$$(2)\quad A + A^* \xrightarrow{k_b} A + A \qquad \text{II-7}$$

$$(3)\quad A^* \xrightarrow{k_1} \text{products}$$

Since at steady state the concentration of activated molecules will remain constant, the rate of activation can be equated to the sum of the rates for deactivation and decomposition; i.e.

$$k_f C_A^2 = k_b C_A C_A^* + k_1 C_A^* \qquad \text{II-8}$$

The net rate of reaction is

$$r_A = -\frac{1}{V}\frac{dn_A}{dt} = k_1 C_A^* \qquad \text{II-9}$$

and a rate expression independent of C_A^* is obtained by eliminating this quantity between Equations II-8 and II-9 to obtain

$$r_A = \frac{k_1 k_f C_A^2}{k_1 + k_b C_A} \qquad \text{II-10}$$

At high pressures, the rate of activated molecule decomposition will be controlling and a state of equilibrium will exist between normal and activated molecules. Equation II-10 is then more revealing when written as

$$r_A = \frac{k_1 C_A^2}{\frac{k_1}{k_f} + \frac{C_A}{K_c}} \qquad \text{II-11}$$

where $K_c = k_f/k_b$. The ratio k_1/k_f at high pressure will be small in comparison with C_A/K_c, thus Equation II-11 will approach the first-order expression

$$r_A = k_1 K_c C_A \qquad \text{II-12}$$

Conversely, at low pressure, the equilibrium between normal and active molecules is not maintained and the term $k_b C_A$ in the denominator of Equation II-11 becomes small in comparison with k_1. Thus, the reaction takes on second-order behavior as given by the expression

$$r_A = k_f C_A^2 \qquad \text{II-13}$$

In analyzing experimental data, and for testing the Lindemann theory, it is convenient to calculate a first-order rate constant $k_c = r_A/C_A$, whether or not the reaction is of first-order, and plot its reciprocal against the reciprocal of C_A. According to theory a straight line should result. This prediction can be shown in the following way. Since

$$r_A = k_c C_A = \frac{k_1 k_f C_A^2}{k_1 + k_b C_A}\ ;\ k_c = \frac{k_1 k_f C_A}{k_1 + k_b C_A} \qquad \text{II-14}$$

then

$$\frac{1}{k_c} = \frac{1}{k_1 K_c} + \frac{1}{k_f C_A} \qquad \text{II-15}$$

In Equation II-15, as concentration increases without limit, k_c approaches $k_1 K_c$: a quantity which it has become customary to call k_∞. Values of k_∞ are obtained by finding the k_c^{-1} intercept from a linear extrapolation of experimental data in a plot of k_c^{-1} against C_A^{-1}. This technique

has been universally accepted by investigators of unimolecular reactions as a means of reporting pressure independent rate constants. The foregoing mathematical treatment of the Lindemann theory is equivalent to the statistical mechanical treatment by Hinshelwood (28), and involves the fundamental assumption that all activated molecules have the same specific reaction rate, independent of their energy content. The result obtained from the Hinshelwood treatment is

$$k_c = \frac{k_\infty}{1+\beta/p} \qquad \text{II-16}$$

A similar result can be obtained from Equation II-15, upon observing that the concentration is proportional to pressure.

Some departure from the linear relationship of Equation II-15, predicted by the Lindemann theory, as indicated in Figure 1, brought about refinements in the theory by Rice and Ramsperger (70), and Kassel (38). These refinements are essentially the same; both are statistical mechanical

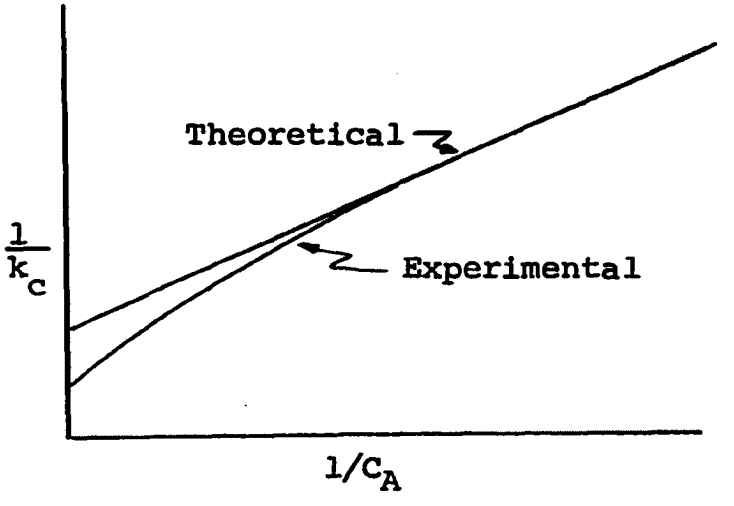

Figure 1

treatments which allow for variation of the specific reaction rate with energy level of the molecule. With these treatments, the general expression for the first-order rate constant, with the same nomenclature of Equation II-14, becomes

$$k_c = \sum_i \frac{(k_1)_i (k_f)_i C_A}{(k_1)_i + (k_b)_i C_A} \qquad \text{II-17}$$

where the summation includes all energy levels of the activated molecule A_i^*. The limiting value of k_c at high pressure is then

$$k_\infty = \sum_i (k_1)_i (K_c)_i \qquad \text{II-18}$$

The specific equations of the Rice-Ramsperger-Kassel theory are too lengthy for inclusion in the present discussion. Briefly, the theory permits calculation of the ratio k_c/k_∞ in terms of pressure, at a given temperature, when only a molecular dimension and the number of degrees of freedom are specified, that is

$$k_c/k_\infty = f(\sigma, n, T, p) \qquad \text{II-19}$$

Testing of the theory is accomplished by plotting log k_c/k_∞ against log p to obtain the characteristic curve shown in Figure 2.

In the case of cyclopropane isomerization, Slater has attempted to calculate directly the specific rate of reaction from a vibrational analysis of the molecule: first, with a classical harmonic oscillator model (76) and, second, with a quantum harmonic oscillator model (78). Though

Slater was unsuccessful in arriving at the correct absolute values of k_c/k_∞; it is significant, however, that he was able to predict the characteristic shape of the curve in Figure 2.

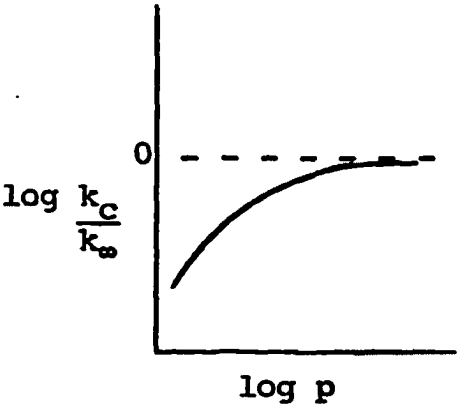

Figure 2

The absolute reaction rate theory is capable of explaining the behavior of unimolecular reactions at high pressure, where the reactant molecules and activated molecules are in equilibrium; but at low pressure, the variation in the specific rate constant is accounted for in an unappealing way through the introduction of a pressure dependent transmission coefficient.

Thermodynamic Activities versus Concentrations in Rate Expressions

The question of whether or not thermodynamic activities should be used in rate expressions for chemical reactions in lieu of concentrations is a point of controversy. To demonstrate the nature and depth of this conflict, some selected, supporting and opposing, views have been extracted from the literature and are quoted in the paragraphs which follow:

Views Opposing Thermodynamic Activities

Leffler and Grunwald
(51, p. 71-72)

"The reaction rate according to transition state theory is proportional to the concentration of the transition state rather than to its activity. The activity of the transition state enters the rate problem only because the concentration of the transition state is given by a thermodynamic equilibrium constant. The resulting expression for the transition state concentration contains the ratio of activity coefficients $\gamma_A \gamma_B / \gamma^*$. Because γ^* is not constant, the rate can be in no constant proportion to the activities of the reagents. If reaction rates were proportional to the activity of the transition state, γ^* would cancel out, and the rates would be proportional to the reagent activities. The failure of the rates to be proportional to reagent activities is one of the main reasons for the development of transition state theory."

Ubbelohde
(86, p. 147)

"Theoretical grounds for using thermodynamic concentration variables in describing the kinetics of early stages in polymerization reactions far from equilibrium seem by no means fully established at present. ..... alternately, the use of fugacities may merely conceal the real significance of the marked pressure dependence for some of these polymerization reactions."

Denbigh
(16, p. 445)

"Because the equilibrium constant must be expressed in forms such as above (comment: i.e. with activities), throughout the period from 1915 to 1930 there was a strong school of thought holding the view that reaction rate must be primarily dependent on activities (i.e. the products of concentrations with their appropriate activity coefficients), rather than on the concentrations themselves."

Denbigh
(15, p. 49)

"Because it (reaction) is a collisional process, the rate of reaction is determined primarily by the concentration, as is expressed in the empirical law of mass action. It is only when the reaction system is close to equilibrium that the rate is also approximately proportional to the thermodynamic force."

Views Supporting Thermodynamic Activities

Prausnitz
(61, p. 7)

"....theoretical considerations based on the activated complex theory suggest that fugacities should be used in expressing high pressure reaction rates. As our understanding of chemical kinetics increases and as more precise kinetic data become available, it will probably become necessary to include fugacity coefficients in an exact formulation of chemical rate laws at advanced pressures."

Whalley
(93, p. 148)

"As Prof. Ubbelohde points out concentrations are not satisfactory close to equilibrium, and there is no reason to believe that they will be better far from equilibrium. This is true not only for the reactions of stable molecules, but also for the reactions of intermediate species produced during a chemical change, and the statement made by Laird, Morrell and Seed that the rate of decomposition of an activated complex is a function only of its concentration and not of its fugacity, must be incorrect. ...It can be argued for reactions far from equilibrium that if the rate of decomposition of the complex were a function of concentration only, it ought to be independent of its environment, and this does not appear to be reasonable. The use of activities is one way of taking account of the environment."

Walas
(90, p. 5-6)

"When operating conditions are such that the gases or solutions concerned do not behave ideally, k as defined by Equation 1-4

$$r = -\frac{1}{V}\frac{dn}{dt} = k\ f(n_A, n_B, \cdots) \qquad 1\text{-}4$$

develops a dependence on concentrations. From thermodynamic considerations in such instances activities should be substituted for concentrations so that

$$r = k\ f(a_A\ a_B, \cdots) \qquad 1\text{-}5$$

"From a study of reversible processes it appears that thermodynamic activities should be regarded as the active mass."

Hougen and Watson
(31)

"The rate equations developed on this basis (i.e. with activities instead of concentrations) have the advantage of a simple relationship to the thermodynamic equilibrium constant which permits the establishment of a simple equation which is applicable to the net rate of a reaction when approaching equilibrium from any direction."

The only direct exchange of views, in those quoted, is that between Whalley and Ubbelohde in connection with the ethylene polymerization study by Laird, Morrell and Seed (46). Laird et al. found that use of fugacities in their correlation made the results more compatible with the free-radical chain mechanism of vinyl polymerization.

From the views quoted, there are some striking disagreements. For example, Prausnitz contends that the absolute reaction rate theory supports the use of thermodynamic con-

centration variables; whereas, Leffler and Grunwald state that failure of rates to be proportional to reactant activities was one of the main reasons for development of the theory. Further, Whalley insists that the rate of decomposition of the activated complex should be a function of environment as well as concentration, while Leffler and Grunwald, and Laird et al. hold that the reaction rate is proportional to the concentration of the transition state and not to its activity. Denbigh and Ubbelohde, while accepting the significance of thermodynamic variables in rate expressions near equilibrium, are more reluctant than Walas, Whalley, and Hougen and Watson to accept a generalization in which thermodynamic variables are considered of primary significance in regions far removed from equilibrium as well. An attempt is made to resolve these conflicting viewpoints in the paragraphs which follow.

The concept of writing rate expressions in terms of thermodynamic activities has its origin in studies of elementary reversible reactions. For purposes of illustration, consider the reversible reaction

$$A_2 + B_2 \rightleftharpoons 2\ AB \qquad \text{II-20}$$

The net reaction rate, of course, can be written as the difference between the forward and backward rates of reactions; i.e.

$$r = r_f - r_b \qquad \text{II-21}$$

Now, in some elementary reactions, the rates are found to be

proportional to the product of the "active masses" of the reactants, each raised to powers corresponding to their stoichiometric coefficient. In such cases, one says that the empirical "principle" of mass action by Guldberg and Waage is obeyed.* The word "principle" rather than "law" is employed here, in agreement with Frost (21) that the principle is not sufficiently general to be considered a law of nature. On the basis of this principle, the net rate for the reaction selected for consideration becomes

$$r = r_f - r_b = k_f(m^*_{A_2})(m^*_{B_2}) - k_b\,(m^*_{AB})^2 \qquad \text{II-22}$$

At equilibrium it is apparent that the net reaction rate must become zero; hence, Equation II-22 may be expressed as

$$\frac{k_f}{k_b} = \frac{(m^*_{AB})^2_e}{(m^*_{A_2})_e (m^*_{B_2})_e} \qquad \text{II-23}$$

From thermodynamics, it is known that regardless of the reaction mechanism, the conditions at equilibrium for the reaction in Equation II-23 must conform to the requirements of the expression

$$K_a = \frac{(\bar{a}_{AB})^2_e}{(\bar{a}_{A_2})_e (\bar{a}_{B_2})_e} \qquad \text{II-24}$$

where K_a is the thermodynamic equilibrium constant, which is a function only of temperature when the standard state for each component is chosen arbitrarily to be unit fugacity

*Gonikberg (24) claims that this principle was first formulated by the Russian physicist and chemist N. N. Beketov.

(i.e. one atmosphere), as is customary for gases. From a comparison of Equations II-23 and II-24, one is led to deduce that thermodynamic activities are the proper "active masses" in the rate expressions and that the equilibrium constant is

$$K_a = \frac{(k_a)_f}{(k_a)_b} \qquad \text{II-25}$$

where the subscript a has been introduced on k_f and k_b to signify their origin from rate expressions in terms of activities.

It is important, however, not to over estimate the demands placed on the form of rate expressions by thermodynamics. For example, thermodynamics does not require that the net rate in Equation II-22 be expressed as a difference in two terms. For as illustrated by Denbigh (16), one could also satisfy the conditions at equilibrium with the rate expression

$$r = f\left[\bar{a}_{A_2}\bar{a}_{B_2} - \frac{\bar{a}_{AB}^2}{K_a}\right]^n \qquad \text{II-26}$$

in which a difference in two terms appears only when n = 1. Still further, a more complicated rate expression such as

$$r = (k_a)'_f \frac{\bar{a}_{A_2}\bar{a}_{B_2}^{\beta}}{\psi_f} - (k_a)'_b \frac{\bar{a}_{AB}^{2\beta}}{\psi_b} \qquad \text{II-27}$$

will meet the conditions required at equilibrium, provided $(\psi_f)_e = (\psi_b)_e$ where ψ may be a complicated function, possibly with a number of adsorption terms, as is often encountered in

reactions catalyzed by solids. A term such as β, which is a function of concentration, has been found necessary in some rate expressions for ionic solutions (3). Since β appears in both terms of Equation II-27, its value in no way affects the equilibrium expression.

Since in principle all reactions may be treated as reversible and the exact rate laws must hold both at equilibrium and away from it, then the restrictions imposed by equilibrium on the forward and backward rate laws are pertinent to the question of formulating rate laws in terms of thermodynamic variables. In general it has been found that conditions imposed by equilibrium are far less restrictive than previously supposed.

At every equilibrium condition, thermodynamics requires that the ratio of the forward to reverse reaction rates be unity; i.e.

$$\frac{r_f}{r_b} = 1 \qquad \text{II-28}$$

Further, the ratio must be greater than unity when ΔG_R is less than zero. For the general reversible reaction

$$aA + bB + \cdots \rightleftharpoons mM + nN \cdots \qquad \text{II-29}$$

Gadsby, Hinshelwood and Sykes (22) proposed the following relationships as necessary conditions in meeting the thermodynamic requirements

$$\frac{r_f}{r_b} = \frac{(k_a)_f \, \bar{a}_A^{\,a} \, \bar{a}_B^{\,b} \cdots}{(k_a)_b \, \bar{a}_M^{\,m} \, \bar{a}_N^{\,n} \cdots} \qquad \text{II-30}$$

$$K_a = \frac{(k_a)_f}{(k_a)_b} \qquad \text{II-31}$$

However, Manes, Hofer and Weller (56) have shown that this requirement is far too restrictive. Instead, they propose that it is <u>sufficient</u> that

$$\frac{r_f}{r_b} = \frac{(k_a)_f}{(k_a)_b}\left[\frac{\bar{a}_A^a \bar{a}_B^b \cdots}{\bar{a}_M^m \bar{a}_N^n \cdots}\right]^z \qquad \text{II-32}$$

where $(k_a)_f/(k_a)_b = K_a^z$ and z is a positive constant, usually a small positive integer or its reciprocal. While this relation is not a necessary or general expression, it does have broad utility, as demonstrated by the fact that Manes et al. were able to apply it to all of the many mechanisms for surface-catalyzed gas-phase reactions proposed by Yang and Hougen (97). Hollingsworth (29, 30) has also considered the less restrictive, necessary conditions imposed on the ratio r_f/r_b by thermodynamics.

In relating the thermodynamic activity to concentration it is convenient to define an activity coefficient

$$\alpha_i = \frac{\bar{a}_i}{C_i} \qquad \text{II-33}$$

Since by definition $\bar{a}_i = \bar{f}_i/f_i^o$ and the concentration C_i may be expressed as $y_i P/Z_m RT$, then the activity coefficient becomes

$$\alpha_i = \frac{Z_m RT}{f_i^o}\,\frac{\bar{f}_i}{y_i P} \qquad \text{II-34}$$

In Equation II-34, the term $\bar{f}_i/y_i P$ is recognized as

the fugacity coefficient $\bar{\Phi}_i$ for component i. Thus,

$$\alpha_i = \frac{Z_m RT}{f_i^o} \bar{\Phi}_i \qquad \text{II-35}$$

Though it is customary, yet quite arbitrary, to specify f_i^o as unit fugacity (one atmosphere), the symbol f_i^o is carried forward in this development to avoid confusion concerning dimensions in subsequent expressions. It is also customary to introduce another activity coefficient $\gamma_i = \bar{\Phi}_i/\Phi_i$ which accounts for deviation from ideal solution behavior. Φ_i is the fugacity coefficient for the pure component at the system temperature and pressure. In terms of these definitions the final expression for the thermodynamic concentration variable becomes

$$\alpha_i C_i = Z_m RT \gamma_i \Phi_i (f_i^o)^{-1} C_i \qquad \text{II-36}$$

From Equation II-36 it is apparent that the expression for K_a in terms of K_c will be

$$K_a = K_c K_\gamma K_\Phi (K_{fo})^{-1} (Z_m RT)^{\Sigma \nu_i} \qquad \text{II-37}$$

where ν_i is the stoichiometric coefficient for component i in the reaction equation; ν_i is positive for products and negative for reactants. Thus, elementrary reversible reactions, with rate expression formulated in the classical way of Guldberg and Waage, yield the equilibrium relationship of Equation II-37 where thermodynamic activities are chosen as the active mass and K_a is observed to be $(k_a)_f/(k_a)_b$.

It is possible to find a relationship between k_c and

k_a for a first-order reaction in the following way. The observed rate of reaction, of course, is not dependent upon the method of writing the rate expression, thus

$$r = \frac{k_a(Z_m RT\Phi_i \gamma_i C_i)}{f_i^o} = k_c C_i \qquad \text{II-38}$$

and

$$k_a = \frac{k_c f_i^o}{Z_m RT\gamma_i \Phi_i} \qquad \text{II-39}$$

Since $RT \ln K_a = \Delta G_R^\circ$, and the standard states are chosen to be independent of pressure, then

$$RT\left[\frac{\partial \ln K_a}{\partial P}\right]_T = 0 \qquad \text{II-40}$$

and

$$\left[\frac{\partial \ln(k_a)_f}{\partial P}\right]_T - \left[\frac{\partial \ln(k_a)_b}{\partial P}\right]_T = 0 \qquad \text{II-41}$$

Equation II-41 may be satisfied in two ways: either by both $(k_a)_f$ and $(k_a)_b$ being independent of pressure, or by both having the same pressure dependence. Assuming that the former is true, then by logarithmic differentiation of Equation II-39, one obtains

$$\left[\frac{\partial \ln k_a}{\partial P}\right]_T = \left[\frac{\partial \ln k_c}{\partial P}\right]_T - \left[\frac{\partial \ln(Z_m \gamma_i \Phi_i)}{\partial P}\right]_T = 0 \qquad \text{II-42}$$

Thus, with this reasoning, rather than k_c being a constant independent of pressure, the indicated constant quantity is

$$\left[\frac{k_c}{Z_m \gamma_i \Phi_i}\right]_T = \text{constant} \qquad \text{II-43}$$

where from Equation II-39 the constant is identified as RTk_a/f_i°. Assuming that the pressure independence of k_a also holds away from equilibrium, then the rate expression for a first-order reaction $k_a(Z_m RT\Phi_i\gamma_i C_i)/f_i^\circ$ has more general utility than $k_c C_i$, since $k_a \equiv k_a(T)$ whereas $k_c \equiv k_c(P, T)$.

Since $C_i = y_i P/Z_m RT$, $\Phi_i P = f_i$, and f_i° is arbitarily chosen as unit fugacity, then for a first-order reaction

$$r = k_a(\gamma_i y_i f_i) \qquad \text{II-44}$$

Further, in many cases ideal solution behavior exists (i.e. Lewis and Randall's Rule applies and $\gamma_i = 1$) so that

$$r = k_a(y_i f_i) \qquad \text{II-45}$$

It is now desirable to compare the foregoing treatment with the results expected from absolute reaction rate theory. For illustration purposes, consider again the reversible reaction of Equation II-20, but now with inclusion of the activated complex to obtain

$$A_2 + B_2 \rightleftharpoons C^* \rightleftharpoons 2AB \qquad \text{II-46}$$

In accordance with the usual absolute reaction rate treatment (23), only the irreversible decomposition of the activated complex to AB is considered initially. The theory assumes that equilibrium exists between an activated complex and the reactants and that the rate of reaction is determined by the rate at which the activated complex passes over the energy barrier along the reaction coordinate; i.e.

$$r = (C^*)'\nu \qquad \text{II-47}$$

where $(C^*)^{\ddagger}$ is the concentration of activated complex at the top of the energy barrier, with one translational degree of freedom oriented along the reaction coordinate, and ν is the frequency of passage over the barrier. Further,

$$(C^*)^{\ddagger} = C^*\frac{(2\pi\ m^*k_BT)^{\frac{1}{2}}\delta}{h} = C^*f_{t(1)} \qquad \text{II-48}$$

where C^* is the total concentration of activated complex and $f_{t(1)}$ is the probability associated with one translational degree of freedom along the reaction coordinate. Since $\nu = \bar{v}/\delta$ and $\bar{v} = (k_BT/2\pi m^*)^{\frac{1}{2}}$, then the rate expression becomes

$$r = \frac{k_BT}{h} C^* \qquad \text{II-49}$$

It is apparent from the nature of the absolute reaction rate model, especially with the physical interpretation of Equation II-47, that Leffler and Grunwald are correct in their statement that the rate is proportional to the concentration of the transition state (i.e. activated complex). Whalley's contention that the rate should be proportional to the fugacity of the activated complex does not have its foundation in the absolute reaction rate theory. However, because of the equilibrium relationship between reactants and the activated complex, the rate of reaction will be a function of reactant activities; that is, since

$$K_a^* = \frac{\alpha^*C^*}{\bar{a}_{A_2}\bar{a}_{B_2}} \quad \text{and} \quad C^* = \frac{K_a^*}{\alpha^*}\bar{a}_{A_2}\bar{a}_{B_2} \qquad \text{II-50}$$

then upon substitution for C^* in Equation II-49, one obtains

$$r = \frac{k_BT}{h}\frac{K_a^*}{\alpha^*}\bar{a}_{A_2}\bar{a}_{B_2} \qquad \text{II-51}$$

The form of Equation II-51 probably prompted the statement by Prausnitz that, "... theoretical considerations based on the activated complex theory suggest that fugacities should be used in expressing high pressure reaction rates."

In comparing the rate equation, $r = k_a \bar{a}_{A_2} \bar{a}_{B_2}$, with Equation II-51, the expression for k_a from absolute reaction rate theory is observed to be

$$k_a = \frac{k_B T}{h} \frac{K_{a^*}}{\alpha^*} \cdot \qquad \text{II-52}$$

For the elementary reversible reaction in Equation II-20, the net reaction rate expression is

$$r = r_f - r_b = (k_a)_f \bar{a}_{A_2} \bar{a}_{B_2} - (k_a)_b \bar{a}_{AB}^2 \qquad \text{II-53}$$

In terms of k_a values from absolute reaction rate theory, Equation II-53 becomes

$$r = r_f - r_b = \frac{k_B T}{h}(K_a^*)_f \frac{\bar{a}_{A_2} \bar{a}_{B_2}}{\alpha^*} - \frac{k_B T}{h}(K_a^*)_b \frac{\bar{a}_{AB}^2}{\alpha^*} \qquad \text{II-54}$$

In comparing Equations II-27 and II-54, for the case of an elementary reaction in which $\psi_f = \psi_b = 1$, it is natural to make the interpretation that $\beta = 1/\alpha^*$, as was done by Bronsted (3). Upon carrying the comparison further, one obtains

$$(k_a)'_f = \frac{k_B T}{h}(K_a^*)_f \text{ and } (k_a)'_b = \frac{k_B T}{h}(K_a^*)_b \qquad \text{II-55}$$

These $(k_a)'$ values are obviously independent of pressure. On the other hand, k_a values predicted by absolute reaction rate theory in Equation II-52 are pressure dependent because of α^*. Thus, the absolute reaction rate theory suggests that

the expression

$$\left[\frac{\partial \ln(k_a)_f}{\partial P}\right]_T - \left[\frac{\partial \ln(k_a)_b}{\partial P}\right]_T = 0 \qquad \text{II-56}$$

holds, not because both $(k_a)_f$ and $(k_a)_b$ are independently free of pressure effect, but instead, because both terms have the same pressure dependence, contrary to the previous assumption.

When the reaction rate is expressed in terms of concentrations, the rate constant k_c from absolute reaction rate theory is

$$k_c = \frac{k_B T}{h} K_c^* \qquad \text{II-57}$$

Thus, the theory indicates that, in general, both k_a and k_c are pressure dependent. However, for the unimolecular isomerization reaction of cyclopropane, since

$$k_a = \frac{(k_a)'}{\alpha^*} = \frac{k_c}{\alpha_\Delta} \qquad \text{II-58}$$

and α^* and α_Δ should be approximately equal, then k_c, by absolute reaction rate theory, is expected to have less pressure dependence than k_a. In fact k_c is predicted to be essentially constant. This observation makes it possible, therefore, to test the absolute reaction rate theory by measuring reactions rates at a number of high pressure levels. Constant k_c values for a given temperature, but varying pressure, support the theory; whereas, constancy of the ratio k_c/α_Δ would support the view that rates expressed in terms

of thermodynamic activities yield a rate constant which is independent of pressure.

It is believed that this study represents the first attempt to obtain evidence which either supports or refutes the absolute reaction rate theory by exploring a homogeneous, gas-phase, unimolecular reaction under nonideal conditions. Very recently, Eckert and Boudart (16a) have attempted to verify the theory by analyzing the second-order, high-pressure, gas-phase, thermal decomposition data for hydrogen iodide, which was obtained by Kistiakowsky (40a) many years ago. While Eckert and Boudart report excellent agreement between their calculations and the experimental results, it remains that their analysis involves many assumptions, particularly with respect to the nature of the activated complex and its virial coefficients. A study of a unimolecular gas-phase reaction under nonideal conditions, such as the thermal isomerization of cyclopropane, offers a more appealing method for testing the theory because of the similarity between the reactant and the activated complex.

Both proponents and opponents of thermodynamic variables in rate expressions agree, in general, that near equilibrium the rate is some function of a thermodynamic force (e.g. Denbigh, 15, p. 49). In fact, it can be shown (see Appendix I) that <u>near</u> equilibrium, the net rate of reaction is proportional to the free energy change of reaction: i.e.

$$r = f' \cdot \Delta G_R \qquad \text{II-59}$$

where f' remains constant for a given equilibrium, regardless of which thermodynamic variables are changed, either singularly or simultaneously. The more general interpretation on the constancy of f' was established by Manes, Hofer and Weller (56). A treatment showing the constancy of f', for variation in a single variable, was given by Prigogine, Outer and Herbo (64). Further, it can be shown that

$$\frac{1}{V}\frac{dS_p}{dt} = \frac{-r \cdot \Delta G_R}{T} > 0 \qquad \text{II-60}$$

Hence, r and ΔG_R must always have opposing signs. This condition is satisfied by f' always being negative.

From Appendix I it will be observed that f' is a function of both thermodynamic and nonthermodynamic variables, thus the relationship of Equation II-59 does not suggest that rates may be predicted from thermodynamics alone. However, Equation II-59 does show that the thermodynamic driving force is important near equilibrium, and lends support to the intuitive argument of Whalley (93) that thermodynamic variables should be of importance away from equilibrium as well.

CHAPTER III

REVIEW OF PREVIOUS WORK

General Background

Thermal isomerization of cyclopropane has been studied extensively at subatmospheric pressures, but the present investigation is the first in which the reaction has been explored at pressures substantially in excess of atmospheric pressure. Past interest in the thermal isomerization of cyclopropane at low pressure has been primarily the result of two considerations: (1) the homogeneous gas phase reaction is one of the few elementary unimolecular reactions occurring in the absence of free radical chain mechanisms and (2) because of this, and the relatively simple molecular structure, the reaction is useful in testing the unimolecular reaction rate theories which predict a decline in the first-order rate constant with reduced pressure. Unimolecular reaction rate theory is discussed in Chapter II.

Trautz and Winkler (84) in 1922 made the first significant study of cyclopropane thermal isomerization. Egloff (17) has reported several investigations prior to the work of Trautz and Winkler, but all were far less comprehensive. Just before the turn of the century, Tanatar (81) observed

the conversion of cyclopropane to propylene upon passing the former through a glass tube at elevated temperatures. Tanatar's results were contested by Volkov and Menshutkin (88) who claimed that the primary product was ethylene. This conflict was resolved through additional experiments by Tanatar (82). Apparently, Volkov and Menshutkin had not eliminated the presence of air in their experiments (17). Several other noncatalytic isomerization studies were made in advance of Trautz and Winkler. Of these, Berthelot (5), in 1900, performed what appears to be the first batch experiment. Ipatieff and Huhn (35) and Tanatar (83) made catalytic studies of cyclopropane isomerization which also predate the work of Trautz and Winkler.

At the time of the Trautz and Winkler investigation, the statistical theories of unimolecular reactions had not been developed, hence the need for a study of rate constant dependence on pressure was not apparent. Their experiments were conducted at approximately 755 mm. of mercury, while temperature was varied from 350 to 650°C. This range of temperature has not been exceeded in any subsequent investigation. The reaction was accomplished in flow-type reactors constructed of either quartz or porcelain tubes. For the most part, they found the reaction to be homogeneous and of first-order, but some surface catalysis was indicated in the porcelain tube; and at the high temperatures, decomposition occurred. Products of the decomposition were reported to be

hydrogen, carbon, methane, ethylene and propylene. From the later work of Hurd and Meinert (30) it is known that propylene will pyrolyze in Pyrex at 600°C.

Some, seemingly, justifiable criticisms of the Trautz and Winkler study have been put forth by Kassel (37) and Chambers and Kistiakowsky (9). The chief objections arise from the fact that a reactor preheater was not used, even though contact times were low, and temperatures were measured at the outside surface of the reactor tube. The activation energies of 63.9 to 65.0 kilocalories, for the temperature range of 550 to 650°C., are reasonably close to values reported in later investigations, but their frequency factor of 1.00×10^{14} was apparently much too low.

Chambers and Kistiakowsky (9) were the first to demonstrate the pseudo-unimolecular behavior in the thermal isomerization of cyclopropane. At 499.5°C. their first-order rate constant was observed to decrease 43.5 per cent upon decreasing pressure from 70.26 to 1.27 cm. of mercury. Values of k_∞ were obtained at each temperature by finding the 1/k intercept in a plot of 1/k against 1/p. The k_∞ values were found to have the expected Arrhenius type temperature dependence, resulting in equation

$$\log k_\infty = 15.17 - \frac{65,000}{2.3\ RT}$$

Chambers and Kistiakowsky also found that, by choosing 3.9×10^{-8} cm. as the molecular diameter and thirteen as the number of degrees of freedom, the experimental values of

k/k_∞ were in close agreement with the values of k/k_∞ calculated from the equation derived in the theoretical treatment of unimolecular reactions by Kassel (38). This agreement was demonstrated in a plot of log k/k_∞ versus log p in which the experimental points were essentially superimposed upon the theoretical curve.

Over a decade passed following the Chambers and Kistiakowsky investigation before another cyclopropane isomerization study was reported. During this period a number of reactions which had previously been thought to be unimolecular were found to proceed by a chain mechanism in the presence of free radicals. In this "open-season" on pseudo-unimolecular reactions, Corner and Pease (12) elected to challenge the cyclopropane isomerization reaction, in spite of the rather overwhelming indication of unimolecular behavior from the work of Chambers and Kistiakowsky. Corner and Pease attempted to show, through the effect of added gases, that their proposed chain mechanism, based on the formation of a trimethylene di-radical, provided a better explanation of the experimental results. With a quasi-unimolecular reaction, added gases are expected to increase the reaction rate; whereas, the rate may either increase or decrease in the case of a chain mechanism. However, in the Corner and Pease mechanism, no change was expected. The added gases used were hydrogen, ethylene, propylene and n-butane. In the presence of decomposing n-butane, isomerization of cyclopro-

pane was accelerated; but otherwise, in the pressure range of their experiments, the added gases had little effect and the results were inconclusive.

Almost another decade passed before decisive results were reported on the effect of added gases. The experiments by Pritchard, Sowden and Trotman-Dickenson (65, 66), in which a number of gases, in varying amounts, were added to cyclopropane at an initial pressure of from 0.01 to 0.1 cm. of mercury, showed a clear-cut restoration of the first-order rate constant. Not only were their results of sufficient precision to demonstrate, beyond any reasonable doubt, the unimolecular character of the cyclopropane isomerization reaction, but calculation of efficiencies for the collisional transfer of energy with the various added gases was permitted as well. Of the collisional efficiencies reported, helium was the lowest with a value of 0.048, while the highest was 1.10 for toluene. Both efficiencies are relative to cyclopropane.

With the pressure range of cyclopropane isomerization extended to a much lower region in the work of Pritchard et al., ample data were available to Slater (76) to permit a thorough check of his theoretically predicted unimolecular reaction rate for cyclopropane isomerization. In this treatment by Slater, the cyclopropane molecule was considered to be a classical vibrating system (the cyclopropane molecule being one of the few in which such an analysis is tractable).

Two models for isomerization were considered. In the first, the reaction was assumed to occur when vibrations carried a hydrogen too near a carbon in another methylene group; while in the second model, isomerization was assumed to result from the over-stretching of a carbon-carbon bond. Both mechanisms had been previously suggested by Chambers and Kistiakowsky. Though Slater's theory fell short of predicting the experimentally observed frequency factor (4×10^{14} theoretical versus 15×10^{14} $sec.^{-1}$ experimental) two important points were established: (1) the shape of the curve resulting from a plot of log k/k_∞ against log p was confirmed without the use of any arbitrary parameters, and (2) the hydrogen migration model gave results which were in closer agreement with experimental observations. General acceptance of the C-H rather than the C-C distance as the critical coordinate in cyclopropane isomerization has not been the result of Slater's work alone, however. Many of the recent cyclopropane isomerization studies have been concerned with establishing the reaction mechanism through the use of isotopes. These investigations are discussed briefly in a later section.

In the classical theory of unimolecular reactions by Slater (77, p. 162) temperature is predicted to affect the plot of log k/k_∞ against log p in the form of a displacement toward the log p axis with increasing temperature, through the relationship $\Delta \log p = \frac{1}{2} n \log (T_2/T_1)$ where n is the

effective number of oscillators. Langrish and Pritchard (49), in studying this effect, found, within experimental error, that their data at 483 and 505°C. could not be distinquished from the data previously reported at 491°C. (66). This observation is in agreement with the earlier work of Chambers and Kistiakowsky, prior to the theory of Slater, where also the temperature effect was not apparent. Langrish and Pritchard reported their high pressure rate constant as

$$\log k_\infty = 15.85 - \frac{67,500}{2.303\ RT}$$

which is not in too close agreement with the equation reported by Chambers and Kistiakowsky.

More recently (1959), Slater (77) has presented a quantum harmonic oscillator model for explanation of the temperature dependence of unimolecular rate constants. However, in testing his theory with the isomerization results of Falconer, Hunter and Trotman-Dickenson (19), he has found that the experimental data agree more closely with the Arrhenius form than with the quantum oscillator theory (78). Falconer et al. had designed their experiments to yield data of sufficient precision to test the Slater theory. All of their runs were conducted at a pressure of 30 cm. of mercury in the temperature range of 420 to 535°C. The Arrhenius type equation

$$\log k_{30} = 15.296 - \frac{65,084}{2.303\ RT}$$

represented their results within the limits of experimental

accuracy. Upon extending the results to infinite pressure, they obtained

$$\log k_\infty = 15.45 - \frac{65,600}{2.303\ RT}$$

which is in very close agreement with the expression reported by Chamber and Kistiakowsky.

Kennedy and Pritchard (39) have recently extended the region of low pressure thermal isomerization of cyclopropane to 6×10^{-4} mm. of mercury. It was their purpose to observe the change in reaction kinetic as the mean free path of the molecules approached the dimensions of the reaction vessel. At 490°C. and 10^{-3} mm. pressure, the reaction became first-order again, where the mean free path was approximately 7 cm., compared with the vessel diameter of 13 cm. The return to first-order kinetics was the expected result, of course, as collisions with the walls of the reaction vessel, rather than in the gas phase, became the primary source of energization.

Davis and Scott (14), in the most recent cyclopropane thermal isomerization study (1964), have extended the temperature range of reliable data on the reaction to 620°C. All of their experiments were at essentially atmospheric pressure and measurements were made in a Pyrex glass, flow-type reactor. Upon combining their data with that of previous investigators (9, 12, 53), they obtained the following equation relating k_∞ to absolute temperature:

$$\ln k_\infty = 35.431 - \frac{65,570}{RT}$$

Reaction Mechanism and Kinetics

It is now generally accepted that the thermal isomerization of cyclopropane is one of the few elementary unimolecular reactions. In Pyrex (borosilicate glass) apparatus the reaction has been found to be homogeneous, and at atmospheric pressure the reaction is of first-order. But in agreement with unimolecular reaction rate theory, the first-order reaction rate constant shows a pressure dependence as pressure is reduced, and a region of second-order behavior exists.

The reaction mechanism studies have been in two categories: (1) unimolecular versus free radical chain theory and (2) after acceptance of the unimolecular course, determination of whether the reaction occurs through hydrogen migration or over-stretching of a C-C bond. As the reaction mechanism is not of primary interest in the present investigation, the past work on the structural mechanism of the reaction will be only briefly reviewed. It should be pointed out that the unimolecular theories themselves are based on mechanisms (or models if preferred) but the discussions of these mechanisms, such as the one proposed by Lindemann (52), have been relegated to the theoretical section.

As previously mentioned, Corner and Pease (12) proposed a free radical chain mechanism to explain their data as well as that of Chambers and Kistiakowsky. Corner and Pease postulated that the trimetylene di-radical was formed,

followed by a chain of other reactions, i.e.

$$C \xrightarrow{k_1} R$$

$$R \xrightarrow{k_2} C$$

$$R \xrightarrow{k_3} P$$

$$R + C \xrightarrow{k_4} 2P$$

where C signifies cyclopropane, R the trimethylene di-radical, and P propylene. As indicated, the di-radical formed is proposed to react along three pathways. In the first, a reversion to cyclopropane occurs through re-pairing of the electrons; while in the second, a proton shift results in the formation of propylene; finally, in a second-order process, the di-radical exchanges hydrogen atoms with a colliding cyclopropane molecule to produce two molecules of propylene.

With the Corner and Pease mechanism, and the usual assumption of steady-state free radical concentration, the rate equation for change in cyclopropane concentration becomes

$$\frac{dC}{dt} = k_1 C \frac{k_3 + 2k_4 C}{k_2 + k_3 + k_4 C}$$

It is remarkable how well Corner and Pease were able to show a constant value of k_1 over the pressure range by proper selection of the ratios $k_3/(k_2+k_3)$ and k_3/k_4. Not only were they able to do this selecting for their own data but for that of Chambers and Kistiakowsky as well by using a different numerical value for the ratio $k_3/(k_2+k_3)$. At this point,

it should be stated that Corner and Pease apparently reported an erroneous value for this ratio in analyzing the data of Chambers and Kistiakowsky, as was discovered by Pritchard, Sowden and Trotman-Dickenson (66).

Since the addition of an inert gas should have no effect on the rate constant with the free radical chain mechanism--whereas, it should increase the rate constant in the quasi-unimolecular theory--this artifice was the logical means for determining the proper mechanism. As previously discussed, the results of Corner and Pease were not conclusive, primarily because their initial pressures were not low enough to produce a significant effect. The unimolecular character of the reaction was strongely indicated in the later added-gas experiments of Pritchard et al. It is apparent, however, from the work of McNesby and Gordon (57) that this evidence has not been overwhelming enough to squelch the desires of some to pursue other possible free radical chain mechanisms for explanation of the reaction behavior. The mechanism which they proposed will not be discussed however, as they were able to show, themselves, through the use of deuterium as a tracer, that the proposed mechanism could not hold.

With acceptance of the intramolecular, or purely physical, nature of the cyclopropane thermal isomerization reaction, the problem of selecting between the two most probable structural mechanisms remained. As previously mention-

ed, both mechanisms were suggested by Chambers and Kistiakowsky. In the first, it is proposed that a hydrogen "migrates" or "disproportionates" along a C-C bond, causing rupture of a second C-C bond and doubling of a third:

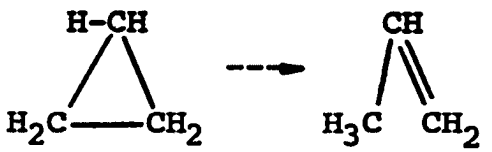

In the parlance of the absolute reaction rate theory, this mechanism involves a transition state in which a hydrogen atom is in the process of transferring from one carbon atom to another. The classical vibrational analysis of Slater (76) has favored this mechanism. In the second mechanism, it is proposed that the initial, and rate determining-step is the rupture of a C-C bond, followed by rearrangement of the di-radical produced.

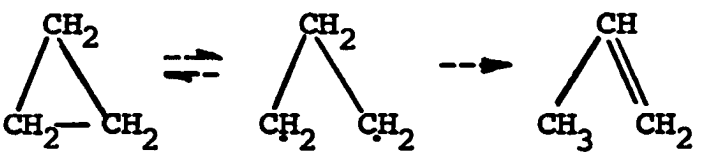

Again in the language of the absolute reaction rate theory, the second mechanism is said to involve the formation of the trimetylene di-radical as the activated complex of the transition state.

Four isotope studies have been made in an attempt to choose decisively between the two proposed mechanisms. Linquist and Rollefson (53) and Weston (91, 92) have investigated the relative rates of isomerization for cyclopropane and cyclopropane-t_1, while Rabinovitch, Schlag and Wiberg

(68) have similarly studied the relative rates using cyclopropane-d_2. And in the most recent report on isotope effects, Blades (6) has used cyclopropane-d_6. As pointed out by Blades, the results of these studies on isotope effects have not been conclusive. However, Blades presents a very appealing intuitive argument for the first mechanism; that is, "..... if the hydrogen does become bridged from one carbon to the next, as it must if it is to be of any assistance in the rupture of the carbon-carbon bond, then it will be most advantageous for it to continue on its path toward that carbon atom." Other arguments by Blades seem to overwhelm those of Benson (4), the strongest proponent of the C-C rupture mechanism.

Thermodynamics and Composition at Equilibrium

Even at the time of the Chambers and Kistiakowsky study, a good estimate of the expected equilibrium composition in the cyclopropane isomerization reaction was not possible because of the lack of specific heat and spectroscopic data on cyclopropane. These authors did, however, estimate that at their lowest temperature of 470°C. the equilibrium concentration of cyclopropane would be less than 1 part in 1000. From the thermodynamic analysis in Appendix B of the present work, one finds that the cyclopropane concentration will be substantially lower than that estimated.

Egloff (17, p. 696) has reported that Rogowski heated propylene at 400 to 405°C. in a sealed tube and obtained more

than fifty per cent cyclopropane. This amount is a highly unlikely result in view of present knowledge. Several, apparently erroneous, thermodynamic analyses are discussed in Appendix B. Also in Appendix B an expression for the standard free energy change as a function of temperature has been developed for the cyclopropane isomerization reaction and references are furnished on the various thermodynamic data sources.

Ranges of Pressure and Temperature

In reading the literature on cyclopropane isomerization, one sees frequent reference to the "high pressure" region. This terminology requires some clarification. With thermal isomerization of cyclopropane, the noticeable on-set of quasi-unimolecular behavior begins at only slightly below atmospheric pressure, and the reaction takes-on second-order characteristics. Near atmospheric pressure, however, the reaction is of first-order. It is this region of first-order behavior near atmospheric pressure which is usually described as the "high pressure" region.

The highest pressure employed in any previous investigation was 910 mm. of mercury in the work of Corner and Pease (12). Chambers and Kistiakowsky obtained reliable data near atmospheric pressure and below, but most investigations have been in the "interesting" region far below atmospheric pressure. In disproving the Corner and Pease free radical chain theory, Pritchard, Sowden, and Trotman-Dickenson carried-out

experiments with initial cyclopropane pressures as low as 0.07 mm. of mercury. However, no one has reported data for pressures below the 6×10^{-4} mm. lower limit in the work of Kennedy and Pritchard (39).

Excluding the early, and somewhat uncertain, work of Trautz and Winkler (84), the present investigation covers a greater range of temperatures than any previous single cyclopropane thermal isomerization study. Outside of the isotope investigations, the minimum temperature at which reliable data have been obtained is 420°C. This temperature was used in the work of Falconer, Hunter and Trotman-Dickenson (19) where pressure was held constant at 300 mm. Davis and Scott (14) have recently extended the high temperature range of reliable data to 620°C. at atmospheric pressure.

The temperature and pressure ranges covered in all the cyclopropane thermal isomerization investigations, starting with Trautz and Winkler, and including the present study, are summarized in Table I.

Types of Apparatus

Practically all of the cyclopropane thermal isomerization studies have been performed in batch-type apparatus constructed of Pyrex glass. Excluding the essentially qualitative work prior to Trautz and Winkler, flow reactors have only been used in two instances; first, in the work of Trautz and Winkler and, second, in the very latest work by Davis and Scott. As previously discussed, the Trautz and Winkler

TABLE I

Temperature and Pressure Ranges
of
Cyclopropane Thermal Isomerization Studies

Reference	Year	Pressure mm Hg	Temperature °C	Temp. Range °C
Trautz and Winkler	(84) 1922	~1 atm.	350-650	300
Chambers and Kistiakowsky	(9) 1934	12.7-764-9.	470-519	49
Corner and Pease	(12) 1945	10-910	440-520	80
Pritchard, Sowden and Trotman-Dickenson	(65) 1952 (66) 1953	0.07-84	470-490	20
*Weston	(91) 1955 (92) 1957	0.4 -700	406-492	86
*McNesby and Gordon	(57) 1956	-300-	-475-	-
*Lindquist and Rollefson	(53) 1956	160-202	447-555	108
*Rabinovich, Schlag and Wiberg	(68) 1958	-15+-	414-474	60
Langrish and Pritchard	(49) 1958	-	483-505	22
Falconer, Hunter and Trotman-Dickenson	(19) 1961	-300-	420-535	115
*Blades	(6) 1961	0.178-760	407-514	107
Kennedy and Pritchard	(39) 1963	$6x10^{-4}$-7	477-517	40
Davis and Scott	(14) 1964	~1 atm.	546-620	74
Present Work	1964	250-2000 psi	454-593	139

*Isotope studies

results have been subject to criticism because of failure to provide preheat for the reactor feed, and because the reaction temperature was taken to be that measured at the outside of the low thermal conductivity quartz and porcelain tubes used as reactors.

Flow-type reactors fell into early disfavor with chemists probably because of a lack of understanding of the flow dynamics in the types of reactors they employed. Often the reactors had quite low length to diameter ratios and inlet and outlet connections were of small cross-section compared with that of the reactor itself; such conditions were favorable to channelling and resulted in effective residence times which were much lower than supposed. Batten (2) has recently discussed this behavior at some length. Kennedy and Pritchard (39) reported the failure of a flow-type experiment for thermal isomerization of cyclopropane at low pressure. They now attribute the causes of failure to this phenomenon. In many instances plug-flow has been erroneously assumed, either tacitly or otherwise. The plug-flow assumption was applicable to the study of Davis and Scott and their apparatus is free of the criticisms given to the apparatus of Trautz and Winkler. In Appendix D the diffusional effects and validity of the plug-flow assumption have been assessed for the present investigation.

All of the batch thermal isomerization studies have been conducted in glass vessels of some type. Pyrex glass

has been used in most cases. However, Lindquist and Rollefson (53) used quartz bulbs, Rabinovitch et al. (68) report the use of silica glass, while Weston used quartz bulbs in preliminary experiments, but does not describe the type of glass in his 1800 ml. flasks. Sizes of the batch reactors have varied from 18 to 2000 ml.

Chambers and Kistiakowsky and Davis and Scott have demonstrated that the reaction is homogeneous in Pyrex glass. Surface effects were shown to be absent upon addition of Pyrex packing to the reactor in each case. The former was a batch reactor, while the latter was of flow-type.

The analytical procedures and apparatus used in previous investigation are discussed in Chapter VI.

Catalysis

Catalytic reactions of cyclopropane and propylene, per se, are not of interest in this investigation. However, it has been necessary to avoid the known catalytic materials in the design of the high-pressure thermal isomerization apparatus. A discussion of the known catalytic effects, as they relate to final selection of the reactor material, is presented under the Reaction Section in Chapter IV.

CHAPTER IV

DESCRIPTION OF EXPERIMENTAL APPARATUS

When any kinetic study is extended into regions of high pressure, the problems associated with equipment design are compounded, particularly where high temperatures are involved and/or where catalytic surfaces must be avoided. In the present investigation it was necessary to design for both high temperature and pressure, while eliminating catalytic surfaces to the extent practicable. These demands have brought forth certain design features which cannot be regarded as ordinary. It is the purpose of this section, therefore, to comment on these special design features in particular, as well as to discuss the process equipment in general.

In this experimental investigation, high-pressure, thermal isomerization of cyclopropane to propylene was accomplished with the apparatus indicated in the process flow diagram of Figure 3. The apparatus is designed for reaction under once-through, continuous-flow conditions. In all the previous work on this reaction at low pressure, only in the very early work of Trautz and Winkler (84) and in the most recent work by Davis and Scott (14) have other than batch

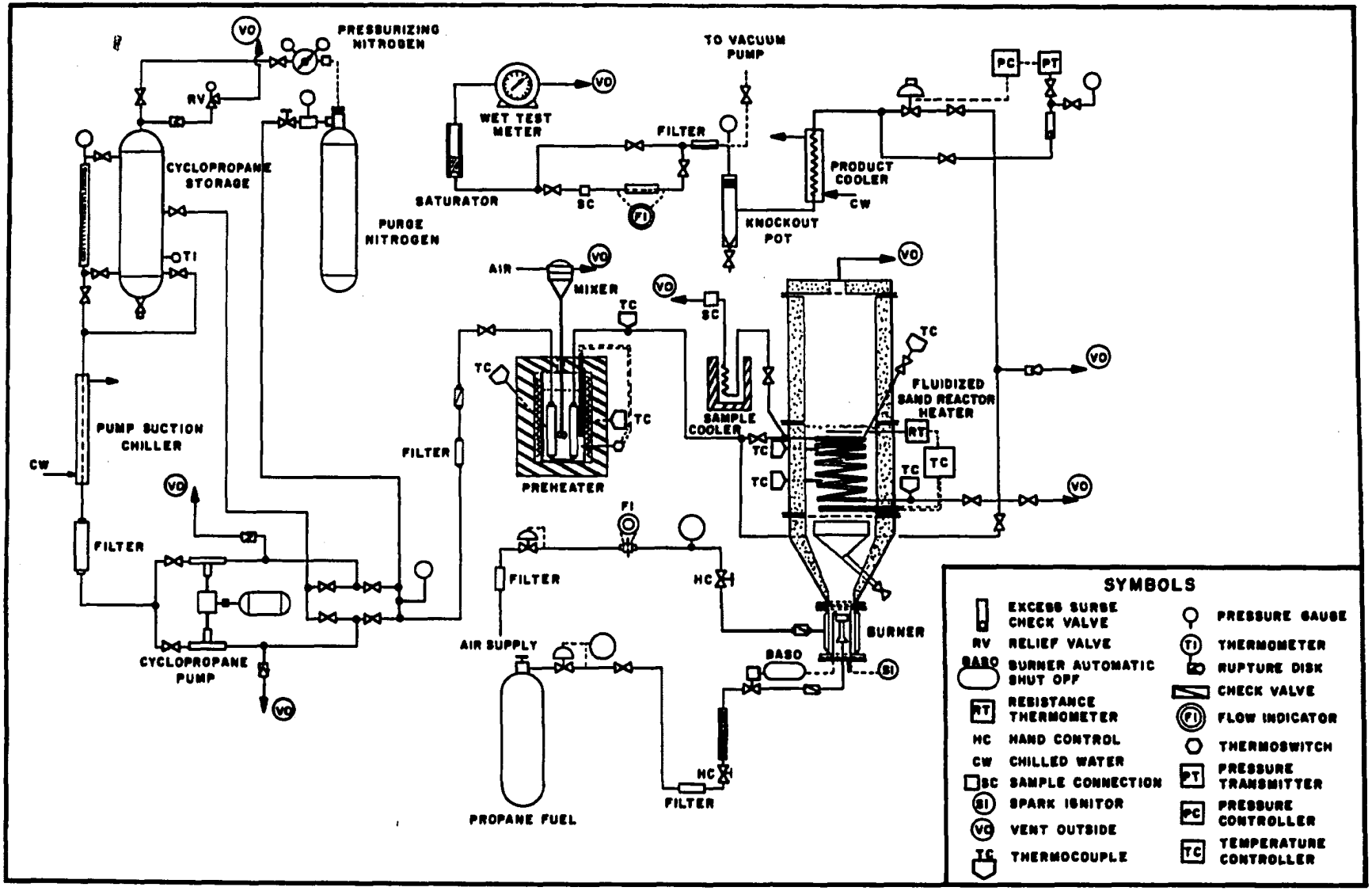

CYCLOPROPANE ISOMERIZATION PROCESS FLOW DIAGRAM

Figure 3

systems been employed. As with commercial processes, equipment for processing on a research scale must have certain design specifications. In the present case, these specifications were:

	Maximum
Cyclopropane Feed Rate	1.0 gal./hr.
Conversion	100 per cent
Temperature	1200°F.
Pressure	5000 p.s.i.

Briefly, the process involves pumping pure liquid cyclopropane from storage to a preheater, and thence to a gold-lined tubular reactor immersed in a constant temperature bath of fluidized sand. Effluent gases from the reactor are throttled through a pressure control valve into a product cooler, followed, in turn, by a receiver and gas measuring system. For purposes of discussion in detail, it is convenient to divide the equipment into five categories: (1) feed system, (2) preheater section, (3) reactor section, (4) product section, and (5) auxiliaries. It will be observed that analytical equipment is discussed in Chapter VI. Further, the calculation of allowable pressures for equipment will be found in Appendix C.

Feed System

The main components of the feed system were the cyclopropane storage drum, the nitrogen pressurizing system, a calibrated sight glass, a pump suction chiller, and a high-pressure, positive-displacement pump.

The storage drum was constructed from a 56-inch length

of 8-inch (N.P.S.), Schedule 80, carbon steel pipe and two 8-inch, Schedule 40, carbon steel pipe caps. With this construction, the volumetric storage capacity for cyclopropane was approximately eleven gallons. Owing to the potential hazards of storing liquefied hydrocarbon gases indoors, and because of the high cost of cyclopropane ($75.00 per gallon of liquid), several measures were taken to assure leak-free service from the storage drum and connecting piping. First, all threaded connections to the drum were made with Teflon tape as a thread sealant. Second, all valves connected to the drum were of ball-type, with O-ring seals, and Underwriter's Laboratory approval for liquefied hydrocarbon gas service (viz., Worcester No. 444TB valves). Third, relief protection was provided with a rupture disc and relief valve in series, with the former on the drum side. This last precaution was taken because relief valves are rarely ever leak-free and, further, one would not wish to take the risk of loosing a complete charge of cyclopropane when using a rupture disc alone. Both the rupture disc and relief valve were designed to relieve at 300 p.s.i. gauge. Normal storage drum pressure was 175 p.s.i. gauge corresponding to the saturation vapor pressure of cyclopropane (approximately 85 p.s.i. gauge at 75°F.) plus an added pressure of 90 p.s.i. from nitrogen pressurization. As indicated in Figure 3, the storage drum was equipped with a sight glass, pressure gauge and thermometer.

Pump suction piping (3/8-inch o.d. by 1/4-inch i.d., Type 304 stainless steel tubing, with Autoclave Engineers, Inc.. Ermeto connections) was provided to permit pumping from either the storage drum or the liquid level gauge (sight glass). The liquid level gauge was a Jerguson tubular glass assembly, four feet in overall length, complete with valves, plastic (Lucite) protector, and guard rods. Ball check valves, located within each gauge valve, functioning on the excess surge principle, provided protection in the event of liquid level gauge failure. Tubing for the level gauge was heat-treated glass with 3/4-inch o.d. and ½-inch i.d. Calibration of the level gauge revealed a uniformity of internal cross-section over the entire length, corresponding to a volumetric capacity of 1.23 ml. per cm. of length. Pumping rates were observed from a numbered centimeter scale taped onto the back-side of the glass tube. Both the level gauge and storage drum may be observed at the left side of the panel in the photograph of Figure 4.

Because of ceiling height limitation, it was not possible to supply the required pump N.P.S.H. from a liquid column of cyclopropane alone. Thus, it was necessary to either pressurize the cyclopropane storage drum or to chill the fluid going to the pump to insure against cavitation at the pump suction. Actually, the best results were obtained when both methods were employed at the same time. Chilling of the pump suction alone was not sufficient. Chilling of

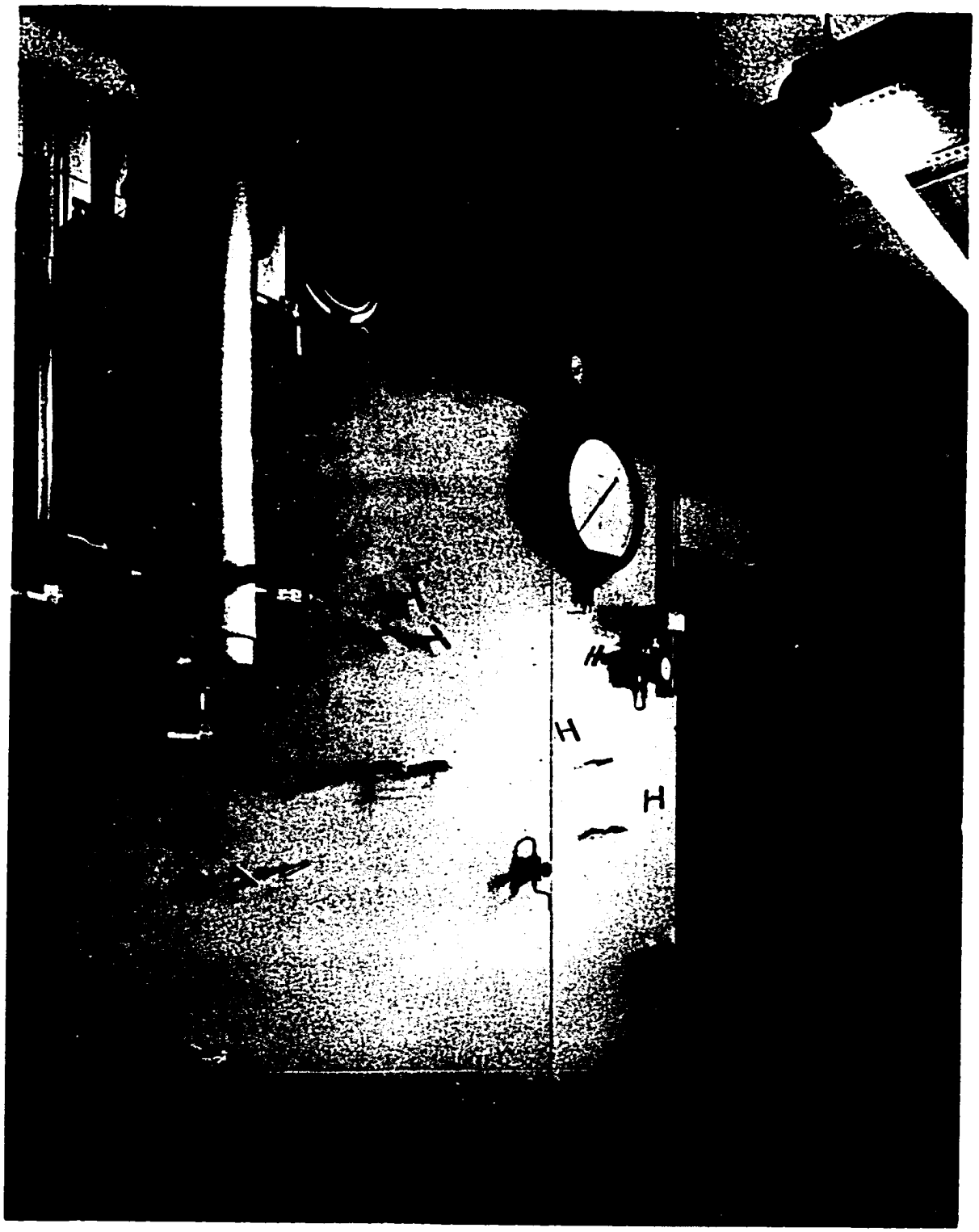

Figure 4 - High-Pressure Cell Front Panel

the feed was accomplished by a counter-current flow of water at 35°F. through the annulus formed by surrounding the 3/8-inch stainless steel tubing with a 40-inch length of, insulated, 3/4-inch brass pipe. Nitrogen was added to the top of the cyclopropane storage drum through a pressure regulator attached to a standard cylinder. Between the suction chiller and pump, a filter was installed to remove rust and other suspended matter which might impair proper operation of the pump check valves. This filter was a standard Kuentzel bomb, with filter-type outlet closure. Inserts of 100-mesh brass gauze were installed at each end, while the bomb proper was filled with 3-mm. diameter soda-lime glass beads.

Cyclopropane was pumped from storage with a Hills-McCanna, Model "UM"-2F, proportioning pump, equipped with cylinders in duplex, each with a maximum capacity of 0.56 gal./hr. at a design discharge pressure of 5000 p.s.i. This pump was used in a previous investigation by Skinner (75) where considerable difficulty was encountered in maintaining reproducible, low flow rates at high pressure. Though this problem also existed to some extent in the present investigation, it was not as severe as reported previously. Standard double-cone check valves were used for both the suction and discharge of each cylinder. Also, each cylinder was equipped with a 5/16-inch alumina-ceramic piston surrounded by seven cylindrical rings of Teflon packing, four of which

were of the compressed-flake type, while the three remaining rings were of solid molded Teflon, two of which were the end rings. As shown in Figure 3, it was possible to circulate either cylinder back to the storage drum. This feature permitted a check-out of flow rate and extent of packing leakage in advance of each run. Each cylinder was also equipped with a rupture disc to avoid over-pressuring. The cyclopropane feed pump, suction chiller, filter and by-pass manifold are shown on the right in the photograph of Figure 5.

Preheater Section

Cyclopropane, after being pumped from storage, passed through a sintered metal filter and check valve before entering the preheater. Use of the filter was necessary to prevent spalled pump packing from being carried into the preheater and reaction sections.

Basically, the preheater was a thermostated bath of well-mixed, molten inorganic salt in which the elements to be heated were immersed. The heating element was either a stainless steel coil or four modified Kuentzel bombs in series. Details of the modified Kuentzel bombs are shown in the cross-section of Figure 6. The complete preheater installation is shown at the center of the photograph in Figure 5.

From Figure 6, it will be observed that the Kuentzel bomb modification involved: (1) application of ceramic lining to the inside surface, (2) alteration of closures to accommo-

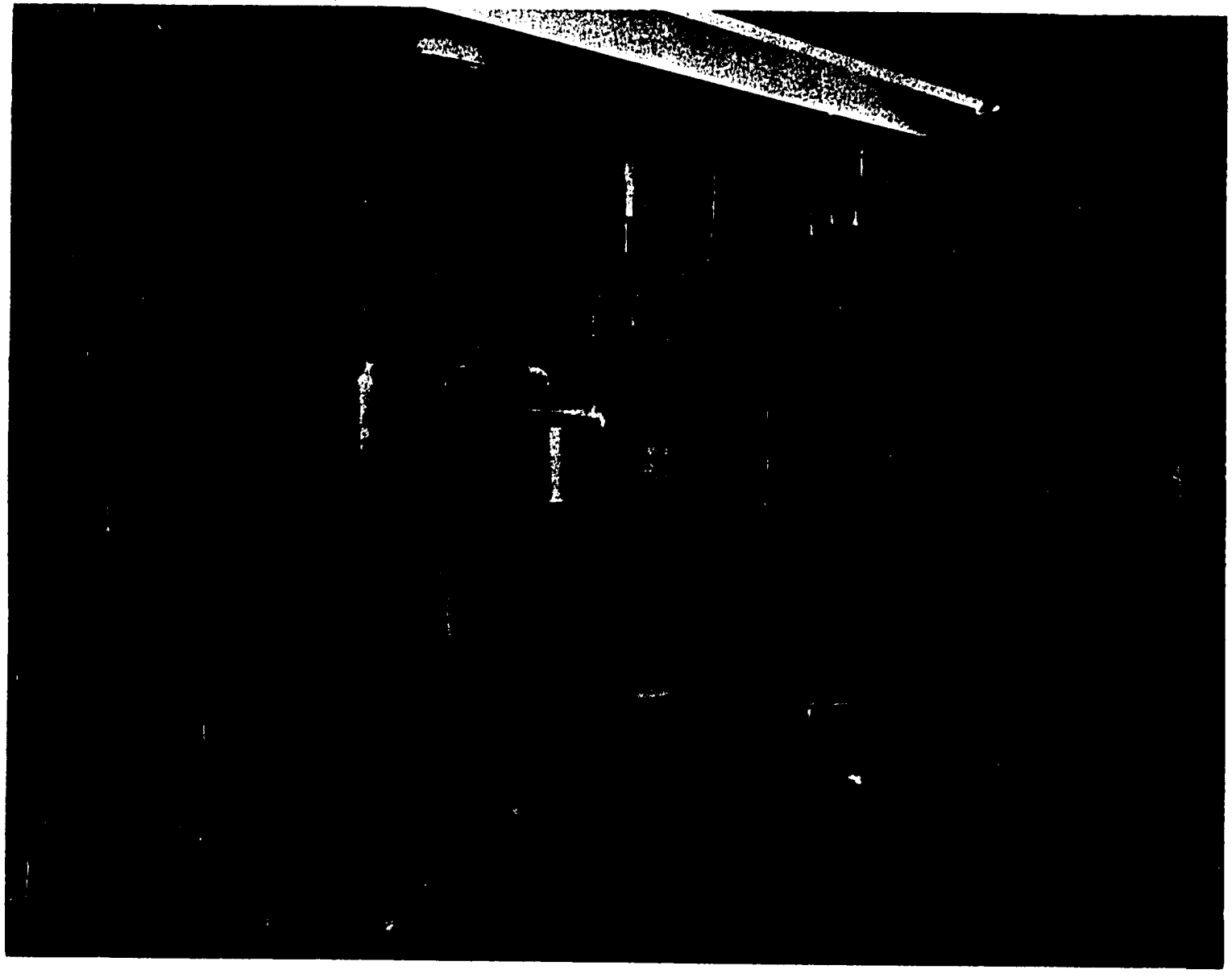

Figure 5 - Equipment Inside High-Pressure Cell

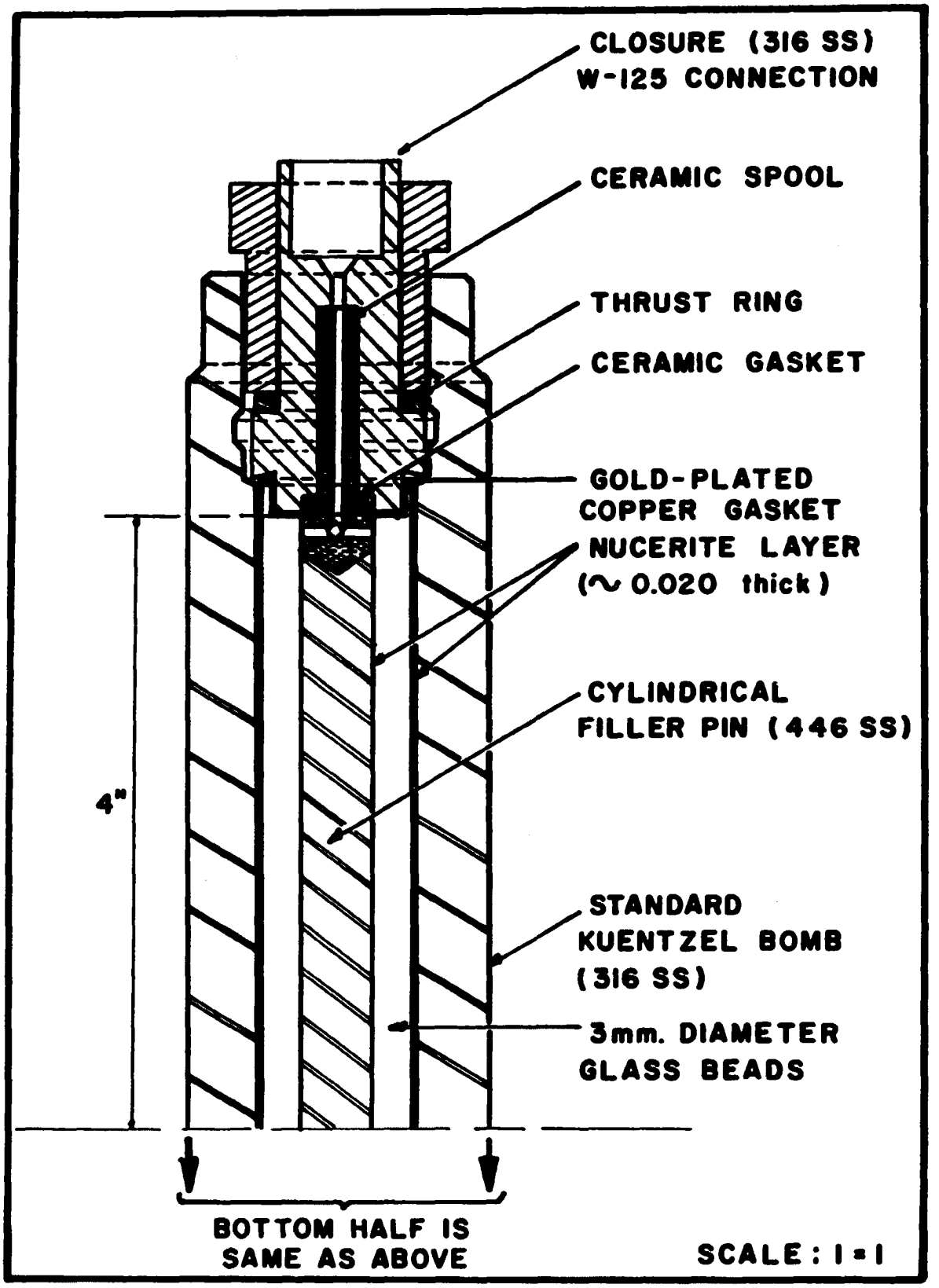

MODIFIED KUENTZEL BOMB PREHEATER (4)

Figure 6

date ceramic spools, and (3) insertion of ceramic-coated filler pins to form an annular flow path. Originally these bombs were designed to be used as reactors and the annular flow and radial entry features were designed to eliminate the channelling effect, such as described by Batten (2). With the decision to use the bombs as preheaters, filling the annular space with glass beads was considered desirable for two reasons: (1) the internal heat transfer coefficient would be improved and (2) the extent of thermal reaction would be minimized owing to the reduced residence time.

The ceramic applied to the surfaces indicated in Figure 6 was Pfaudler's Nucerite RC formulation. This coating was an experimental application, and the work was done by the Pfaudler Company in their facilities at Rochester, New York. Nucerite is a trade name for a ceramic formulation in which crystal growth within a glass matrix is controlled, both as to size and number. The crystalline structure contributes to improved mechanical strength and resistance to thermal shock. The method of application involves bringing the base metal to a red heat, followed by grit blasting, spraying of the surface with the ceramic, firing at a high temperature to accomplish the ceramic to metal bond, and finally heat treatment for control of the nucleated glass crystallization.

Ceramics of this type are suitable for operating temperature up to 1400°F., depending upon the base metal used.

It is desirable that the metal thermal coefficient of expansion be slightly greater than that of the ceramic so that the latter will be in compression when cooled. Carbon steel and 400 Series stainless steels have thermal coefficients of expansion (6.7×10^{-6} and 6.0×10^{-6} in./(in.)(°F.), respectively) which more nearly match that of the ceramic; whereas, 300 Series stainless steels, with their higher thermal coefficients of expansion (8.9×10^{-6} in./(in.)(°F.), tend to overcompress the ceramic in the cooled state. Nevertheless, the four, Type 316 stainless, Kuentzel bombs were successfully lined, even though the small inside diameter (1-inch) and thick wall (1/2-inch) presented additional complications. Surface coverage was essentially 100 per cent complete and no cracking of the lining was observed.

Application of ceramic to the inside face of the closures was more difficult and some spalling did occur on the convex surfaces with small radius of curvature. The filler pins could not be successfully coated when made of Type 316 stainless steel. Type 446 stainless steel, however, proved to be entirely satisfactory. The thickness of ceramic applied was approximately 0.020-inch on all surfaces.

The spools shown in Figure 6 served both as filler pin supports and flow distributors, while at the same time reducing the amount of metal surface exposed to the gas stream. They were machined from hydrous aluminum silicate (American Lava Corporation, Grade A) and the final anhydrous

ceramic form was obtained by firing in an oven at 1850 to 2000°F. The opening along the axis of the spools was 3/32-inch in diameter. In the head of the spools, this opening branched into six, equally spaced, radial passages with diameter of 1/32-inch. A gasket of Fiberfrax ceramic paper was inserted between the spools and the end closures. The gaskets between the Kuentzel bombs and closures were at first made of gold-plated copper, where standard copper gaskets were plated in Atomex immersion gold solution (Engelhard Industries, Inc.) at 145°F. to give an approximate plating thickness of 0.7 mg. of gold per sq. in. These gaskets were later found to be unsatisfactory and were replaced with gaskets made of annealed Type 316 stainless steel.

In the annular space between the filler pin and the inside wall of each Kuentzel bomb, a charge of 3-mm. diameter soda-lime glass beads was added. The total free volume of the four Kuentzel bombs was measured to be 126.2 cu. cm., excluding the short sections of 1/8-inch o.d. by 1/16-inch i.d., Type 304 stainless steel, connecting tubing. The preheater assembly was hydrostatically test at 10,000 p.s.i. before being placed in service.

The preheater salt bath was constructed from a 20-inch length of 10-inch, Schedule 20, carbon steel pipe. All four Kuentzel bombs were mounted on a stainless steel rack which was designed to permit simultaneous removal of the bombs from the bath. The salt bath top closure was con-

structed as an integral part of the bomb rack. The 15-ft. x 7-3/8-in. long, 1/8-inch o.d. by 1/16-inch i.d., stainless steel preheater coil was wound around the Kuentzel bomb assembly. Separate inlet and outlet connections make it possible to change from one preheater to the other without entering the salt bath.

Hitec salt (a eutectic mixture consisting of 40% sodium nitrite, 7% sodium nitrate, and 53% potassium nitrate) was used as the heat transfer medium. This material could be heated to 1100°F. and thus provided the full level of preheat required for all of the runs. Heat was supplied to the salt through the walls of the bath by six, 500-watt, Chromolox resistance heating elements embedded in Thermon. Power for these heaters was supplied by two Powerstat variable voltage transformers operating with 200-volt, single-phase, electrical supply. Three heaters were wired in parallel with each Powerstat. Insulation for the sides of preheater assembly was provided by two-half-sections of 12-inch nominal size Unibestos pipe insulation, 3-1/2 inches thick. Insulation for the top of the preheater was furnished by, 4-inch thick, Kast-O-Lite blocks of refractory concrete formed into the particular shapes required.

In order to improve the coefficient of heat transfer, and to assure isothermal operation of the bath, the Hitec salt was continuously agitated with an air motor driven "Lightnin" mixer, (Model No. AR-25). Trim heat for control

of salt bath temperature was supplied by a 675-watt Chromalox cartridge heating element placed in a copper well extending through the salt bath top cover plate. The temperature controller was a Fenwal No. 16050-0, high temperature, Thermoswitch which opened or closed the trim-heater power supply circuit as required (i.e., an on-off control). Temperature of the bath was measured with two chromel-alumel thermocouples located in stainless steel wells deeply immersed in the salt. Recorded values of these temperatures were obtained from a Leeds and Northrup Micromax multi-point recorder.

Reactor Section

There are three major equipment items in the reactor section: (1) a gold-lined, stainless steel, tubular reactor, (2) an isothermal bath of fluidized sand, and (3) an enclosed propane burner which supplied heated air and combustion products as a fluidizing medium for the bath. These items, along with the associated auxiliary equipment, are indicated schematically in Figure 3. The fluidized sand bath is on the left-hand side in the photograph of Figure 5. Appearing at the base of the bath cone section is the propane burner. When the center section of the fluidized sand bath is removed, the reactor coil appears as shown in Figure 7.

In selecting the reactor section equipment, it was necessary to solve the problem of surface catalysis, as well as to provide a high temperature, isothermal environment for the reactor. Methods used in solving these problems, and

Figure 7 - Reactor Section of Sand Bath Heater

the reasons for them, are discussed in the paragraphs which follow.

Most previous studies of cyclopropane thermal isomerization have been performed in borosilicate glass (Pyrex) equipment. This glass is the only material which has been definitely established as noncatalytic to the reaction. Davis and Scott (14) found borosilicate glass to be noncatalytic in the complete range of reaction temperatures up to 620°C., the maximum temperature of their study. In the early work by Trautz and Winkler (84), a change in reactor material, from quartz to unglazed porcelain, was reported to affect the reaction rate. Their results have been questioned however, because of the analytical procedure used and for other reasons (9).

Very little is known about the catalytic effect of metals on the isomerization of cyclopropane. Platinum is the only metal definitely established as catalytic (17). The catalytic effect of iron is not certain. Ipatieff and Huhn (35) reported that iron fillings promoted the reaction at 100°C. Later, however, Ipatieff (34), in referring to the same study, stated that the reaction was carried-out at 600°C. If the latter is true, then he could have been observing the thermal reaction instead. Egloff (17), in his book on reaction of pure hydrocarbons, quotes the low temperature results of Ipatieff and Huhn. Roberts (71), in his article on catalytic effect of acidic solids, has also noted

this inconsistency.

Apart from the catalytic effect of metals on cyclopropane, one must also considered the influence of metals on the propylene product formed. Egloff (17) has reported that nickel, monel metal, and iron are catalysts for the decomposition of propylene. Thus, it would appear that these metals, and platinum as well, should be avoided in reactor construction.

Though the catalytic effect of gold upon reactions of cyclopropane and propylene has not been studied, a review of the literature, for reactions in which gold is known to be a catalyst, does not suggest that difficulty would be encountered. For example, gold is known to be a catalyst for the hydrogenation of olefins, but in the present investigation hydrogen is not present. Or taking another case, gold has been used as a catalyst for the oxidation of olefins, but again oxygen is not present in the system. Gold's role as a catalyst for the polymerization of acetylene, when suspended on activated charcoal or silica gel, is the one case where difficulty might be suggested.

A decision was made to try gold as a reactor material on an experimental basis. However, owing to the low strength of gold and the high pressures and temperatures required (aside from cost) it was not feasible to use a reactor constructed of gold alone. The problem was resolved by applying a gold lining to the inside of a stainless steel tube.

It was found that Engelhard Industries, Inc., and others, had developed the technology for application of precious metal linings to tubing of various materials. In the case of stainless steel, it is not possible to bond chemically with gold. Instead, a mechanical bond is obtained by first inserting a cold gold sleeve into the stainless steel tube and then pulling through a "torpedo" to press the lining firmly against the tubing inside surface.

The lining was applied to a 14-ft. long, 9/16-inch o.d. by 3/8-inch i.d., piece of Type 316 stainless steel, Super Pressure tubing, purchased from Superior Tube Company. This high creep resistance material was guaranteed to meet a 1000-hour stress rupture test at 1200°F. with a stress of 25,000 p.s.i. Though a tubing with smaller inside diameter was desired, 3/8-inch was the minimum size which could be lined by Engelhard. Also, the 14-ft. length was approximately the maximum which could be handled with their facilities. The tube, as actually lined, contained 26.91 troy ounces of gold. This amount corresponds to an average lining thickness of approximately 0.015-inch.

Coiling of the tube was accomplished on a lathe, using a piece of 6-inch pipe as a spool, and an improvised wiper die. A uniform coil spacing of 9/16-inch was obtained by bending the gold-lined tube simultaneously with another piece of tubing of the same diameter. After expanding, the final average coil diameter was 7½-inches. Thus, the 14-ft.

section was wound in seven turns. Negligible flattening occurred in the bending process, as was confirmed by volume measurement.

Coupling of the gold-lined reactor coil to the transfer tubing with 9/16-inch cone to 1/8-inch Ermeto adapters proved to be unsuccessful because of leakage. The final installation was made by welding as shown in Figure 8. By coincidence, after correction for removal of the threaded end sections, the final reactor volume was exactly 250 ml.

Use of fluidized sand as a heating medium for the reactor was the result of two considerations: (1) Hitec salt decomposes at the maximum reaction temperatures; whereas, with fluidized sand, one is limited only by the sand softening point, and (2) in well-designed fluidized beds, almost perfect backmixing is achieved by both the gas and solid phases, and a high effective thermal conductivity assures a close approach to isothermal behavior. High thermal conductivity is an important attribute of fluidized systems. As reported by Frantz (20), in an excellent review of the literature on fluidization, thermal conductivities may in some cases be as much as 100 times greater than that of silver.

Acceptance of fluidized system as a general research tool, until recently, has lagged well behind the approval of such systems in industrial applications. One is made aware of a reversal in this trend by the many references to fluidized systems employed in recently reported investigations of

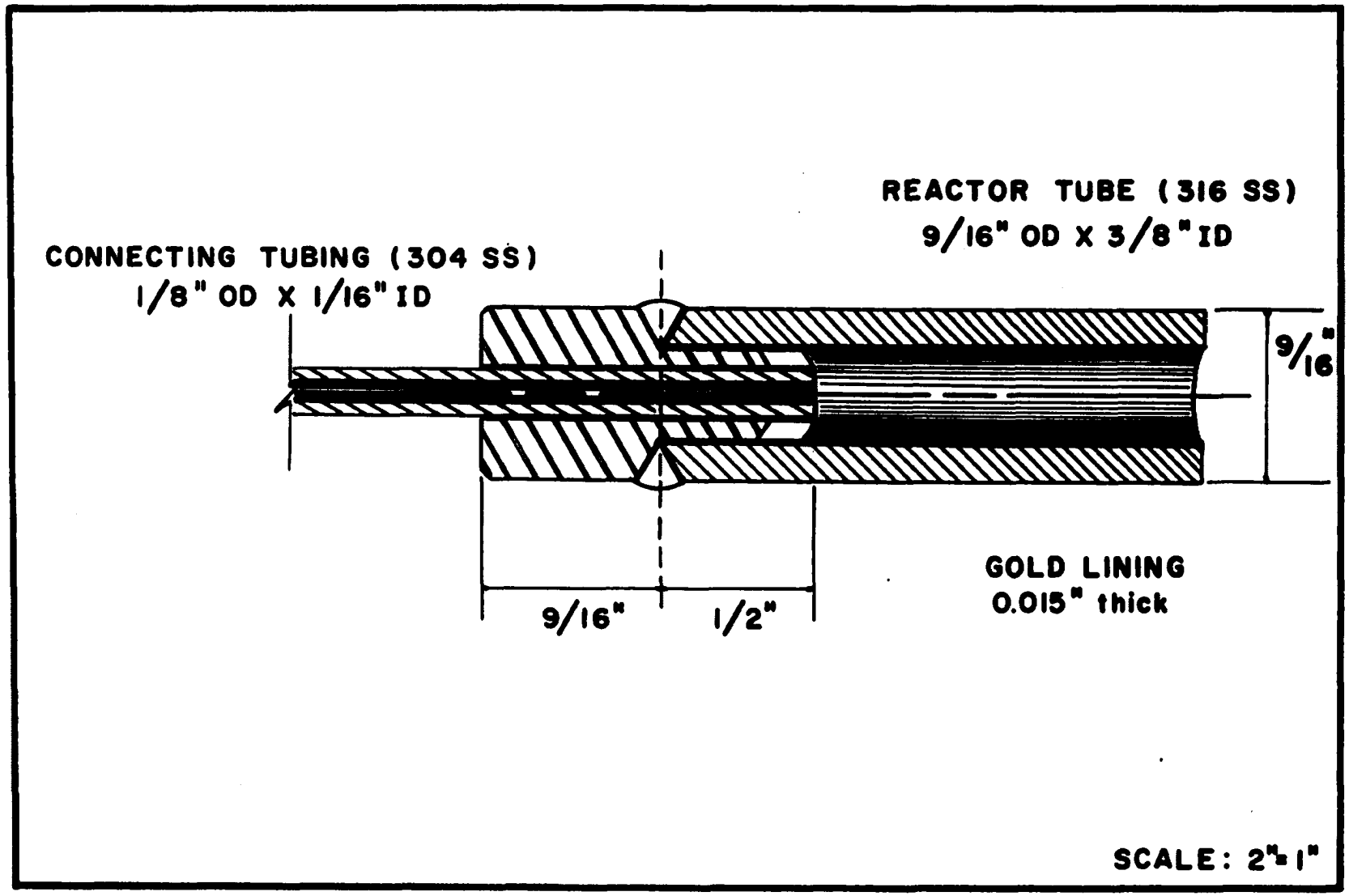

REACTOR WELDED COUPLING

Figure 8

all types. For example, in a very recent investigation, Hall and Rase (26) employed a fluided sand bath for maintaining isothermal reaction conditions in their study on the effect of dislocation density on catalytic activity. In another study, almost as recent, Korbach and Stewart (43) report "simple and effective" temperature control with a fluidized sand system in their kinetic and equilibrium study of benzene hydrogenation in a batch recycle reactor.

Though the use of a fluidized solid system as an isothermal bath in this investigation cannot be considered a new concept, it is believed that the overall design of the equipment for sand fluidization, heating, and handling is unique. From Figure 5, the fluidized sand heater is observed to be a vertical structure consisting of four flanged sections stacked in series. These sections, identified from bottom to top, are: (1) a burner section, (2) a sand trap and flame section, (3) a reactor or fluidized sand section, and (4) a sand addition and disengaging section. Mechanical and dimensional details of the top three sections are given in Figure 38 of Appendix F. Details of the burner design are found in Figure 40, also of Appendix F.

In brief, operation of the fluidized sand heating system involves heating a controlled volume of air which, upon passing through a grid-plate distributor, fluidizes a charge of sand in which the gold-lined reactor coil is immersed. The air-flue gas mixture leaving the fluidized bed

then passes through a disengaging section in which all but the smallest entrained particles of sand are removed. Control of the base heat supply for maintenance of bath temperature was accomplished by hand regulation of propane flow to the burner. Trim heat for the final control of bath temperature was supplied by a heating element immersed in the sand. Electrical power to this trim heater was regulated by a temperature controller with a resistance thermometer sensing element.

Air for fluidization was first reduced from supply line pressure to a constant metering pressure of 15 p.s.i. gauge with a Fisher No. 95L pressure regulator. Rate of air flow was measured with an orifice meter. Pressure differential across a 0.5075-inch diameter sharp-edged orifice located in a standard run of 1-inch, Schedule 40, galvanized pipe was indicated on a Barton Model 200 pressure differential indicator with a range of 20 inches of water. The design air flow was 18 std. cu. ft./min. which yields a superficial velocity of approximately 1-ft./sec. in the fluidized bed at 1100°F. With pressure held constant by the pressure regulator, it was possible to control the air flow rate by hand adjustment of a standard brass glove valve.

The air was heated with a propane burner specifically designed for this application by John Zink Company. A sectional elevation of the burner is shown in Figure 40 of Appendix F. Burner design capacity was 30,000 B.t.u./hr. By

designing the burner with an air plenum surrounding it, the air was preheated in this manner and insulation was not required. The spiralling admission of air at the top of the burner served the useful purpose of reducing flame length and hence the amount of flame impingement on the sand trap-out pan. Since the burner is operated under pressure, the normal supply of low pressure natural gas could not be used as a fuel. Instead, commercial propane from a 16-gallon storage cylinder was used. Propane pressure was reduced to 9 p.s.i. gauge with a Matheson No. 70A pressure regulator. Flow of propane was controlled with a stainless steel needle valve and the rate observed from a Matheson No. 622 PBV rotameter with No. 604 tube. As a safety feature, a BASO device, activated by a shielded thermocouple above the burner, was used to close a solenoid valve in the propane line in the event of flame-out. With the burner enclosed, and operating under pressure, a spark ignitor was used. This ignition system, not unlike that for automobiles, included a spark plug, high tension coil, breaker points, and a 12-volt d.c. battery (also the power supply for the chromatograph). Electrical diagrams for the ignitor and BASO devise are given in Figure 37 of Appendix E.

The heated air-flue gas mixture passes through an annular space between the trap-out pan and the cone insulation before contacting the grid plate of the fluidized sand bath. The grid was constructed from a piece of 11-gauge,

Type 316 stainless steel, 17-3/4 inches in diameter. A total of 195 holes, 1/16-inch in diameter and located on 3/4-inch triangular spacing, were drilled within a radius of 5-1/2 inches about the center. Each hole was coned on the flame side of the grid with a 1/4-inch drill to leave a thickness of 1/32-inch. With this design, pressure drop through the grid was approximately equal to that through the bed. Zenz and Othmer (98) report a usual design practice for commercial fluidized units to be 40 per cent of bed pressure drop.

Wilcox sand was used in the fluidized bed. Particle size distribution for this material from a Tyler shaker analysis was as follows:

Screen Mesh No.	Weight % on screen	Cumulative % greater than
60	2.98	2.99
70	16.76	19.74
80	7.11	26.85
100	44.40	71.75
140	18.80	90.05
170	5.50	95.55
200	2.87	98.42
300	1.15	99.57
Pan	0.11	99.68

From this analysis, the median particle diameter is approximately 170 microns. A sixty-five pound charge of sand in the fluidized state was found to give ample coverage of the reactor coil and resistance thermometer. The bed as confined by the insulation had a diameter of 13 inches.

Length of the fluidized bed section was 14 inches, compared with 24 inches for the disengaging section. Both of these sections, as well as the cone section, were lined

with a light-weight, castable, refractory insulation of Kast-O-Lite. This material is a product of the A. P. Green Fire Brick Company, consisting chiefly of silica, alumina and lime. The thermal conductivity at 1200°F. is reported to be 2.21 B.t.u./(sq.ft.)(hr.)(°F.)/(in.). The lining was held in place by stainless steel end plates and studs spot-welded to the shell interior. Thickness of application was 4 inches in the fluidizing and disengaging sections.

Temperature of the fluidized sand bath was controlled with a modified Bayley, Model 96, Precision Temperature Controller. As modified, temperatures up to 650°C. could be measured and controlled. The modification included a special resistance thermometer probe with quartz lead insulation and a change in three bridge resistors. This instrument under ideal conditions is capable of controlling temperature to within $\pm$0.001°C. (the manufacturer's stated electronic bridge accuracy). Trim heat from the controller was supplied to a 675-watt Chromalox cartridge heater located in a horizontal copper well directly above the grid plate. Temperature of the sand bath was measured at three locations with chromel-alumel thermocouples. Two of these thermocouples were Conax WTG-24-B2 Safetywell assemblies. The well at center of the bath was 6 inches in length and the one at the top, 12 inches. Both wells were made of 3/16-inch o.d. stainless steel tubing. The third thermocouple was placed in a retractable well located in the sand addition connection. This well was

constructed of 1/4-inch stainless steel tubing and its 26-inch length permitted immersion to the center of the bath. All three temperatures were monitored on a multipoint Leeds and Northrup Micromax recorder, primarily for trend indication. For more precise temperature measurement, either a Leeds and Northrup Model 8662 or Model 8686 precision potentiometer was used.

Product Section

Reactor pressure was regulated by throttling of product gases with a single-port, diaphragm-operated, control valve; viz., a 1/4-inch, Type 304 stainless steel, ATO, valve with P2 or P4 trim as required. Control air beneath the valve diaphragm was supplied by a Foxboro M-58 Consotrol, indicating type, pressure controller located outside of the high pressure cell. A pneumatic signal to this controller was supplied by a Bristol, Series 650, Metagraphic pressure transmitter located inside the cell.

A 0-2000 p.s.i. range Heise gauge, with 2-p.s.i. scale divisions, was used for indication of reactor pressure. The gauge was dead-weight tested before use. An excess-surge check valve was installed in the lead line to the pressure gauge.

Product gases from the pressure control valve passed to a product cooler where cooling was accomplished by counter-current flow of chilled water entering at 35°F. The cooling coil was constructed from 11 feet of 1/4-inch stainless steel

tubing. The knock-out pot following the cooler was constructed from a piece of 2-inch diameter copper pipe, 14 inches long. A 2-inch thick stainless steel wool demister was installed at the top of the receiver. The connection to the vacuum pump for start-up and shut-down evacuation was located at the outlet of the knock-out pot.

Gas from the knock-out pot passed through a sintered metal filter before being measured. Two methods of flow measurement were used. In the first case, pressure differential across a short section of 1/4-inch copper tubing was measured and indicated continuously with a Barton, Model 200, pressure differential indicator with range of 20 inches of water. This instrument was used primarily for observation of flow continuity. Following the flow indicator was a rubber septum sample connection which permitted removal of product samples with a syringe and needle. Final measurement of product flow was with a Precision Scientific wet test meter, preceded by a saturator constructed of transparent plastic.

Auxiliaries

As previously mentioned, chilled water was used for product cooling, as well as for cooling cyclopropane going to the charge pump. This chilled water system included a refrigeration unit, storage drum, and water circulating pump. The refrigeration unit was a Copeland Model E75C. Freon 12 refigerant was expanded into a copper coil immersed

in a 30-gallon water reservoir. This reservoir was constructed from a 30-gallon barrel which was coated internally with a polyester resin to prevent rusting. Fiber glass insulation was provided around the drum. Water was circulated continuously with a small Eastern pump through the coolers and back to the drum through 3/8-inch i.d. by 9/16-inch o.d. Tygon tubing.

Other than the high pressure cell itself, which was constructed on 1/4-inch thick cold-rolled steel, additional safety features were provided. A 4-ft. by 7½-ft. blast mat, woven to a thickness of three inches from 1-inch diameter Manila rope, was used to cover the cell access door during periods of operation. Further, a spray nozzle was installed over the equipment in the cell with remote operation of a solenoid valve in a water line provided for activation in case of fire. All relief valves, rupture discs, and vents were connected to a common vent line which extended outside the building. A 1725 r.p.m. exhaust fan located in the cell and driven by a 1/4-h.p. explosion-proof motor, prevented accumulation of explosive mixtures resulting from a leak.

At shut-down and start-up the system was evacuated with a Cenco-Pressovac No. 4 vacuum pump. The vacuum pump exhaust was also vented outside the building. A bottle of high pressure nitrogen connected to the cyclopropane pump discharge provided a means for inert gas purging at start-up and shut-down. At this same connection, compressed air from

standard high pressure cylinders could be admitted for de-coking when required.

CHAPTER V

EXPERIMENTAL PROCEDURE

Discussion in this section is divided among six pertinent subtitles: preliminary procedures, startup procedure, run procedure, shutdown procedure, calibrations and measurement of variables, and difficulties encountered. Details of the analytical procedure are presented in Chapter VI.

Preliminary Procedures

Owing to the expense of cyclopropane, a number of preliminary runs were made using technical-grade normal propane as charge material. Out of these "dry" runs evolved workable startup, run, and shutdown procedures which are described in subsequent sections. Another useful function of these preliminary runs was the establishment of approximate controller set points for the various levels of temperature and pressure anticipated in the isomerization runs. At each operating temperature, a propane fuel rate was found which would supply the basic heat requirement for the fluidized sand heater. Simultaneously, the Bayley temperature controller coarse and fine pot settings were obtained to give the desired reactor temperature and corresponding supply of

trim heat. In a like manner, Powerstat settings for the basic heat duty of the preheater salt bath were determined at each anticipated temperature of operation, while the Fenwal thermoswitch was adjusted to give the trim heat requirement for temperature control.

The preliminary runs, with normal propane as feed, were most useful in finding the conditions under which uniform pumping with the Hills-McCanna charge pump could be assured. It was found that cooling the feed with 35°F. chilled water at the pump suction was not sufficient to prevent cavitation. A combination of suction chilling and storage drum pressurization with nitrogen did prove to be adequate, however. Nitrogen was supplied through a pressure regulator to give storage drum pressures which were 70 to 100 p.s.i. in excess of the liquid vapor pressure. Since extremely low pumping rates were not required, standard double-cone check valves, for both suction and discharge, were found to be satisfactory when used in conjunction with a special rod packing consisting of cylindrical rings of compressed Teflon flakes supported between rings of solid Teflon. With this packing, leakage could be prevented with only moderate pressure being applied with the packing gland nut. Thus, very little heat was released owing to friction between the rod and packing and spalling of packing into the cylinder and valves was minimized.

To assure that the cyclopropane feed in storage was

essentially free of contact with oxygen, the cyclopropane storage drum was evacuated and purged with cyclopropane vapor three times before transferring the liquid from the shipping cylinder.

Startup Procedure

The most time consuming element in the process of bringing the unit up to operating conditions was warmup of the fluidized sand heater. Though warmup of the preheater salt bath from the solidified state was also time consuming, usually enough heat was constantly maintained on the bath to assure that it remained in the liquid state. Thus, warmup of the preheater to the selected operating temperature was not a bottleneck.

Because from 5 to 7 hours were required to bring the reactor fluidized sand heating system to equilibrium at the selected run temperature, the first step in the startup procedure involved initiation of air flow through the fluidized sand heater, followed by burner ignition. When igniting the burner with the spark ignitor, the air rate was held at 8 std. cu.ft./min. and the propane fuel supply adjusted to a rate of approximately 0.3 lb./hr., corresponding to a reading of 2.5 at the location of the rotameter Pyrex float. These conditions for ignition were found to be satisfactory through experimentation. Circuit diagrams for the burner ignitor and the BASO safety devise are included in Appendix E. Power supply to the ignitor was furnished in each instance, for the

short time required, through jumper cables from the chromatograph 12-volt battery. The start button activates a solenoid valve which permits gas to flow to the burner during the lighting process. This button must be suppressed for a period of approximately 30 seconds after ignition until the BASO solenoid is activated by the burner thermocouple.

After burner ignition, the air rate and propane fuel rate were increased simultaneously to 10 std. cu. ft./min. and 0.675 lb./hr., respectively. These conditions were maintained until the bath thermocouples indicated a temperature of 400°F. At that time, a 65-pound charge of Wilcox sand was added above the grid plate through the temperature probe connection located in the disengaging section. Once the sand was added, the air rate was then increased to the normal operating level of 16 std. cu. ft./min. and the burner fired at a maximum propane fuel rate of 1.5 lb./hr. (11.0 reading on the Pyrex float). Fuel to the burner was supplied at the maximum rate until the chosen run temperature was reached, then the firing rate was reduced to a base load which permitted control of the sand bath temperature by the intermittent supply of trim heat from the Bayley temperature controller.

During the preheater and reactor bath warmup period all other preparatory operations were easily accomplished. First, the chilled water refrigeration unit was started and set for control of water temperature at 35°F., then the chilled water circulating pump was put into operation supply-

ing water to the charge pump suction chiller and the product gas cooler. The preheater air-powered mixer was also placed in service.

Next, the entire system was evacuated through the vacuum pump connection at the outlet of the knock-out pot. During this operation, the cyclopropane storage drum suction and recycle valves were closed, as were the bypass and block valves at the product gas flow indicator. The reactor bypass valve was closed and the pressure control valve bypass valve was opened. All other valves within the system remained open during evacuation. Cyclopropane pump packing was maintained sufficiently tight to prevent inleakage of air. After the first evacuation, the system was purged with nitrogen until atmospheric pressure was reached with the vacuum pump continuing in operation. Nitrogen flow was then discontinued and the system again evacuated. This procedure was repeated twice-more before closing the two pump feed valves. Following this isolation of the feed pumping system from the preheater and reactor sections, the cyclopropane storage drum suction and recycle valves were opened, thus allowing liquid cyclopropane to equalize into the evacuated pump circuit. The rod packing was then loosened and the pump started. Recycling operation was continued as long as required for the adjustment of packing, chilling of the suction piping and pump cylinders, and observation of pumping consistency.

After putting the charge pump into recycle operation,

the vacuum pump was shutdown and the balance of the system pressurized to 10 p.s.i. with nitrogen. Then the pressure control valve bypass was closed and the product gas flow indicator block valves were opened, thus permitting the product gas section to reach atmospheric pressure while purging the saturator and wet test meter with nitrogen. A low flow rate of nitrogen was then passed through the system to allow putting the pressure control valve into operation at 200 p.s.i. Nitrogen flow was then discontinued and a pressure of 200 p.s.i. maintained on the system until temperature control on the preheater and reactor had been established for acceptance of charge.

After pressurizing the preheater and reactor sections, the nitrogen cylinder was disconnected, provided with a pressure regulator, and connected through a section of 1/8-inch stainless steel tubing to the top of the cyclopropane storage drum. Then the regulator was adjusted to maintain approximately 175 p.s.i. on the drum. This maintenance of nitrogen pressure was continued throughout the run.

The chromatograph warmup was started approximately three hours in advance of the expected time for start of runs. Near the end of the reactor warmup period, standard samples were analyzed to assure satisfactory operation of the chromatograph before run samples were available. Details of the chromatograph operation are given in Chapter VI.

Run Procedure

When temperature control was established on both the preheater salt bath and the reactor fluidized sand heater, cyclopropane recycling was discontinued and charge was directed to the preheater and reactor section. Usually only one cylinder of the pump was used. The inactive cylinder remained lined-up for recycle operation, but with the suction valve closed. Switching from recycling to charging operation on the active cylinder involved closing the recycle valve and opening the feed valve, simultaneously, on that particular cylinder by means of extension handles provided through the cell wall. The desired pumping rate was obtained by adjusting the length of stroke prior to the start of recycle operation.

After the start of cyclopropane flow, approximately 30 minutes were required to achieve steady-state operation at the chosen operating pressure. The approach to steady-state operation could be followed quite clearly from the recorded preheater and reactor outlet temperatures. When these temperatures ceased to increase, steady-state was assumed to exist. In all cases this condition was confirmed by subsequent chromatograph analyses.

Each time the unit was brought on stream it was for one temperature of operation only. Because of the large heat capacity of both the preheater and the fluidized sand heater, several hours were required to change from one temperature

level to another. In most cases only one pump stroke setting was used each time, though in some instances a change in pumping rate was made while operating. Reactor pressure was the variable most easily changed during any run period. Usually data were obtained at five pressure levels: 250, 500, 1000, 1500 and 2000 p.s.i. Hence, for each day of operation, five data points were obtained provided difficulties were not encountered. At each pressure level, data were recorded for five observation periods, usually five minutes in length, but subject to change depending upon the pumping rate and level of cyclopropane in the storage drum. Normally, cyclopropane was pumped from the level glass connection. At the start of each observation period, the cyclopropane level was recorded and the level glass then instantly isolated from the bottom of the storage drum by rapid action of a 1/4-turn, Worcester ball valve. The start of each observation period was always simultaneous with a zero reading on the wet test meter dial. At the close of each observation period, the final cyclopropane level and the cumulative wet gas volume were recorded, then the Worcester ball valve was again opened. During each observation period a 2 cu. cm. sample of product gas was transferred by syringe from the product gas sample septum to the septum at the inlet of the chromatograph column. Thus for each observation period a product analysis was obtained, thereby providing a total of five separate analyses at each pressure level. Temperature of the fluidized

bed was also measured during each observation period with the millivolt potentiometer. Other pertinent data were recorded for each pressure of operation; such as, barometric pressure, cyclopropane storage drum temperature and wet test meter temperature. A sample run data sheet has been included in Appendix I. In addition to the data mentioned, seven temperatures were continuously monitored by the Leeds-Northrup Micromox recording potentiometer. These temperatures were for three locations in the fluidized bed, two locations in the preheater salt bath, and one each for thermocouples located at both the preheater and reactor outlets.

Samples of gas at the reactor inlet were obtained by either one of two methods. In the first method samples were withdrawn, at the close of each run at a given pressure, by throttling with a sample valve, through a cooler, and thence through a septum connection located outside the cell. One disadvantage of this procedure was the difficulty in withdrawing the sample at a rate sufficiently low so that flow through the reactor was not interrupted. On at least two occasions, it is believed that this technique of sampling caused partial plugging in the 1/8-inch tubing at the outlet of the reactor, owing to polymer formation arising from excessive residence time. With Run IX-2 through XIII-4 an entirely different procedure was used to find the reactor inlet composition. This procedure was as follows: Upon completion of a series of runs at various pressures, the charge

pump was switched to recycle operation, then the system was depressurized, evacuated, purged with nitrogen, and evacuated again. The reactor was then isolated under a vacuum by closing the inlet and outlet block valves. This operation was followed by opening the reactor bypass and pressurizing the system with nitrogen as is done during normal startup. Feed was then switched through the preheater, with pressure controlled as usual, but with the reactor bypassed. The preheater temperature was maintained at the same level as during previous runs, and the various pressure levels of operation were rapidly reproduced. At each pressure level, samples were withdrawn at the normal product sample connection and analyzed as usual.

At the end of each run at a given pressure liquid product, if present, was withdrawn from the knock-out pot drain.

During periods of operation, the blast mat was down and the cell entered only for occasional checks for pump packing leakage by soap test.

Shutdown Procedure

As the first step in the shutdown process, the feed valve of the active pump cylinder was closed, followed by immediate opening of the recycle valve. The pump was then stopped and the suction valve of the active cylinder closed. The system was then rapidly depressurized through the pressure control valve bypass, or by opening the emergency vent.

After gas ceased to flow through the wet test meter, the block valves at the flow indicator were closed and evacuation of the system begun. During evacuation, the nitrogen for cyclopropane storage pressurization was disconnected and then reconnected to the preheater and reactor section for purging. Also during evacuation, fuel to the fluidized sand heater was shutoff and power supply to the preheater reduced. Air supply to the fluidized bed was continued at the normal rate in order to cool the sand in preparation for later withdrawal from the unit.

The same evacuation and purge procedures used at startup were repeated on shutdown. Upon completion of the last evacuation, the vacuum pump was shutdown and the system pressurized to 10 p.s.i. with nitrogen. The flow indicator block valves were then opened to permit flow of nitrogen through the saturator and wet test meter. A strong flow of nitrogen through the system was maintained for approximately five minutes. During this period, any remaining liquid in the knock-out pot was thoroughly drained. Nitrogen flow was then discontinued and the system blocked-in under approximately 10 p.s.i. nitrogen pressure.

Air flow to the fluidized bed was continued until it was cooled to 400°F. This operation requires approximately 2 hours. Once the air flow was stopped, the valve on the sand trap-out pan was opened and sand flowing through the grid was collected in a metal container.

Calibrations and Measurement of Variables

Temperature of the fluidized sand bath, in which the reactor coil was immersed, was measured with three chromel-alumel thermocouples, each at a different location. All three temperatures were monitored continuously with the Leeds-Northrup Micromox recorder. Precise temperature measurements were made using the thermocouple located in the deeply immersed well at the center of the bed. Output from this thermocouple, in addition to being received by the recorder, was also measuring with either a Leeds-Northrup Model 8662 or Model 8686 millivolt potentiometer. The latter, slightly more accurate instrument, $\pm$(0.03% of reading + 3 micro-volts), was used when it became available, starting with Run VII-1. The thermocouple lead wires were also of chromel-alumel, hence the temperature of interest for reference junction compensation was that at the terminals of the potentiometer. This temperature was measured by a mercury thermometer with bulb located between the two terminals.

A calibrated platinum resistance thermometer was used to check the temperature-electromotive force relationship of the chromel-alumel couple at two temperature levels (518 and 873°F.). The method used was essentially the same as described by Scott (74, p. 137). The thermocouple was attached to the resistance thermometer by wrapping with fiber glass ribbon so that the thermocouple bead was in close proximity of the platinum resistance element. Both the thermocouple

and resistance thermometer were then inserted into a copper well already immersed in the preheater Hitec salt bath. With a transisterized d.c. power source, a low current was passed through the platinum resistance thermometer and a certified standard resistance wired in series. Reduction in potential across both the platinum resistance thermometer and the standard resistance was measured simultaneously on two Leeds-Northrup Model 8662 millivolt potentiometers. In this manner, the resistance of the platinum thermometer at the prevailing bath temperature was determined from the product of the ratio of voltage drops and the known resistance; i.e., $R_t = \frac{E_t}{E_r} \cdot R_r$, where the subscripts t and r signify thermometer and standard resistance, respectively. Once R_t was established, then the temperature was found by trial and error from the Callendar formula (a quadratic curve fit) using the known calibration constants provided by the manufacturer of the thermometer. The thermocouple e.m.f. was measured simultaneous, also on a Model 8662 millivolt potentiometer. A temperature corresponding to this measured e.m.f. was then read from the standard tables for chromel-alumel couples provided in the National Bureau of Standards Circular No. 561 and compared with that obtained from the resistance thermometer calibration. The maximum difference in these temperatures at the 873°F. level was 1.6°F., slightly in excess of that expected with the combined accuracy of the three potentiometer readings. Hence, the standard e.m.f.

tables for chromel-alumel thermocouples were used with the fluidized bed thermocouple. At the maximum reactor temperature employed, the millivolt potentiometers were capable of measuring temperature accurate to within ±0.3°F. In practically all cases it was possible to control the fluidized bed temperature within a range of ±0.5°F. during the course of a run, and in many cases the extent of fluctuation was within the range of potentiometer accuracy.

While checking the reactor thermocouple with the resistance thermometer, the preheater thermocouple at the center well was also in service in the Hitec salt bath. Its indicated temperature was in close agreement with that of the resistance thermometer (difference 0.6°F. at 873°F.).

Reactor pressure was measured with a dead-weight tested Heise gauge of Bourdon tube type with guaranteed accuracy of 0.2%. Scale divisions were 2 p.s.i. Owing to the reciprocating action of the charge pump, there were pressure fluctuations about the controller set-point. However, for practically all runs, this fluctuation was not more than ±10 p.s.i., or 2% at 500 p.s.i. and 0.5% at 2000 p.s.i. The pressure gauge connection was located 2 feet downstream from the reactor outlet, but the pressure drop correction was negligible for the pressure levels employed. In fact, total pressure drop through the system was never greater than 50 p.s.i., even when using the 1/16-inch i.d. stainless steel coil as a preheater. This pressure drop of course excludes

the few instances when partial plugging occurred as the result of polymer formation.

Measurement of the volumetric rate of cyclopropane liquid charge to the system was obtained by observing the change in level in a sight glass for a selected observation period. The sight glass of ½-inch nominal i.d. and 4-ft. length was calibrated by observing the incremental increase in liquid height upon addition of successive 10 ml. quantities of water. The calibration was found to be linear with a volume of 1.258 ml. per centimeter of length. Precision of the cyclopropane liquid measurement is a function of the pumping rate and length of the observation period. The estimated precision of measurement is one per cent when pumping 30 centimeters of liquid during a 5-minute observation period. Greater precision was not possible because of level fluctuations arising from the reciprocating action of the charge pump. Precision of product gas measurement with the wet test meter is estimated to be 0.5 per cent when 0.4 cu. ft. of wet gas are metered during an observation period.

In order to make weight balance calculations, saturated liquid densities of cyclopropane at various temperatures near ambient were required. This information has not been reported in the open literature, nor was it available from the manufacturer of the cyclopropane. Further, the critical volume of cyclopropane has not been measured; thus, estimation of the density from the generalized correlation

of Lydersen, Greenkorn and Hougen (55, p. 12) was precluded. In view of this situation, it was necessary that these densities be determined in some manner in this investigation. These densities were obtained with a continuous flow technique using the isomerization equipment itself, described as follows: the high pressure laboratory was isolated, permitting the room and cyclopropane storage drum to reach an equilibrium temperature of 74.0°F. with the aid of air conditioning. Then cyclopropane was pumped from the calibrated level glass and through the preheater, where it was vaporized, but not reacted. The reactor was bypassed and the vaporized cyclopropane allowed to pass through the control valve continuously at a pressure of 200 p.s.i. Pure cyclopropane vapor at atmospheric pressure was then allowed to flow through the product cooler and knock-out pot, and thence to the saturator and wet test meter. For a selected observation period, the total wet gas flow and volume of liquid pumped were measured. This procedure was repeated four times for check of consistency and to permit obtaining suitable average values. A similar procedure was performed without air conditioning, where room temperature and cyclopropane storage temperature were allowed to reach an equilibrium temperature of 85.7°F. Upon applying temperature, pressure and percentage moisture corrections to the wet test meter gas volume measured, the standard dry gas volume was obtained and hence the weight of gas could be calculated. The liquid

densities determined in this manner were 0.600±0.006 grams/cu.cm. at 74.0°F. and 0.594±0.006 grams/cu.cm. at 85.7°F. In most runs the cyclopropane storage drum temperature was between 74.0 and 85.7°F. and the densities were estimated assuming a linear relationship. It will be observed that the densities for saturated cyclopropane liquid are substantially higher than for either propane or propylene. Two liquid densities for cyclopropane have been reported in the literature, but both are for temperatures far removed from ambient. Trautz and Winkler (84) gave a value of 0.720 grams/cu.cm. at -79°C.,while Grosse and Linn (75) list the density at -32.7°C. (N.b.p.) as 0.6807 grams/cu.cm.

Difficulties Encountered

One of the most perplexing problems was that of obtaining a consistent cyclopropane pumping rate. Solution of this problem was discussed under the Preliminary Procedure Section. Actually the difficulty was resolved while performing propane test runs; therefore, when the isomerization runs began, good pumping consistency prevailed. Usually the maximum deviation in pumping rate for a single observation was less than 3.5 per cent of the average rate for the five observation periods of each run.

Another problem encountered on some runs was that of partial plugging in the reactor outlet tubing owing to a buildup of polymer. The method used in removing these obstructions will be discussed briefly. Since mechanical

cleaning would have been a formidable task, requiring dismantling of the reactor section and perhaps replacement of the 1/8-inch stainless steel tubing connected to the reactor, "decoking" with compressed air was tried as an alternate. This procedure proved to be extremely successful. At the start of the procedure the system was evacuated and purged with nitrogen three times, as during normal shutdown. Then the fluidized bed and preheater temperatures were held at operating level while compressed air was allowed to flow through the system at a rate permitted by the obstruction. In some cases, it was necessary to supply compressed air at a pressure of 2000 p.s.i. to obtain a significant air flow. A burning period of up to 15 minutes duration was sometimes required before "break-through" occurred. Successful removal of the obstruction was manifested in a rapid drop of inlet pressure and sudden increase in air rate through the saturator and wet test meter. This method of "decoking" is of course only successful in the case of partial plugging. Fortunately, complete plugging never occurred. It is of interest to note that during the "decoking" operation the fluidized bed of sand serves as a useful high temperature heat sink.

The recycle valves at the discharge of the cyclopropane pump, while serving a useful function, also had their disadvantages. On several occasions leakage through these valves, back to the storage drum, during a run was suspected

and later confirmed by nitrogen testing at the conclusion of the runs. Such leakage was usually the result of supplying insufficient seating pressure through the valve handle extensions. The results from those runs in which leakage was known to have occurred were, nevertheless, useful; but, obviously, weight balance checks were not permitted.

One difficulty arose during the preliminary runs with normal propane, which has not been previously discussed; viz., "freeze-up" of the pressure control valve owing to condensation of liquid upstream from it. Initially, the tubing extending from the reactor onlet to the pressure control valve was uninsulated. Under these conditions, the control valve would pass fluid only by continuously opening and closing it by manual adjustment of the diaphragm air pressure. Insulation alone was not sufficient to prevent the difficulty. The problem was finally solved by applying heat to the transfer line with a heating coil wrapped around it and embedded between two layers of insulation. The coil was constructed from 20 feet of 24-gauge Nichrome wire and supplied with electrical power from a Variac variable voltage transformer.

Another difficulty encountered during the preliminary tests with normal propane was leakage at the preheater Kuentzel bomb closures. On one occasion this leakage resulted in a fire which, however, was readily extinguished with the emergency sprays. The system was immediately depressurized through the emergency vent, and no damage was incurred as a

result of the fire. Leakage at the closures was attributed to a combination of thermal shock and loss of elastic action in the gold-plated copper gaskets. The copper gaskets were therefore replaced with gaskets made of annealed Type 316 stainless steel. After the preliminary runs, the startup procedure was modified to minimize the initial shock on admitting feed to the unit. Whereas, initially the system was evacuated at the time of starting feed through the unit, later, the procedure was altered so that the system would be pressured to 200 p.s.i. with nitrogen at the time of feed addition, as previously described in the startup procedure.

CHAPTER VI

ANALYTICAL PROCEDURE AND APPARATUS

The cyclopropane-propylene mixtures of this investigation were analyzed through use of gas-liquid partition chromatography. This method of analysis was selected after a review of the merits of all previously used analytical procedures. Owing to the past interest in the quasi-unimolecular behavior of cyclopropane isomerization at low pressures (subatmospheric), a large number of analytical schemes has evolved.

Previous Methods of Analysis

In the first study of the thermal conversion of cyclopropane to propylene, Trautz and Winkler (84) employed the purely physical measurement of reaction product liquid specific volume as a means of detecting the extent of conversion. They observed that at -80°C. the liquid volumes of cyclopropane and propylene are essentially additive. This method was not used by later investigators, primarily because of the large amount of sample required. Trautz and Winkler conducted their experiments in a flow system, where the required amount of sample could be made available, but most subsequent

investigations were performed with batch apparatus.

Since the Trautz and Winkler study (1922), analytical procedures have progressed through a variety of chemical methods only to return to physical tests of a more sophisticated nature; viz., infrared spectrophotometry and gas chromotography. The chemical methods have been based, for the most part, on the selective absorption of propylene by various solvents. Chambers and Kistiakowsky (9), in analyzing their batch isomerization results, found a 3 per cent aqueous neutral solution of potassium permanganate suitable for quantitative absorption of propylene without attack of cyclopropane. They were able to show that previous reported failures of the method could be attributed to the neglect of physical absorption. Chambers and Kistiakowsky considered their method of analysis to be more accurate than the low temperature density method of Trautz and Winkler and reported the average deviation from the mean for duplicate experiments to be 0.1 cu. cm. for every 10 cu. cm. of gas absorbed.

The selective chemical absorption of propylene from cyclopropane-propylene mixtures has been reported by other investigators using different solutions. Ipatieff (34) reports the results of propylene absorption in both 2 per cent potassium permanganate and bromine solutions. In more recent wet chemical methods, Pritchard, Sowden and Trotman-Dickenson (66) have employed mixtures of mercuric acetate and mercuric nitrate, while Weston (92) absorbed propylene in a saturated

solution of mercuric sulfate in 22 per cent sulfuric acid. In the latter, a precision (mean error) of 2 per cent was reported for 10 micro-mole samples of 50-50 mixtures, with accuracy slightly less than the precision and declining with departure from equimolar mixture.

In a study which followed that of Chambers and Kistiakowsky, Corner and Pease (12) in 1945 introduced a method of selective catalytic hydrogenation for analysis of cyclopropane-propylene mixtures. In this method the sample to be analyzed, along with hydrogen, is passed, first, over a mercury-poisoned nickel catalyst which converts the propylene only to propane, then, in sequence, the cyclopropane is hydrogenated over an unpoisoned nickel catalyst. The principle objection raised by Corner and Pease to the 3 per cent potassium permanganate method of Chambers and Kistiakowsky was that since only propylene content was measured, and cyclopropane was determined by difference, then no account could be made of possible propylene polymerization or decomposition. Corner and Pease report known samples were analyzed to within ± 0.5 per cent. Selective catalytic hydrogenation of cyclopropane-propylene mixtures apparently did not find favor with later investigators.

In the past decade chemical analyses in general have been revolutionized by the introduction of such analytical techniques as infrared spectrophotometry and chromatography. The analysis of cyclopropane-propylene mixtures is no excep-

tion. In fact, in all of the more recent investigations, only these methods have been used, with gas chromatography being more prevalent. Infrared spectrophotometry has been used in at least two studies. Lindquist and Rollefson (53) in 1956 reported infrared calibrations for cyclopropane-propylene mixtures with an average deviation of 0.5 per cent. Roberts (71) in 1959 also used infrared spectrophotometry in the analysis of products from the catalytic isomerization of cyclopropane. Gas chromatography was reported by Blade (6) in 1961 for the separation of cyclopropane-propylene mixtures. A 15 ft. column of dodecyl phthalate at room temperature was employed, with Hydrogen as the carrier gas. In the same month, in another journal, Falconer, Hunter and Trotman-Dickenson (19) describe a chromatographic analysis in which the sample and carrier gas (carbon dioxide) are first passed over a 1 ft. column of activated alumina and then over 3 ft. of firebrick with 20 per cent of ethylene glycol saturated with silver nitrate, elution being observed with a Janak nitrometer detector. In 1963, Kennedy and Pritchard (39) reported a chromatographic method of analysis in which a 4 ft. column of 20 per cent molar $AgNo_3$/glycol on firebrick was operated at -30°C. in conjunction with a Pye Argon detection system. In the most recently reported study of cyclopropane isomerization (February, 1964), Davis and Scott (14) state that the reaction products were analyzed by gas chromatography, but details of the apparatus are not given.

Several solvents are available for resolution of cyclopropane-propylene mixtures. In addition to those solvents already mentioned, Knox (42) has reported the utility of a column, containing alumina poisoned with a few per cent of squalane, for C_3 mixtures and acetylene at room temperature. From the tabulation of most widely used solvents by Purnell (67), tricresyl phosphate is expected to be suitable, as it has proven to be useful in the separation of olefins and paraffins.

Principles of Chromatographic Analysis

If one sought to apply the chromatographic method as an analytical tool on the basis of theory alone, complexity would vitiate the utility of the method. Fortunately, as an empirical tool, it is extremely useful because of recent advances in detection systems.

Chromatography is a broad topic, involving many methods. Consequently, only the principles of the specific type of chromatography used in this investigation will be discussed; i.e., elution chromatography with gas-liquid partitioning. Essentially, the method involves the dynamic and selective absorption and desorption of components from a gas sample injected instantaneously into an inert gas stream which passes continuously through a column containing a liquid solvent supported on porous solid packing. Owing to the difference in affinity which the liquid solvent has for the various components of the injected sample (i.e., difference in partition

coefficients), it first absorbs some components more readily than others, but later desorbs these same components less freely. As a result of the selective absorption-desorption process, some components tend to remain absorbed in the solvent liquid for longer periods of time than others; i.e., their retention times are greater. This process brings about a resolution of the components and they are eluted from column by the carrier gas in inverse order of affinity.

The resolved components appear as separate bands in the carrier gas stream. These bands may be detected by various means (e.g., by color, whence came the name chromatography). The concentration profile of the resolved component within a band ideally follows a Gaussian error curve (42). Thus, where instantaneous concentration detection systems are employed, the recorded values will appear in characteristic shapes called peaks. The area of these peaks are a measure of the amount of each component resolved.

Katharometers are the most widely used detectors. These instruments (also called thermal conductivity cells) are capable of detecting the concentration of resolved components in the carrier gas by the change which occurs in thermal conductivity. This change in thermal conductivity is sensed by a pair of matched, electrically heated resistors. One resistor is exposed to the pure carrier gas and the other to the carrier gas containing the eluted components. The resistor in the stream with the higher thermal conductivity

will assume a lower equilibrium temperature for the same current flow, hence the resistance of the two will no longer be the same. It is customary to use the matched resistors as two elements of a wheatstone bridge. The change in resistance causes an unbalanced condition which is detected and recorded.

Katharometers are not excelled as detectors where moderate sensitivity is required, and according to Knox (42), "---they are the standard against which any other detector is assessed." Flame temperature detectors and gas density balances have sensitivities comparable to the katharometer, but lack the katharometer simplicity. When high sensitivities are required for the measurement of very low concentrations, usually flame ionization or argon ionization detectors are used.

Chromatograph Equipment Description

The chromatograph used in this investigation is a modified version of the home-made apparatus previously described by Perkins (58). Figure 9 is a photograph of the equipment as it was installed for the present study. A schematic diagram of the apparatus is shown in Figure 10. There are essentially four main functional categories of equipment involved: (1) carrier gas supply, control and flow measurement equipment, (2) a thermostated packed column, (3) a thermostated detector, associated electrical circuitry, and recorder, and (4) a sample injection system. Details of the

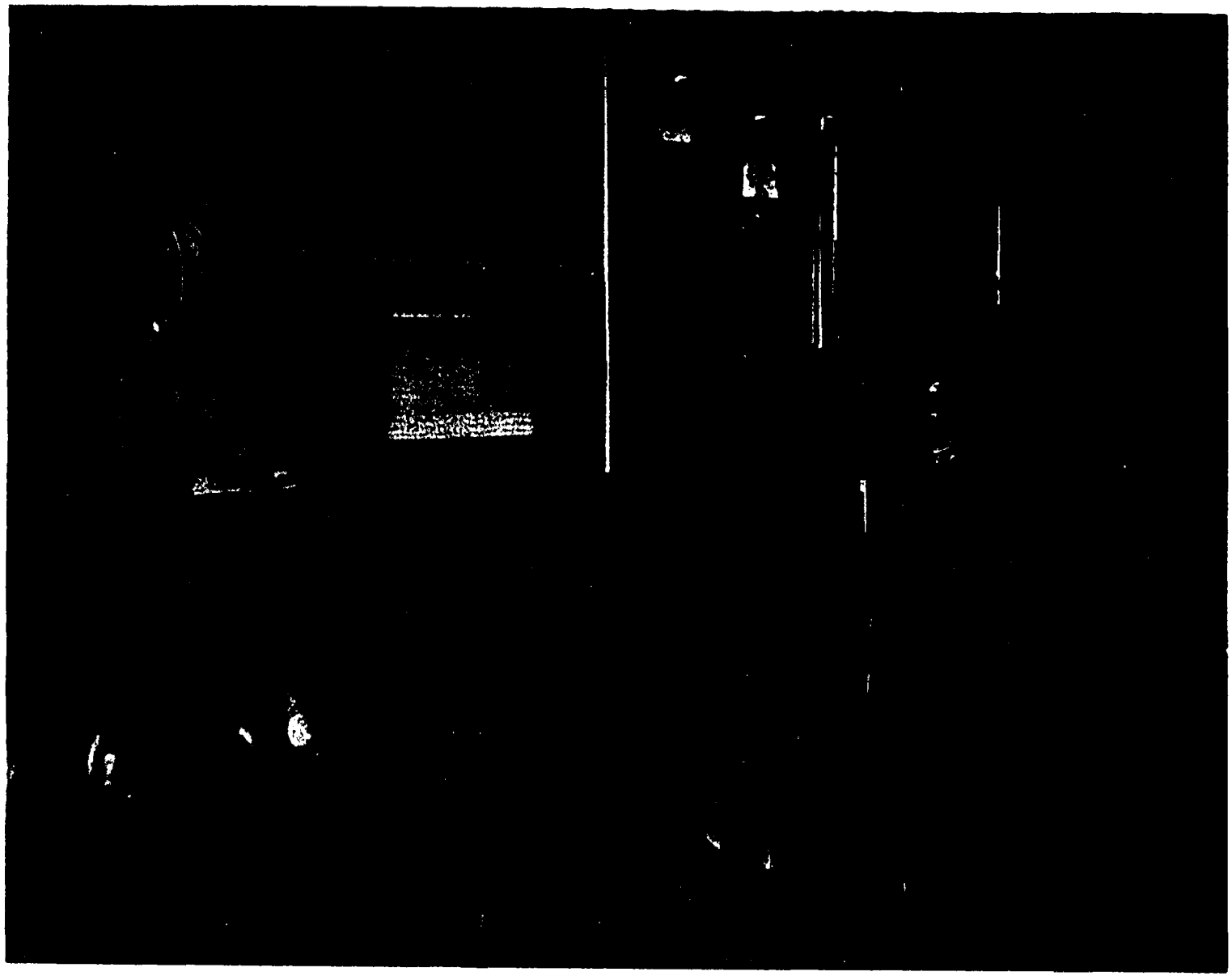

Figure 9 - Photograph of Chromatograph

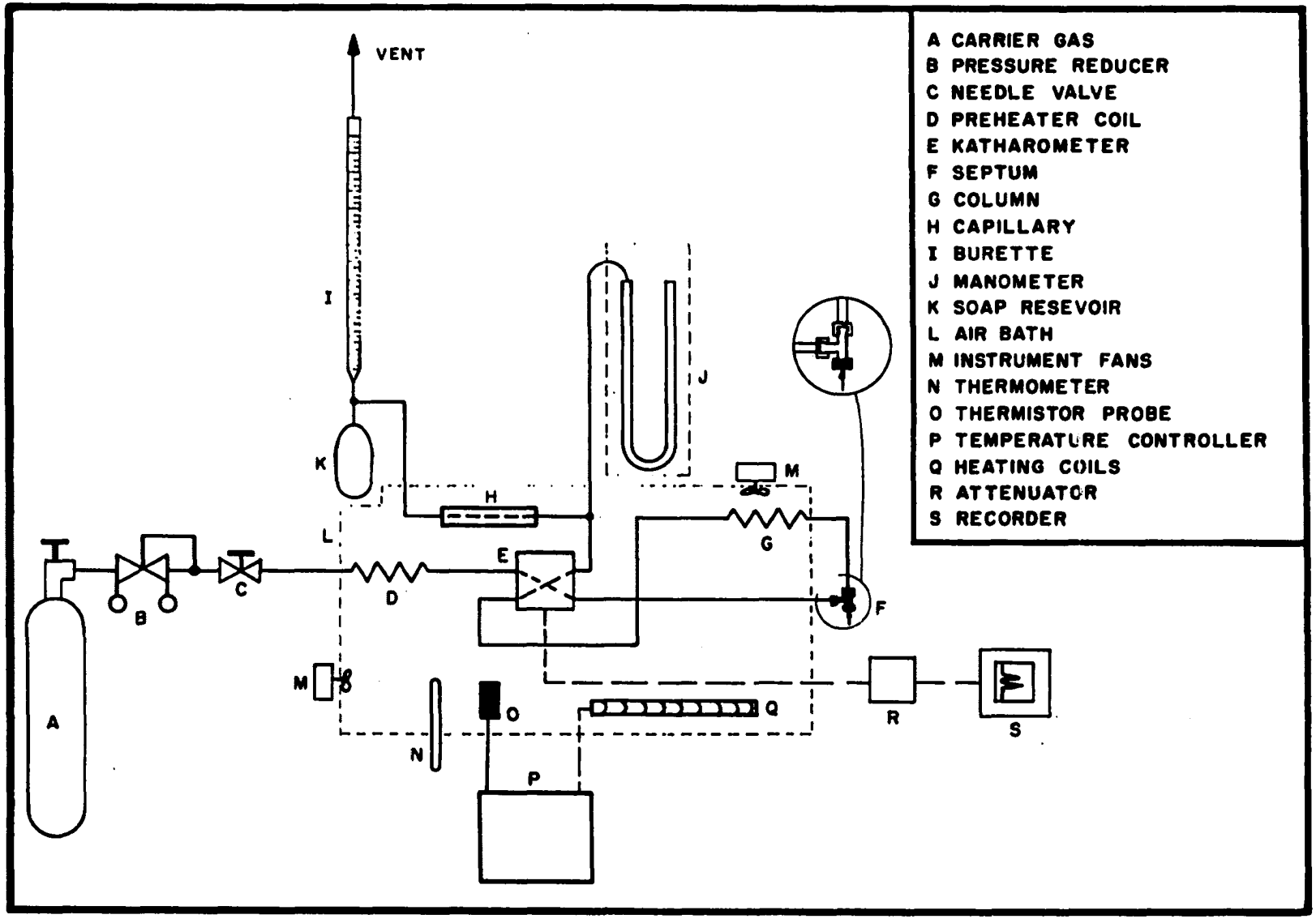

GAS CHROMATOGRAPHY SCHEMATIC DIAGRAM

Figure 10

equipment in each category are given in the paragraphs which follow:

Carrier gas was supplied from a standard ICC high pressure shipping cylinder of 220 std.cu.ft. capacity (standard conditions 70°F. and atmospheric pressure). Essentially pure helium (99.99+% minimum purity) was used as carrier gas. A Hoke-Phoenix pressure reducer was used to regulate the helium flow from a variable storage drum pressure to a constant upstream pressure at a needle valve. Helium flow rate was controlled by adjustment of the needle valve. Two methods were used for measurement of carrier gas flow: (1) a soap bubble flow meter and (2) a capillary differential flow meter. In the first method, the carrier gas flow was determined absolutely by the extremely simple procedure of measuring the time require for a soap film to progress from the bottom to the top of a 50 ml. burette. An accuracy of 0.1 per cent can be obtained with this method (67). The second method was used to provide instantaneous indications of flow rate, whereby any gross changes in flow rate occurring at intervals between soap bubble meter readings could be observed. The capillary was of annular type, constructed from 2½ inches of pipette glass tubing, with inside bore of 0.1 cm. diameter, through which a piece of 20 gauge (A.W.G.) Nichrome wire was inserted. Capillary differential was measured with a manometer which permitted a maximum head of 15 inches of water.

The column used for the chromatographic resolution

of the cyclopropane-propylene mixtures was prepared by packing a 20-ft. length of standard 1/4-inch aluminum tubing with 42/60 mesh firebrick, containing 10 per cent by weight tricresyl phosphate as substrate. The coiled column, as well as the carrier gas preheater, thermistor detector and capillary flow meter were enclosed in an insulated air bath provided with two instrument fans for air circulation. A Sargent, Model S, "Thermonitor" was used to control bath temperature. This instrument is a thermistor actuated controller, of proportional power output type, from which power was supplied to a pair of heaters capable of 250 and 300 watt output. This controller is capable of maintaining temperature control within $\pm$0.01°C. of a chosen set-point, in those cases where the system thermal capacitance and resistance are negligible. For the particular construction of the air bath used in this work, it was possible to hold the temperature at 143.0°F. within 1.0°F. Both Knox (42) and Purnell (67) state that temperature control within a range of 1°C. is satisfactory in most cases with katharometer detectors. The adequacy of the temperature control in this work was confirmed by the absence of temperature cycling of the recorder base line at the attenuations required for most of the sample analyses.

The chromograph detector was a Gow-Mac katharometer of the thermistor type. A matched pair of 8000-ohm resistors, one each mounted in the carrier gas and column effluent chan-

nels of a stainless steel block, provided the sensing elements of a wheatstone bridge with which changes in thermal conductivity, and hence concentration could be detected. An attenuator was used to convert the unbalanced cell current into a millivolt signal acceptable to the recorder. The recorder was a Bristol's Dynamaster d.c. millivolt unit, Model 1PH 560-51-T46-T66X-T71, with 0.0 to 1.0 mv. range and chart speed of 1 inch per minute. The detector electrical circuit diagram (Figure 34) is included in Appendix A.

The method of sample injection was extremely simple. Samples of gas were displaced from a 2 ml. syringe, through a 1½-inch long, 24-gauge needle which was inserted through a rubber septum located in a standard 1/4-inch tubing tee at the column inlet.

Chromatograph Operation and Calibration

Before each cyclopropane isomerization run, the chromatograph was adjusted to a set of steady-state conditions within the range of those previously used for the preparation of calibration curves. The standard conditions for calibration and their maximum range were:

	Mean	Max. Range
Helium Flow Rate (std.cu.ft./min.)	48.5	± 1.5
Air Bath Temperature (°F.)	143.0	± 1.0
Cell Current (milliamps)	10.05	± 0.05

With these operating conditions, and particular chromatograph construction, the average elapse times from injection to elution, using the 20-ft. column of TCP on firebrick, were

3.02 and 3.36 minutes for propylene and cyclopropane, respectively. A sample analysis could be completed in less than five minutes. Samples were transferred directly from the product gas stream septum to the injection point septum with a 2 cu.cm. syringe.

Seven propylene-cyclopropane mixtures were prepared for chromatograph calibration. The propylene used was Phillips Petroleum Company research grade material with 99.99 mol per cent minimum purity. Anesthetic grade cyclopropane of 99.5 mol per cent minimum purity was obtained from Ohio Chemical and Surgical Equipment Company. A chromatographic analysis of this material indicated impurities to be less than the 0.5 mol per cent reported. The propylene content was approximately 0.09 mol per cent. Gas mixing was accomplished in 500 cu. in. stainless steel bombs, connected by manifold to a vacuum pump and the two gas supplies. A triple evacuation and purge procedure assured essentially complete air removal. The desired mixture composition was obtained in each case by adding cyclopropane and propylene, in sequence, to give predetermined differentials on a mercury manometer, with absolute sample bomb pressure being found by adding to, or subtracting from, atmospheric pressure the manometer reading, depending on whether the differential was positive or negative. The accuracy of the calculated standard composition depends on the precision of the manometer readings. The estimated maximum relative error is only $\pm$ 3 per

cent for the lowest sample composition percentage and is less, of course, for all other compositions.

The calibration curve determined upon analysis of the seven standard samples is given in Figure 32 of Appendix A. Each data point shown on the calibration curve is the arithmetic mean of the results obtained for at least five chromatographic analyses of the particular standard sample. From Figure 32 it will be observed that composition percentage has been correlated versus peak height ratio. This procedure was used for two reasons: first, owing to the sharpness and symmetry of the peaks, less error is involved in the measurement of peak height than in area and, second, the ratio of peak heights is insensitive to small variations in carrier gas flow rate and sample size. From Appendix A it is seen that, for a single analysis, Figure 32 may be used with 95 per cent confidence, that the relative error will not exceed from $\pm$0.80 to $\pm$2.57 per cent, depending upon the composition level. With duplicate and triplicate samples, the error is further reduced. For example, at the 63.25 per cent cyclopropane composition level, with two analyses the relative error is $\pm$1.0 per cent, compared with $\pm$1.23 per cent for a single analysis and $\pm$0.73 per cent for analyses in triplicate. According to both Purnell (67) and Knox (42) it is difficult to achieve accuracies with a range less than $\pm$1.0 per cent, even with the best chromatograph design.

Five product samples were analyzed for each run of

this study. Thus, the precision in the measurement of composition with the chromatograph can be expected to be better than the estimated accuracy in the preparation of standard samples.

A typical chromatogram is shown in Figure 33 of Appendix A.

CHAPTER VII

METHOD OF DATA ANALYSIS

In this investigation integral rate data were obtained with conditions which, in most instances, permitted the assumption of isothermal behavior and plug-flow. These conditions, and the fact that the reaction occurs in a simple binary mixture with essentially constant molar density (except under extreme conditions when polymerization takes place), greatly simplify the kinetic analysis.

Development of Expression for Calculation of k_c from Experimental Data

An expression for the first-order specific rate constant k_c, defined in terms of concentration, can be obtained either through simplification of the general continuity equation or by starting with a conservation of species balance, for a differential element of reactor volume, in which all of the appropriate assumptions are made. The first method is used in the present derivation. In a subsequent development, in which the deviation from isothermal behavior is explored, the latter method is employed to permit comparison of the two methods of derivation.

The general equation of continuity for component A in a reacting binary mixture is (5a, p. 557)

$$\frac{\partial C_A}{\partial t} + \nabla \cdot C_A v^* = \nabla \cdot C\, D_{AB} \nabla y_A - r_A \qquad \text{VII-1}$$

In Equation VII-1, where subscript A is chosen to represent cyclopropane, r_A signifies the molar rate of cyclopropane transformation per unit volume, consistent with Equation II-2. When the mixture molar density C and the binary diffusion coefficient D_{AB} remain constant, Equation VII-1 becomes

$$\frac{\partial C_A}{\partial t} + C_A \nabla \cdot v^* + v^* \cdot \nabla C_A = D_{AB} \nabla^2 C_A - r_A \qquad \text{VII-2}$$

Further, since the isomerization of cyclopropane involves no change in the number of moles present, the divergence of the molar average velocity v* is zero; and because there is no change in molecular weight, the molar average velocity v* is equal to the mass average velocity v. Thus, the continuity equation becomes

$$\frac{\partial C_A}{\partial t} + v \cdot \nabla C_A = D_{AB} \nabla^2 C_A - r_A \qquad \text{VII-3}$$

For axial symmetric flow in a tubular reactor, the appropriate form of Equation VII-3 in terms of cylindrical coordinates is

$$\frac{\partial C_A}{\partial t} + \left[v_r \frac{\partial C_A}{\partial r} + v_z \frac{\partial C_A}{\partial z} \right] = D_{AB} \left[\frac{1}{r} \frac{\partial}{\partial r} \left(r \frac{\partial C_A}{\partial r} \right) + \frac{\partial^2 C_A}{\partial z^2} \right] - r_A \qquad \text{VII-4}$$

In the case of fully-developed, steady-state, laminar flow with negligible axial diffusion, Equation VII-4 transforms to

$$v_o\left[1 - \frac{r^2}{R^2}\right]\frac{\partial C_A}{\partial z} = D_{AB}\left[\frac{\partial^2 C_A}{\partial r^2} + \frac{1}{r}\frac{\partial C_A}{\partial r}\right] - r_A \qquad \text{VII-5}$$

From Equation VII-5 one can obtain the dimensionless partial differential equation (D-1) of Appendix D which was solved by Cleland and Wilhelm (11). In Appendix D it is shown that the criterion for plug-flow established by Cleland and Wilhelm is satisfied by the experimental runs of this study. When the plug-flow assumption is applicable, and when axial diffusion is negligible (as is also shown to be true in Appendix D), Equation VII-4 reduces to the simple result

$$\langle v\rangle\frac{dC_A}{dz} = -r_A \qquad \text{VII-6}$$

where $\langle v\rangle$ is the average velocity over the reactor cross-section. The velocity $\langle v\rangle$ can be expressed as

$$\langle v\rangle = \frac{F_o}{A_{cs}C} = \frac{Z_m RTF_o}{A_{cs}P} \qquad \text{VII-7}$$

where F_o is molar flow rate of feed to the reactor and A_{cs} is the reactor cross-sectional area. With this equation for $\langle v\rangle$ and the first-order rate expression, $r_A = k_c C_A$, Equation VII-6 is converted to a form convenient for integration; i.e.,

$$\frac{Z_m RTF_o}{A_{cs}P} \cdot \frac{dy_A}{y_A} = -k_c dz \qquad \text{VII-8}$$

With ideal solution behavior, the expression for the mixture compressibility factor is $Z_m = Z_A y_A - Z_B(1-y_A)$. Upon substitution of this value for Z_m in Equation VII-8 and integrating, one obtains the following explicit result for k_c

$$k_c = \frac{RTF_o}{V_R P}\left[(Z_A - Z_B)\{(y_A)_I - (y_A)_o\} + Z_B \ln\frac{(y_A)_I}{(y_A)_o}\right] \qquad \text{VII-9}$$

in which V_R is the reactor volume. Since the compressibility factors for cyclopropane and propylene are not widely different, and in no instance deviating more than 10 per cent from unity with the temperatures and pressures prevailing in the experimental runs, one can calculate the first-order rate constant without significant error (less than 0.2% from a number of calculations) by using the simplified expression

$$k_c = (Z_m)\frac{RTF_o}{V_R P} \ln \frac{(y_A)_I}{(y_A)_o} \qquad \text{VII-10}$$

where (Z_m) is an average compressibility factor determined from pseudo-critical properties calculated by Kay's rule at the arithmetic average composition of the reaction mixture. Equation VII-10 is obtained by integrating Equation VII-8 with the constant (Z_m) value substituted for Z_m. This method of calculation has two advantage: (1) only one reading from a compressibility chart is required and, (2) the error involved in subtracting two compressibility factors which are of essentially the same magnitude is avoided. All k_c values reported in Table G-1 of Appendix G were calculated using Equation VII-10.

In Equation VII-10, the prefix to the logarithmic term is the reciprocal of the average residence time $\langle\tau\rangle$. For a given temperature, first-order behavior is confirmed

by a straight line through the origin, the slope of which is the first-order rate constant k_c.

Calculation of Reaction Energy of Activation

The Arrhenius equation (Equation II-1) in logarithmic form is

$$\ln k_c = -\frac{E_A}{RT} + \ln A \qquad \text{VII-11}$$

Upon plotting $\ln k_c$ against the reciprocal of temperature, a straight line is obtained whose slope is $-E_A/R$. For each of the five pressures of operation in this investigation, a least squares line in the form of Equation VII-11 was obtained from the experimental data.

Estimation of Maximum Departure from Isothermal Behavior

In the derivation of Equation VII-9 for calculation of k_c, it was assumed that isothermal conditions prevailed, both radially and axially, throughout the reactor. From the analogy between the heat and mass transfer processes, and the results of Appendix D, the radial temperature gradients are expected to be negligible. On the other hand, the axial temperature gradients may not be negligible, owing to the heat generated by the reaction and the resistance to heat transfer at the reactor inside surface. With laminar flow in the reactor, the heat transfer coefficient at the inside surface is controlling, and the tube wall temperature is essentially equal to the temperature of the fluidized sand.

To determine the axial temperature variation it is necessary to obtain a simultaneous solution of the mass and energy transfer equations. The appropriate differential equations are derived in abbreviated form in the paragraphs which follow.

Consider a differential element of reactor volume $A_{cs}\Delta z$ through which the reacting fluid passes with a plug-flow velocity $\langle v \rangle$.

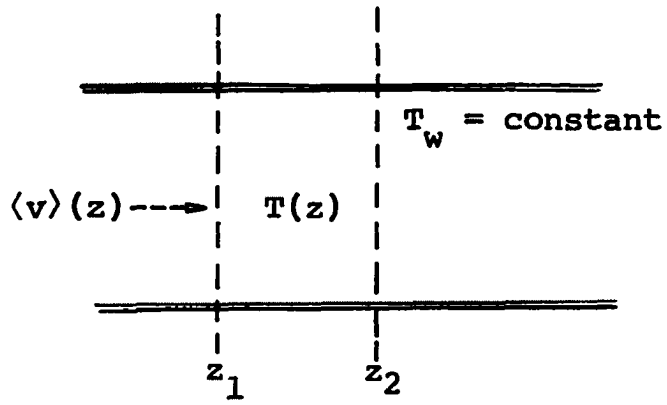

With plug-flow and negligible axial diffusion, the steady-state mass balance for component A (cyclopropane) in difference form is

$$0 = \dot{n}_A\Big]_{z_1} \Delta t - \dot{n}_A\Big]_{z_2} \Delta t - r_A \cdot A_{cs} \Delta z \cdot \Delta t \qquad \text{VII-12}$$

With the limiting process, Equation VII-12 transforms to the differential equation

$$\frac{d\dot{n}_A}{dz} = - A_{cs} \cdot r_A \qquad \text{VII-13}$$

Observing that the following auxiliary equations apply

$$r_A = k_c C_A = y_A C A e^{-E_A/RT}$$

$$\dot{n}_A = A_{cs}\langle v\rangle C y_A$$

$$A_{cs}\langle v\rangle C = \text{constant}$$

Then Equation VII-13 becomes

$$\langle v\rangle \frac{dy_A}{dz} = - y_A A e^{-E_A/RT} \qquad \text{VII-14}$$

This result is equivalent to Equation VII-6 which was derived from the general conservation equation.

The steady-state energy balance for the differential element of reactor volume, with negligible axial conduction and no radial temperature gradients, becomes in difference form

$$0 = \dot{H}]_{z_1}\Delta t - \dot{H}]_{z_2}\Delta t + q\cdot(\pi D)\cdot\Delta z\cdot\Delta t \qquad \text{VII-15}$$

where q is the wall heat transfer flux. Upon applying the limiting process to Equation VII-15, one obtains the simple differential equation

$$\frac{d\dot{H}}{dz} = \pi D q \qquad \text{VII-16}$$

Equation VII-16 is expanded into more useful form with the auxiliary equations

$$q = h(T_w - T)$$

$$\dot{H} = A_{cs}\langle v\rangle C \Sigma_i y_i \bar{H}_i$$

$$A_{cs}\langle v\rangle C = \text{constant}$$

The expanded result is

$$\langle v\rangle C \frac{d\Sigma_i y_i \bar{H}_i}{dz} = \frac{4h}{D}(T_w - T) \qquad \text{VII-17}$$

With ideal solution behavior

$$\sum_i y_i \bar{H}_i = \sum_i y_i \underline{H}_i = y_A \underline{H}_A + (1-y_A)\underline{H}_B$$

Further, since $\underline{H}_B - \underline{H}_A = \Delta H_R$, then

$$\sum_i y_i \bar{H}_i = \underline{H}_A + (1-y_A)\,\Delta H_R$$

In addition, if it is assumed that the axial temperature change is not sufficiently great to cause a significant change in the value of ΔH_R evaluated at the wall temperature T_w, then Equation VII-17 becomes

$$C_p \langle v \rangle C \frac{dT}{dz} - \Delta H_R \langle v \rangle C \frac{dy_A}{dz} = \frac{4h}{D}(T_w - T) \qquad \text{VII-18}$$

Equations VII-14 and VII-18 are the two differential equations to be solved. The appropriate boundary conditions are

$$T = T_w \quad \text{at } z = 0$$

$$y_A = (y_A)_I \quad \text{at } z = 0$$

It is convenient to eliminate the independent variable z between Equations VII-14 and VII-18 and to introduce the dimensionless temperature variable $\theta = T/T_w$. With some manipulation, one obtains

$$\frac{d\theta}{dy_B} = -\frac{\Delta H_R}{C_p T_w} - \frac{4hZ_m R T_w \theta(\theta-1)}{D(1-y_B)C_p P k_c \exp \frac{E_A}{RT}(1-\frac{1}{\theta})} \qquad \text{VII-19}$$

where k_c is the specific rate constant evaluated at T_w, and y_B is the propylene mole fraction. The proper boundary condition for Equation VII-19 is

$$y_B = (y_B)_I \text{ at } \theta = 1$$

Thus,

$$\left.\frac{d\theta}{dy_B}\right]_{y_B = (y_B)_I} = -\frac{\Delta H_R}{C_p T_w}$$

Equation VII-19 with its appropriate boundary condition can be solved conveniently by the method of isoclines. Such a solution is given in Figure 11 for Run XXIII-250. In illustrating the method, the run with greatest severity has been purposely chosen to shown the maximum effect. The pertinent data used in the solution of Equation VII-19 for Run XXIII-250 are listed for reference:

Run XXIII-250

Wall Temperature	T_w	= 1100°F.
Pressure	P	= 250 p.s.i.
Propylene MF at Inlet	$(y_B)_I$	= 0.0314
Propylene MF at Outlet	$(y_B)_o$	= 0.704
Compressibility Factor	Z_m	= 0.9975
Rate Constant	k_c(@ T_w)	= 7.705×10^{-2} sec.$^{-1}$
Molar Density	C(@ T_w)	= 0.0159 lb.-mole/cu.ft.
Heat of Reaction	ΔH_R(@ T_w)	= -7,813 Cal./g-mole
Heat Capacity	C_p	= 33.07 B.t.u./lb.-mole-°F.
Energy of Activation	E_A	= 66,410 Cal./g-mole
Reactor Diameter	D	= 0.02856 ft.
Thermal Conductivity	k	= 0.072 B.t.u.-ft./hr.-ft.^{2}-°F.
Transfer Coefficient	h	= 14.4 B.t.u./hr.-ft.^{2}-°F.

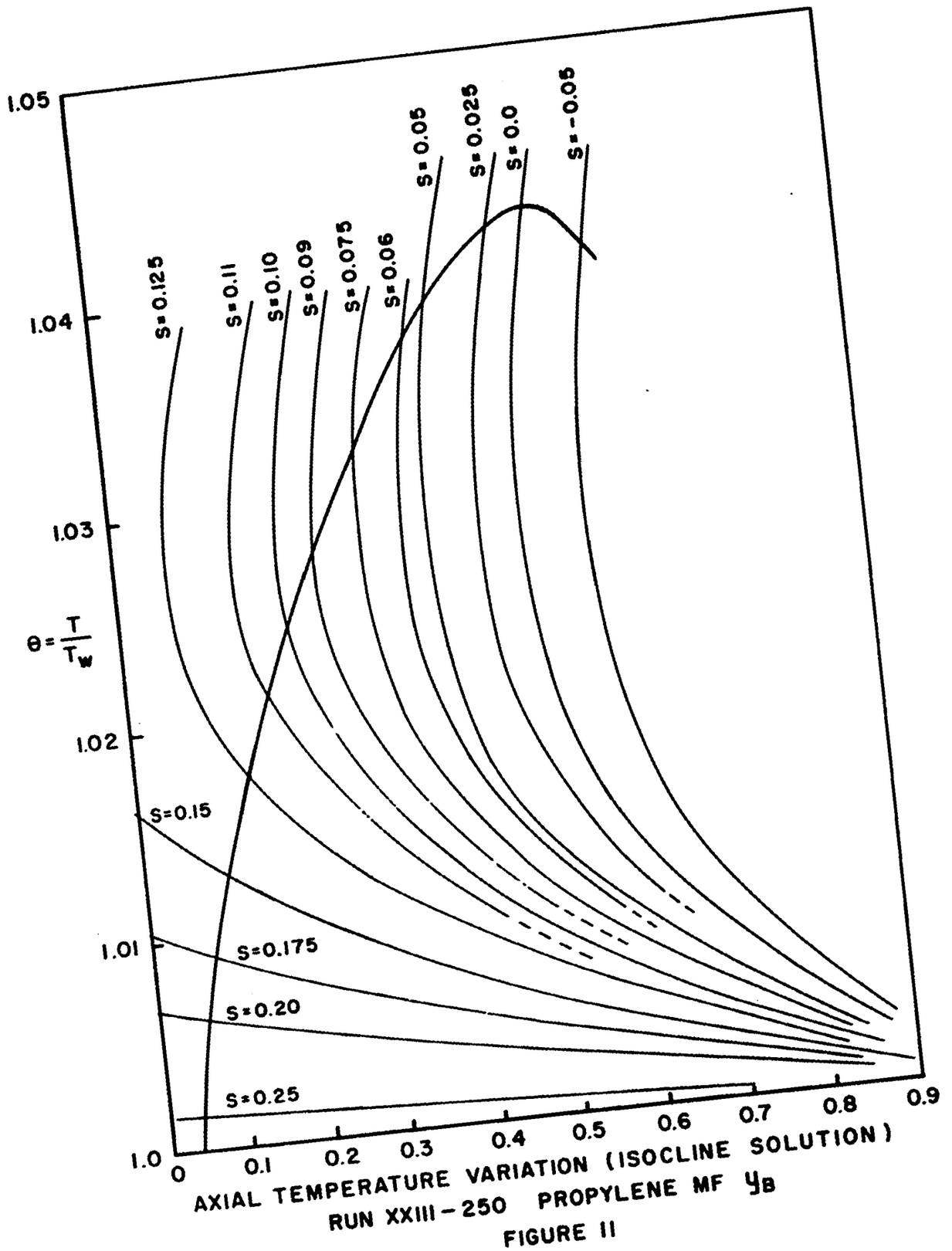

AXIAL TEMPERATURE VARIATION (ISOCLINE SOLUTION)
RUN XXIII-250 PROPYLENE MF y_B

FIGURE 11

Similar solutions were obtained for other selected runs. The estimated maximum error introduced by the assumption of isothermal behavior is discussed in the next section.

Estimation of Maximum Error in the Calculation of k_c

The temperature dependence of k_c is given by the Arrhenius equation. In differential form, the temperature effect is

$$dk_c = A\frac{E_A}{RT^2} \exp(-E_A/RT)dT$$

Thus, for a small temperature error ΔT, the percentage error in k_c is given by the expression

$$\text{Percentage Error in } k_c = 100 \frac{\Delta k_c}{k_c} = 100 \frac{E_A}{RT^2}\Delta T \qquad \text{VII-21}$$

In Run X-4 where the cyclopropane conversion was 9.56 per cent (a value which is greater than that attained in 72 per cent of the experimental runs correlated), the maximum rise in axial temperature above T_w was calculated to be 0.816°F. With this result, the maximum error in k_c calculated from Equation VII-21, assuming the maximum temperature to prevail over the whole reactor length, is 4.4 per cent. In the high temperature runs where conversion was much greater, the calculated maximum error is more significant. In Run XI-250 at 1050°F., in which a conversion of 30.63 per cent was attained, the maximum temperature rise is calculated to be 10.95°F. If this maximum temperature prevailed over the complete re-

actor length, then the assumption of isothermal behavior would introduce an error of 52 per cent. Only one run had conditions more severe than those of Run XI-250: viz., Run XXIII-250, for which the estimated axial temperature variation is given in Figure 11. In this case, where cyclopropane conversion is 69.44 per cent, the indicated maximum temperature rise is 67°F. which would yield an intolerable maximum error of 300 per cent.

Calculation of k_a Values

A relationship was derived in Chapter II (Equation II-39) which permits calculation of the first-order rate constant k_a from a known value of k_c; i.e.,

$$k_a = \frac{k_c f_i^{\circ}}{Z_m RT \gamma_i \Phi_i} \qquad \text{II-39}$$

The values of k_c are calculated from the experimental data through use of Equation VII-10. In studying the effect of pressure on k_a and k_c, it is convenient to compare the quantities RTk_a and k_c which are of the same dimension and order of magnitude. When the standard state fugacity f_i° is chosen to be unity and ideal solution behavior prevails, these quantities are related by the expression

$$RTk_a = \frac{k_c}{Z_m \Phi_i} \qquad \text{VII-22}$$

While in principle, the activity coefficient γ_i for cyclopropane can be calculated rigorously by the equation

$$\ln \gamma_i = \ln \frac{\bar{f}_i}{f_i y_i} = \frac{1}{RT} \int_0^p (\bar{v}_i - v_i) dp \qquad \text{VII-23}$$

the fact remains that the necessary data for such calculations are not available. As an alternative, an equation of state method can be used to obtain an estimate of γ_i. Several calculations of this type, using the Redlich-Kwong equation of state, have shown that γ_i is essentially unity for the range of conditions covered in this investigation. This result is not unexpected, since in all cases the reaction temperature is far above the critical temperature for cyclopropane or propylene, and the two components do not have widely different properties.

Values of Z_m in Equation VII-22 were calculated by the method previously described in this chapter. The pure component fugacity coefficients Φ_i for cyclopropane were determined from the customary generalized correlation (59), with reduced properties corresponding to the pressure and temperature of the reacting system.

Estimation of Net Propylene Yield with Simultaneous Isomerization and Polymerization

In general, those isomerization runs in which polymerization occurred have been excluded from analysis in this investigation. It has been of interest, however, to see how closely the net propylene yield could be predicted in those runs in which significant polymerization occurred and in

which the reaction was permitted to proceed until a maximum propylene composition was reached in the reactor effluent.

The net propylene yield is determined by the two simultaneous reactions

$$\begin{aligned} &(1) \qquad A \xrightarrow{k_c} B \\ &(2) \qquad B + B \xrightarrow{k_2} \text{polymer} \end{aligned} \qquad \text{VII-24}$$

where A signifies cyclopropane and B represents propylene. The second reaction has been shown to be of second order (44), thus the rate expression for propylene production is

$$\frac{1}{V}\frac{dn_B}{dt} = k_c C_A - k_2 C_B^2 \qquad \text{VII-25}$$

If the analysis is limited to the region where the extent of polymerization has little effect on the molar density in the reactor, then the propylene composition at the reactor outlet is given the integral equation

$$\int_{(y_B)_I}^{y_B} \frac{dy_B}{y_B^2 + \frac{k_c}{Ck_2}(y_B - 1)} = -Ck_2 \int_o^{\langle\tau\rangle} dt \qquad \text{VII-26}$$

where $\langle\tau\rangle = CV_R/F_o$ is the average reactor contact time. The solution of Equation VII-26 is

$$\ln \frac{2y_B+\alpha-\beta}{2y_B+\alpha-\beta} - \ln \frac{2(y_B)_I + \alpha-\beta}{2(y_B)_I + \alpha-\beta} = -Ck_2\beta\langle\tau\rangle \qquad \text{VII-27}$$

where $\alpha = \frac{k_c}{Ck_2}$ and $\beta = [\alpha^2+4\alpha]^{\frac{1}{2}}$

In Chapter VIII, values of y_B from Equation VII-27

are compared with those of an actual run in which the reaction was allowed to proceed into the polymerization region.

Pressure Dependence of the Rate Constant k_c

It is desirable to consider the pressure dependence of the rate constant k_c from a different point of view than presented in Chapter II. For unimolecular reactions in general, the specific rate constant according to absolute reaction rate theory is

$$k_c = \varkappa \frac{k_B T}{h} K_a^* \frac{\alpha_A}{\alpha^*} \qquad \text{VII-28}$$

where $\varkappa$ is a transmission coefficient which accounts for the quasi-unimolecular behavior at low pressure. The logarithmic differentiation of Equation VII-28 with respect to pressure at constant temperature yields

$$\frac{\partial \ln k_c}{\partial p} = \frac{\partial \ln \varkappa}{\partial p} + \frac{\partial \ln(\alpha_A/\alpha^*)}{\partial p} \qquad \text{VII-29}$$

In terms of the Lindemann-Hinshelwood theory for unimolecular reactions, the transmission coefficient $\varkappa$ can be replaced by the expression $1/(1+\beta/p)$, or alternately by the expression $1/(1+\xi k_\infty/p)$ in which ξ is the slope of the straight line resulting from a plot of $1/k_c$ versus $1/p$. Further, if ideal solution behavior is assumed, then the ratio α_A/α^* reduces to the fugacity ratio f_A/f^*. Upon substitution of these results into Equation VII-29, one obtains

$$\frac{\partial \ln k_c}{\partial p} = \frac{\partial \ln(f_A/f^*)}{\partial p} - \frac{\partial \ln(1+\xi k_\infty/p)}{\partial p} \qquad \text{VII-30}$$

Since $\frac{\partial \ln f}{\partial p} = \frac{\underline{v}}{RT}$, then Equation VII-30 becomes

$$\frac{\partial \ln k_c}{\partial p} = \frac{\underline{v}_A - \underline{v}^*}{RT} - \frac{\partial \ln(1+\xi k_\infty/p)}{\partial p} \qquad \text{VII-31}$$

As pointed out in Chapter III, it is the accepted view that the activated complex (or transition state) in the cyclopropane isomerization reaction is simply a cyclopropane molecule in which a hydrogen atom is in the process of migrating from one carbon atom to another. With this view, $\underline{v}_A$ and $\underline{v}^*$ should be essentially equal, or at most, $\underline{v}^*$ should be only slightly greater than $\underline{v}_A$ because of the stretching of a C-C bond. At high pressures, the second term on the right hand side of Equation VII-31 becomes small. Thus, in effect, at high pressure, the rate constant for a unimolecular reaction is expected to be essentially independent of pressure, though the volume term in Equation VII-31 could contribute to a small reduction in k_c as pressure is increased.

CHAPTER VIII

DISCUSSION OF RESULTS

In this chapter the experimental results are discussed in terms of the theoretical treatment of Chapter II, after being analyzed by the methods of Chapter VII. Rate data for the thermal isomerization of cyclopropane were obtained in a gold-lined reactor, previously described, for the following range of variables:

	Range
Pressure (p.s.i.)	250 -2000
Temperature (°F.)	850 -1100
Residence Time (Sec.)	15.4 -2016
Feed Rate (lb.-Moles/Sec.x10^6)	0.66-10.33
Conversion (per cent)	0.59-69.44

For completeness, all of the experimental results are recorded in Table G-1 of Appendix G. Sample run data sheets and calculation work sheets are provided in Appendix H.

In many of the runs recorded in Table G-1 polymerization was encountered. This occurrence was not unexpected, however, as polymerization of propylene had been anticipated under certain conditions, based on the previous work by Sullivan, Ruthruff and Kuentzel (80), and by Krauze, Nemtzov

and Soskina (44). In selecting the results which were suitable for isomerization correlation, all runs were excluded in which (1) the weight recovery was in error by 4 per cent or more, (2) a measureable quantity (more than a trace) of liquid was detected in the product receiver. In addition, some runs were excluded because of various difficulties encountered. These difficulties have been discussed in the footnote comments to Table G-1 in Appendix G. All runs free of apparent difficulties, and meeting the two requirements mentioned, are tabulated in Table G-2 of Appendix G. In total, there are forty-three data points available for correlation, all of which fall within the shaded area representing the isomerization region in Figure 12.

Figure 12 is based on the results of this investigation. At each temperature level, pressure was increased until the formation of liquid product was observed (it should be noted that pressure is reflected in the residence time, τ). Since, in most instances, pressure was increased in 500 p.s.i. increments, the hyperbolic-shaped boundary line in Figure 12 should not be interpreted as a precise dividing line between a region of pure isomerization and region of significant polymerization. The dividing line is the approximate locus of points which are from 0 to 500 p.s.i. below the pressure required to produce a measureable quantity of liquid polymer product at the particular temperature of operation.

In Chapter VII it was shown that in an isothermal,

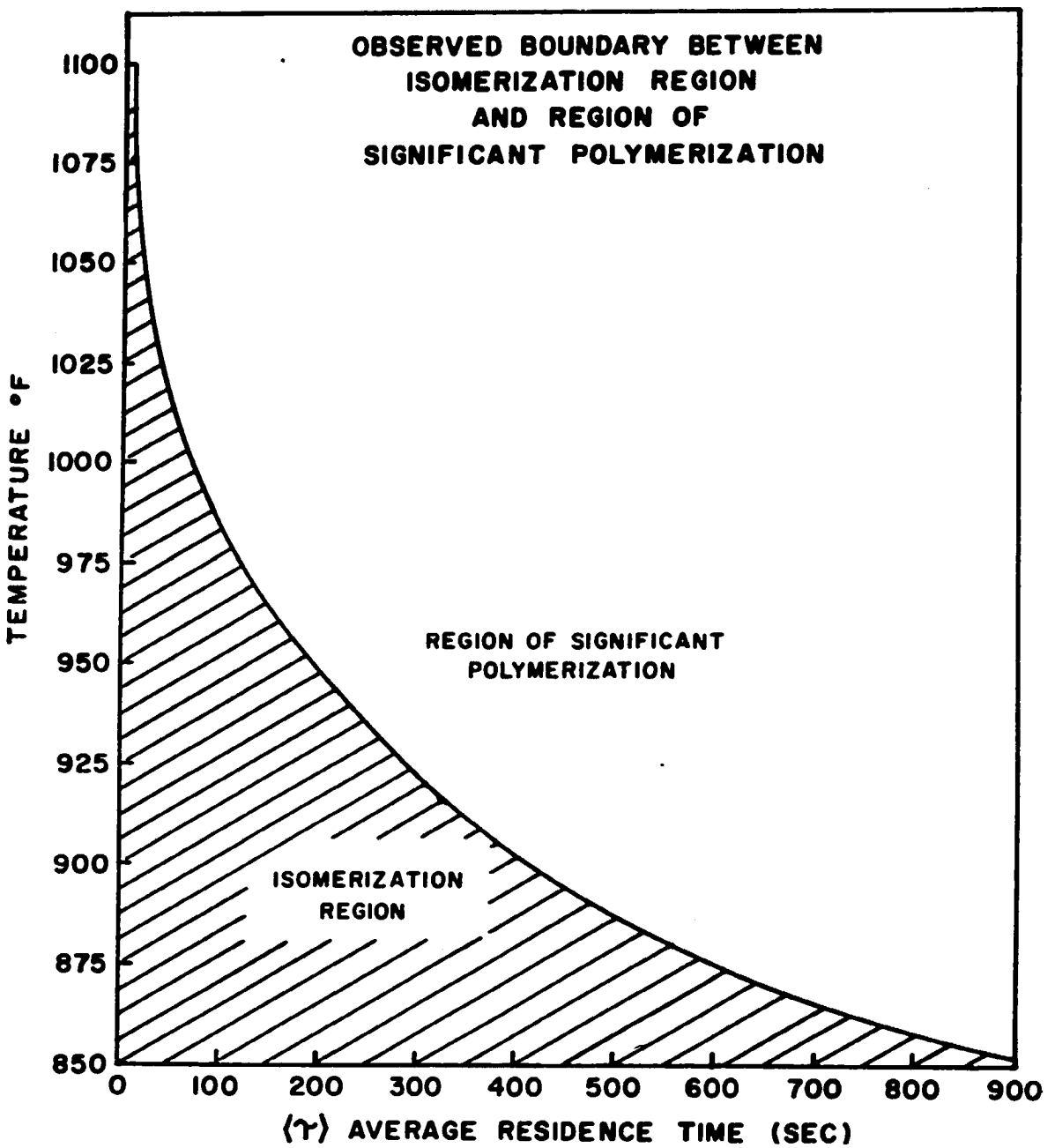
OBSERVED BOUNDARY BETWEEN
ISOMERIZATION REGION
AND REGION OF
SIGNIFICANT POLYMERIZATION
REGION OF SIGNIFICANT
POLYMERIZATION
ISOMERIZATION
REGION
TEMPERATURE °F
1100
1075
1050
1025
1000
975
950
925
900
875
850
0
100
200
300
400
500
600
700
800
900
⟨τ⟩ AVERAGE RESIDENCE TIME (SEC)

Figure 12

plug-flow reactor, the integral rate data for a first-order reaction should be correlated by the expression $\ln (y_A)_I/(y_A)_o = k_c\langle\tau\rangle$. Thus, upon plotting $\ln (y_A)_I/(y_A)_o$ against $\langle\tau\rangle$, a straight line through the origin should be obtain whose slope is k_c. Figure 13 is such a plot for the runs at 900°F. The slope of the line through the origin in Figure 13 was calculated from Davis and Scott's equation for k_∞ given in Chapter III. It is observed that first-order behavior is confirmed. The experimental results are in quite close agreement with the prediction. Figure 14 is a similar plot for the data at 950°F. The slopes determined from both the Davis and Scott, and Chambers and Kistiakowsky equations for k_∞ are shown for comparison. The experimental results agree more closely with the Davis and Scott equation----a desirable result----since the Davis and Scott equation for k_∞ was derived from their own results combined with those from three other sources, including Chambers and Kistiakowsky. In both Figure 13 and 14 there is some indication of a decline in k_c at the higher residence times (or pressures). One possible explanation of this behavior might be the presence of undetected polymerization.

As expected, the rate constant temperature dependence is well represented by the Arrhenius equation. An Arrhenius plot of log k_c versus $1/T$ has been prepared for each of the five pressure levels studied. These plots are shown in Figures 15 thru 19. In each figure the least squares line

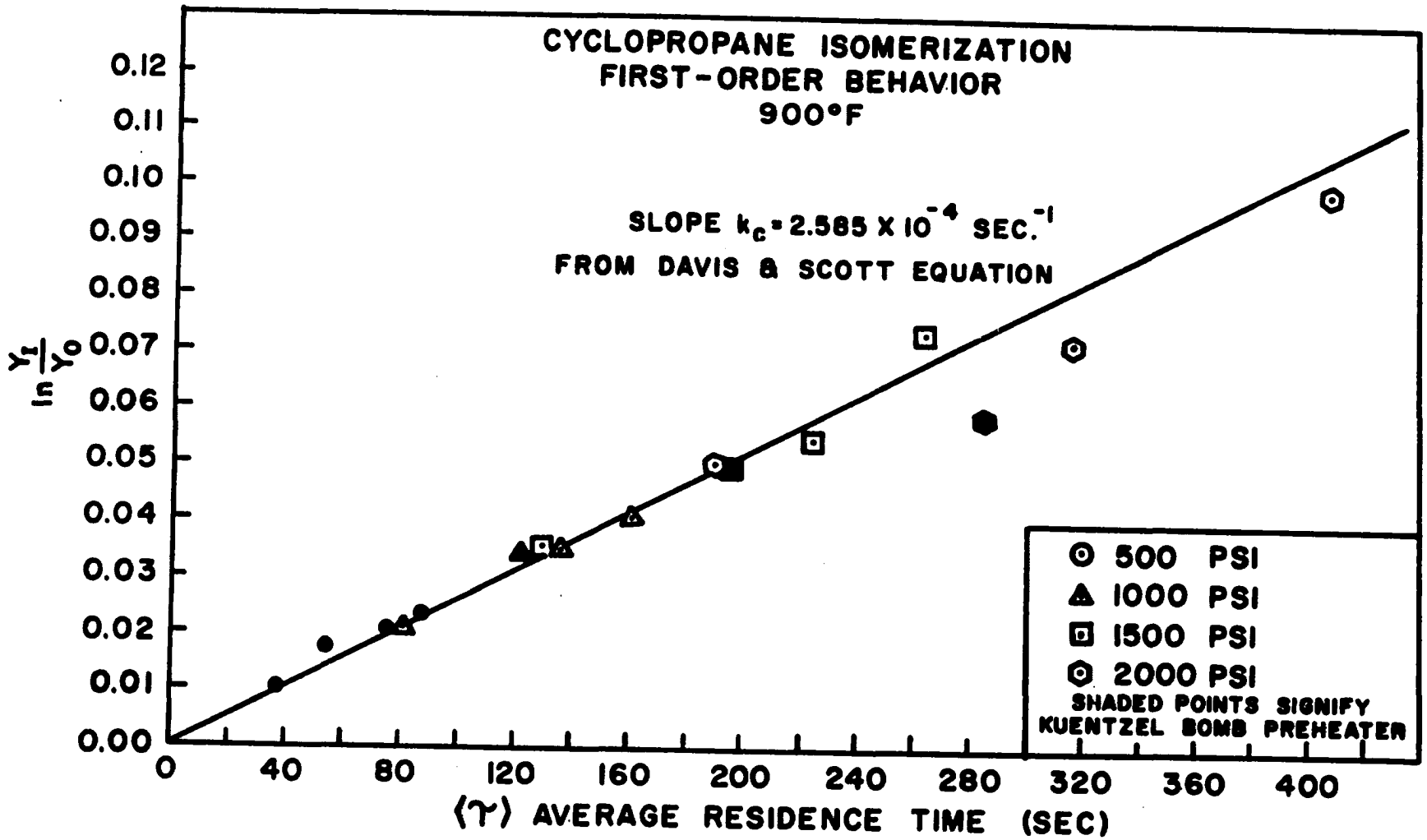
CYCLOPROPANE ISOMERIZATION
FIRST-ORDER BEHAVIOR
900°F
SLOPE $k_c = 2.585 \times 10^{-4}$ SEC.$^{-1}$
FROM DAVIS & SCOTT EQUATION
$\ln \frac{Y_t}{Y_o}$
0.12
0.11
0.10
0.09
0.08
0.07
0.06
0.05
0.04
0.03
0.02
0.01
0.00
0
40
80
120
160
200
240
280
320
360
400
⟨τ⟩ AVERAGE RESIDENCE TIME (SEC)
500 PSI
1000 PSI
1500 PSI
2000 PSI
SHADED POINTS SIGNIFY
KUENTZEL BOMB PREHEATER

Figure 13

TABLE 2

SUMMARY OF DATA FOR FIGURE 13

900°F.

$$\ln(y_A)_I/(y_A)_o = k_c\langle\tau\rangle$$

Run No.	$\langle\tau\rangle$(Sec.)	$\ln(y_A)_I/(y_A)_o$
	500 psi	
II-1	88.0	0.02353
IX-1	38.3	0.01038
X-1	75.8	0.02077
XIV-1 (KB)	54.2	0.01765
	1000 psi	
II-2	137.2	0.03507
IX-2	80.7	0.02146
X-2	160.8	0.04017
XIV-2 (KB)	123.0	0.03433
	1500 psi	
II-3	225.3	0.0547
IX-3	130.3	0.0354
X-3	265.3	0.0742
XIV-3 (KB)	196.3	0.0500
	2000 psi	
II-4	317.1	0.0722
IX-4	189.6	0.0506
X-4	407.8	0.1003
XIV-4 (KB)	285.6	0.0585

KB - Kuentzel Bomb Preheater

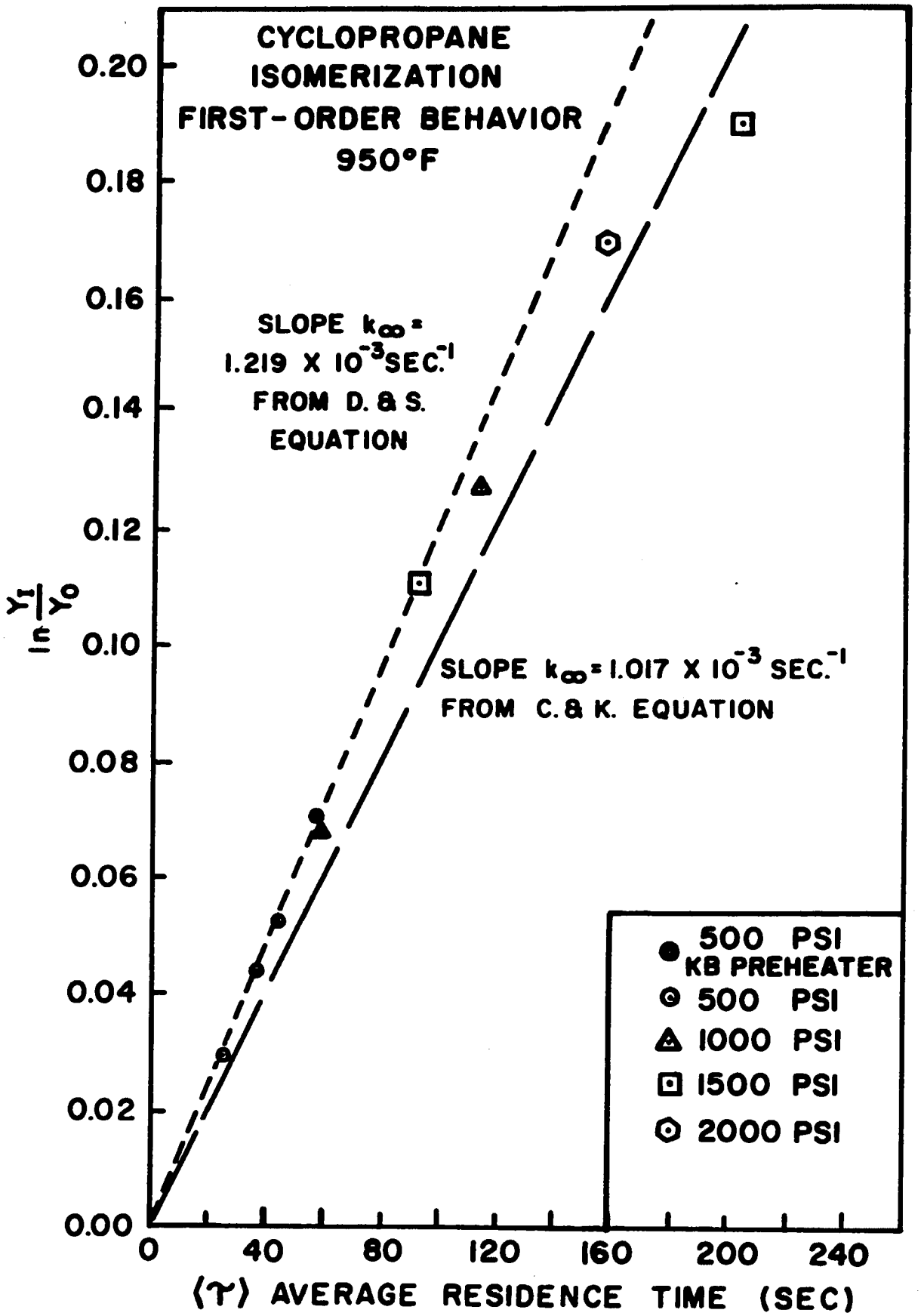
CYCLOPROPANE
ISOMERIZATION
FIRST-ORDER BEHAVIOR
950°F
SLOPE k_∞ =
1.219 X 10^{-3} SEC.$^{-1}$
FROM D. & S.
EQUATION
SLOPE k_∞ = 1.017 X 10^{-3} SEC.$^{-1}$
FROM C. & K. EQUATION
500 PSI
KB PREHEATER
500 PSI
1000 PSI
1500 PSI
2000 PSI
$\ln \frac{\gamma_\infty}{\gamma_\infty - \gamma}$
0.00
0.02
0.04
0.06
0.08
0.10
0.12
0.14
0.16
0.18
0.20
0
40
80
120
160
200
240
⟨τ⟩ AVERAGE RESIDENCE TIME (SEC)

Figure 14

TABLE 3

SUMMARY OF DATA FOR FIGURE 14

950°F.

$$\ln(y_A)_I/(y_A)_o = k_c\langle\tau\rangle$$

Run No.	$\langle\tau\rangle$(Sec.)	$\ln(y_A)_I/(y_A)_o$
	500 psi	
I-1	25.60	0.02970
XV-1 (KB)	57.24	0.07095
XXI-1	37.13	0.04300
XXII-1	44.54	0.05265
	1000 psi	
I-2	59.21	0.06760
XXII-2	113.4	0.1270
	1500 psi	
I-3	92.08	0.1110
XXII-3	201.9	0.1900
	2000 psi	
I-4	156.7	0.1695

KB - Kuentzel Bomb Preheater

of correlation is shown along with the experimental data points. It will be observed that at the 500 p.s.i. pressure level (Figure 16), where the greatest number of data points are available for correlation, the least squares line

$$\ln k_c = 35.309 - \frac{65,380}{RT}$$

is in quite close agreement with the equation

$$\ln k_\infty = 35.431 - \frac{65,570}{RT}$$

reported by Davis and Scott. In fact, both the frequency factor logarithms and the activation energies differ in each case by only approximately 0.3 per cent. The maximum departure from the Davis and Scott equation was at the 2000 p.s.i. pressure level (Figure 19), where the fewest number of data points were available for correlation. In this case, the experimental activation energy is 5 per cent below the Davis and Scott results, while the experimental frequency factor logarithm is 6.5 per cent lower.

The location of the data point for Run XXIII-250 at 1100°F. in Figure 15 is of special interest because of the significant departure from isothermal behavior predicted in Chapter VII. As will be observed, this particular data point falls well in line with the other results at 250 p.s.i. Apparently, therefore, the departure from isothermal behavior is far less than predicted----a result most readily explained by underestimation of the heat transfer coefficient.

In Figure 20 the Arrhenius correlation least squares

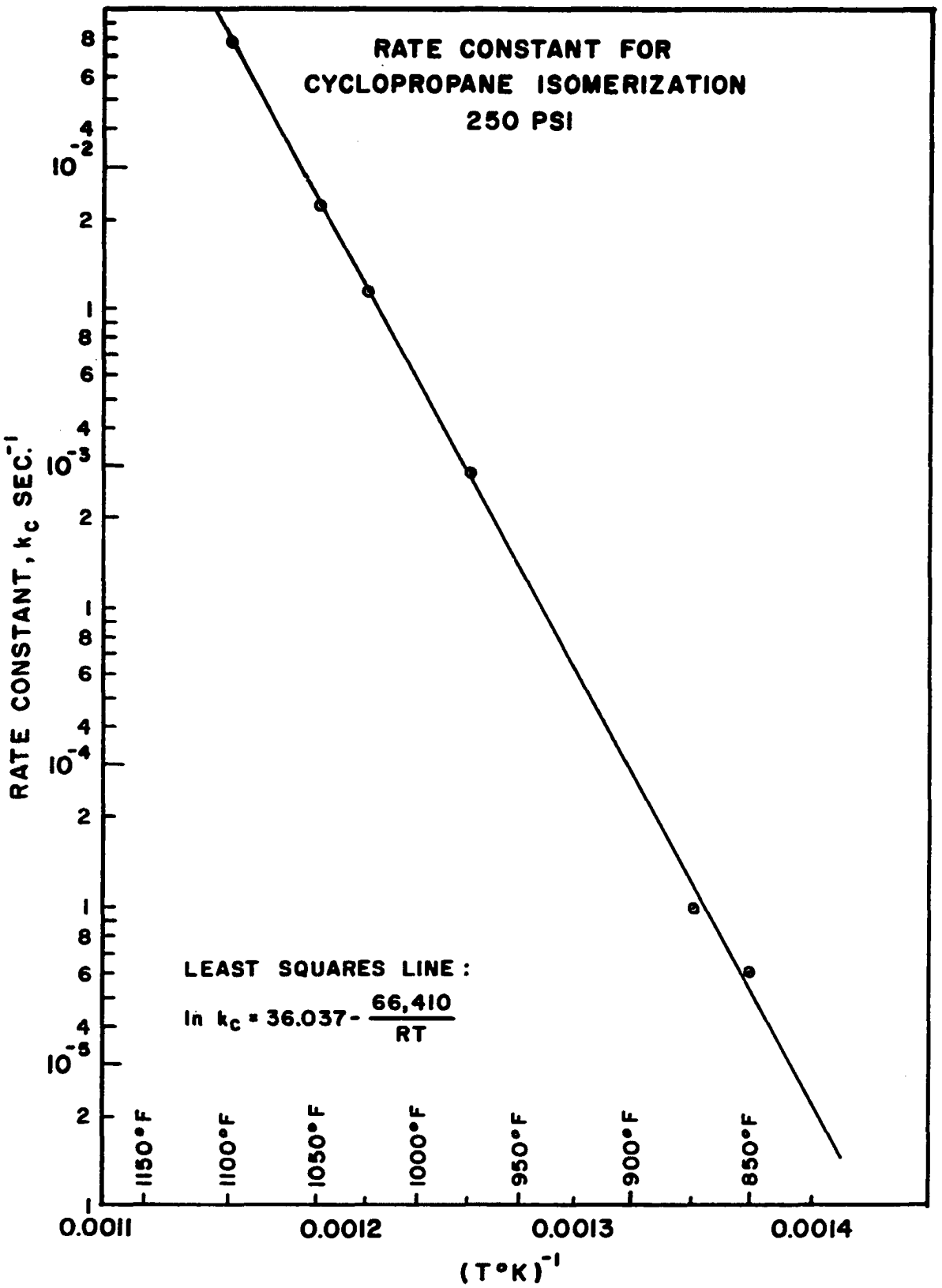
RATE CONSTANT FOR
CYCLOPROPANE ISOMERIZATION
250 PSI
RATE CONSTANT, k_c SEC.$^{-1}$
LEAST SQUARES LINE :
$\ln k_c = 36.037 - \frac{66,410}{RT}$
1150°F
1100°F
1050°F
1000°F
950°F
900°F
850°F
0.0011
0.0012
0.0013
0.0014
$(T°K)^{-1}$

Figure 15

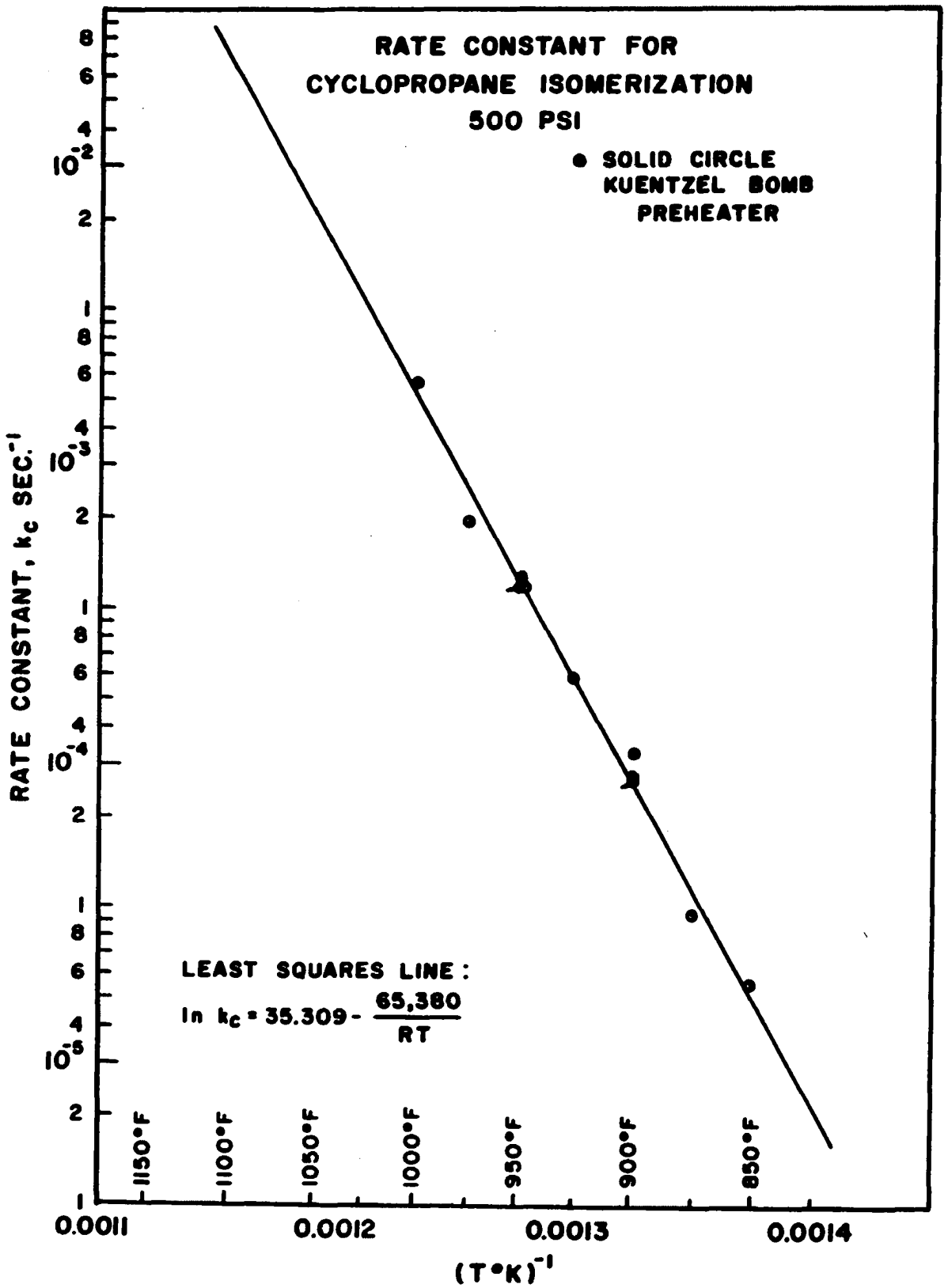
RATE CONSTANT FOR
CYCLOPROPANE ISOMERIZATION
500 PSI
● SOLID CIRCLE
KUENTZEL BOMB
PREHEATER
LEAST SQUARES LINE :
ln kc = 35.309 - 65,380/RT
RATE CONSTANT, kc SEC.-1
(T°K)-1
1150°F
1100°F
1050°F
1000°F
950°F
900°F
850°F
0.0011
0.0012
0.0013
0.0014

Figure 16

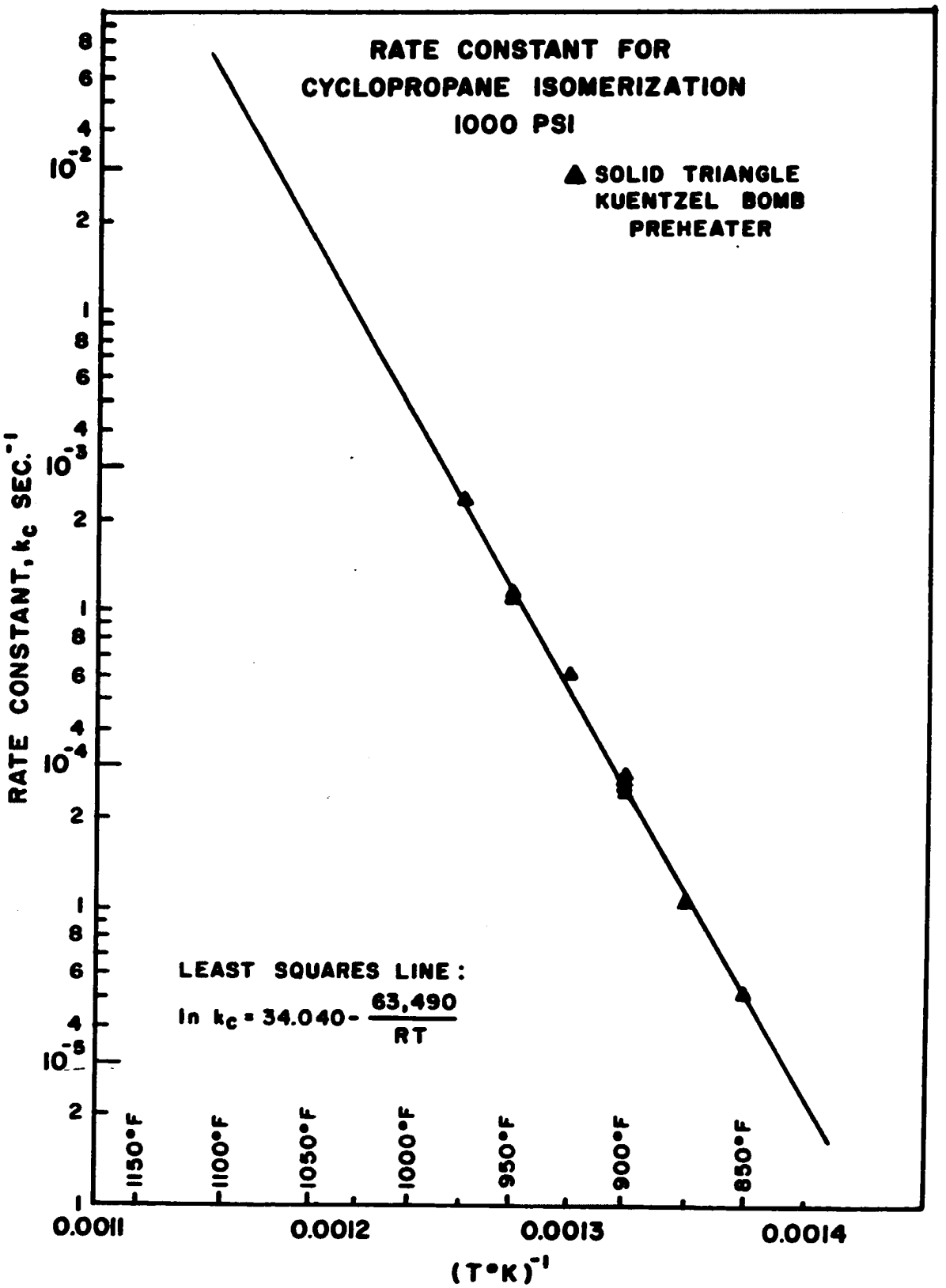
RATE CONSTANT FOR
CYCLOPROPANE ISOMERIZATION
1000 PSI
▲ SOLID TRIANGLE
KUENTZEL BOMB
PREHEATER
LEAST SQUARES LINE:
ln kc = 34.040 - 63,490/RT
RATE CONSTANT, kc SEC.-1
(T°K)-1
1150°F
1100°F
1050°F
1000°F
950°F
900°F
850°F
0.0011
0.0012
0.0013
0.0014

Figure 17

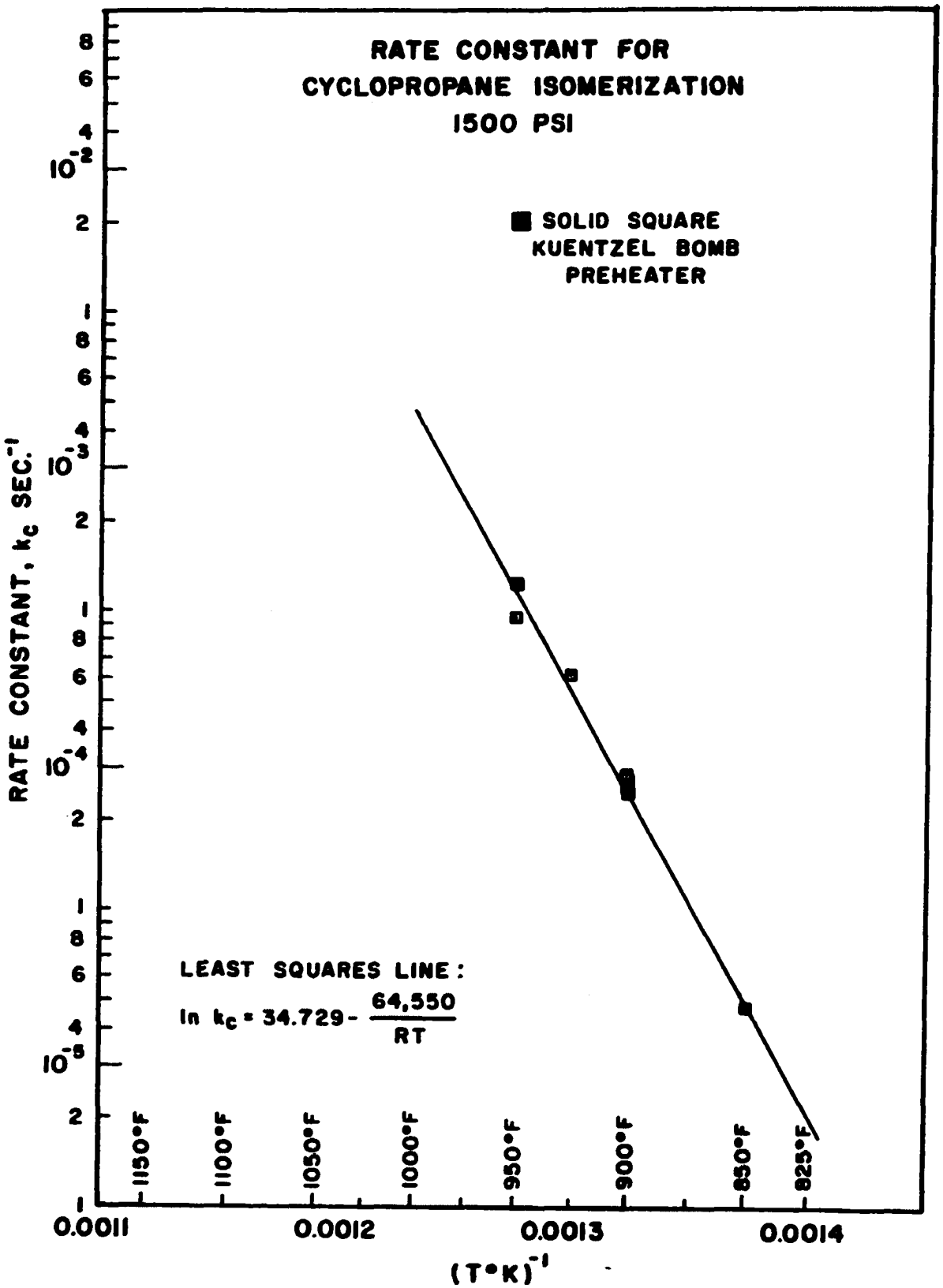
RATE CONSTANT FOR
CYCLOPROPANE ISOMERIZATION
1500 PSI
SOLID SQUARE
KUENTZEL BOMB
PREHEATER
LEAST SQUARES LINE:
ln kc = 34.729 - 64,550/RT
RATE CONSTANT, kc SEC.-1
(T°K)-1
0.0011
0.0012
0.0013
0.0014
1150°F
1100°F
1050°F
1000°F
950°F
900°F
850°F
825°F

Figure 18

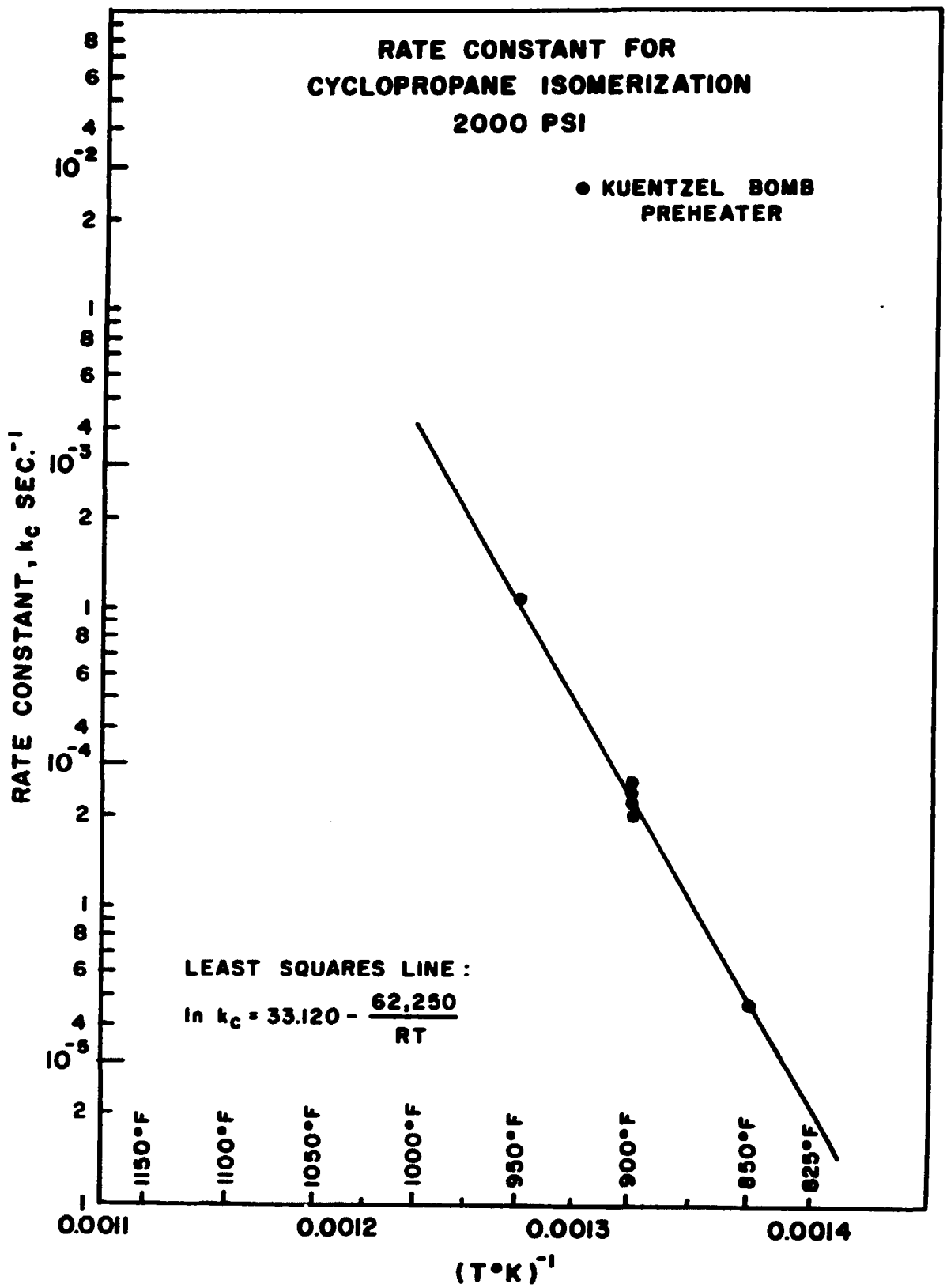
RATE CONSTANT FOR
CYCLOPROPANE ISOMERIZATION
2000 PSI
● KUENTZEL BOMB
PREHEATER
RATE CONSTANT, k_c SEC.$^{-1}$
LEAST SQUARES LINE :
$\ln k_c = 33.120 - \frac{62,250}{RT}$
1150°F
1100°F
1050°F
1000°F
950°F
900°F
850°F
825°F
0.0011
0.0012
0.0013
0.0014
$(T°K)^{-1}$

Figure 19

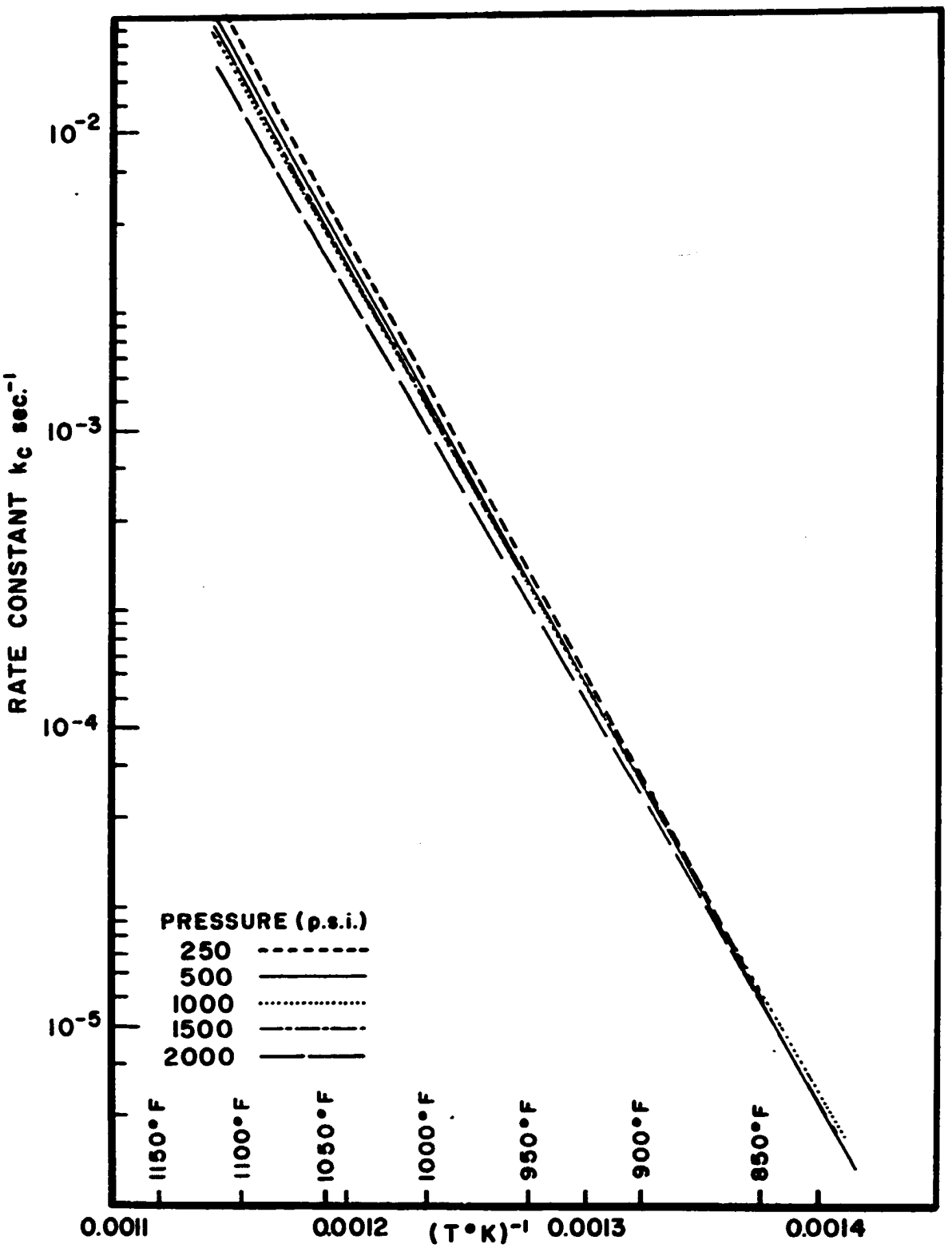

RATE CONSTANT TEMPERATURE DEPENDENCE AT VARIOUS PRESSURES.

FIGURE 20

lines for all five pressures are included in a single plot so that the pressure effect will be more apparent. Only a small pressure effect is observed. The small effect which does exist is in the direction of a decline in k_c with increasing pressure. The effect of pressure on the rate constant is considered in more detail in later paragraphs.

As previously discussed, in finding the region where polymerization is important, some runs were extended into the polymerization region to such an extent that a maximum was reached in the net propylene yield. This behavior is shown in Figure 21 for Runs V and XXII. In Figure 22, it is seen that the polymerization effect in Run V brings about an apparent (but not real) departure from the first-order behavior for the isomerization reaction. It should be pointed out that the data points at 1500 and 2000 p.s.i. for Run V do not survive the restrictions placed on the data used in the isomerization correlations. These points are included in Figure 22 simply to illustrate the polymerization effect. The points at the three lower pressures meet the requirement for correlation, and are seen to yield a first-order slope k_c which is intermediate to values calculated by the Davis and Scott, and the Chamber and Kistiakowsky equations.

In Chapter VII a method was presented for estimating the net propylene yield when isomerization and polymerization are occurring simultaneously. Curve No. 2 in Figure 23 represents the calculated net propylene yield for Run V when

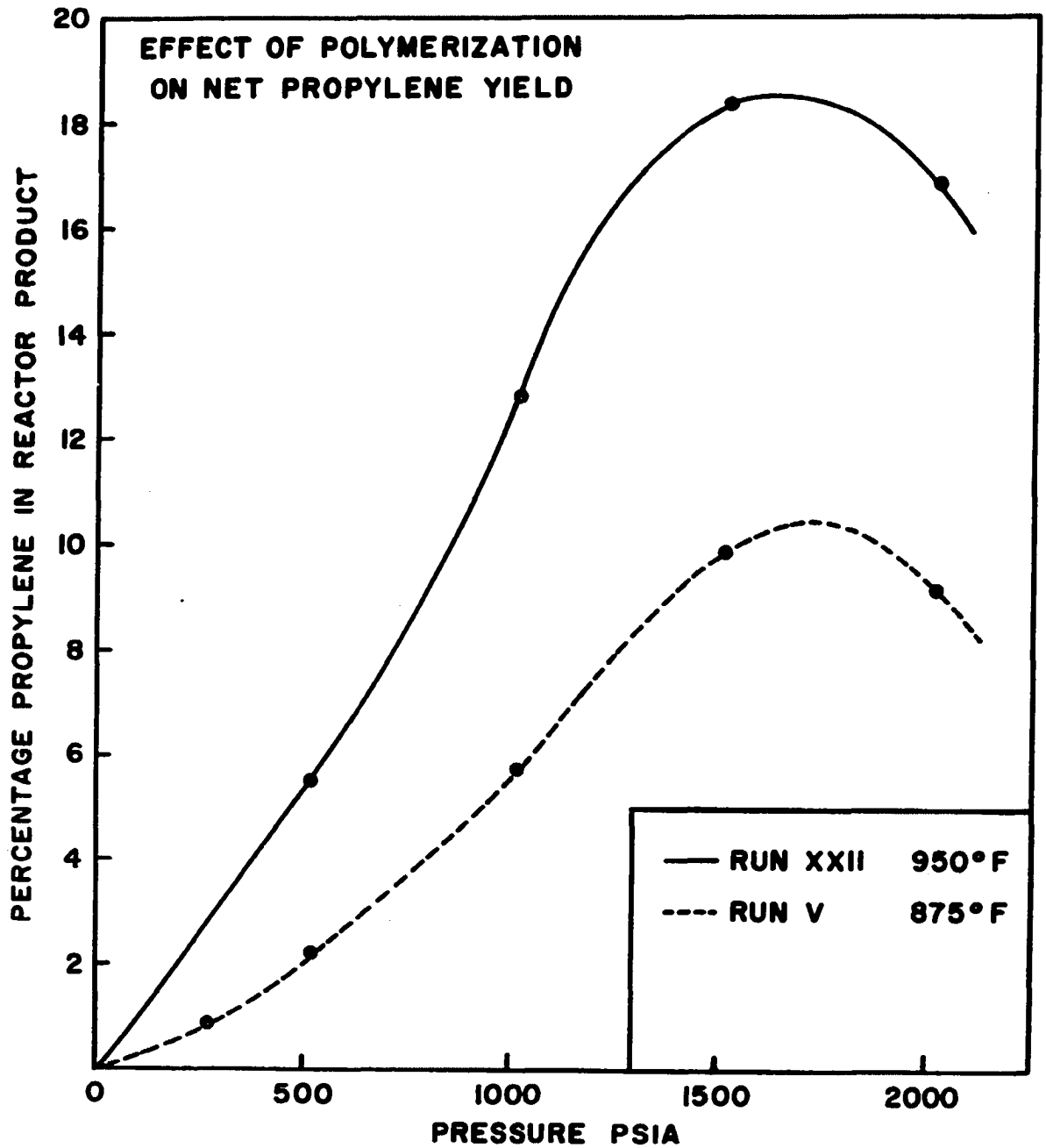
EFFECT OF POLYMERIZATION
ON NET PROPYLENE YIELD
PERCENTAGE PROPYLENE IN REACTOR PRODUCT
20
18
16
14
12
10
8
6
4
2
0
500
1000
1500
2000
PRESSURE PSIA
RUN XXII 950°F
RUN V 875°F

Figure 21

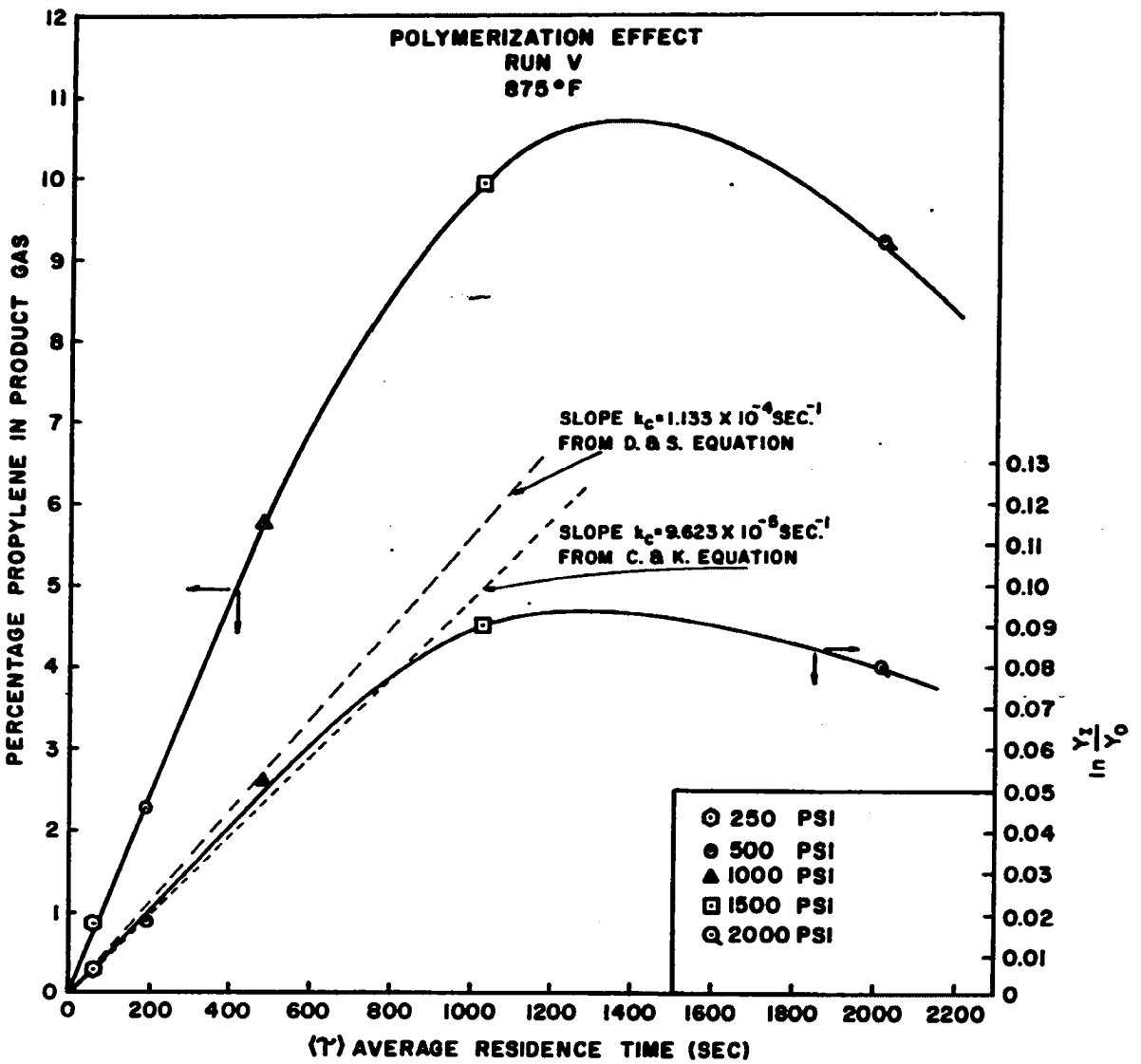
POLYMERIZATION EFFECT
RUN V
875°F
SLOPE k_c=1.133 X 10^{-4}SEC.$^{-1}$
FROM D. & S. EQUATION
SLOPE k_c=9.623 X 10^{-5}SEC.$^{-1}$
FROM C. & K. EQUATION
250 PSI
500 PSI
1000 PSI
1500 PSI
2000 PSI
PERCENTAGE PROPYLENE IN PRODUCT GAS
$\ln \frac{Y_1}{Y_0}$
(τ) AVERAGE RESIDENCE TIME (SEC)
0
200
400
600
800
1000
1200
1400
1600
1800
2000
2200
1
2
3
4
5
6
7
8
9
10
11
12
0.01
0.02
0.03
0.04
0.05
0.06
0.07
0.08
0.09
0.10
0.11
0.12
0.13

Figure 22

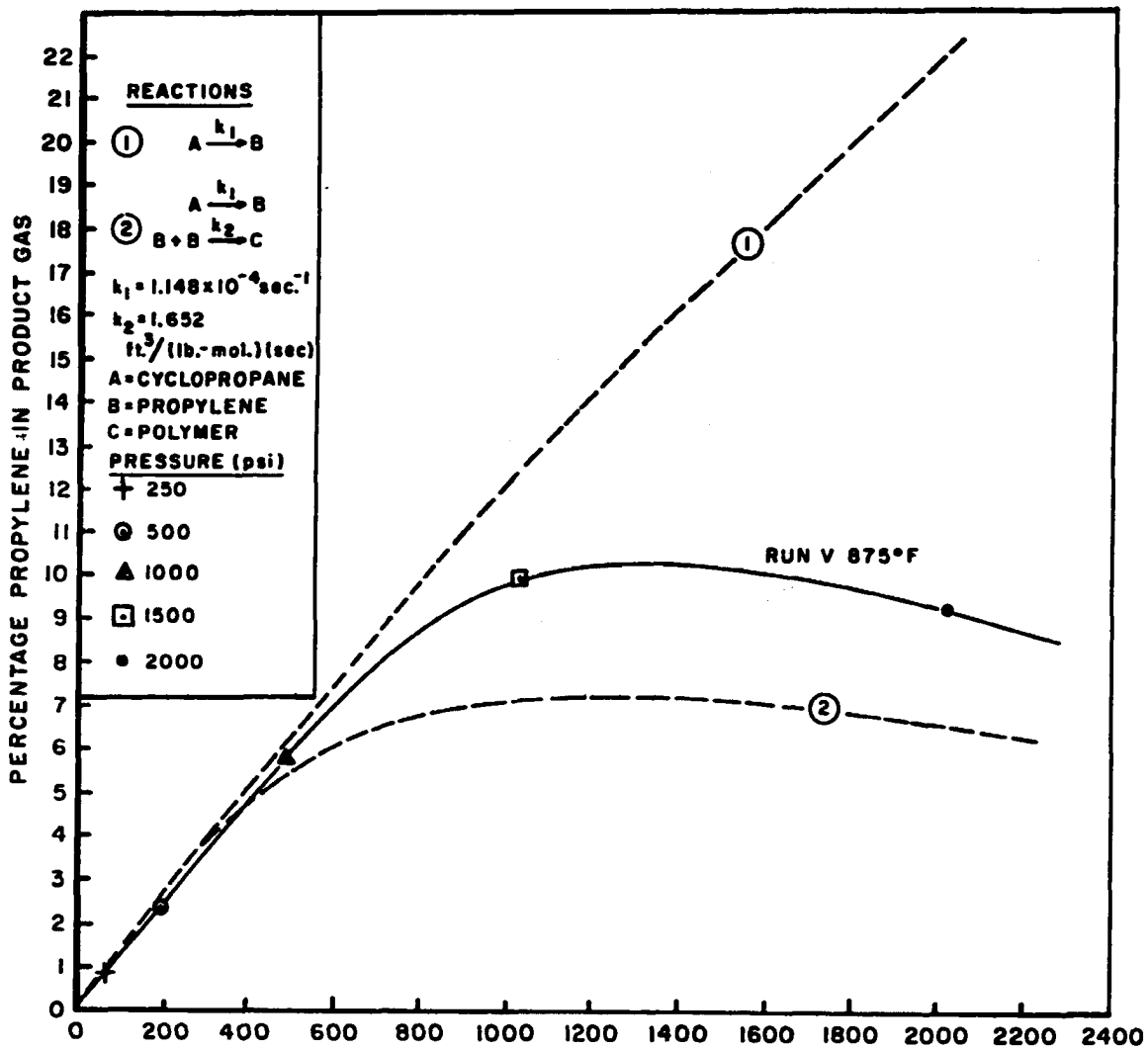

COMPARISON OF ACTUAL AND PREDICTED NET PROPYLENE YIELD FOR RUN V.

Figure 23

using an estimated second-order rate constant derived from the results of Krauze, Nemtzov and Soskina (44), as reported by Egloff (17). At 370°C. the second-order rate constant for propylene polymerization is reported to be 2.0×10^{-3} liters/g-mole sec., while the activation energy is 38,000 calories/g-mole. In Figure 23 the shape of the net propylene curve is reproduced, but the location of the calculated curve below the actual curve suggests that the estimated second-order rate constant for polymerization is too high. Curve No. 1 in Figure 23 is the calculated curve for first-order isomerization in the absence of polymerization.

This investigation did not include experiments designed to show, beyond all doubt, that gold is noncatalytic to the cyclopropane isomerization reaction. However, the noncatalytic nature of gold is very strongly indicated by the close agreement between the activation energies calculated from these experiments and those previously obtained in Pyrex glass. The question of whether or not the reactor would have been catalytic without the gold lining was answered by the results following Run XXIII-250. Apparently, during the evacuation following Run XXIII-250, the gold lining collapsed and subsequent runs gave conversions which were much higher than predicted by thermal reaction alone. Following the lining collapse, products other than propylene and cyclopropane began to appear in the product gas. A qualitative chromatographic analysis of the product gas from Run

XXVII-1 showed the presence of hydrogen, methane, ethane, ethylene, and propane. One chromatograph peak was unidentified. When the reactor was cut in two after Run XXVII-2, a large quantity of fine carbon was found around the gold lining. The lining had collapsed for practically the full reactor length.

In most runs the preheater constructed from 1/16-inch i.d. stainless steel tubing was used. From Figure 24, it is observed that the extent of catalytic conversion in this preheater must be low, since the actual observed conversion is lower than the calculated maximum thermal conversion. The greater significance of catalytic conversion in the unlined reactor, as compared with the coiled stainless steel preheater, is explained by the difference in residence times. The stainless steel preheater had a volume which was only 4.35 per cent of the gold-lined reactor volume. One indication that this preheater was not completely void of catalytic effect came from the occasional buildup of fine carbon powder which had to be removed at intervals. Another preheater, discussed in detail in Chapter IV, was constructed from four modified Kuentzel bombs connected in series. While this construction was hoped to be free of catalytic effects, the experimental results showed otherwise. An interesting observation was made on Run XII, the first in which the Kuentzel bombs were used. At the time of this run, the handle was broken on the reactor inlet sample valve; thus it was neces-

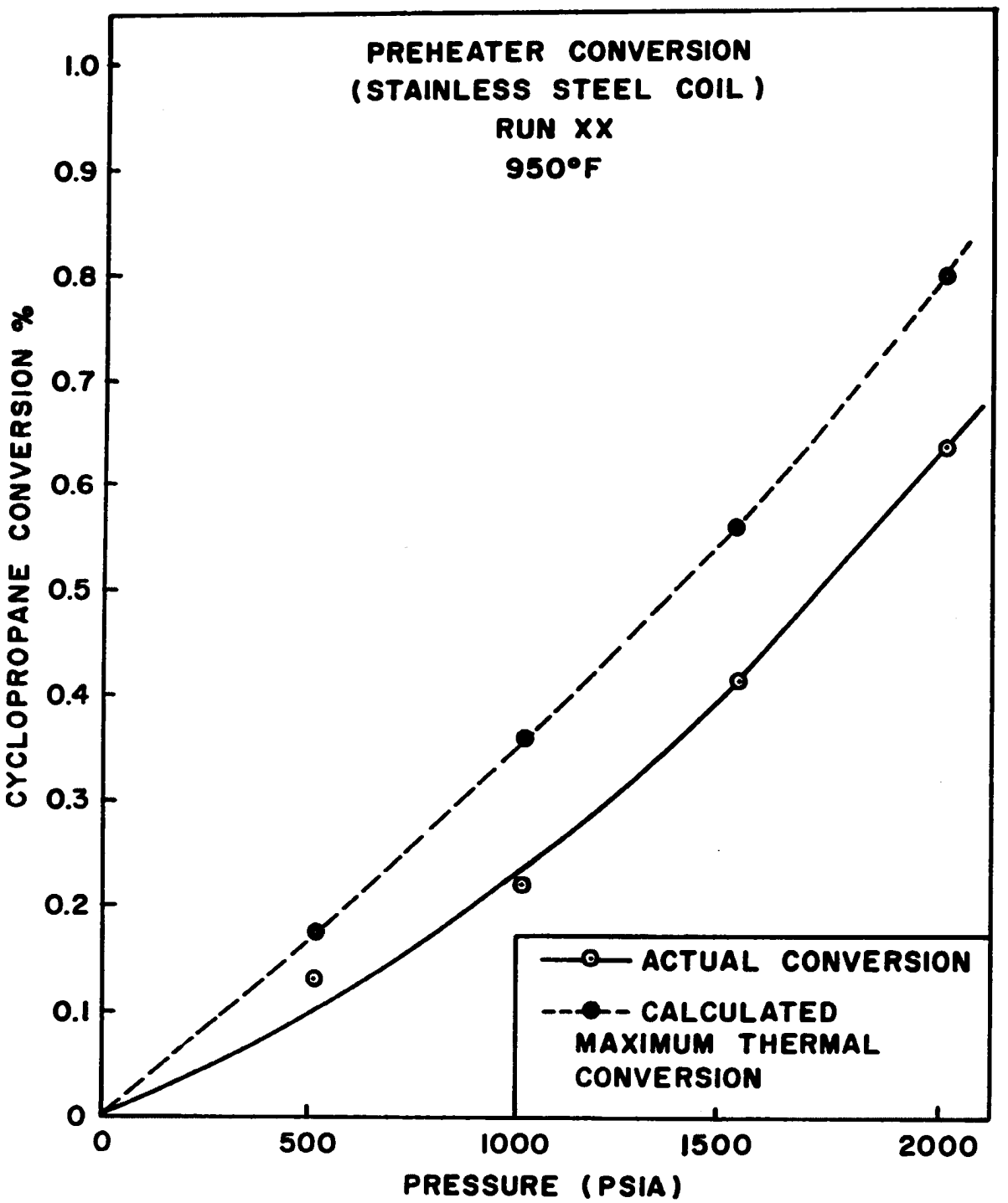
PREHEATER CONVERSION
(STAINLESS STEEL COIL)
RUN XX
950°F
CYCLOPROPANE CONVERSION %
1.0
0.9
0.8
0.7
0.6
0.5
0.4
0.3
0.2
0.1
0
0
500
1000
1500
2000
PRESSURE (PSIA)
ACTUAL CONVERSION
CALCULATED MAXIMUM THERMAL CONVERSION

Figure 24

sary to obtain the preheater outlet composition after the completion of the run by by-passing the reactor and passing the preheater product through the reactor product sample connection. However, at the close of Run XII, the preheater began to plug, and a decoking operation was necessary before the preheater outlet composition could be determined. Following the decoking operation, the preheater product was found to contain, in some cases, more propylene than was present in the reactor product of the preceding run. Thus, the decoking process also served as an activating process for the Kuentzel bomb preheaters. The nature of the activation is not known. In Figure 25 the actual preheater conversion, following the decoking process after Run XII, is compared with the calculated maximum thermal conversion. The catalytic conversion is obviously substantial. From Figure 26, it is seen that after several runs the catalytic activity had declined, but some catalytic effect is still present. It will be observed in Figures 25 and 26 that the thermal conversion alone can be significant in the Kuentzel bomb preheaters. This observation can be explained by their large total volume which was 50.5 per cent of the reactor volume.

In Chapter II it was shown that for the simple Lindemann-Hinshelwood theory of unimolecular reactions a plot of $1/k_c$ versus $1/p$ should yield a straight line whose intercept on the $1/k_c$-axis is the reciprocal of k_∞. This method

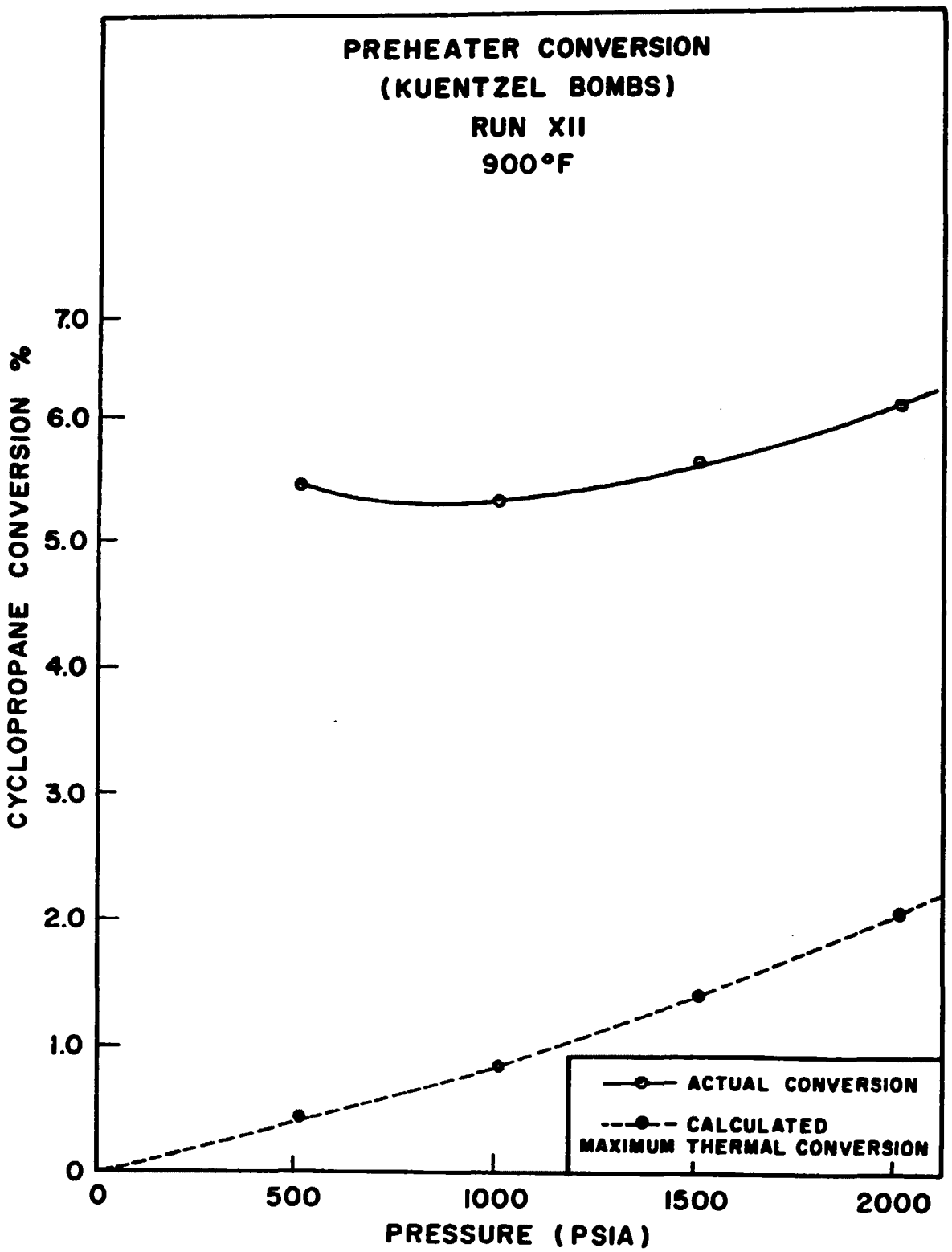
PREHEATER CONVERSION
(KUENTZEL BOMBS)
RUN XII
900°F
CYCLOPROPANE CONVERSION %
7.0
6.0
5.0
4.0
3.0
2.0
1.0
0
0
500
1000
1500
2000
PRESSURE (PSIA)
ACTUAL CONVERSION
CALCULATED
MAXIMUM THERMAL CONVERSION

Figure 25

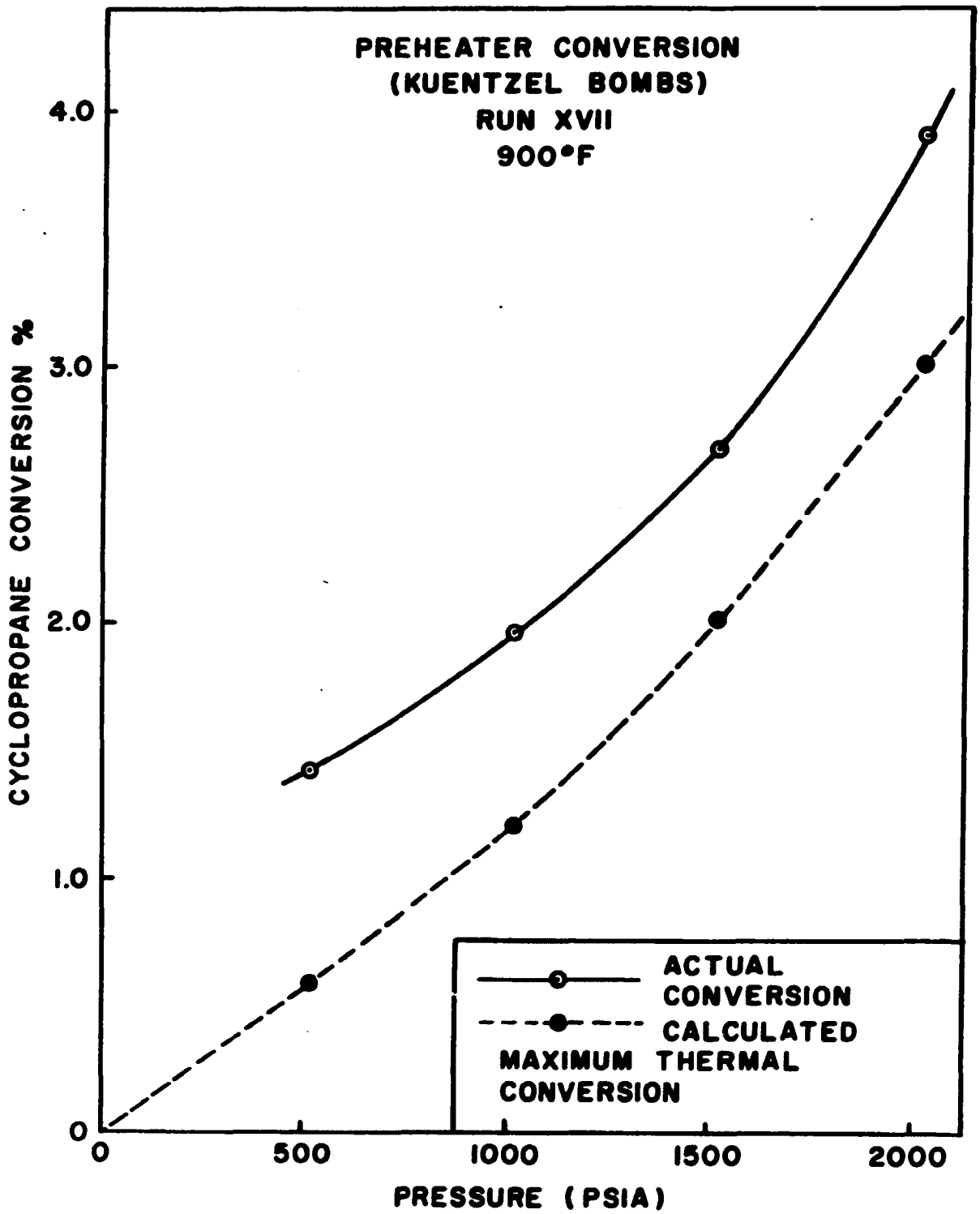
PREHEATER CONVERSION
(KUENTZEL BOMBS)
RUN XVII
900°F
CYCLOPROPANE CONVERSION %
4.0
3.0
2.0
1.0
0
0
500
1000
1500
2000
PRESSURE (PSIA)
ACTUAL CONVERSION
CALCULATED MAXIMUM THERMAL CONVERSION

Figure 26

of extrapolating low pressure data for unimolecular reactions to obtain values of k_∞ has been used universally as a means of comparing the results of different experiments. According to the Rice-Ramsperger-Kassel refinement of the theory, some slight departure from the straight line relationship is predicted at high pressure; that is, at high pressures, values of k_c are expected to be higher than predicted by the linear extrapolation of the simple theory. However, Kassel (37) has said that the linear extrapolation gives good results when the values of $1/k_c$ used in the extrapolation do not exceed the high pressure value by more than 50 per cent. In general, however, unimolecular reactions have not been studied in the region substantially above atmospheric pressure. Thus, for example, in the case of cyclopropane isomerization, the linear extrapolation has been neither prove or disproved for pressures well above one atmosphere. In comparing the Davis and Scott equations for k_c at one atmosphere and for k_∞, the k_∞ value is observed to exceed the atmospheric value by approximately 16 per cent at the 900°F. temperature level.

In Figures 27 and 28, the slopes of the $1/k_c$ versus $1/p$ lines are determined by the Davis and Scott equations. The results of Run III at 850°F. and the smoothed data from the Arrhenius plots are included in Figure 27 for comparison. One observes that, while the smoothed data are within $\pm$ 5 per cent of the $1/k_c$ extrapolation, considerable deviation exists for Run III. The nature of the $1/k_c$ variation with

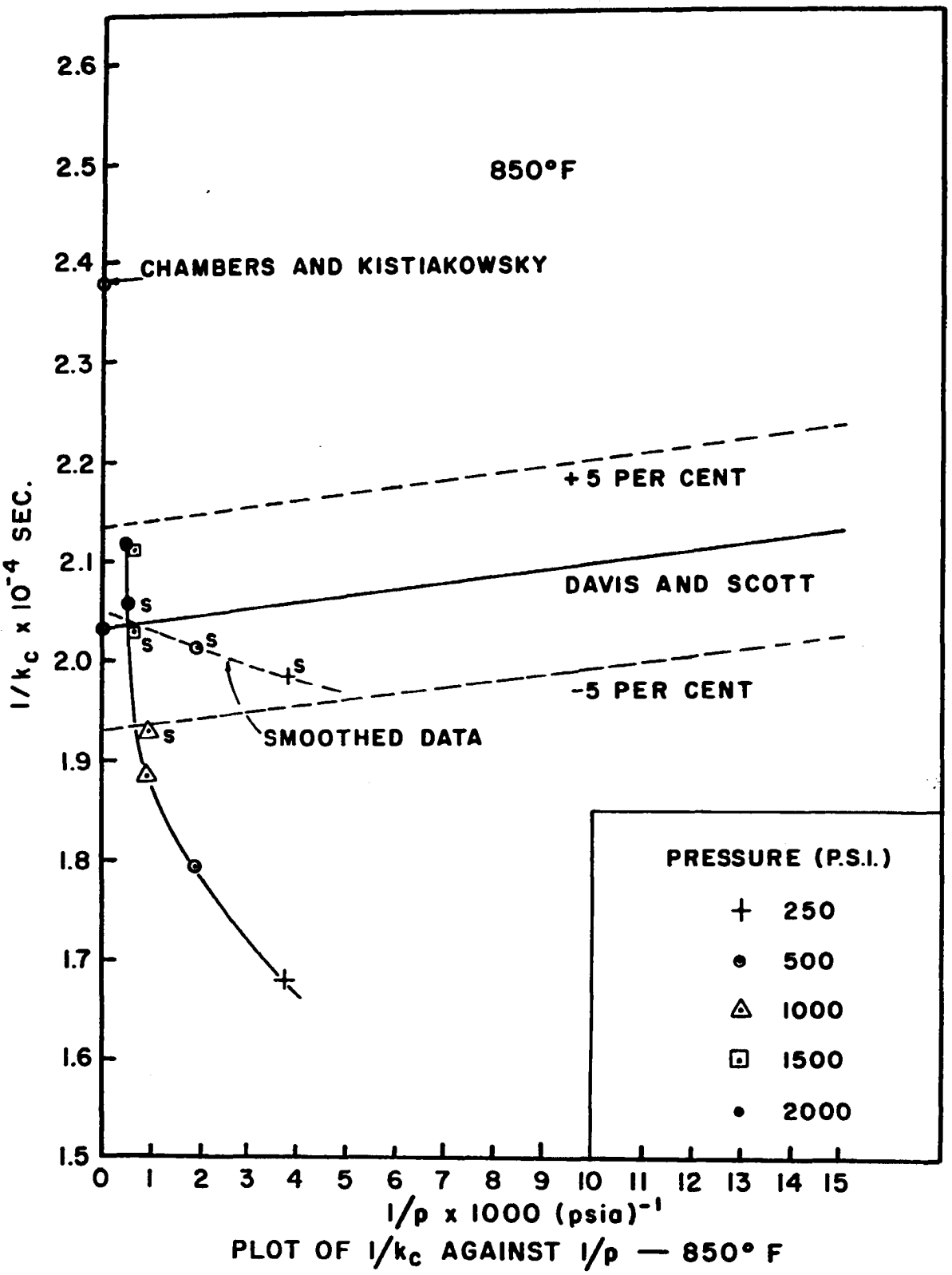

PLOT OF $1/k_c$ AGAINST $1/p$ — 850° F

FIGURE 27

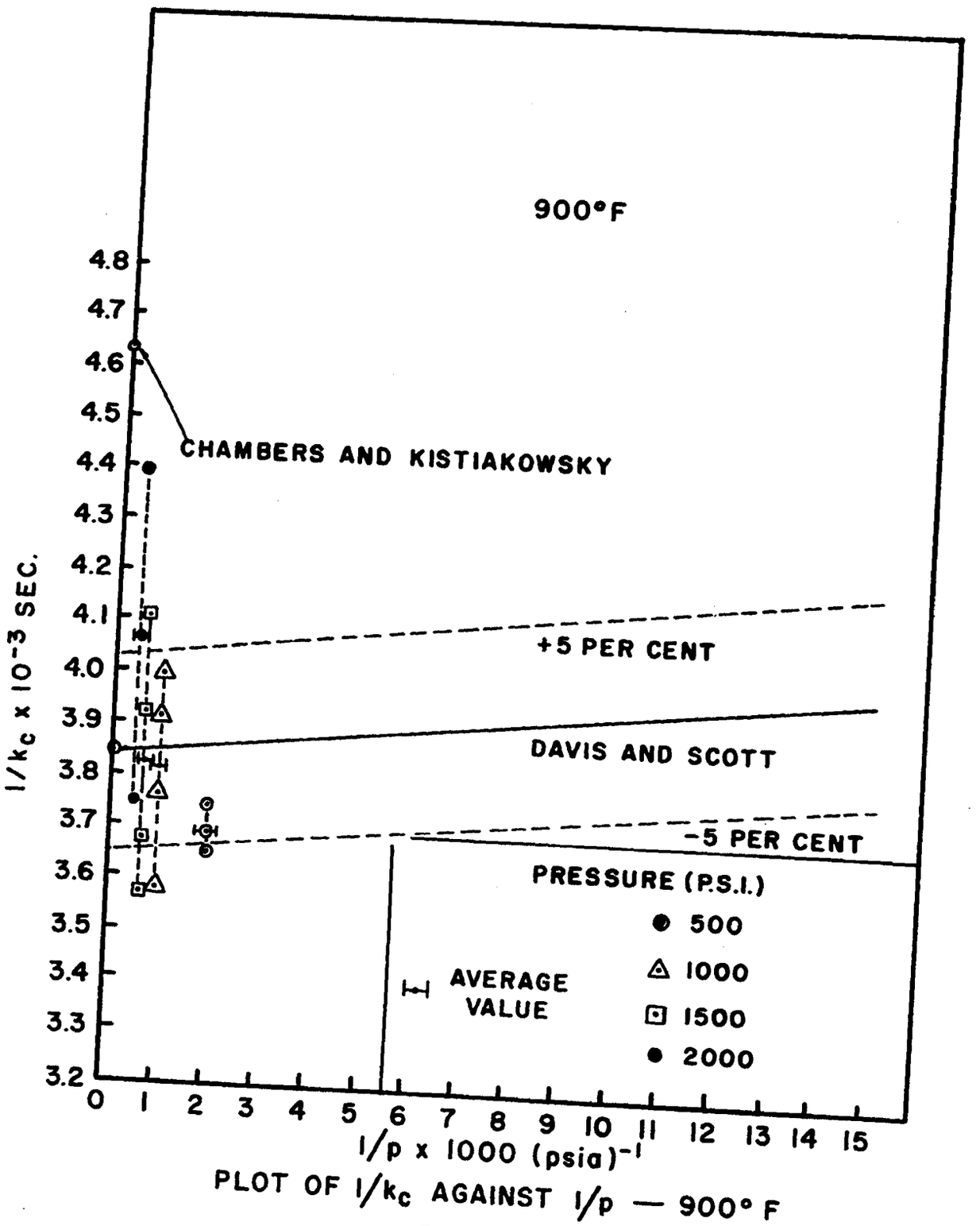

PLOT OF $1/k_c$ AGAINST $1/p$ — 900° F

FIGURE 28

pressure in Figure 27 is of special interest. Both Run III and the smoothed data show $1/k_c$ versus $1/p$ slopes which are negative instead of positive as predicted by theory. Directionally at least, this behavior could be explained by the presence of undetected polymerization. With such an explanation, the low pressure values would be considered more nearly correct; thus, especially with Run III, the values of $1/k_c$ would fall substantially below the predicted line of correlation.

At 900°F. a greater number of runs are available for analysis. These results are shown in Figure 28, where the average values at each pressure level are also identified. One observes that most of the data points are within ± 5 per cent of k_∞ calculated from the Davis and Scott equation. Again, the values of $1/k_c$ are observed to increase, rather than decrease, as pressure is increased. However, the overall effect between 500 and 2000 p.s.i., based on the average values, is only 10 per cent.

In Chapter II it was shown to be in conflict with the absolute reaction rate theory to assume that rates of elementary reactions are proportional to thermodynamic activities of the reactants. Further, for a first-order reaction, such as the thermal isomerization cyclopropane at higher pressure, the theory predicts that k_c will be essentially independent of pressure. Thus, since k_c and k_a are related by the expression

$$RTk_a = \frac{k_c}{z_m \Phi_i}$$

from Chapter VII, it is apparent that if the experimental results indicate that k_c at a given temperature is independent of pressure, then k_a, of necessity, must vary with pressure. Such results, therefore, would support the view that the reaction rate is proportional to the concentration of the activated complex----the fundamental concept of the absolute reaction rate theory. At the same time, these results would refute the argument that the rate is proportional to the reactant activity. On the other hand, if values of k_a at constant temperature were found to be invariant with respect to pressure, then the opposing view would be supported.

In Figure 29, values of RTk_a are compared with k_c for runs at 900°F. where sufficient data were available to establish trends with pressure. Unfortunately, the results presented in Figure 29 are not conclusive. For Run II the quantity RTk_a is more nearly constant and independent of pressures; whereas, with Run IX the opposite is true and k_c is the more constant quantity. The data for Run X are too widely scattered to be analyzed with certainty. In Figure 29, the results of Run IX conform with the predicted behavior from absolute reaction rate theory; that is, k_c is essentially independent of pressure, but does show a slight decrease as pressure is increased, in agreement, trend-wise, with the volume contribution term of Equation VII-31 in Chapter VII.

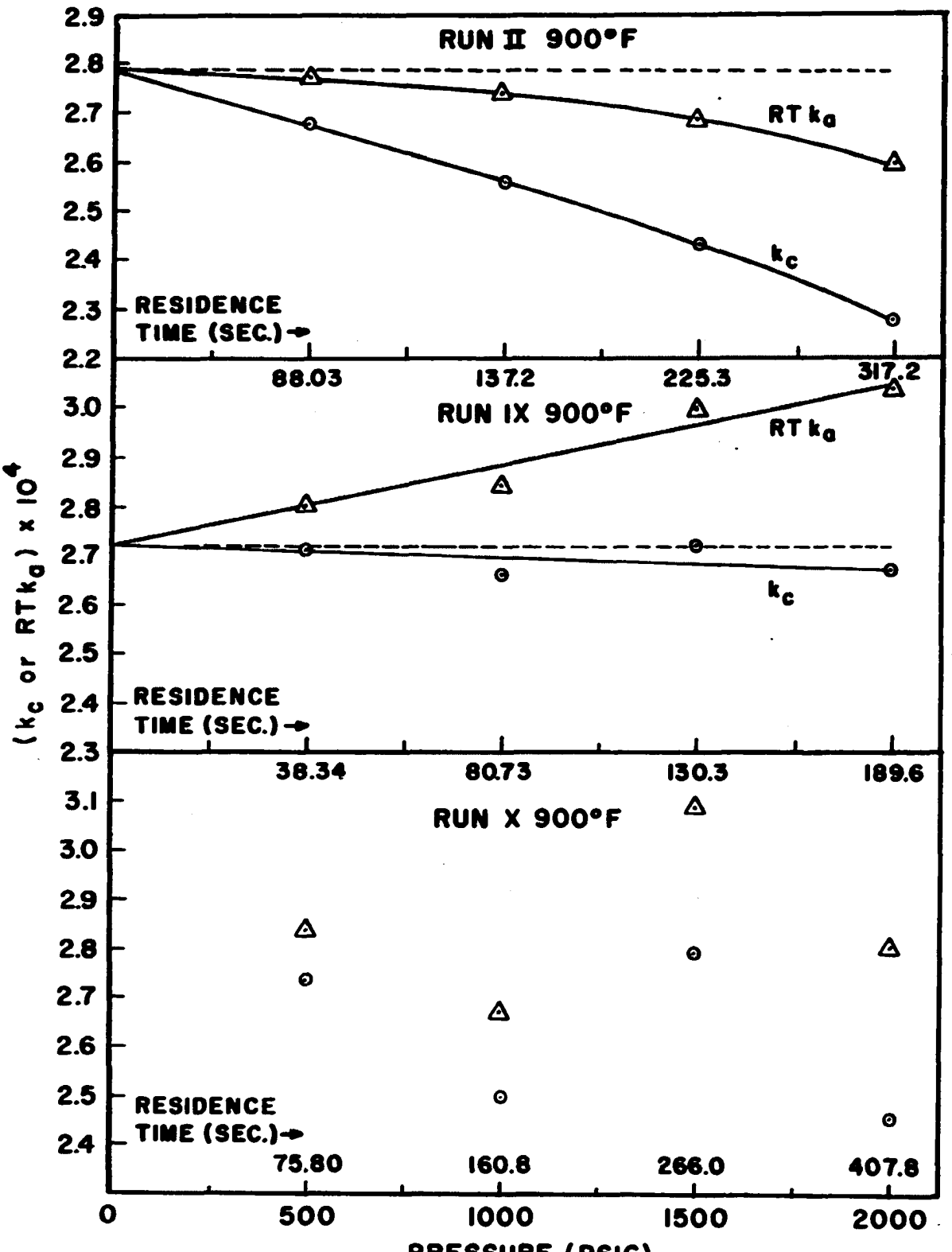

RATE CONSTANT VARIATION WITH PRESSURE

FIGURE 29

The lack of constancy in k_c for Run II could possibly be the result of undetected polymerization. It will be observed that the residence times are lower for Run IX----a fact which would reduce any polymerization effect. For this reason, the results of Run IX are perhaps more reliable than those for Runs II and X.

Plots of k_c and RTk_a against pressure for 950°F. are given in Figure 30 for Runs I and XXII. The decline in k_c with increasing pressure for Run XXII is definitely believed to be the result of undetected polymerization since when pressure was increased from 1500 to 2000 p.s.i., liquid accumulated in the product receiver. Run I was made with lower residence times and less of a decline in k_c is observed. However, from Run I, one cannot say that k_c is more independent of pressure than RTk_a.

In the preceding discussion, undetected polymerization was offered as one explanation for the negative slopes observed when the experimental data were presented in the $1/k_c$ versus $1/p$ plots of Figures 27 and 28. However, excluding polymerization, a fundamental explanation exists for negative slopes at low values of $1/p$. The simple Lindemann-Hinshelwood theory of unimolecular reactions and the statistical refinement of that theory by Rice, Ramsperger, and Kassel are represented schematically in Sketch (a) of Figure 31. Both theories yield a positive slope at the $1/k_c$ intercept. It is important to remember, however, that the statistical

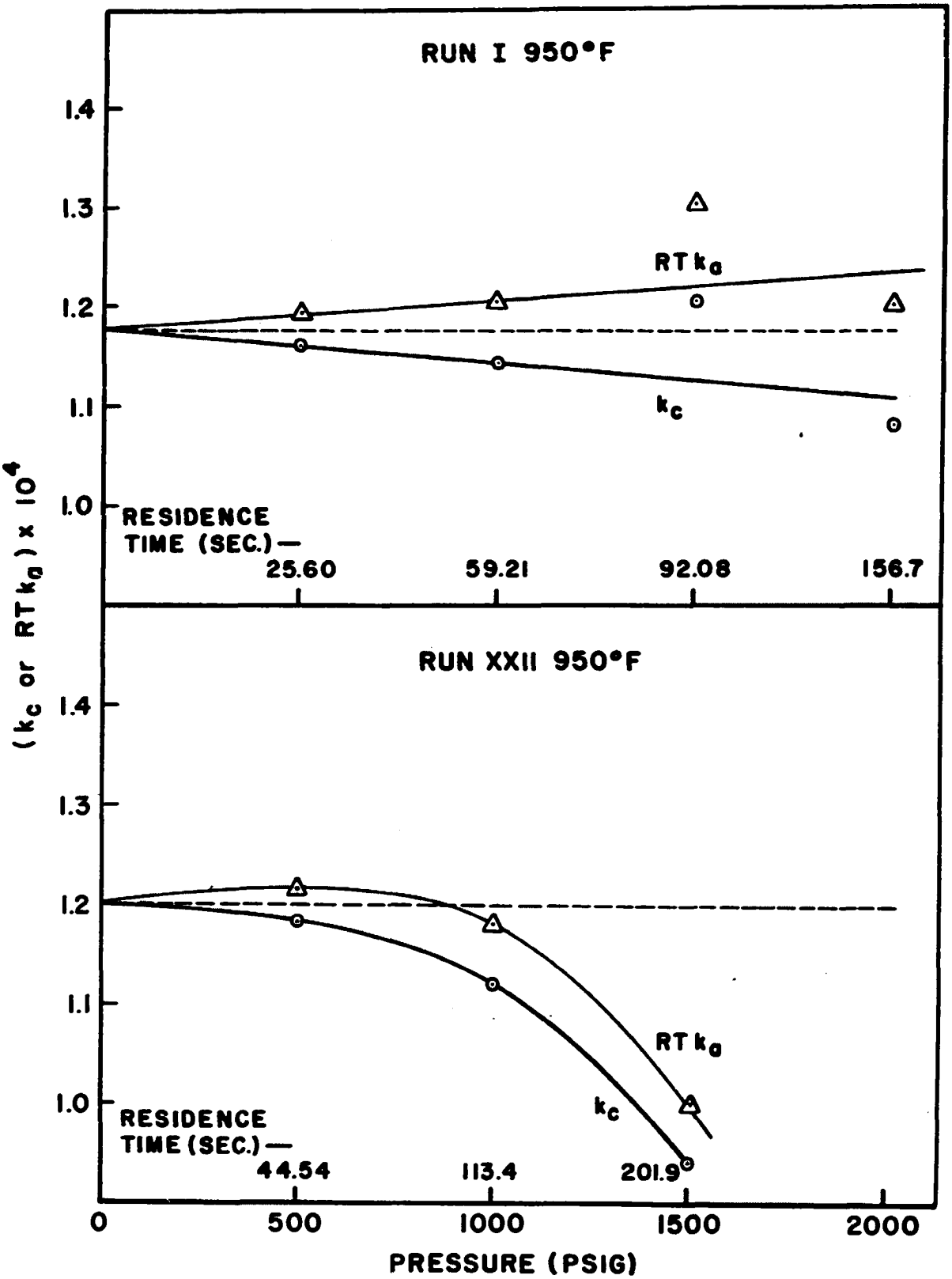

RATE CONSTANT VARIATION WITH PRESSURE

FIGURE 30

TABLE 4

SUMMARY OF DATA FOR FIGURES 29 AND 30

Run No.	(Z_m)	Φ_Δ	$(Z_m)\Phi_\Delta$	$k_c(\text{sec.})^{-1}$	$RTk_a(\text{sec.})^{-1}$
			900°F.		
II-1	0.985	0.980	0.965	2.673×10^{-4}	2.770×10^{-4}
II-2	0.972	0.962	0.935	2.555×10^{-4}	2.733×10^{-4}
II-3	0.955	0.947	0.904	2.428×10^{-4}	2.686×10^{-4}
II-4	0.942	0.932	0.878	2.276×10^{-4}	2.592×10^{-4}
IX-1	0.985	0.980	0.965	2.707×10^{-4}	2.805×10^{-4}
IX-2	0.973	0.962	0.936	2.658×10^{-4}	2.840×10^{-4}
IX-3	0.956	0.947	0.905	2.718×10^{-4}	3.003×10^{-4}
IX-4	0.942	0.932	0.878	2.669×10^{-4}	3.040×10^{-4}
X-1	0.984	0.980	0.964	2.740×10^{-4}	2.842×10^{-4}
X-2	0.972	0.962	0.935	2.498×10^{-4}	2.672×10^{-4}
X-3	0.955	0.947	0.904	2.797×10^{-4}	3.094×10^{-4}
X-4	0.941	0.932	0.877	2.459×10^{-4}	2.804×10^{-4}
			950°F.		
I-1	0.989	0.983	0.972	1.160×10^{-3}	1.193×10^{-3}
I-2	0.979	0.968	0.948	1.142×10^{-3}	1.205×10^{-3}
I-3	0.964	0.958	0.924	1.205×10^{-3}	1.304×10^{-3}
I-4	0.952	0.945	0.900	1.082×10^{-3}	1.202×10^{-3}
XXII-1	0.988	0.983	0.971	1.182×10^{-3}	1.217×10^{-3}
XXII-2	0.978	0.968	0.947	1.120×10^{-3}	1.183×10^{-3}
XXII-3	0.965	0.958	0.924	0.941×10^{-3}	1.018×10^{-3}

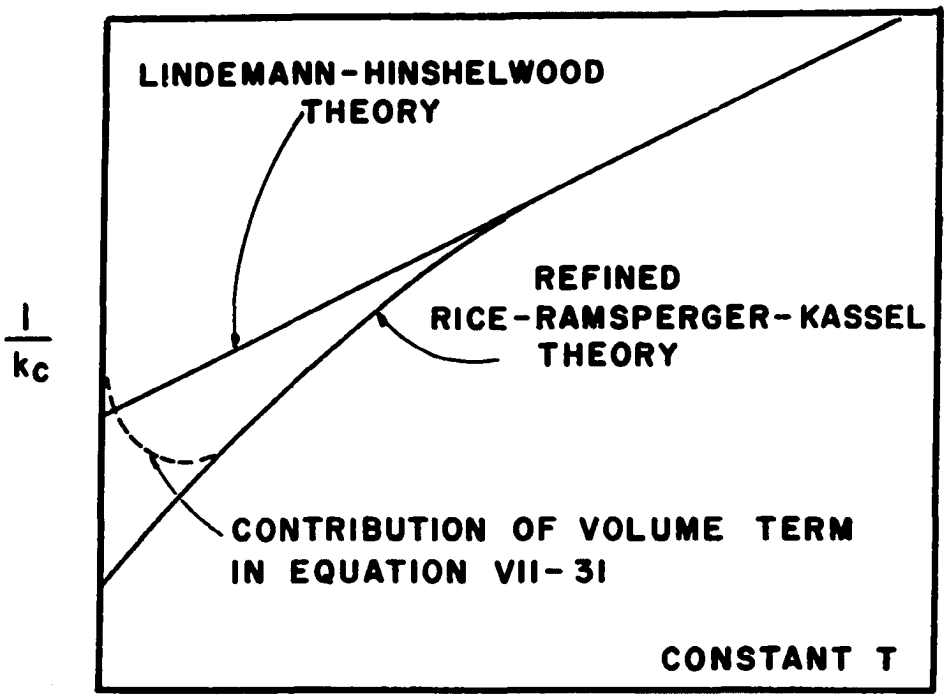

SKETCH (a)

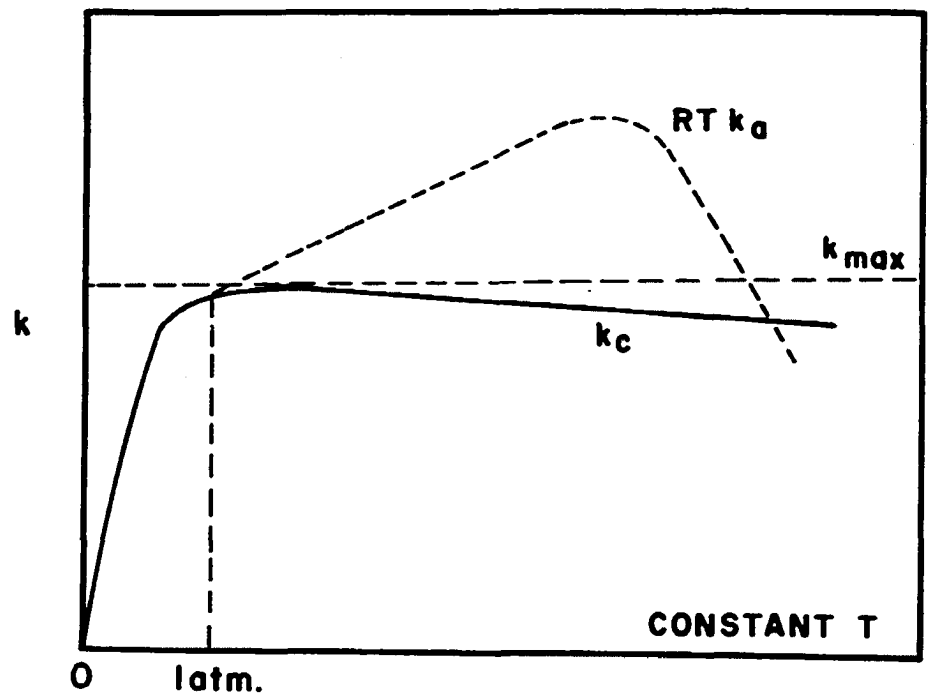

SKETCH (b)

EFFECT OF NONIDEAL BEHAVIOR AT HIGH PRESSURE ON THE UNIMOLECULAR REACTION RATE CONSTANT.

FIGURE 31

treatments do not consider the nonideal behavior at high pressure represented by the contribution of the volume term in Equation VII-31. From Equation VII-31 it is apparent that at some pressure the quantity k_c will pass through a maximum value where the derivative $\partial \ln k_c/\partial p$ vanishes and the result $\frac{v_A - v}{RT} = \frac{\partial \ln(1+\xi k_\infty/p)}{\partial p}$ holds. Though Equation VII-31 is developed in terms of the Lindemann-Hinshelwood theory, the same argument applies with the Rice-Ramsperger-Kassel refinement. The maximum k_c value will of course be represented by a minimum $1/k_c$ value in a plot of $1/k_c$ versus $1/p$, as indicated schematically in Sketch (a) of Figure 31.

The expected k_c versus p relationship from Equation VII-31 is also shown schematically in Sketch (b) of Figure 31. Below atmospheric pressure the departure from first-order behavior is indicated. At some pressure above one atmosphere, the two terms on the right hand side of Equation VII-31 will cancel each other at the point of maximum k_c. As pressure is increased, the second term on the right hand side of Equation VII-31 declines in importance and the slope of the k_c versus p curve is controlled by the volume term. The expected behavior of RTk_a is also indicated in Sketch (b) of Figure 31.

Returning again to the $1/k_c$ versus $1/p$ plots in Figure 27 and 28, and to Sketch (a) of Figure 31, it appears that one might profitably seek a minimum $1/k_c$ value in the

pressure range from one atmosphere to 250 p.s.i. Such an investigation could be carried-out in Pyrex glass apparatus. Additional high pressure data at very low residence times would be helpful in establishing whether or not undetected polymerization is significant.

CHAPTER IX

CONCLUSIONS

As was shown in the theoretical treatment, page 14-30, the viewpoint that reaction rates for elementary reactions under nonideal conditions are directly proportional to the thermodynamic activities is in conflict with absolute reaction rate theory. This study is believed to be the first attempt to resolve this discrepancy by an experimental investigation of a unimolecular, homogeneous, gas-phase reaction at elevated pressures. The advantage of this particular reaction system lies in the similarity in the properties of the reactant and its activated complex.

In total, these results for the thermal isomerization of cyclopropane at high pressure have not supported the absolute reaction rate theory, conclusively. However, those runs which are least likely to be affected by undetected polymerization (i.e., those runs with low residence times) have yielded values of k_c which are essentially constant, but which decline slightly with increasing pressure in accordance with the result predicted by absolute reaction rate theory.

In general, the experimental values of k_c at high

pressure are in close agreement with the k_∞ values from the equation by Davis and Scott. For example, at 500 p.s.i. where the most data were available for correlation, the experimental activation energy of 65,380 calories/g-mole, as determined by least squares fit of the Arrhenius equation, is only 0.3 per cent lower than the value reported in the equation for k_∞ by Davis and Scott.

Plots of $1/k_c$ versus $1/p$ reveal an interesting departure from the usual representation of the unimolecular reaction theory. The experimental results show an increase in $1/k_c$ as $1/p$ approaches zero; whereas, even in the refined unimolecular theory, a positive slope is predicted at the $1/k_c$ intercept. While it has not been possible to resolve to what extent the anomolous behavior may be the result of undetected polymerization, it has been shown that there is a fundamental explanation for negative slopes at low values of $1/p$. In fact, the usual straight line extrapolation to the $1/k_c$ intercept is erroneous because of failure to consider the nonideal behavior at high pressure.

Gold has been shown to be noncatalytic to the cyclopropane isomerization reaction, beyond reasonable doubt. Type 316 stainless is catalytic to the reaction and promotes the formation of other products in addition to propylene. The fluidized sand technique has been demonstrated to be a reliable means for obtaining isothermal reaction conditions at high temperature.

There are two areas in which continued study of the cyclopropane thermal isomerization reaction would be profitable: (1) the pressure region between one atmosphere and 250 p.s.i. where a maximum value of k_c is indicated, and (2) the high pressure region, but with low residence times to reduce the possibility of undetected polymerization.

Further, if a unimolecular, homogeneous, gas-phase reaction should be found which is free of such complications as polymerization and the formation of multiple products, and for which the deviation from ideal gas behavior is greater than was the case for the cyclopropane isomerization reaction, a high pressure kinetic study of that reaction would be recommended to provide an additional test of the theory.

NOMENCLATURE

a = thermodynamic activity

A = species A in stoichiometric equation

= frequency factor in Arrhenius equation

A^* = concentration of activated molecules A*

A_{cs} = reactor cross-sectional area

B = species B in stoichiometric equation

c = molar concentration, Appendix D

C = molar concentration

= dimensionless concentration, c/c_o, Appendix D

C_p = heat capacity at constant pressure

d = reactor diameter

D = diffusion coefficient

E = Young's modulus

E_A = energy of activation

f = fugacity

= partition function, Equation II-48

= indication of functional relationship

f' = proportionality constant, Equation II-59

F_o = reactor molar feed rate

F_T = residence time distribution function, Appendix D

G = Gibbs free energy

ΔG° = reaction standard state free energy change

h = Planck's constant

= heat transfer coefficient

H = enthalpy

$\dot{H}$ = rate of enthalpy transport by bulk flow

ΔH_R = heat of reaction at constant pressure

ΔH^O = standard state heat of reaction

$H(\tau-\tau_o)$ = residence time step function, Appendix D

k = specific rate constant

= thermal conductivity

k_a = specific rate constant defined in terms of activities

k_B = Boltzman constant

k_C = specific rate constant defined in terms of concentration

k_∞ = extrapolated high pressure rate constant from unimolecular theory

K = equilibrium constant

= ratio of cylinder outside to inside diameter, Appendix C

K_C^* = concentration equilibrium constant for reactants and activated complex

L = axial length of cylinder, Appendix C

m = number of product stream analyses used in obtaining mean peak height ratio $\overline{x}_m$, Appendix A

m* = active mass, Equation II-22

= effective mass of activated complex, Equation II-48

M = molecular weight

n = number of moles

= number of degrees of freedom, Equation II-19

= exponential in Equation II-26

= number of standard sample analyses used in obtaining the mean peak height ratio, $\bar{x}_n$, Appendix A

$\dot{n}$ = molar rate of transport

P = pressure

q = reactor wall heat transfer flux

q_1 = a generic term representing arbitrary independent variable, Appendix A

Q = dependent variable, Appendix A

r = rate of reaction

= radius variable, Equation VII-4

= molecular radius, Equation II-4

R = gas law constant

= reactor inside radius

= peak height ratio, cyclopropane peak height divided by propylene peak height, Appendix A

s = estimate of population standard deviation for n analyses, Appendix A

S = numerical value of tangent, Figure 11 and Appendix A

= entropy

$\Delta S°$ = entropy of reaction in standard state

t = reaction time variable

= "Student" t statistic, Appendix A

T = temperature

T_w = reactor wall temperature

U = dimensionless radius, Appendix D

v = local velocity of flow in reactor

v_o = reactor central streamline velocity

v* = molar average velocity

$\langle v \rangle$ = average velocity over reactor cross-section

$\underline{v}^*$ = activated complex specific molar volume

$\underline{v}_A$ = specific molar volume of pure component A

V = volume

V_R = total reactor volume

x_i = peak height ratio for a single analysis i, Appendix A

$\overline{x}_m$ = mean peak height ratio for m analyses of the product gas stream, Appendix A

$\overline{x}_n$ = mean peak height ratio for n analyses of a standard sample, Appendix A

y = mole fraction

z = positive integer or its reciprocal, Equation II-32

= reactor length variable

z_o = number of collisions from kinetic theory of gases

z = compressibility factor

(Z_m) = mixture average compressibility factor, Equation VII-10

Greek

α = thermal coefficient of expansion, Appendix C

= dimensionless diffusion parameter, $D/k_c R^2$, Appendix D

= dimensionless ratio, $k_c/C\ k_2$, Equation VII-27

α = activity coefficient, defined as a/C

β = concentration dependent term in Equation II-27

= constant in Equation II-16

= the quantity $\alpha E \Delta T/(1-\nu)$, Appendix C

= the dimensionless quantity $(\alpha^2+4\alpha)^{\frac{1}{2}}$, Equation VII-27

γ = the functional form of Q in terms of the q_n independent variables, Appendix A

= activity coefficient for departure from ideal solution behavior

δ = length at top of energy barrier, Equation II-48

Δ = symbol for Difference

ϵ = strain, Appendix C

θ = dimensionless temperature, T/T_w

= radial angle, Appendix C

$\varkappa$ = transmission coefficient

λ = contact time parameter, $k_c z/v_o$, Appendix D

μ = true population mean, Appendix A

μ_m = mixture viscosity, Appendix D

ν = stoichiometric coefficient

= frequency in Equation II-47

= Poisson's ratio, Appendix C

ξ = slope in $1/k_c$ versus 1/p plot

= de Donder's degree of advancement, Appendix I

ρ_m = mixture mass density, Appendix D

σ = true population standard deviation, Appendix A

= molecular dimension Equation II-19

σ = principal stress, Appendix C

$\bar{\sigma}_m$ = true standard deviation of the means for sample size m, Appendix A

σ_r = radial tensile stress, Appendix C

σ_t = tangential tensile stress, Appendix C

τ = residence time

= shear stress, Appendix C

τ_o = residence time of center streamline

$\langle\tau\rangle$ = average residence time over reactor cross-section

Φ_i = fugacity coefficient of pure component i, f_i/P

$\bar{\Phi}_i$ = fugacity coefficient of component i in the mixture, $\bar{f}_i/y_iP$

ψ = function of nonthermodynamic variables, Equation II-27

Subscripts

a = definition in terms of activities

A = component A (usually signifies cyclopropane)

AB = property of binary AB

b = backward

B = component B (usually signifies propylene)

c = definition in terms of concentrations

= compressive, Appendix C

e = equilibrium condition

f = forward

i = component i or variable i

I = inlet condition

j = variable j

m = mixture property

n = n-th variable

o = outlet condition

r = radial

R = property of reaction; e.g., ΔG_R = free energy of reaction

t = tangential

t(1) = one translational degree of freedom

w = wall

y = yield point

z = axial

∞ = infinite pressure value by extrapolation

γ = equilibrium ratio of activity coefficients, Equation II-37

Δ = Cyclopropane

1,2 = location 1 and 2, or reaction 1 and 2

Superscripts

° = standard state property

* = activated complex or active mass

Super-bar = partial property of component in solution

Sub-bar = specific property; e.g., $\underline{v}$ is specific molar volume

LITERATURE CITED

1. Bak, T., "Contributions to the Theory of Chemical Kinetics," W. A. Benjamin, Inc., New York, (1963).

2. Batten, J. J., "A Possible Error in the Measurement of Rate Constants of Gaseous Reactions by Flow Techniques," Aust. J. Appl. Sci. (No. 1), 12, 12 (1961).

3. Bell, R. P., "Acid-Base Catalysis, Oxford University Press, London, (1941).

4. Benson, S. W., "Reaction of Cyclopropane with Iodine and Some Observations on the Isomerization of Cyclopropane," J. Chem. Phys. 34, 521 (1960).

5. Berthelot, M. P. E., Ann. Chim. Phys. (7), 20, 27 (1900).

5a. Bird, R. B., W. E. Stewart and E. N. Lightfoot, "Transport Phenomena," John Wiley and Sons, Inc., New York, (1960).

6. Blade, A. T., "The Hydrogen Isotope Effect in the Pyrolysis of Cyclopropane," Can. J. Chem. 39, 1401 (1961).

7. Bosworth, R. C. L., "Distribution of Reaction Times for Laminar Flow in Cylindrical Reactors," Phil. Mag. (London) (No. 7), 39, 847 (1948).

8. Brown, B., "Catalytic Isomerization of Cyclopropane," Ph. D. Thesis, University of Washington, (1953).

9. Chambers, T. S. and G. B. Kistiakowsky, "Kinetics of the Thermal Isomerization of Cyclopropane," J. Am. Chem. Soc. 56, 399-405 (1934).

10. Chambre, P. L., "On Chemical Reactions in Internal Flow Systems," Appl. sci. Res., A9, 157 (1960).

11. Cleland, F. A., and R. H. Wilhelm, "Diffusion and Reaction in Viscous-flow Tubular Reactor," A.I.Ch.E. Journal 2, 489 (1956).

12. Corner, E. S. and R. N. Pease, "Kinetics and Mechanism of the Isomerization of Cyclopropane," J. Am. Chem. Soc. 67, 2067-2071 (1945).

13. Danckwerts, P. V., "Continuous Flow Systems-distribution of residence times," Chem. Eng. Sci., 2, 1 (1953).

14. Davis, B. R. and D. S. Scott, "Rate of Isomerization of Cyclopropane in a Flow Reactor," Ind. Eng. Chem. 3, 20 (1964).

15. Denbigh, K. G., "The Thermodynamics of the Steady State," Methuen and Co. Ltd., London, (1958).

16. Denbigh, K. G., "The Principles of Chemical Equilibrium," Cambridge University Press, London, (1961).

16a. Eckert, C. A. and M. Boudart, "On the Use of Fugacities in Gas Kinetics," Chem. Eng. Sci. 18, 144 (1963).

17. Egloff, G., "Reaction of Pure Hydrocarbons," Reinhold Publishing Corp., (1937).

18. Eyring, H. and F. M. Eyring, "Modern Chemical Kinetics," Reinhold Publishing Corp., New York, (1963).

19. Falconer, W. E., T. F. Hunter and A. F. Trotman-Dickenson, "The Thermal Isomerization of Cyclopropane," J. Chem. Soc. 164, 609 (1961).

20. Frantz, J. F., "Design for Fluidization," Part 2, Chemical Engineering, p. 89, (Oct. 1, 1962).

21. Frost, A. A., "Effect of Concentration on Reaction Rate and Equilibrium, "J. Chem. Ed. 18, 272 (1941).

22. Gadsby, Hinshelwood, and Sykes, Proc. Roy. Soc. (London) 187, 129 (1946).

23. Glasstone, S., K. J. Laidler, and H. Eyring, "The Theory of Rate Processes," McGraw-Hill Book Company, Inc. New York, (1941).

24. Gonikberg, M. G., "Chemical Equilibria and Reaction Rates at High Pressure," N. S. F. Publication (translated from Russian), Washington, D. C., (1963).

25. Grosse, A. V. and C. B. Linn, "Refraction Data on Liquid C_3-Hydrocarbons," J. Am. Chem. Soc. 61, 75 (1939).

26. Hall, J. W. and H. F. Rase, "Relation between Dislocation Density and Catalytic Activity and Effects of Physical Treatment," Ind. Eng. Chem. 3, 158 (1964).

27. Hamann, S. D., "Physico-Chemical Effects of Pressure," Butterworths, London, (1957).

28. Hinshelwood, C. N., "On the Theory of Unimolecular Reactions," Proc. Roy. Soc., 113A, 230 (1926).

29. Hollingsworth, C. A., "Equilibrium and the Rate Laws for Forward and Reverse Reactions," J. Chem. Phys. 20, 921 (1952).

30. Hollingsworth, C. A., "Equilibrium and the Rate Laws," J. Chem. Phys. 20, 1649 (1952).

31. Hougen, O. A. and K. M. Watson, "Kinetics and Catalysis," John Wiley and Sons, Inc., New York, (1947).

32. Hougen, O. A., K. M. Watson and R. A. Ragatz, "Chemical Process Principles," (2nd. Ed.), John Wiley and Sons, Inc., New York, (1958).

33. Hurd, C. V. and R. N. Meinert, "The Pyrolysis of Propylene," J. Amer. Chem. Soc. 52, 4978 (1930).

34. Ipatieff, V. N., "Catalytic Reactions at High Pressure and Temperatures," Macmillan, (1936).

35. Ipatieff, W., and W. Huhn, Ber. 35, 1063 (1902).

36. Ipatieff, W., and W. Huhn, Ber. 36, 2014 (1903).

37. Kassel, L. S., "Kinetics of Homogeneous Gas Reactions," The Chemical Catalog Co., Inc., New York, (1932).

38. Kassel, L. S., "Studies in Homogeneous Gas Reactions," J. Phys. Chem. 32, 235 (1928).

39. Kennedy, A. D. and H. O. Pritchard, "The Thermal Isomerization of Cyclopropane at Low Pressures," J. Phys. Chem. 67, 161 (1963).

40. Kistiakowsky, G. B. and O. K. Rice, "Gaseous Heat Capacities II," J. Chem. Phys. 8, 610 (1940).

40a. Kistiakowsky, G. B., J. Amer. Chem. Soc., 50, 2315 (1928).

41. Knowlton, J. W. and F. D. Rossini, "Heats of Combustion and Formation of Cyclopropane," J. Research NBS 43, 113 (1949) RP2012.

42. Knox, J. H., "Gas Chromatography," Methuen and Co., Ltd. (London), (1962).

43. Korback, P. F. and W. E. Stewart, "Kinetic and Equilibrium Studies of Benzene Hydrogenation in Batch Recycle Reactor," Ind. Eng. Chem. 3, 24 (1964).

44. Krauze, M. V., M. S. Nemtzov and E. A. Soskina, Compt. rend. Acad. Sci. U.S.S.R., 2, 301-306 (1934).

45. Laidler, K. J., "Chemical Kinetics," McGraw-Hill Book Co., New York, (1950).

46. Laird, R. K., A. G. Morrell and L. Seed, "The Velocity of Ethylene Polymerization at High Pressures," Disc. Farad. Soc., No. 22, 126 (1956).

47. Lamé, G., "Lecons sur la Theorie Mathematique de L'Elasticite des Corps Solides," pp. 188-91, Bachelier, Paris, (1852).

48. Lambert, J. D. et al., Proc. Roy. Soc. A231, 280 (1955).

49. Langrish, J. and H. O. Pritchard, "Secondary Effects in the Thermal Decompositions of Cyclopropane and Cyclobutane," J. Phys. Chem. 62, 761 (1958).

50. Lauwerier, H. A., "A Diffusion Problem with Chemical Reaction," Appl. sci. Res., A8, 366 (1959).

51. Leffler, J. E. and E. Grunwald, "Rates and Equilibria of Organic Reactions," John Wiley and Sons, Inc., New York, (1963).

52. Lindemann, F. A., Discussion on "The Radiation Theory of Chemical Action," Trans. Faraday Soc. 17, 598 (1922).

53. Lindquist, R. H. and G. K. Rollefson, "Relative Rates of Isomerization of Cyclopropane and Cyclopropane-t_1," J. Chem. Phys. 24, 725 (1956).

54. Linnett, J. W., "Infra-red and Raman Spectra of Polyatomic Molecules, V Cyclopropane and Ethylene Oxide," J. Chem. Phys. 6, 692 (1938).

55. Lydersen, A. L., R. A. Greenkorn and O. A. Hougen, "Generalized Thermodynamic Properties of Pure Fluids," University of Wisconsin, Engineering Experiment Station, Report No. 4, (1955).

56. Manes, M., L. J. E. Hofer and S. Weller, "Classical Thermodynamics and Reaction Rates Close to Equilibrium," J. Chem. Phys. 18, 1355 (1950).

57. McNesby, J. R. and A. S. Gordon, "Mechanism of the Isomerization of Cyclopropane," J. Chem. Phys. 25, 582 (1956).

58. Perkins, T. D., "The Effect of Solid State Dislocations upon the Catalytic Activity of Metals," Ph. D. Thesis, Oklahoma University, (1963).

59. Perry, R. H., C. H. Chilton and S. D. Kirkpatrick, "Chemical Engineers' Handbook," McGraw-Hill Book Co., Inc., New York, (1963).

60. Perrin, J., Ann. Phys., (9), 11, 1 (1919).

61. Prausnitz, J. M., "Fugacities in High-Pressure Equilibria and in Rate Processes," A.I.Ch.E. Journal 5, 3 (1959).

62. Present, R. D., "Kinetic Theory of Gases," McGraw-Hill Book Co., Inc., New York, (1958).

63. Prigogine, I. and R. Defay, "Chemical Thermodynamics," John Wiley and Sons, Inc., New York, (1962).

64. Prigogine, I., P. Outer and Cl. Herbo, "Affinity and Reaction Rate Close to Equilibrium," J. Phys. Colloid Chem. 52, 321 (1948).

65. Pritchard, H. O., R. G. Sowden and A. F. Trotman-Dickenson, "The Isomerization of Cyclopropane-A Quasi-Unimolecular Reaction," J. Am. Chem. Soc. 74, 4472 (1952).

66. Pritchard, H. O., R. G. Sowden and A. F. Trotman-Dickenson, "II. The Isomerization of Cyclopropane-A Quasi-Unimolecular Reaction," Proc. Royal Soc. A217, 563 (1953).

67. Purnell, H., "Gas Chromatography," John Wiley and Sons, Inc. (1962).

68. Rabinovitch, B. S., E. W. Schlag and K. B. Wiberg, "Geometrical and Structural Unimolecular Isomerization of Symcyclopropane-d_2," J. Chem. Phys. 28, 504 (1958).

69. Reid, R. C. and T. K. Sherwood, "The Properties of Gases and Liquids," McGraw-Hill, New York, (1958).

70. Rice, O. K., and H. C. Ramsperger, "Theories of Unimolecular Gas Reactions at Low Pressure," J. Am. Chem. Soc. 49, 1617 (1927).

71. Roberts, R. M., "Catalytic Isomerization of Cyclopropane," J. Phys. Chem. 63, 1400 (1959).

72. Roginski, S. Z. and F. H. Rathmann, J. Am. Chem. Soc. 55, 2800 (1933).

73. Ruehrwein, R. A. and T. M. Powell, "The Heat Capacity, Vapor Pressure, Heats of Fusion and Vaporization of Cyclopropane. Entropy and Density of the Gas," J. Am. Chem. Soc. 68, 1063 (1946).

74. Scott, R. B., "Cryogenic Engineering," D. Van Nostrand Company, Inc., New York, (1959).

75. Skinner, J. L., "Kinetic Study of the Formation of Cyclohexene from Ethylene and Butadiene at Elevated Pressures and Temperatures," Ph. D. Thesis, Oklahoma University, (1962).

76. Slater, N. B., "The Theoretical Rate of Isomerization of Cyclopropane," Proc. Royal Soc. (London) A218, 224 (1953).

77. Slater, N. B., "Theory of Unimolecular Reactions," Cornell University Press, Ithaca, N. Y., (1959).

78. Slater, N. B., "Theoretical Temperature Dependence of the Rate of Isomerization of Cyclopropane," J. Chem. Soc. 164, 606 (1961).

79. Spencer, H. M., "Empirical Heat Capacity Equations of Various Gases," J. Am. Chem. Soc. 67, 1859 (1945).

80. Sullivan, F. W., R. F. Ruthruff and W. E. Kuentzel, "Pyrolysis and Polymerization of Gaseous Paraffins and Olefins," Ind. Eng. Chem. 27, 1072 (1935).

81. Tanatar, S., Ber. 29, 1297 (1896).

82. Tanatar, S., Ber. 32, 702 (1899).

83. Tanatar, S., Z. Physik Chem. 41, 735 (1902)

84. Trautz, M. and K. Winkler, J. Prakt. Chem. (2) 104, 53 (1922).

85. Timoshenko, S., and J. N. Goodier, "Theory of Elasticity," 2nd. Ed., McGraw-Hill, New York, (1951).

86. Ubbelohde, A. R., General Discussion, Disc. Farad. Soc., No. 22, 147 (1956).

87. Volk, W., "Applied Statistics for Engineers," McGraw-Hill Book Co., New York, (1958).

88. Volkov, A. and B. N. Menshutkin, Ber. 31, 3067 (1898).

89. Voorhees, H. R., C. M. Sliepcevich and J. W. Freeman, "Thick-Walled Pressure Vessels," Ind. Eng. Chem. 48, 872 (1956).

90. Walas, S. M., "Reaction Kinetics for Chemical Engineers," McGraw-Hill Book Co., New York, (1959).

91. Weston, Jr., R. E., "Tritium Isotope Effect in the Isomerization of Cyclopropane," J. Chem. Phys. 23, 988 (1955).

92. Weston, Jr., R. E., "Effect of Pressure on the Isotope Effect in a Unimolecular Gaseous Reaction: Tritium and Carbon-13 Effects in the Isomerization of Cyclopropane," J. Chem. Phys. 26, 975 (1957).

93. Whalley, E., General Discussion, Disc. Farad. Soc., No. 22, 148 (1956).

94. Whalley, E., "The Design of Pressure Vessels Subjected to Thermal Stress-I. General Theory for Monoblock Vessels," Can. J. Tech. (5) 34, 268 (1956).

95. Whalley, E., "The Design of Pressure Vessels Subjected to Thermal Stress-II. Steady State Temperature Distribution," Can. J. Tech. (5) 34, 291 (1956).

96. Wissler, E. H. and R. S. Schechter, "A Further Note on a Diffusion Problem with Chemical Reaction," Appl. sci. Res., A10, 198 (1961).

97. Yang, K. H. and O. A. Hougen, "Determination of Mechanism of Catalyzed Gaseous Reactions," C.E.P. 46, 146 (1950).

98. Zenz, F. A. and D. F. Othmer, "Fluidization and Fluid-Particle Systems," Reinhold Publishing Corp., New York, (1960).

APPENDIX A

ANALYSIS OF CHROMATOGRAPH CALIBRATION

The objective of this section is to demonstrate the precision with which Figure 32 may be used to predict composition of the product gas stream, when either single or multiple samples are employed.

For each standard sample analyzed, and hence for each point used in the preparation of Figure 32, the best estimate of the peak height ratio standard deviation from n analyses is

$$s = \frac{\sum_{i}^{n} (x_i - \bar{x}_n)^2}{n-1} \qquad \text{A-1}$$

where x_i is the peak height ratio for a single analysis i and $\bar{x}_n$ is the arithmetic mean peak height ratio for n analyses; i.e., $\bar{x}_n = n^{-1}\Sigma_i^n x_i$, (See Table 5).

Since the estimated standard deviation of peak height ratio, s, applies to variation about the true mean, it is necessary to obtain some estimate of the true mean, μ, from the arithmetic mean, $\bar{x}_n$, for n samples. This estimate can be accomplished through use of the "Student" t statistic (87, p. 100), defined as

$$t = \frac{(\bar{x}_n - \mu)}{s/\sqrt{n}} \qquad \text{A-2}$$

where t is a function of degrees of freedom (i.e., D.F. = n-1) and probability (or confidence limits). Thus, for a specified confidence limit, the true mean will be in a range $\pm ts/\sqrt{n}$ about the arithmetic mean for the n analyses.

For a system of normal distribution the true mean, μ, can be estimated from a single measurement, x_i, within a specified confidence range, by the expression

$$\mu = x_i \pm z\sigma \qquad \text{A-3}$$

where σ is the true standard deviation for the normally distributed propulation of analyses and z is the standard deviate, another statistic analogous to t which is a function only of the confidence range demanded in the estimation of μ. The true standard deviation, σ, is not known, of course, but one has available the best estimate s.

Since the true mean is within a range $\pm tx/\sqrt{n}$ of $\bar{x}_n$ for a specified confidence limit, and a single analysis is within the range $\pm$ zs of the true mean for the same confidence limit, then x_i may differ from $\bar{x}_n$ by as much as $\pm(\frac{ts}{\sqrt{n}} + zs)$.

The case is now explored where the mean peak height ratio, $\bar{x}_m$, for m samples is used in Figure 32 to determine the composition. From a theorem in statistics (87, p. 101), it is known that $\bar{\sigma}_m = \frac{\sigma}{\sqrt{m}}$; i.e., the standard deviation of the means of sample size m is equal to the true population standard deviation divided by the square root of number of

samples used in determining the mean. It is important to note that m does not correspond to n, the number of samples used in obtaining the mean peak height ratio for Figure 32. Again using the best estimate of the standard deviation, $\bar{s}_m \approx \frac{s}{\sqrt{m}}$, then, within certain specified confidence limits, $\bar{x}_m$ will be in the range $\pm \left(\frac{ts}{\sqrt{n}} + z\frac{s}{\sqrt{m}}\right)$ about $\bar{x}_n$. These values are tabulated in Table 6 and may be related to an expected range of variation in the predicted composition as shown in the paragraph which follows.

In general, any dependent quantity Q can be related to the various independent variables q_n in the functional form

$$Q = \gamma(q_1, q_2 \ldots q_n) \qquad \text{A-4}$$

and the differential change in Q is

$$dQ = \sum_{i=1}^{n} \frac{\partial \gamma}{\partial q_i} dq_i \qquad \text{A-5}$$

For small changes in the independent variable, such as errors in measurement or calculation, Equation A-5 can be expressed in finite difference form

$$\Delta Q = \sum_{i=1}^{m} \frac{\partial \gamma}{\partial q_i} \Delta q_i \qquad \text{A-6}$$

Thus, in the use of Figure 32 for the prediction of cyclopropane composition, Equation A-6 reduces the following simple expression for relating the confidence range in peak height ratio to a confidence range in cyclopropane composition:

$$\Delta Q = \frac{d\gamma}{dq_1} \Delta q_1 \qquad \text{A-7}$$

In Equation A-7, ΔQ represents the confidence range for cyclopropane composition, $d\gamma/dq_1 = S$ is simply the slope of the curve in Figure 32 at the particular peak height ratio envolved, and Δq_1 represents the confidence range in peak height ratio; i.e., $\Delta q_1 = \bar{x}_m - \bar{x}_n$. The estimated ranges of absolute and relative errors occurring in the prediction of cyclopropane composition from Figure 32 are recorded in Table 7.

TABLE 5

STANDARD SAMPLE COMPOSITIONS AND PEAK HEIGHT RATIOS

Bomb No.	Cyclopropane Percentage	Number of Samples Analyzed n	Peak Height Ratio** Arithmetic Mean $\bar{x}_n$	Peak Height Ratio Standard Deviation* s
1	6.19	8	0.0648	0.000667
2	17.27	9	0.2092	0.00260
3	26.92	5	0.3472	0.00193
4	40.67	5	0.5822	0.00209
5	63.25	6	1.179	0.00771
7	78.49	5	2.130	0.00885
9	87.42	5	3.702	0.0163

$$* \quad s = \frac{\Sigma_i^n (x_i - \bar{x}_n)^2}{n - 1}$$

** Peak Height Ratio = $\frac{\text{Cyclopropane Peak Height}}{\text{Propylene Peak Height}}$

TABLE 5

PEAK HEIGHT RATIO 95 PER CENT CONFIDENCE RANGE

FOR SINGLE, DUPLICATE AND TRIPLICATE SAMPLING

Bomb No.	n	t	$\frac{ts}{\sqrt{n}}$	$\bar{x}_m - \bar{x}_n = \pm \frac{ts}{\sqrt{n}} + \frac{zs}{\sqrt{m}}$		
				m = 1	m = 2	m = 3
1	8	2.365	0.000557	±0.001867	±0.001483	±0.001313
2	9	2.306	0.00200	±0.00710	±0.00561	±0.00494
3	5	2.776	0.00239	±0.00614	±0.00504	±0.00455
4	5	2.776	0.00259	±0.00686	±0.00561	±0.00505
5	6	2.571	0.00809	±0.02319	±0.01877	±0.01680
7	5	2.776	0.01098	±0.02828	±0.02321	±0.02096
9	5	2.776	0.02022	±0.05211	±0.04278	±0.03862

Note:

t and z values from Volk's (87) Table 6.1

TABLE 7

RANGE OF ERROR IN THE PREDICTION OF COMPOSITION

FROM FIGURE 32 (WITH 95 PER CENT CONFIDENCE)

Cyclopropane Percentage	$S = \frac{d\Delta\%}{d\ R}$	Cyclopropane Percentage Absolute Error Range $s\ (\bar{x}_m - \bar{x}_n)$			Relative Per Cent Error		
		m = 1	m = 2	m = 3	m = 1	m = 2	m = 3
6.19	85	0.159	0.126	0.112	2.57	2.04	1.81
17.27	78	0.554	0.438	0.386	3.21	2.54	2.24
26.92	68.4	0.420	0.345	0.311	1.56	1.28	1.16
40.67	47.5	0.326	0.266	0.240	0.80	0.65	0.59
63.25	33.6	0.779	0.631	0.564	1.23	1.00	0.73
78.49	26.4	0.747	0.613	0.553	0.95	0.78	0.70
87.42	16.2	0.844	0.693	0.626	0.97	0.79	0.72
				Average	1.61	1.30	1.14

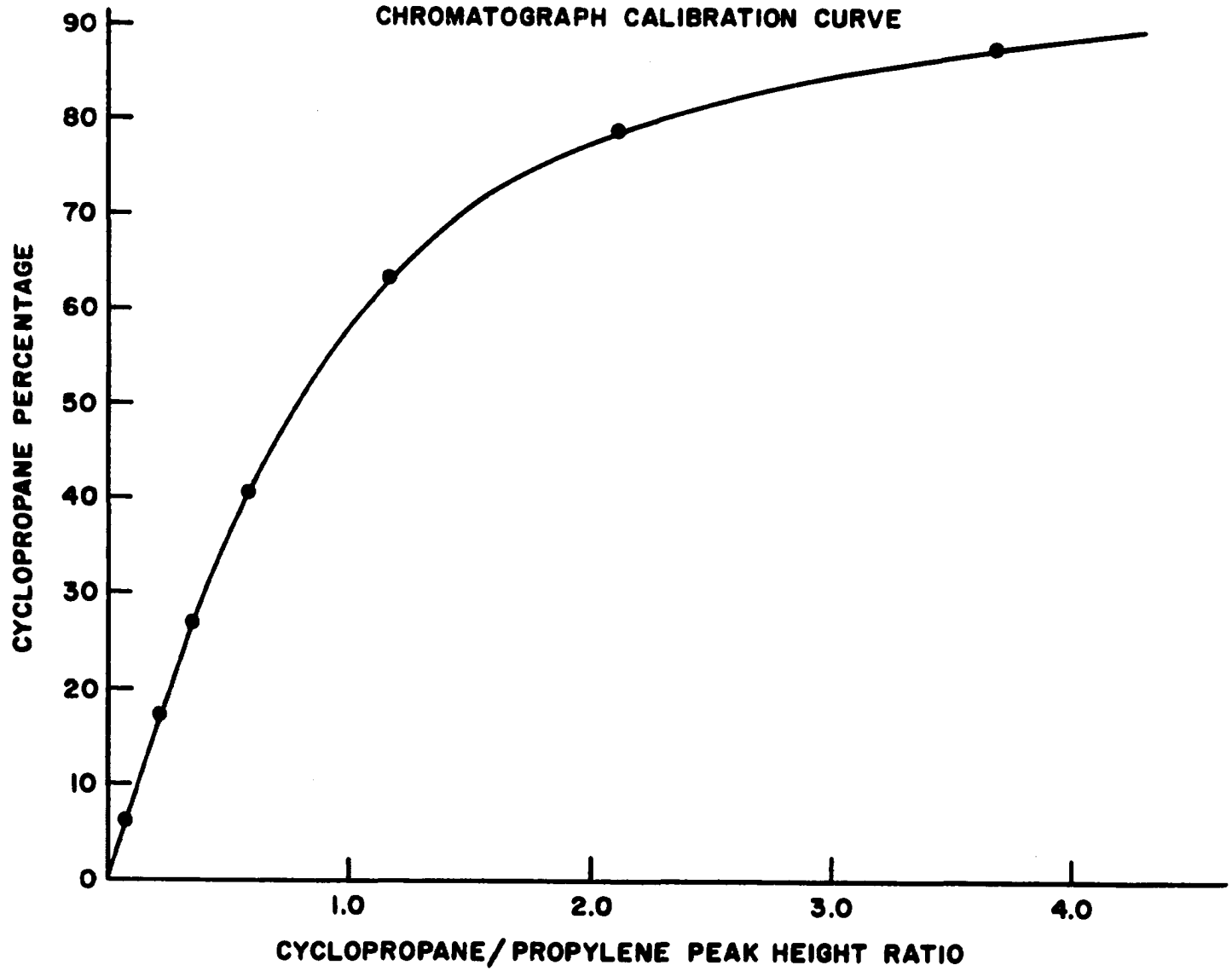
CHROMATOGRAPH CALIBRATION CURVE
CYCLOPROPANE PERCENTAGE
90
80
70
60
50
40
30
20
10
0
1.0
2.0
3.0
4.0
CYCLOPROPANE/PROPYLENE PEAK HEIGHT RATIO

FIGURE 32

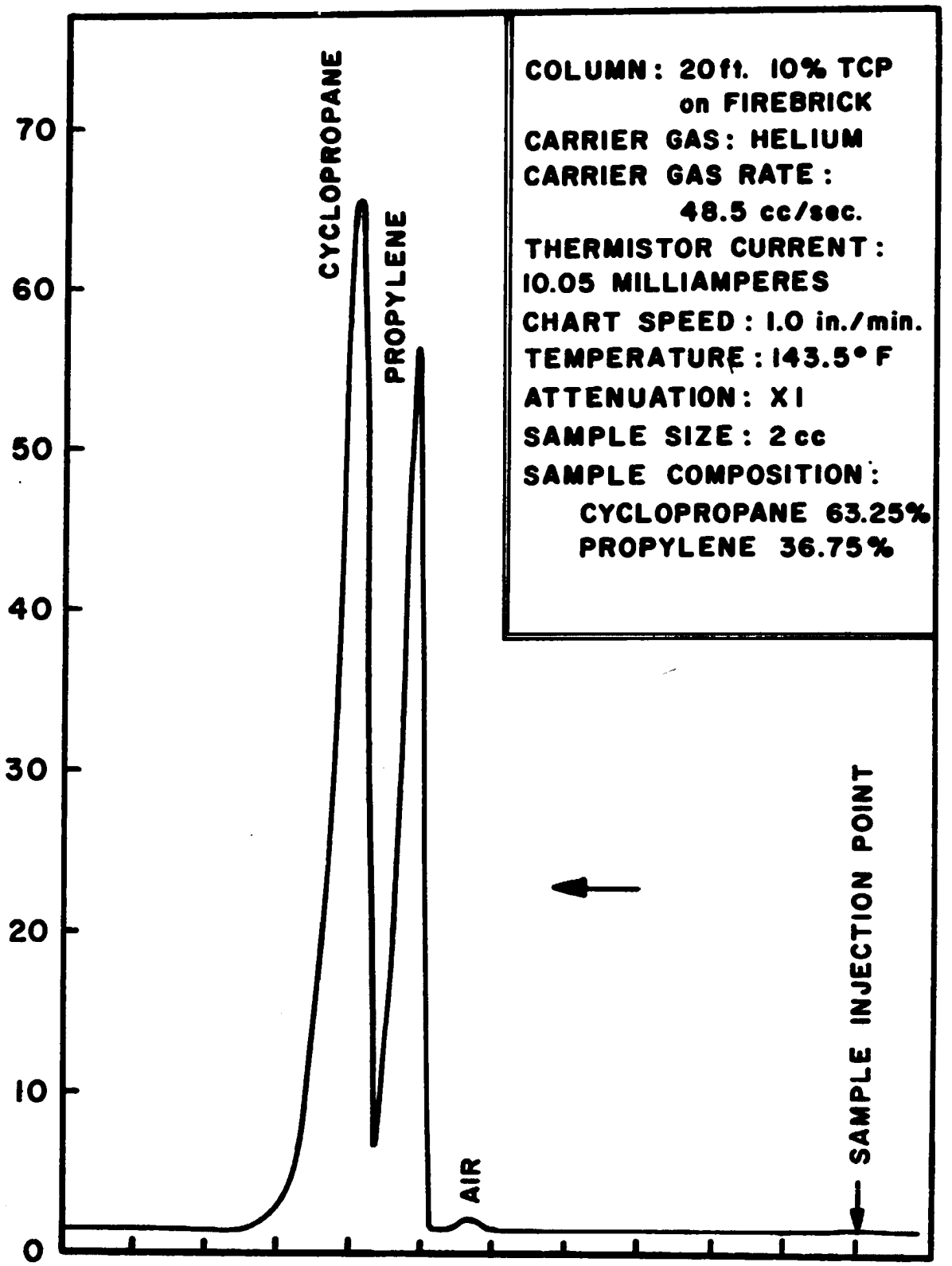

TYPICAL CHROMATOGRAM

Figure 33

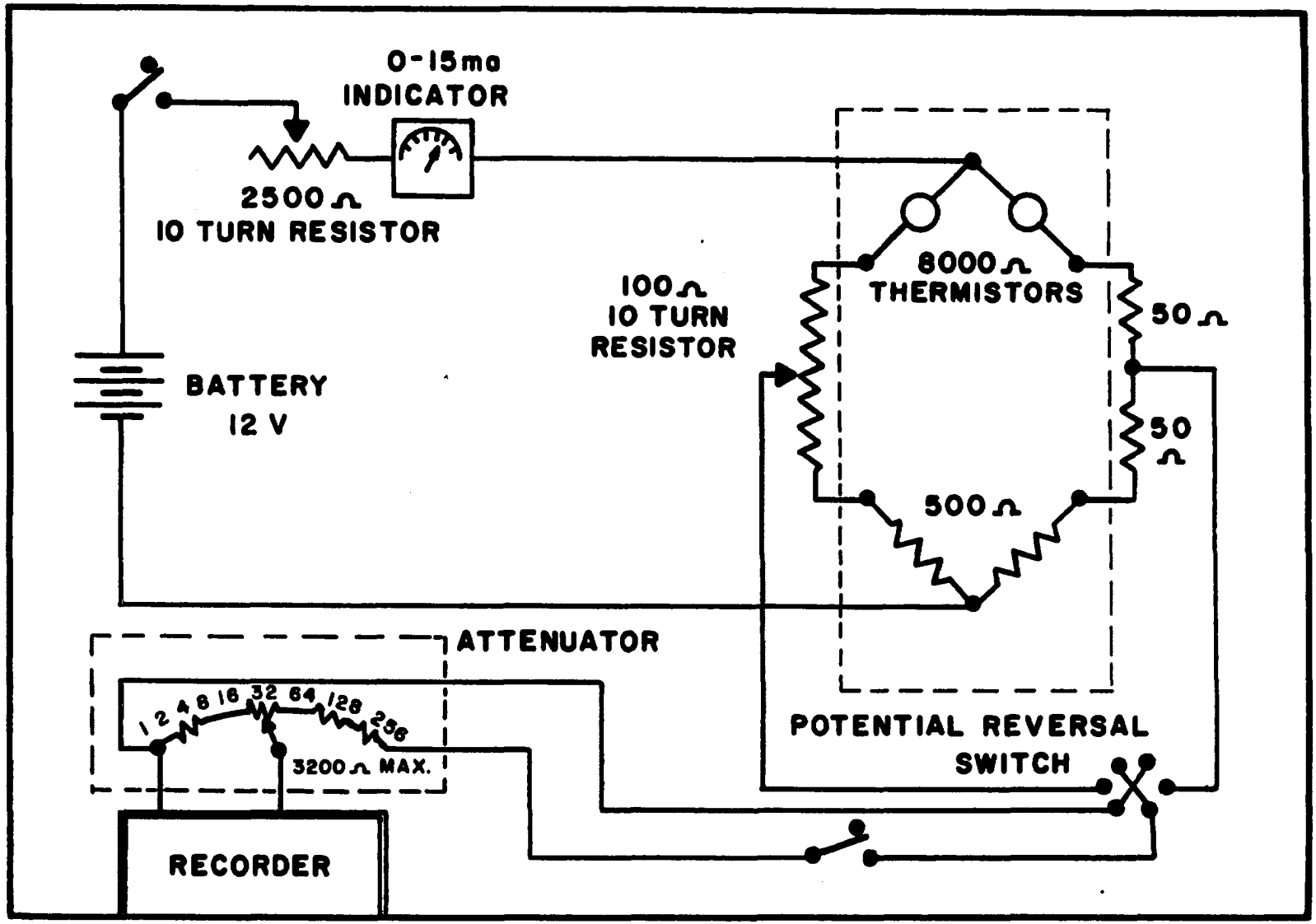

CHROMATOGRAPH ELECTRICAL CIRCUIT DIAGRAM

Figure 34

APPENDIX B

THERMODYNAMICS OF CYCLOPROPANE ISOMERIZATION

Isomerization of cyclopropane to propylene is an exothermic reaction with a heat of reaction at 25°C. of -7.86 kilocalories/g-mole reported by Knowlton and Rossini (41).

Owing to the likeness of cyclopropane and propylene heat capacities, the heat of reaction is only a mild function of temperature. Equilibrium conditions strongly favor the formation of propylene. But as expected with an exothermic reaction, the formation of propylene at equilibrium tends to decrease as temperature is increased, though it is still substantial at high temperatures.

With the heat of reaction known at one temperature, and with equations for heat capacity of both cyclopropane and propylene available, one can find ΔH^{o} as a function of temperature. From the analysis of spectroscopic data by Spencer (79), the heat capacity for cyclopropane in the ideal gas state is

$$c_p^o(\text{cyclopropane}) = -3.562 + 0.065107T - 26.349 \times 10^{-6}T^2 \quad \text{B-1}$$

where T is the temperature in degrees Kelvin and the recommended range of application is 250-1000°K. Similarly, the equation reported by Houqen et al. (32, p. 255) for propylene

heat capacity is

$$c_p^o(\text{propylene}) = 1.97 + 27.69 \times 10^{-3}T - 5.25 \times 10^{-6}T^2 \quad \text{B-2}$$

where T is in degrees Rankine and the recommended range of application is 50-1400°F. The heat of reaction in the ideal gas state is

$$\Delta H^o = \int c_p^o dT + I \quad \text{B-3}$$

where the integration constant I is evaluated through use of the known heat of reaction at 25°C. Thus, the final expression for the heat of reaction in the ideal gas state as a function of temperature is

$$\Delta H^o = 5.532T - 0.007632T^2 + 3.113 \times 10^{-6}T^3 - 8913.4 \quad \text{B-4}$$

where T is in degrees Kelvin and the units of ΔH^o are calories/g-mole. Equation B-4, of course, is only suitable for the range covered by both heat capacity equations; i.e., 283 to 1000°K. Only temperatures inside this range are employed in the present study.

With the value of ΔH^o available as a function of temperature, the value of ΔG^o can likewise be found as a function of temperature from the fact that

$$\frac{\partial \frac{\Delta G^o}{T}}{\partial T} = -\frac{\Delta H^o}{T^2} \quad \text{B-5}$$

Solution of Equation B-5 requires a knowledge of ΔG^o at one temperature. Information is available in the literature for the evaluation of ΔG^o at 25°C. from the relationship

$$\Delta G^o = \Delta H^o - T\Delta S^o \quad \text{B-6}$$

The entropy of propylene at 25°C. is 63.80 calories/g-mole °K. (Rossini, API Project 44). Linnett (54) has provided an equation for the entropy of cyclopropane as a function of temperature, that is

$$S^{o}(\text{cyclopropane}) = 119.34 - 33.086 \log T + 8.791 \times 10^{-2} T - 2.085 \times 10^{-5} T^{2} - \frac{15.095 \times 10^{2}}{T} \qquad \text{B-7}$$

where T is in degrees Kelvin and S^{o} has the units calories/g-mole °K. It is known that Linnett's results are slightly in error, as pointed out in a later paper by Kistiakowsky and Rice (40). However, Equation B-7 gives results which are in good agreement with those in the latter paper at low temperatures. From Equation B-7, the entropy of cyclopropane in the ideal gas state at 25 °C. is 56.77 calories/g-mole °K. Thus, with the previously stated heat of reaction at 25°C. and the entropy values given above, ΔG^{o} at 25°C. is calculated from Equation B-6 to be -9,955.5 calories/g-mole.

Finally, upon substitution of ΔH^{o} from Equation B-4 into Equation B-5, followed by integration and evaluation of the integration constant, the resulting expression for ΔG^{o} as a function of temperature is

$$\Delta G^{o} = -5.532\, T \ln T + 0.007632\, T^{2} - 1.5565 \times 10^{-6} T^{3} + 25.89 T - 8913.5 \qquad \text{B-8}$$

where T is in degrees Rankine and ΔG^{o} has the units calories/g-mole. The values of ΔG^{o} from Equation B-8 have been plotted in Figure 35 along with results obtained independently from tabulations of the free energy function for cyclopropane and

propylene by Kistiakowsky and Rice (40) and Rossini (API Project 44), respectively. The data used in the preparation of Figure 35 are also tabulated in Table B-1 for comparison.

TABLE 8

ΔG° FOR CYCLOPROPANE ISOMERIZATION

		Equation B-8	
T °K	Functions*	ΔG°	$\ln K_a = -\frac{\Delta G^{\circ}}{RT}$
300	- 9,968	- 9,968	16.721
400	-10,694	-10,697	13.454
500	-11,445	-11,431	11.520
600	-12,201	-12,219	10,234
700	-13,106	-12,903	9.423
800	-13,697	-13,637	8.617
900	-14,433	-14,366	8.071
1000	-15,262	-15,051	7.681

*$(G^{\circ}-H^{\circ}_{o})/T$ values for propylene from Rossini (API Project 44) and similar values for cyclopropane from Kistiakowsky and Rice (40).

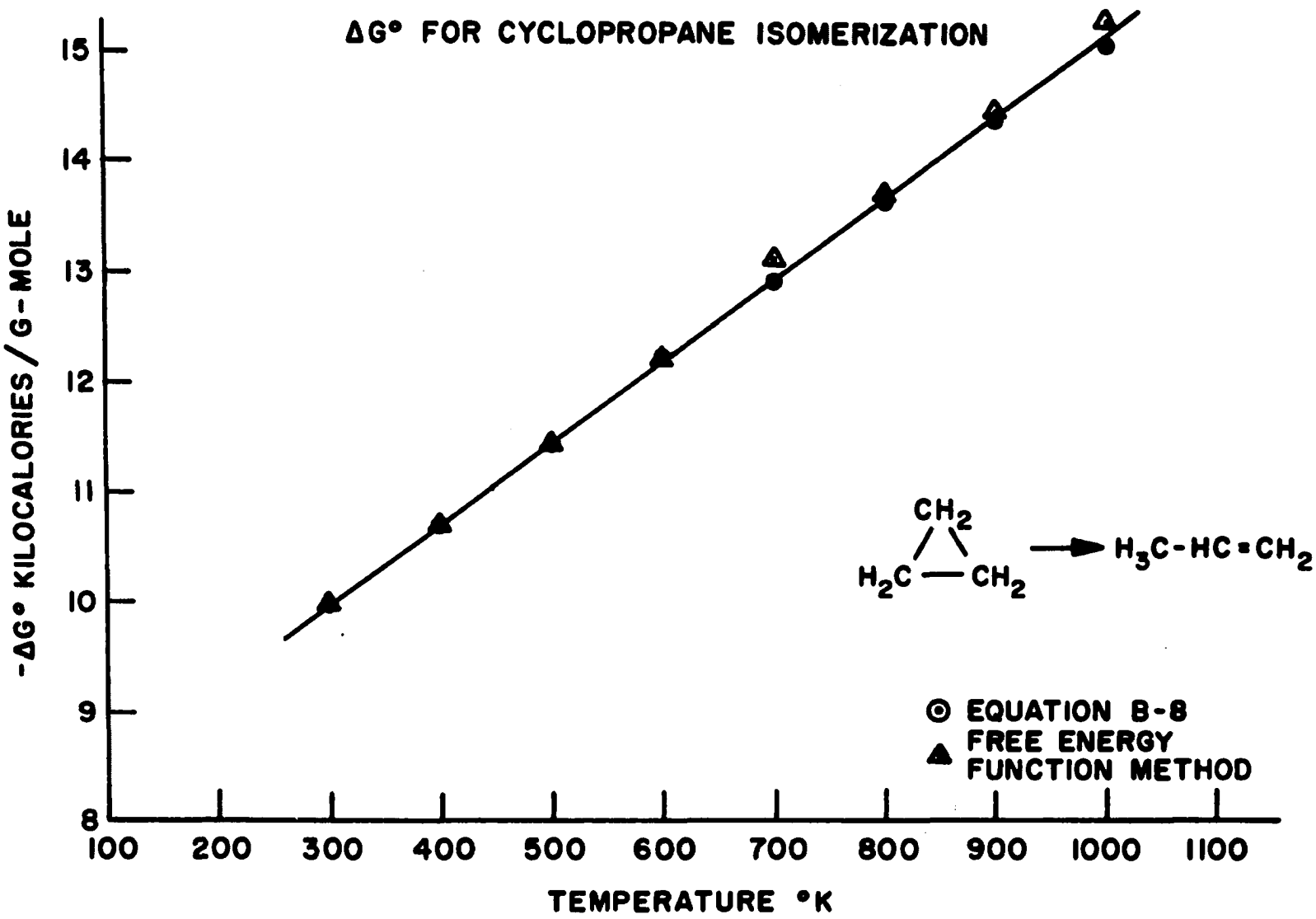
ΔG° FOR CYCLOPROPANE ISOMERIZATION
-ΔG° KILOCALORIES / G-MOLE
15
14
13
12
11
10
9
8
100
200
300
400
500
600
700
800
900
1000
1100
TEMPERATURE °K
CH2
H2C — CH2
H3C-HC=CH2
EQUATION B-8
FREE ENERGY FUNCTION METHOD

FIGURE 35

Roberts (71), in his study of catalytic isomerization of cyclopropane, reported that $Log_{10} K_a$ values were between 9 and 10 for the 100°C. to 150°C. range. This range of values appears to be inconsistent with the results given in Table 8. With the ΔG^o values from Figure 35 for these temperatures, it is found that $\log_{10} K_a$ values (i.e., $\frac{-\Delta G^o}{2,303RT}$) values are approximately 6.2 and 5.6, respectively. Roberts further stated that the equilibrium constant increases with increasing temperature. This statement is contrary to the results presented in Table 8 and is in conflict in general with the observation that for exothermic reactions the equilibrium yield is reduced as temperature is increased. In any case, for the temperature range of the present study, essentially 100 per cent conversion of cyclopropane is possible.

Brown (8) in his thesis stated that the free energy change at 175°C. is on the order of -3 kilocalories. This statement appears to be erroneous.

APPENDIX C

EQUIPMENT DESIGN FOR HIGH PRESSURE AND TEMPERATURE

The operating conditions of this investigation, from the point of view of equipment design, are probably best described as being intermediate in severity. Operating pressures were sufficiently high to require thicknesses of vessels and tubing which do not permit use of the usual thin-wall design equations without significant error. On the other hand, the pressures used were not so high as to require such special techniques as cylinder compounding and autofrettage, nor was the use of special high strength materials demanded. The maximum metal temperature level, for the purpose of design, was 1200°F. At this temperature level, with Type 304 and Type 316 stainless steels as construction materials, creep rate and rupture life are important factors to be considered in the specification of an allowable stress design criterion.

The preheater Kuentzel bombs and the gold-lined reactor coil are subjected to the most severe operating conditions. In order to determine the allowable internal pressure for these, thick-walled, cylindrical shapes, it is first necessary to establish the stress distribution within them. The general problem of elastic stress distribution in long cylin-

ders, with uniform axial stress, was solved by Lamè (47) more than one-hundred years ago. It has been instructive for the writer to proceed with his own development of the Lame equations. This development is presented in an abbreviated form in the paragraphs which follow:

The Lamé Equations for Stress Distribution

As a starting point, one considers an equilibrium force balance on an arbitrary differential element of cylinder wall, with geometry as shown in Figure C-1.

Figure C-1

In difference form, the force balance in the radial direction (positive outward) is

$$-2(\sin\frac{\Delta\theta}{2})\sigma_t \Delta r \Delta L - r\Delta\theta\sigma_r\Big]_{r_1}\Delta L + r\Delta\theta\sigma_r\Big]_{r_2}\Delta L = 0 \qquad \text{C-1}$$

where σ_r is the radial tensile stress, equal in magnitude but opposite in sign to the radial compressive stress, $(\sigma_r)_c$. Upon dividing Equation C-1 by the product $\Delta r \Delta\theta \Delta L$ and taking

the limit as $\Delta\theta$ and Δr approach zero, one obtains

$$\lim_{\Delta\theta \to 0} \left(2 \frac{\sin \frac{\Delta\theta}{2}}{\Delta\theta} \right) \sigma_t - \frac{d(r\sigma_r)}{dr} = 0 \qquad \text{C-2}$$

The first term in Equation C-2 is an indeterminant form, but the difficulty is resolved by application of L'Hospital's rule as follows

$$\lim_{\Delta\theta \to 0} \left(2 \frac{\sin \frac{\Delta\theta}{2}}{\Delta\theta} \right) = \lim_{\Delta\theta \to 0} \left(2 \frac{\frac{\Delta\theta}{2}}{d(\Delta\theta)} \right) = \lim_{\Delta\theta \to 0} \left(\frac{\cos \frac{\Delta\theta}{2}}{1} \right) = 1$$

With this result, and upon completing the differentiation in Equation C-2 and rearranging, one obtains the desired differential equation relating the tangential and radial stresses. i.e.,

$$\sigma_t - \sigma_r = r \frac{d\sigma_r}{dr} \qquad \text{C-3}$$

From Hooke's law and the observed linear superposition of strains, the expression for axial strain may be written as

$$\epsilon_z = \frac{\sigma_z}{E} - \nu \left[\frac{\sigma_r}{E} + \frac{\sigma_t}{E} \right] \qquad \text{C-4}$$

The basic assumption of the derivation is that plane sections are maintained; hence, ϵ_z and σ_z are not expected to be functions of the radius. This being the case, Equation C-4 reduces to a second relationship between σ_t and σ_r only; viz.,

$$\sigma_r + \sigma_t = C_1 \qquad \text{C-5}$$

where C_1 is a constant to be evaluated from boundary condi-

tions. Upon eliminating σ_t between Equations C-3 and C-5, one obtains a differential equation which can be readily integrated.

$$\frac{d\sigma_r}{dr} + \frac{2\sigma_r}{r} = \frac{C_1}{r} \qquad \text{C-6}$$

The integrating factor for Equation C-6 is $e^{\int \frac{2dr}{r}}$ and the resulting solution is

$$r^2\sigma_r = C_1\frac{r^2}{2} + C_2 \qquad \text{C-7}$$

The constants C_1 and C_2 can be evaluated through use of the two boundary conditions

(1) $\sigma_r = -P_1$ at r_1

(2) $\sigma_r = -P_2$ at r_2

Their values are:

$$C_1 = -2\left[P_1 + \frac{r_2^2}{r_1^2 - r_2^2}(P_1 - P_2)\right] \qquad \text{C-8}$$

$$C_2 = \frac{r_2^2 r_1^2}{r_1^2 - r_2^2}(P_1 - P_2)$$

Finally, the expressions for radial and tangential stress resolve to

$$\sigma_r = \frac{P_1 - K^2P_2 - (r_2/r)^2(P_1 - P_2)}{K^2 - 1} \qquad \text{C-9}$$

$$\sigma_t = \frac{P_1 - K^2P_2 + (r_2/r)^2(P_1 - P_2)}{K^2 - 1} \qquad \text{C-10}$$

where K is the ratio of the cylinder outside and inside radius. The axial stress is obviously

$$\sigma_z = \frac{\pi r_1^2 P_1 - \pi r_2^2 P_2}{\pi(r_2^2 - r_1^2)} = \frac{P_1 - K^2 P_2}{K^2 - 1} \qquad \text{C-11}$$

Inspection of Equation C-11 reveals that the axial stress is equal to one-half the sum of the radial and tangential stresses. The three equations, Equations C-9 thru C-11, are the expressions developed by Lamé for the triaxial stresses in a long, thick-walled cylinder. These equations alone are not a basis for design. However, when they are used in conjunction with a criterion for failure, a design method evolves.

Design Equations and Criteria for Failure

It is apparent that for design purposes, the points of maximum stress are of primary concern. In most cases of interest, the outside pressure, P_2, will be small in comparison with the internal pressure, P_1. Hence, the Lamé equations for radial and tangential stress reduce to the simple expressions

$$\sigma_r = \frac{P_1 - (r_2/r)^2 P_1}{K^2 - 1} \qquad \text{C-12}$$

$$\sigma_t = \frac{P_1 + (r_2/r)^2 P_1}{K^2 - 1} \qquad \text{C-13}$$

The tangential stress is observed to always be greater in

magnitude than the radial stress; and since the axial stress is the average of the other two principle stresses, then the tangential stress, at any arbitrary location, will always exceed either the radial or axial stress at that same location. Further, upon inspection of Equation C-13, it is seen that the maximum tangential stress occurs at the inside radius. Hence,

$$\sigma_t(\text{max.}) = \frac{(K^2 + 1)}{K^2 - 1} P_1 \qquad \text{C-14}$$

If the specification of a maximum allowable principal stress is considered to be a suitable criterion for failure, then Equation C-14 becomes a design equation. The basic difficulty arises in the relating of the results of simple tension tests to the case of triaxial stress. There are two theories of failure which are generally considered superior to the maximum principal stress theory: (1) the maximum shear stress theory and (2) the maximum distortion energy theory. These theories are discussed in turn.

In the maximum shear stress theory it is assumed that the breakdown of elastic behavior occurs when the maximum shear stress in the material under the influence of triaxial stress becomes equal to the maximum shear stress at the yield point in the simple tension test. There is rather strong experimental support for this theory, as both tension test specimens and pressure vessels are observed to fail through shear.

It can be shown that the maximum shearing stress is

one-half the difference between the maximum and minimum principal stresses (85, p. 15). Thus, for a thick-walled cylinder

$$\tau(\text{max.}) = \frac{\sigma_t - {}_r\sigma}{2} \qquad \text{C-15}$$

Upon substitution of the values of σ_r and σ_t from Equations C-12 and C-13, Equation C-15 becomes

$$\tau(\text{max.}) = \frac{(r_2/r)^2 \, P_1}{K^2-1} \qquad \text{C-16}$$

Equation C-16 gives the maximum shearing stress at any arbitrary value of r. It is apparent, however, that the greatest shearing stress is always at r_1 where

$$\tau(\text{max.}) \text{ @ } r_1 = \frac{K^2 \, P_1}{K^2-1} \qquad \text{C-17}$$

With the maximum shear stress criterion for breakdown of elastic behavior, $\tau(\text{max.})$ @ r_1 is replaced by τ_y, the shear stress at the yield point in the simple tension test. The value of τ_y in terms of the principal stress at the yield point is

$$\tau_y = \frac{(\sigma_y - 0)}{2} \qquad \text{C-18}$$

The combination of Equations C-17 and C-18 results in an expression for the maximum internal pressure which can be tolerated within the limits of elastic action.

$$P_1 \text{ (max.)} = \frac{\sigma_y(K^2 - 1)}{2 \, K^2} \qquad \text{C-19}$$

Equation C-19 is the design equation resulting from the maximum shear stress theory. Its counterpart in the maximum principal stress theory is Equation C-14. Customarily, the maximum allowable stress in Equation C-19 is taken as some value less than σ_y in order to provide a margin of safety.

The basic concept of the maximum distortion energy theory of von Mises is that breakdown of elastic behavior occurs when a certain level of distortion energy per unit volume of material is imposed, regardless of how the distortion is brought about. A development of the theory may be found elsewhere (85, Chapter 6). The practical result of the theory arises from the ability to equate the distortion energy at elastic breakdown for a triaxial stress condition to that in a simple tension test; in so doing, one obtains the relationship

$$\frac{1+\nu}{6E}\left[(\sigma_t-\sigma_r)^2+(\sigma_r-\sigma_z)^2+(\sigma_z-\sigma_t)^2\right]=\frac{1+\nu}{3E}\sigma_y^2 \qquad \text{C-20}$$

where σ_y is the yield stress of the material in simple tension.

Observing that $2\sigma_z = \sigma_t + \sigma_r$ and also that $2\tau(\text{max.}) = \sigma_t-\sigma_r$, Equation C-20 reduces to the following expression relating $\tau(\text{max.})$ and σ_y. That is,

$$\tau(\text{max.}) = \frac{\sigma_y}{3} \qquad \text{C-21}$$

With this substitution made in Equation C-17, the design equation with the von Mises theory becomes

$$P_1 = \frac{\sigma_y (K^2 - 1)}{\sqrt{3}\ K^2} \qquad \text{C-22}$$

This result may be compared with the design Equation C-14 for the maximum principal stress theory and Equation C-19 for the maximum shear stress theory.

Voorhees, Sliepcevich and Freeman (89), in their study of creep rate and stress for rupture in metals at high temperature, report better agreement with the von Mises theory. They further suggest two design criteria, one for high creep rate materials and another for those materials in which creep is slow. For high creep materials, a design stress of 80 per cent of the stress for 2 per cent creep in the anticipated life is recommended; whereas, with materials of low creep rate, the recommended allowable stress is 80 per cent of the stress for rupture with a specified life.

Design Calculations

The reactor was constructed of seamless, Type 316, stainless steel tubing with guaranteed minimum life of 1000 hours in a stress rupture test at 1200°F. with a 25,000 p.s.i. stress. The tubing dimensions were 9/16-inch outside diameter and 3/8-inch inside diameter, giving a K value of 1.5. Thus, the calculated allowable internal pressure by the three design methods is as follows:

$$\sigma(\text{allowable}) = (0.8)(25{,}000) = 20{,}000 \text{ p.s.i.}$$

I. Maximum Principal Stress Method

$$P_1 = \frac{(K^2-1)}{(K^2+1)}\,\sigma = \frac{(1.25)(20{,}000)}{(3.25)} = 7{,}700 \text{ p.s.i.}$$

II. Maximum Shear Stress Method

$$P_1 = \frac{(K^2-1)}{2K^2}\sigma = \frac{(1.25)(20,000)}{2(2.25)} = 5,550 \text{ p.s.i.}$$

III. Maximum Distortion Energy Method

$$P_1 = \frac{(K^2-1)}{\sqrt{3}\ K^2}\sigma = \frac{(1.25)(20,000)}{3\quad(2.25)} = 6,400 \text{ p.s.i.}$$

All other tubing (Type 304 stainless) used in the high pressure system, and the preheater Kuentzel bombs (Type 316 stainless) as well, had a diameter ratio of K = 2.0. Hence, the reactor allowable pressure establishes the operating limit.

Effect of Thermal Stress

To this point, thermal stresses have not been considered. In the reactor, the steady state, outward flow of heat actually contributes to a reduction in the maximum tangential stress; hence, the calculated maximum allowable pressures are conservative. The contribution of thermal stresses in the design of monoblock vessels has been discussed thoroughly by Whalley (94, 95). From his results, for steady-state heat flow in cylinders, the contribution of thermal stress to the tangential stress σ_t is

$$-\frac{\beta}{2}\left\{\frac{K^2}{K^2-1}\left[1+\frac{r_1^2}{r^2}\right] - \frac{\ln r/r_1}{\ln K} - \frac{1}{\ln K}\right\} \qquad \text{C-23}$$

where

$$\beta = \frac{\gamma E \Delta T}{1-\nu} \ ,$$

α is the thermal coefficient of expansion and ΔT is defined as $(T_1 - T_2)$. Upon applying Equation C-23 at the reactor inside radius, it is found that for each 1°F. the inside wall temperature exceeds that of the outside wall, the tangential stress is reduced by approximately 220 p.s.i.

APPENDIX D

EVALUATION OF DIFFUSIONAL EFFECTS AND VALIDITY OF THE PLUG-FLOW ASSUMPTION

When turbulent flow exists in a tubular reactor, the simplifying assumption of plug-flow is usually satisfactory in the analysis of kinetic data. In the laminar flow regime, however, plug-flow can be assumed, without significant error, only under certain conditions. It is the purpose of this section to explore the suitability of the plug-flow assumption for the experimental runs of the present investigation.

From the summary of Reynolds number calculations in Table 9, it will be observed that laminar flow prevailed in all runs, and that the maximum Reynolds number (1524) occurred in Run I-1. It is, of course, well known that for fully developed laminar flow in a circular tube, in the absence of diffusion, natural convection, and thermal effects, the radial velocity distribution is given by the Poiseuille equation,

$$v(r) = v_o\left(1 - \frac{r^2}{R^2}\right)$$

Further, it is apparent that with such flow, the molecules along the central streamline will have a residence

time (or reaction time) which is less than that of a volume element at any radius, $0<r\leq R$. Bosworth (7) has considered, at length, the distribution of reaction times for laminar flow in cylindrical reactors. In the absence of diffusion, he has shown that the reaction time distribution function is $F_\tau = H(\tau - \tau_o)\,\frac{2\tau_o^2}{\tau^3}$, where $F_\tau d\tau$ represents the fraction of molecules with reaction times between τ and $\tau + d\tau$. Bosworth also developed the more complicated distribution functions which account for radial and longitudinal diffusion. Out of his mathematical treatment, two very practical relationships were derived. First, he has shown that the reaction time distribution in laminar flow is essentially unchanged by longitudinal diffusion provided the length of the reaction section is greater than $360\sqrt{D\tau_o}$. Secondly, radial diffusion does not significantly alter the distribution if the radius of the reactor is greater than $18\sqrt{D\tau_o}$.

In Table 10, the calculated values of $18\sqrt{D\tau_o}$ and $360\sqrt{D\tau_o}$ have been tabulated for each run. Since the dimensions of the gold-lined reactor were R = 0.01428 ft. and L = 13.786 ft., it is apparent from Table 10 that while the influence of longitudinal diffusion on the reaction time distribution is negligible for all runs, the opposite is true for radial diffusion. The fact that the quantity $18\sqrt{D\tau_o}$ is large in comparison with R suggests that radial diffusion may be of sufficient magnitude to make plug-flow a reasonable assumption. This possibility is explored with a criterion

developed by Cleland and Wilhelm (11). These authors, by numerical integration, obtained a solution for the basic partial differential equation describing the concentration field in a circular tube where a fluid in the laminar-flow regime is undergoing a first-order reaction. In dimensionless form, the equation which they solved was

$$-(1-U^2)\frac{\partial C}{\partial \lambda} + \alpha\left[\frac{\partial^2 C}{\partial U^2} + \frac{1}{U}\frac{\partial C}{\partial U}\right] - C = 0 \qquad \text{D-1}$$

where

$$\lambda = \frac{k_c Z}{v_o} \quad , \quad C = \frac{c}{c_o} \quad , \quad \alpha = \frac{D}{k_c R^2} \quad \text{and} \quad U = \frac{r}{R}$$

Equation D-1 involves the assumptions that, (1) laminar flow is fully developed, (2) axial diffusion is negligible in comparison with radial diffusion, (3) isothermal conditions prevail, and (4) diffusivity remains constant throughout the reactor. The solution was with the boundary conditions:

(1) when $\lambda = 0$, $C = 1$

(2) when $U = 1$, $\frac{\partial C}{\partial U} = 0$

For the present analysis, the important result obtained from the Cleland and Wilhelm solution is their criterion for approach to plug-flow conversions; viz., that the product $\alpha\lambda$ must be greater than unity. From Table 11 it is seen that this criterion is satisfied for all runs except I-1, I-2 and I-3. However, upon further analysis of the Cleland and Wilhelm solution (from their Figure 3), it is observed that for the combination of high diffusion parameter, α, and low

contact time parameter, λ, such as exist for Run I, the approach to plug-flow conversion still prevails.

It should be pointed out that the problem which Cleland and Wilhelm solved by numerical methods has since been solved analytically by Lauwerier (50). Recently, Wissler and Schechter (96) have calculated the eigenvalues for the Lauwerier solution and compared the results predicted by the two methods. The numerical results of Cleland and Wilhelm were found to be in excellent agreement with the formal solution.

Danckwerts (13) has analyzed the influence of longitudinal diffusion on tubular reactor conversion for first-order reactions in the absence of velocity gradients. He found that while longitudinal diffusion tends to lower the conversion below that expected for plug-flow. The effect is, nevertheless, negligible provided the relationship $k_c 2\ DL/\langle v\rangle^3 \ll 1$ holds. All runs in this investigation fulfill this criterion.

In summary, it can be said that though all the runs of this investigation were in the laminar region, radial diffusion was sufficiently high, and longitudinal diffusion sufficiently low, to permit the assumption of plug-flow in analysis of the kinetic data without introducing significant error. Further, it is known that disturbances such as those arising from entrance effects, natural convection, temperature gradients, and deviation from axial symmetric flow owing to the coiled construction of the reactor, all contribute to

an increase in the effective radial diffusion, and hence a closer approach to plug-flow. Concerning the entrance effect, fully developed laminar flow is approached only after approximately 0.03 Re pipe diameters; thus, since the reactor has a length of 482.7 pipe diameters, calculations, using the Reynolds numbers of Table 9, reveal that the length of the entrance region for all runs is between 1.0 to 9.5 per cent of the total reactor length.

Since the properties ρ_m, μ_m and D for cyclopropane-propylene mixtures have not been measured and reported in the literature, even at low pressures, the values used in the tables of this appendix have been estimated by the procedures described below:

(1) Densities were calculated from the expression $\rho_m = PM/Z_mRT$ using the arithmetic average of the inlet and outlet reactor compositions. Z_m was read from the conventional generalized correlation (59), with pseudo-reduced temperature and pressure calculated by Kay's rule.

(2) Viscosities of cyclopropane were used in all cases for μ_m, for two reasons: First, in most runs the conversion was low and hence cyclopropane was the predominant component. Secondly, over the temperature range of operation, the maximum difference between cyclopropane and propylene viscosities is only 6 per cent, as seen from Figure 36. In Figure 36, the available low temperature viscosity data have been extended through linear extrapolation on a plot $T^{3/2}/\mu^{o}$

versus T. Because of the limited amount of data available on the viscosity of cyclopropane, the extrapolation has been made with the aid of one viscosity calculated from the Bromley and Wilke equation; i.e., Equation 6-16 of Reid and Sherwood (69). The measured viscosities of cyclopropane used in Figure 36 are from the work of Lambert (48). Viscosities at atmospheric pressure obtained from Figure 36 were extended to higher pressures using the values of μ/μ^{o} from Figure 6-1 of Reid and Sherwood.

(3) Diffusivities for the cyclopropane-propylene binary mixtures were calculated from Slattery's empirical equation: Equation 8-19 of Reid and Sherwood. Pressure corrections were estimated from Figure 8-2 of the same reference.

TABLE 9

Reynolds Number Calculations

d = 0.02856 ft.

Run No.	ρ_m lb_m/ft^3	$\mu_m \times 10^5$ $lb_m/ft\text{-}sec$	$\nu_m \times 10^6$ ft^2/sec	$\langle v \rangle$ ft/sec	$Re = \frac{d\langle v \rangle}{\nu_m}$
I-1	1.504	1.519	10.100	0.539	1524
I-2	2.883	1.563	5.421	0.233	1228
I-3	4.372	1.592	3.641	0.150	1177
I-4	5.885	1.678	2.851	0.088	882
II-1	1.507	1.480	9.821	0.157	457
II-2	3.011	1.522	5.055	0.100	565
II-3	4.576	1.550	3.387	0.061	514
II-4	6.169	1.635	2.650	0.043	463
III-250	0.800	1.396	17.450	0.122	200
III-1	1.576	1.437	9.118	0.070	219
III-2	3.141	1.478	4.706	0.036	218
III-3	4.808	1.505	3.130	0.023	210
III-4	6.507	1.587	2.439	0.014	164
IV-1	1.396	1.568	11.232	0.276	702
V-250	0.787	1.418	18.017	0.229	363
V-1	1.539	1.460	9.487	0.072	217
V-2	3.077	1.502	4.881	0.028	164
VI-1	1.476	1.501	10.169	0.257	722
VI-2	2.950	1.544	5.234	0.115	628
VI-3	4.472	1.572	3.515	0.069	561

TABLE 9----Continued

Run No.	ρ_m lb_m/ft^3	$\mu_m \times 10^5$ $lb_m/ft\text{-}sec$	$\nu_m \times 10^6$ ft^2/sec	$\langle v \rangle$ ft/sec	$Re = \frac{d\langle v \rangle}{\nu_m}$
VII-250	1.726	1.502	20.688	0.518	715
VII-1	1.420	1.546	10.887	0.201	723
VII-2	2.831	1.590	5.616	0.115	575
VIII-250	0.701	1.542	21.997	0.581	754
IX-1	1.507	1.480	10.182	0.360	1009
IX-2	3.010	1.522	5.056	0.171	966
IX-3	4.571	1.550	3.391	0.106	865
IX-4	6.168	1.635	2.651	0.073	818
X-1	1.509	1.480	9.808	0.182	529
X-2	3.011	1.522	5.055	0.086	486
X-3	4.626	1.550	3.351	0.052	443
X-4	6.175	1.635	2.648	0.034	367
XI-250	0.690	1.564	22.666	0.826	1041
XIV-1	1.509	1.480	9.808	0.254	740
XIV-2	3.008	1.522	5.060	0.112	632
XIV-3	4.569	1.550	3.392	0.070	589
XIV-4	6.169	1.635	2.650	0.048	517
XV-1	1.4465	1.519	10.501	0.241	655
XXI-1	1.448	1.519	10.490	0.371	1010
XXII-1	1.449	1.519	10.483	0.310	845
XXII-2	2.887	1.563	5.414	0.122	644
XXII-3	4.366	1.592	3.646	0.068	533
XXIII-250	0.667	1.607	24.090	0.896	1062

TABLE 10

Parameters for Evaluation of Significance of Longitudinal and Radial Diffusion

Run No.	$Dx10^5$ ft^2/sec	τ_o Sec	$D\tau_o x10^4$ ft^2	$\sqrt{D\tau}_o$ ft	$18\sqrt{D\tau}_o$ ft	$360\sqrt{D\tau}_o$ ft
I-1	1.218	12.80	1.559	0.01248	0.225	4.49
I-2	0.628	29.61	1.860	0.01364	0.246	4.91
I-3	0.413	46.04	1.901	0.01380	0.248	4.97
I-4	0.306	78.35	2.398	0.01549	0.279	5.58
II-1	1.185	44.02	5.216	0.02284	0.411	8.22
II-2	0.588	68.60	4.034	0.02009	0.362	7.23
II-3	0.386	112.7	4.350	0.02086	0.375	7.51
II-4	0.287	158.6	4.552	0.02397	0.431	8.63
III-250	2.195	56.70	12.45	0.03529	0.635	12.70
III-1	1.105	98.80	10.92	0.03304	0.595	11.89
III-2	0.549	190.4	10.45	0.03233	0.582	11.64
III-3	0.360	295.4	10.63	0.03260	0.587	11.74
III-4	0.268	485.9	13.02	0.03608	0.649	12.99
IV-1	1.331	24.94	3.320	0.01822	0.328	6.56
V-250	2.278	30.10	6.857	0.02619	0.471	9.43
V-1	1.146	95.45	10.94	0.03308	0.596	11.92
V-2	0.570	243.0	13.85	0.03720	0.670	13.39
VI-1	1.224	26.81	3.282	0.01812	0.326	6.52
VI-2	0.608	60.15	3.657	0.01912	0.344	6.88
VI-3	0.399	100.3	4.002	0.02002	0.360	7.21

TABLE 10--Continued

Run No.	$Dx10^5$ ft^2/sec	τ_o Sec	$D\tau_o x10^4$ ft^2	$\sqrt{D\tau}_o$ ft	$18\sqrt{D\tau}_o$ ft	$360\sqrt{D\tau}_o$ ft
VII-250	2.592	13.30	3.447	0.01857	0.334	6.69
VII-1	1.306	34.30	4.480	0.02375	0.428	8.55
VII-2	0.648	59.70	3.869	0.01967	0.354	7.08
VIII-250	2.874	11.86	3.409	0.01846	0.332	6.65
IX-1	1.185	19.17	2.272	0.01525	0.275	5.49
IX-2	0.588	40.37	2.374	0.01541	0.277	5.55
IX-3	0.386	65.15	2.515	0.01586	0.285	5.71
IX-4	0.287	94.80	2.721	0.01650	0.297	5.94
X-1	1.185	37.90	4.491	0.02378	0.428	8.56
X-2	0.588	80.40	4.728	0.02174	0.391	7.83
X-3	0.386	133.0	5.134	0.02266	0.408	8.16
X-4	0.287	203.9	5.852	0.02419	0.435	8.71
XI-250	2.850	8.34	2.377	0.01542	0.278	5.55
XIV-1	1.185	27.10	3.211	0.01792	0.323	6.45
XIV-2	0.588	61.50	3.616	0.01902	0.342	6.85
XIV-3	0.386	98.15	3.789	0.01947	0.350	7.01
XIV-4	0.287	142.8	4.098	0.02024	0.364	7.29
XV-1	1.218	28.62	3.493	0.01869	0.336	6.73
XXI-1	1.265	18.57	2.349	0.01533	0.276	5.52
XXII-1	1.265	22.27	2.817	0.01682	0.303	6.06
XXII-2	0.628	56.70	3.561	0.01887	0.340	6.79
XXII-3	0.413	100.9	4.167	0.2041	0.367	7.35
XXIII-250	3.019	7.69	2.322	0.01524	0.274	5.49

TABLE 11

Parameters for Evaluation of Validity of Plug Flow Assumption

R = 0.01428 ft. L = 13.786 ft.

Run no.	k_c sec^{-1}	$Dx10^5$ ft^2/sec	Diffusion Parameter $\lambda = \frac{D}{k_c R^2}$	V_o ft/sec	Contact Time Parameter $\lambda = \frac{k_c L}{V_o}$	$\alpha\lambda$
I-1	$1.160x10^{-3}$	1.218	51.40	1.078	0.01484	0.7643
I-2	$1.142x10^{-3}$	0.628	26.97	0.466	0.3378	0.9110
I-3	$1.205x10^{-3}$	0.413	16.81	0.300	0.05537	0.9924
I-4	$1.082x10^{-3}$	0.306	13.87	0.176	0.0875	1.175
II-1	$2.673x10^{-4}$	1.185	217.4	0.314	0.01174	2.552
II-2	$2.555x10^{-4}$	0.588	112.9	0.200	0.01761	1.988
II-3	$2.428x10^{-4}$	0.386	77.97	0.122	0.02744	2.139
II-4	$2.276x10^{-4}$	0.287	61.84	0.086	0.03648	2.256
III-250	$5.953x10^{-5}$	2.195	1808.0	0.244	0.003364	6.082
III-1	$5.577x10^{-5}$	1.105	971.7	0.140	0.005492	5.337
III-2	$5.305x10^{-5}$	0.549	507.6	0.072	0.010158	5.156
III-3	$4.740x10^{-5}$	0.360	372.5	0.046	0.01420	5.290
III-4	$4.728x10^{-5}$	0.268	278.0	0.028	0.02328	6.472
IV-1	$5.624x10^{-3}$	1.331	116.1	0.552	0.14050	16.310
V-250	$9.883x10^{-5}$	2.278	1130.0	0.458	0.002975	3.362
V-1	$9.390x10^{-5}$	1.146	598.5	0.144	0.008990	5.381
V-2	$1.060x10^{-4}$	0.570	263.7	0.056	0.02609	6.880
VI-1	$5.875x10^{-4}$	1.224	102.2	0.514	0.01576	1.611
VI-2	$6.154x10^{-4}$	0.608	48.45	0.230	0.03689	1.787
VI-3	$6.123x10^{-4}$	0.399	31.96	0.138	0.06117	1.955

TABLE 11 --Continued

Run No.	k_c sec^{-1}	$Dx10^5$ ft^2/sec	Diffusion Parameter $\lambda = \frac{D}{k_c R^2}$	V_o ft/sec	Contact Time Parameter $\lambda = \frac{k_c L}{V_o}$	$\alpha\lambda$
VII-250	$2.819x10^{-3}$	2.592	45.09	1.036	0.03751	1.691
VII-1	$1.941x10^{-3}$	1.306	33.00	0.402	0.06656	2.196
VII-2	$2.317x10^{-3}$	0.648	13.72	0.230	0.1389	1.906
VIII-250	$1.130x10^{-2}$	2.874	12.47	1.162	0.1341	1.672
IX-1	$2.707x10^{-4}$	1.185	214.7	0.720	0.005184	1.113
IX-2	$2.658x10^{-4}$	0.588	108.5	0.342	0.01071	1.162
IX-3	$2.718x10^{-4}$	0.386	69.65	0.212	0.01767	1.231
IX-4	$2.669x10^{-4}$	0.287	52.74	0.146	0.02520	1.329
X-1	$2.740x10^{-4}$	1.185	212.1	0.364	0.01038	2.202
X-2	$2.498x10^{-4}$	0.588	115.4	0.172	0.02002	2.310
X-3	$2.797x10^{-4}$	0.386	67.68	0.104	0.03708	2.510
X-4	$2.459x10^{-4}$	0.287	57.24	0.068	0.04985	2.853
XI-250	$2.194x10^{-2}$	2.850	6.368	1.652	0.1831	1.166
XIV-1	$3.256x10^{-4}$	1.185	178.5	0.508	0.008835	1.577
XIV-2	$2.791x10^{-4}$	0.588	103.3	0.224	0.01718	1.775
XIV-3	$2.547x10^{-4}$	0.386	74.33	0.140	0.02508	1.864
XIV-4	$2.049x10^{-4}$	0.287	68.69	0.096	0.02942	2.021
XV-1	$1.239x10^{-3}$	1.218	49.89	0.482	0.03515	1.754
XXI-1	$1.158x10^{-3}$	1.265	53.58	0.742	0.0215	1.152
XXII-1	$1.182x10^{-3}$	1.265	52.49	0.620	0.0263	1.380
XXII-2	$1.120x10^{-3}$	0.628	27.50	0.244	0.0633	1.741
XXII-3	$0.941x10^{-3}$	0.413	21.52	0.136	0.0954	2.053
XXIII-250	$7.705x10^{-2}$	3.019	1.922	1.792	0.593	1.140

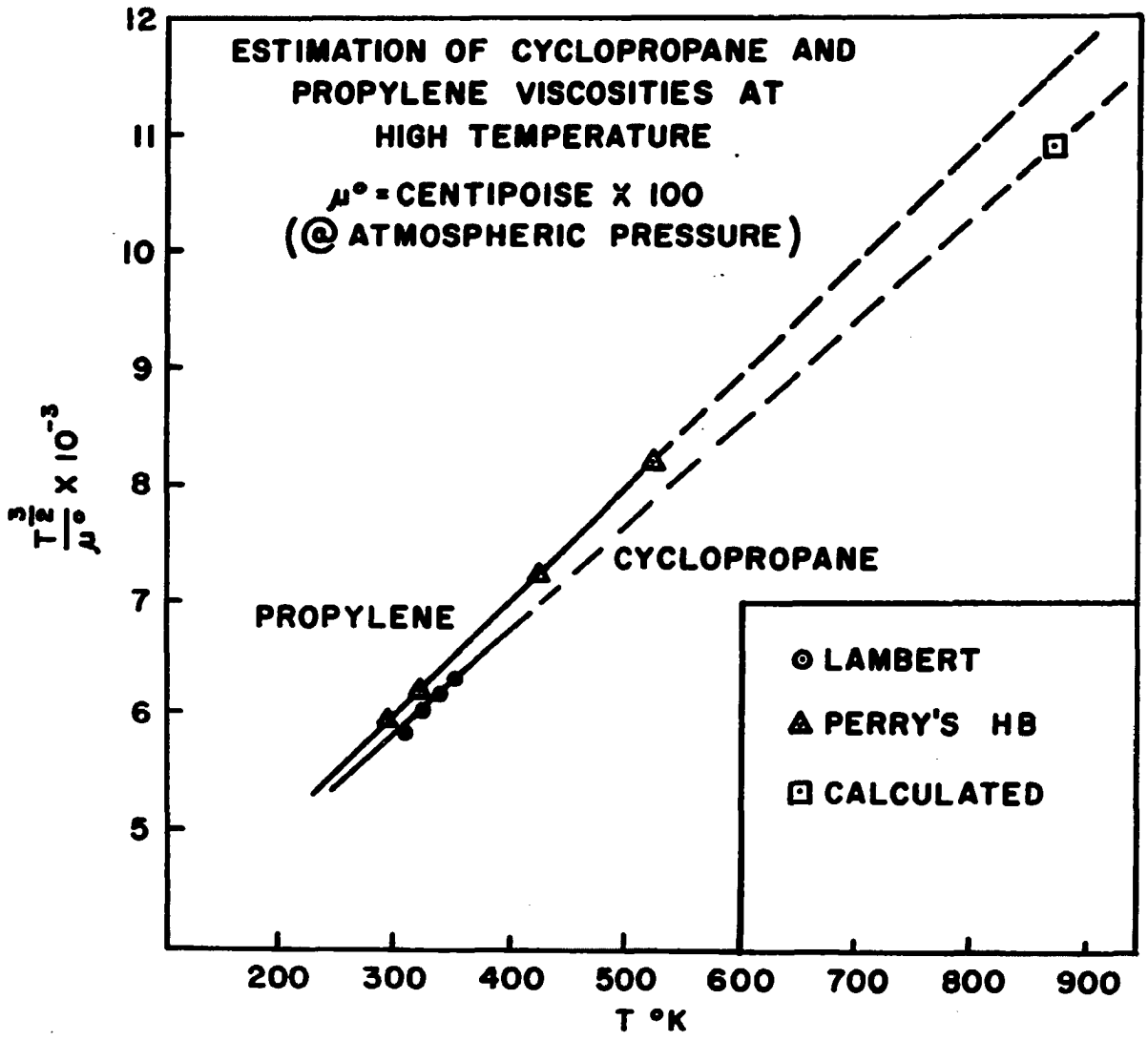
ESTIMATION OF CYCLOPROPANE AND
PROPYLENE VISCOSITIES AT
HIGH TEMPERATURE
μ° = CENTIPOISE X 100
(@ ATMOSPHERIC PRESSURE)
CYCLOPROPANE
PROPYLENE
LAMBERT
PERRY'S HB
CALCULATED
T °K
200
300
400
500
600
700
800
900
5
6
7
8
9
10
11
12

Figure 36

APPENDIX E

IGNITOR AND BASO DEVICE ELECTRICAL CIRCUITS

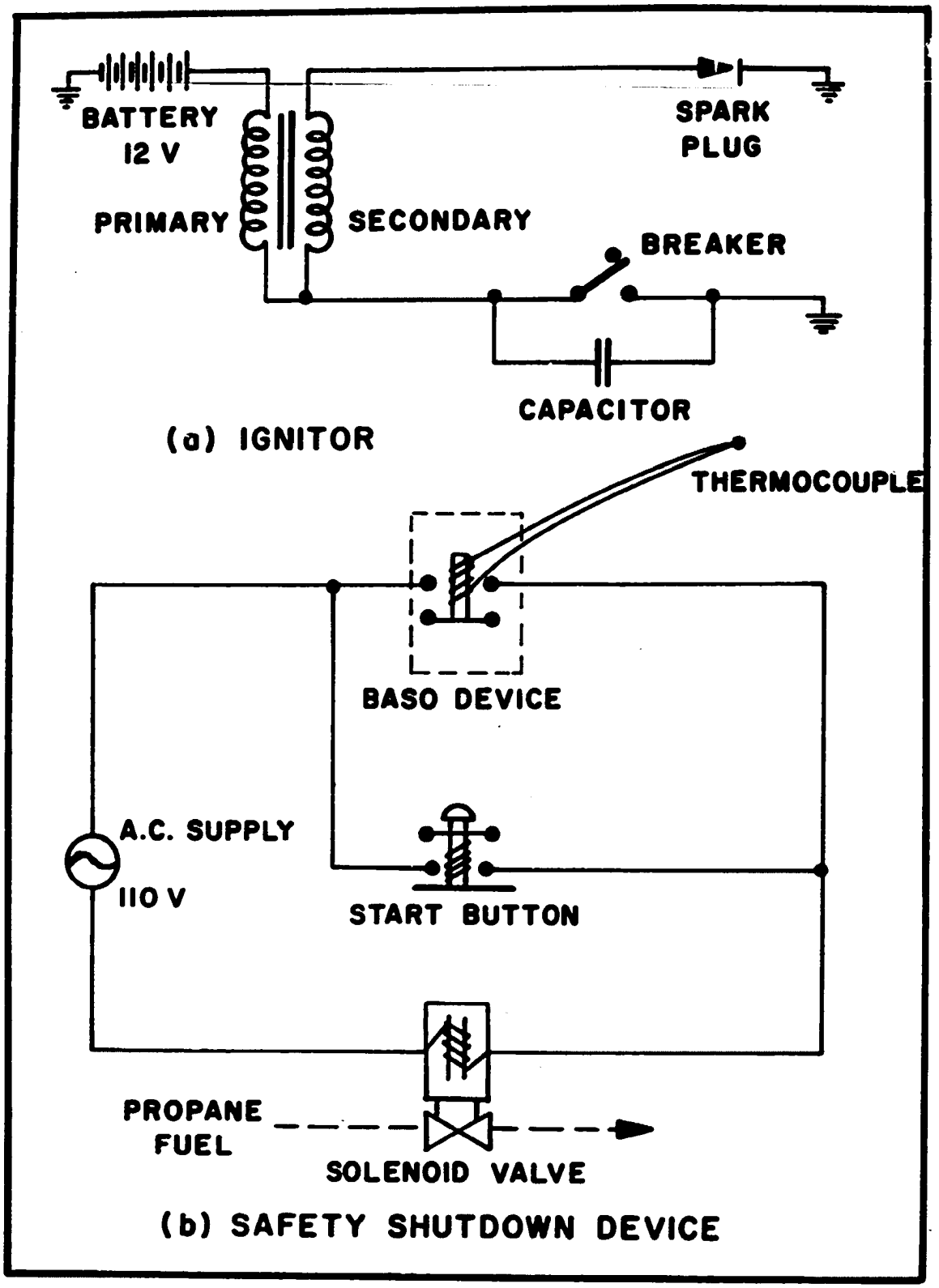

BURNER IGNITION SYSTEM
ELECTRICAL CIRCUIT DIAGRAMS

Figure 37

APPENDIX F

BURNER AND SAND BATH HEATER DRAWINGS

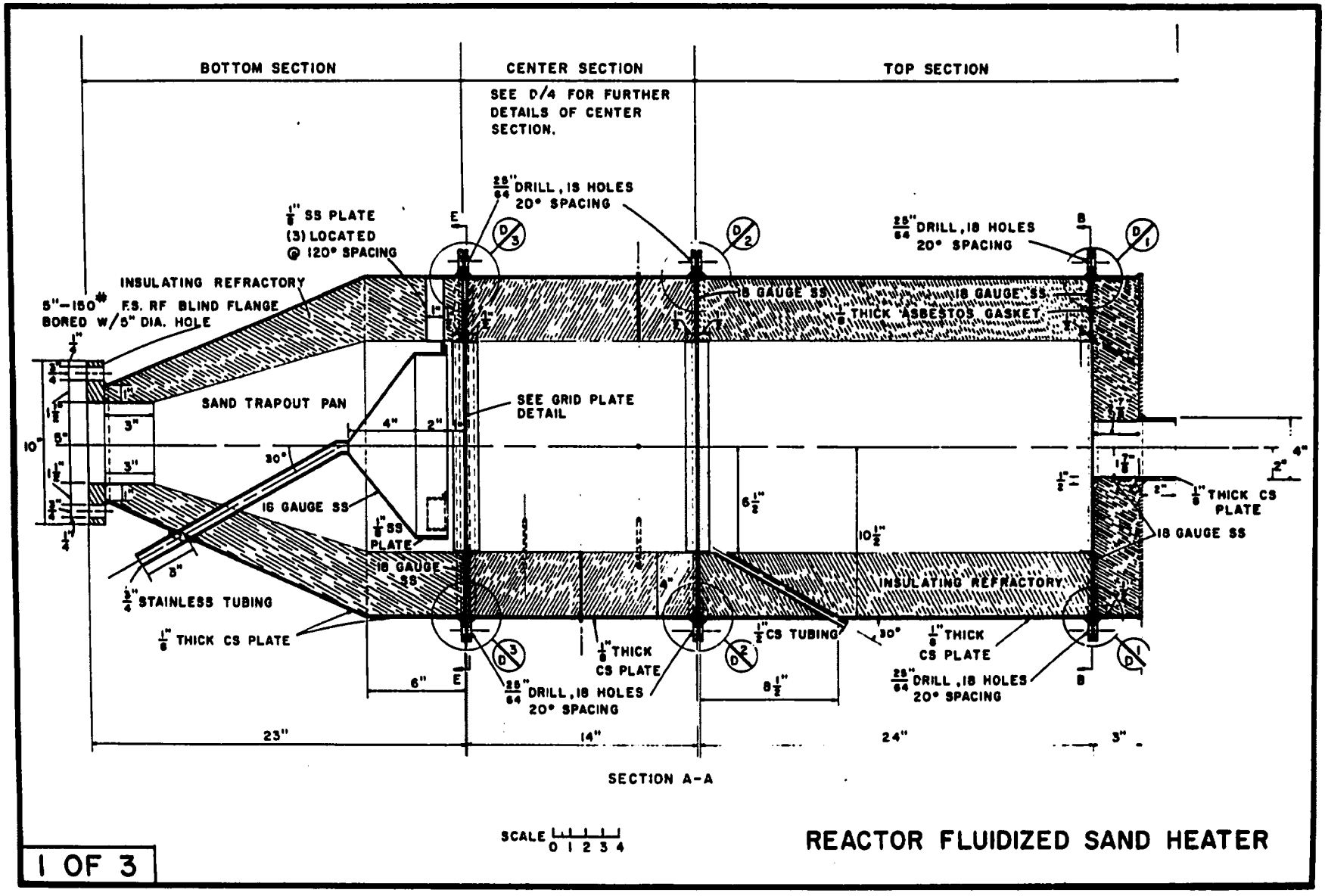
BOTTOM SECTION
CENTER SECTION
TOP SECTION
SEE D/4 FOR FURTHER DETAILS OF CENTER SECTION.
25/64" DRILL, 18 HOLES 20° SPACING
1/8" SS PLATE (3) LOCATED @ 120° SPACING
INSULATING REFRACTORY
5"-150# F.S. RF BLIND FLANGE BORED W/5" DIA. HOLE
18 GAUGE SS
1/8" THICK ASBESTOS GASKET
SAND TRAPOUT PAN
SEE GRID PLATE DETAIL
16 GAUGE SS
1/8" SS PLATE
3/4" STAINLESS TUBING
1/8" THICK CS PLATE
1/2" CS TUBING
1/8" THICK CS PLATE
INSULATING REFRACTORY
18 GAUGE SS
23"
14"
24"
3"
SECTION A-A
SCALE 0 1 2 3 4
REACTOR FLUIDIZED SAND HEATER
1 OF 3

Figure 38

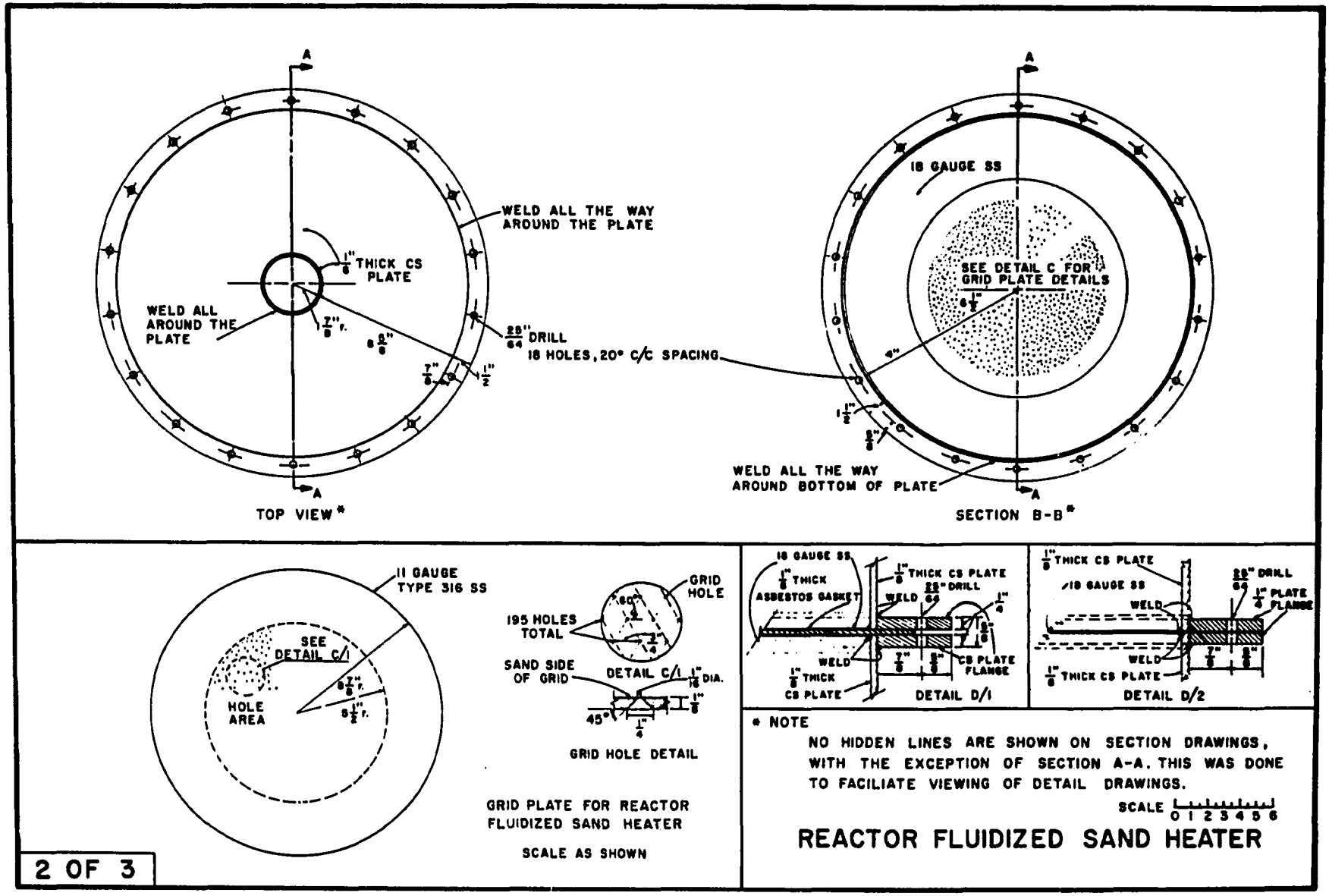
A
WELD ALL THE WAY AROUND THE PLATE
1/8" THICK CS PLATE
WELD ALL AROUND THE PLATE
7/8" R.
8 5/8"
7/8"
1/2"
25/64" DRILL
18 HOLES, 20° C/C SPACING
TOP VIEW *
18 GAUGE SS
SEE DETAIL C FOR GRID PLATE DETAILS
1 1/8"
4"
1 1/2"
5/8"
WELD ALL THE WAY AROUND BOTTOM OF PLATE
SECTION B-B *
11 GAUGE TYPE 316 SS
SEE DETAIL C/1
HOLE AREA
8 7/8" R.
8 1/2" R.
GRID HOLE
195 HOLES TOTAL
.60"
3/4"
SAND SIDE OF GRID
DETAIL C/1
1/16" DIA.
1/8"
45°
1/4"
GRID HOLE DETAIL
GRID PLATE FOR REACTOR FLUIDIZED SAND HEATER
SCALE AS SHOWN
18 GAUGE SS
1/8" THICK ASBESTOS GASKET
1/8" THICK CS PLATE
25/64" DRILL
WELD
1/4"
5/8"
7/8"
1 1/8"
CS PLATE FLANGE
1/8" THICK CS PLATE
DETAIL D/1
1/8" THICK CS PLATE
18 GAUGE SS
25/64" DRILL
1/4" PLATE FLANGE
WELD
7/8"
1 1/8"
1/8" THICK CS PLATE
DETAIL D/2
* NOTE
NO HIDDEN LINES ARE SHOWN ON SECTION DRAWINGS, WITH THE EXCEPTION OF SECTION A-A. THIS WAS DONE TO FACILIATE VIEWING OF DETAIL DRAWINGS.
SCALE 0 1 2 3 4 5 6
REACTOR FLUIDIZED SAND HEATER
2 OF 3

Figure 39A

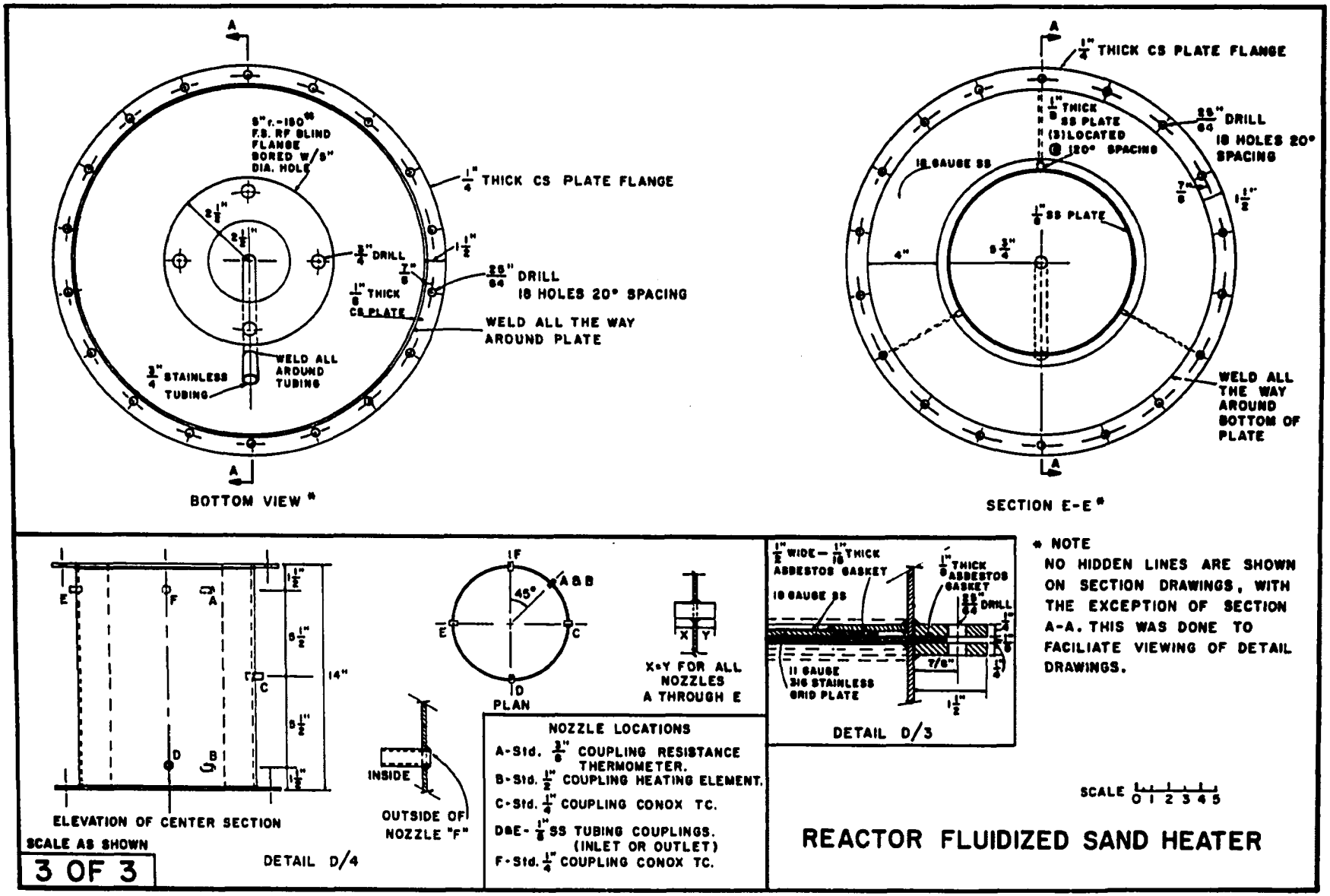
8"r.-150# F.S. RF BLIND FLANGE BORED W/ 5" DIA. HOLE
1/4" THICK CS PLATE FLANGE
3/4" DRILL
1/8" THICK CS PLATE
25/64" DRILL 18 HOLES 20° SPACING
WELD ALL THE WAY AROUND PLATE
3/4" STAINLESS TUBING
WELD ALL AROUND TUBING
BOTTOM VIEW *
1/4" THICK CS PLATE FLANGE
1/8" THICK SS PLATE (3) LOCATED @ 120° SPACING
25/64" DRILL 18 HOLES 20° SPACING
18 GAUGE SS
1/8" SS PLATE
WELD ALL THE WAY AROUND BOTTOM OF PLATE
SECTION E-E *
ELEVATION OF CENTER SECTION
SCALE AS SHOWN
DETAIL D/4
PLAN
X=Y FOR ALL NOZZLES A THROUGH E
INSIDE
OUTSIDE OF NOZZLE "F"
NOZZLE LOCATIONS
A-Std. 3/8" COUPLING RESISTANCE THERMOMETER.
B-Std. 1/2" COUPLING HEATING ELEMENT.
C-Std. 1/4" COUPLING CONOX TC.
D&E- 1/8" SS TUBING COUPLINGS. (INLET OR OUTLET)
F-Std. 1/4" COUPLING CONOX TC.
1/8" WIDE - 1/16" THICK ASBESTOS GASKET
1/8" THICK ASBESTOS GASKET
18 GAUGE SS
11 GAUGE 316 STAINLESS GRID PLATE
DETAIL D/3
* NOTE
NO HIDDEN LINES ARE SHOWN ON SECTION DRAWINGS, WITH THE EXCEPTION OF SECTION A-A. THIS WAS DONE TO FACILIATE VIEWING OF DETAIL DRAWINGS.
SCALE 0 1 2 3 4 5
REACTOR FLUIDIZED SAND HEATER
3 OF 3

Figure 39 B

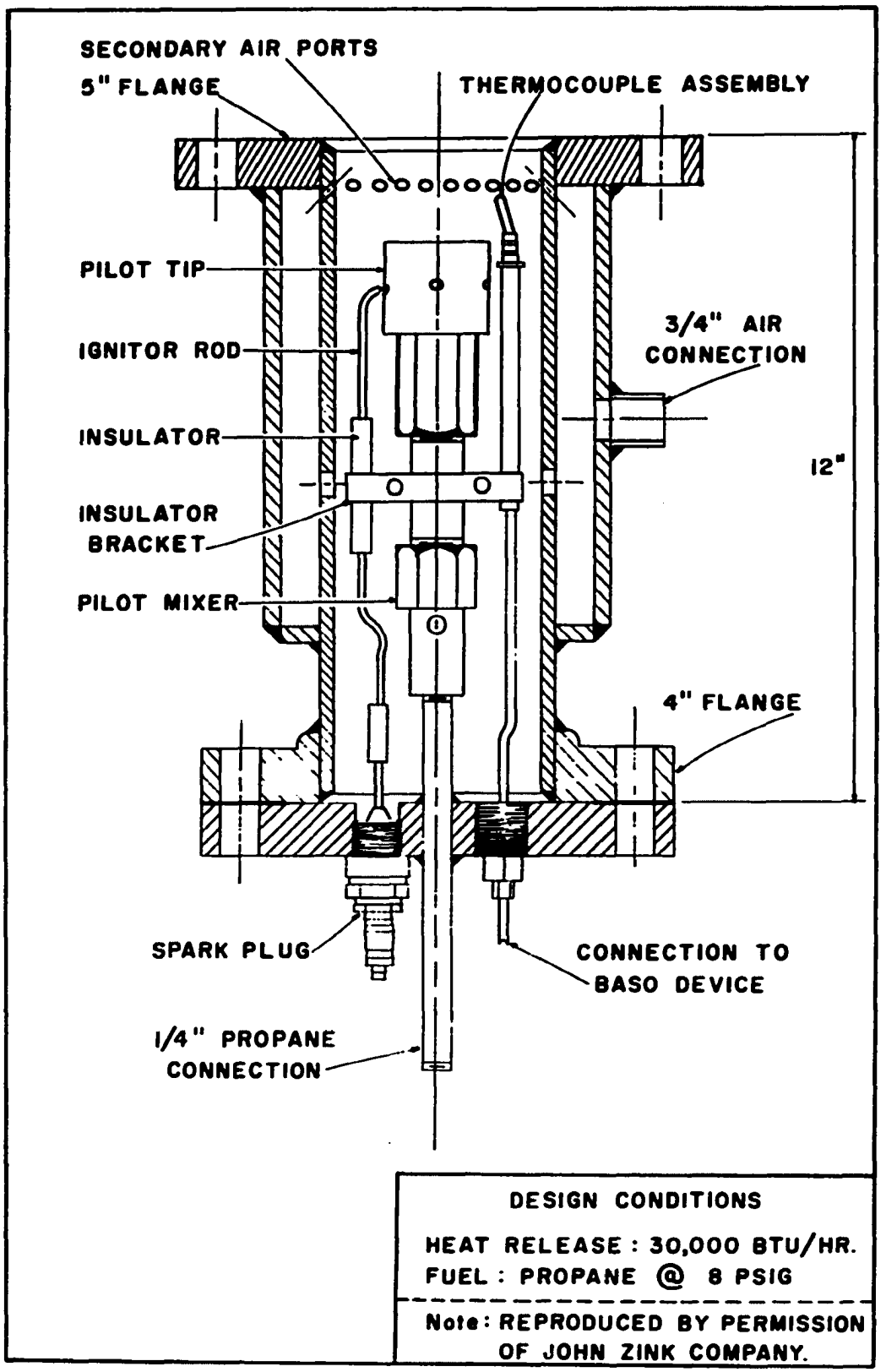

SECTIONAL ELEVATION OF BURNER
FOR SAND BATH HEATER

Figure 40

APPENDIX G

SUMMARY OF EXPERIMENTAL DATA

TABLE 12

SUMMARY OF EXPERIMENTAL RESULTS

Run No.	Temp. °F	Press. psig	Average Residence Time ⟨τ⟩ (sec)	Average Velocity ⟨v⟩ (ft/sec)	Propylene Outlet %	Propylene Inlet %	Conv. %	Rate Constant k_c $(sec)^{-1}$	Dry Product Gas (SCFM)	Product/Feed SCFM Ratio x100	Notes
I-1	948.3	520	25.60	0.539	3.08	0.16	2.92	1.160×10^{-3}	0.2352	97.24	CP, MLP
I-2	950.8	1000	59.21	0.233	6.83	0.31	6.54	1.142×10^{-3}	0.2326	97.39	CP, MLP
I-3	949.9	1500	92.06	0.150	11.00	0.53	10.53	1.205×10^{-3}	0.2267	98.88	CP, MLP
I-4	950.3	2000	156.7	0.088	16.03	0.52	15.59	1.082×10^{-3}	0.1795	96.44	CP, TLP
II-1	900.1	500	88.03	0.157	2.44	0.14	2.30	2.673×10^{-4}	0.0818	98.61	CP, MLP
II-2	900.0	1000	137.2	0.100	3.73	0.29	3.45	2.555×10^{-4}	0.1048	99.14	CP, MLP
II-3	899.6	1500	225.3	0.061	5.67	0.37	5.32	2.428×10^{-4}	0.0970	99.23	CP, MLP
II-4	899.9	2000	317.2	0.043	7.63	0.71	6.97	2.276×10^{-4}	0.0929	99.04	CP, MLP
III-250	850.5	250	113.4	0.122	0.72	0.05	0.67	5.953×10^{-5}	0.0337	100.44	CP, MLP, (a)
III-1	850.9	500	197.6	0.070	1.20	0.10	1.10	5.577×10^{-5}	0.0381	99.33	CP, MLP, (a)
III-2	850.4	1000	380.8	0.036	2.11	0.21	1.90	5.305×10^{-5}	0.0394	100.16	CP, MLP, (a)
III-3	850.4	1500	590.7	0.023	3.08	0.33	2.76	4.740×10^{-5}	0.0389	100.55	CP, MLP
III-4	850.1	2000	971.8	0.014	4.94	0.47	4.49	4.728×10^{-5}	0.0320	100.06	CP, MLP
IV-1	999.5	500	49.87	0.276	25.3	1.1	24.2	5.624×10^{-3}	0.1337	100.70	CP, MLP
IV-2	999.9	1000	—	—	—	—	—	—	0.1106	86.67	CP, LP, (b)
V-250	874.6	250	60.20	0.229	0.85	0.26	0.59	9.883×10^{-5}	0.0624	100.16	CP, MLP
V-1	875.4	500	190.9	0.072	2.27	0.50	1.78	9.390×10^{-5}	0.0385	96.68	CP, MLP
V-2	874.7	1000	485.9	0.028	5.73	0.75	5.02	1.060×10^{-4}	0.0303	91.08	CP, MLP, (c)
V-3	875.2	1500	1025.1	0.013	9.90	1.40	8.62	8.789×10^{-5}	0.0219	88.66	CP, MLP, (c)
V-4	875.1	2000	2015.7	0.007	9.18	1.71	7.60	3.969×10^{-5}	0.0154	79.35	CP, LP
VI-1	925.4	500	53.62	0.257	3.43	0.34	3.10	5.875×10^{-4}	0.1315	99.80	CP, MLP
VI-2	925.1	1000	120.3	0.115	7.55	0.44	7.14	6.154×10^{-4}	0.1171	99.27	CP, MLP
VI-3	925.3	1500	200.6	0.069	12.00	0.51	11.55	6.123×10^{-4}	0.1065	98.43	CP, MLP
VI-4	924.8	2000	293.2	0.047	14.62	1.26	13.53	4.956×10^{-4}	0.0983	96.83	CP, LP
VII-250	974.8	250	26.60	0.518	8.03	0.87	7.22	2.819×10^{-3}	0.1303	99.00	CP, MLP
VII-1	975.0	500	68.59	0.201	13.40	1.06	12.47	1.941×10^{-3}	0.1214	100.14	CP, MLP
VII-2	974.7	1000	119.4	0.115	25.10	1.25	24.15	2.317×10^{-3}	0.1133	96.96	CP, TLP
VII-1200	974.9	1200	—	—	—	—	—	—	0.1034	91.68	CP, LP
VIII-250	1024.6	250	23.74	0.581	24.04	0.72	23.49	1.130×10^{-2}	0.1412	101.02	CP, MLP
VIII-1	1025.0	500	54.76	0.252	44.65	1.84	43.61	1.046×10^{-2}	0.1195	95.06	CP, TLP, (d)
IX-1	899.6	500	38.34	0.360	1.17	0.14	1.03	2.707×10^{-4}	0.1878	97.85	CP, TLP
IX-2	899.6	1000	80.73	0.171	2.34	0.22	2.12	2.658×10^{-4}	0.1781	98.51	CP, TLP, (e)
IX-3	899.7	1500	130.3	0.106	3.74	0.27	3.48	2.718×10^{-4}	0.1676	98.32	CP, TLP, (f)
IX-4	900.0	2000	189.6	0.073	5.33	0.42	4.93	2.669×10^{-4}	0.1554	97.84	CP, TLP, (f)
X-1	899.9	500	75.80	0.182	2.28	0.23	2.05	2.740×10^{-4}	0.0951	99.12	CP, TLP, (f)
X-2	899.7	1000	160.8	0.086	4.19	0.26	3.94	2.498×10^{-4}	0.0895	98.90	CP, TLP, (f)
X-3	900.3	1500	266.0	0.052	7.58	0.46	7.15	2.797×10^{-4}	0.0823	99.54	CP, TLP, (f)
X-4	899.9	2000	407.8	0.034	10.15	0.65	9.56	2.459×10^{-4}	0.0723	98.38	CP, TLP, (f)
XI-250	1049.4	250	16.68	0.826	31.50	1.26	30.63	2.194×10^{-2}	0.1975	98.53	CP, MLP, (f)
XI-1	1050.6	500	—	—	—	—	—	—	0.1809	93.12	CP, LP, (f)

SUMMARY OF EXPERIMENTAL RESULTS--Continued

Run No.	Temp. °F	Press. psig	Average Residence Time (τ) (sec)	Average Velocity (v) (ft/sec)	Propylene Outlet %	Propylene Inlet %	Conv. %	Rate Constant k_c $(sec)^{-1}$	Dry Product Gas (SCFM)	Product Feed SCFM Ratio x100	Notes
XII-1	900.3	500	--	--	3.57	5.55	-2.10	--	0.1889	97.50	KB, TLP, (f), (g)
XII-2	899.4	1000	--	--	5.10	5.40	-0.32	--	0.1818	98.36	KB, TLP, (f), (g)
XII-3	900.7	1500	--	--	6.64	5.70	1.00	--	0.1689	97.89	KB, MLP, (f), (g)
XII-4	899.8	2000	--	--	8.20	6.16	2.17	--	0.1560	98.01	KB, MLP, (f), (g)
XIII-1	899.9	500	--	--	4.19	2.97	1.26	--	0.0803	100.03	KB, MLP, (f), (g)
XIII-2	900.0	1000	--	--	9.04	6.45	2.77	--	0.0720	100.23	KB, MLP, (f), (g)
XIII-3	900.4	1500	--	--	(h)	--	--	--	0.0618	98.26	KB, MLP, (f), (g)
XIII-4	900.2	2000	--	--	(h)	--	--	--	0.0445	90.82	KB, LP, (f), (g)
XIV-1	899.6	500	54.20	0.254	3.43	1.71	1.75	3.256×10^{-4}	0.1330	97.99	KB, MLP, (i)
XIV-2	900.0	1000	123.0	0.112	6.04	2.76	3.37	2.791×10^{-4}	0.1168	97.72	KB, MLP, (i)
XIV-3	900.0	1500	196.3	0.070	8.35	3.63	4.90	2.547×10^{-4}	0.1112	96.45	KB, MLP, (i)
XIV-4	899.8	2000	285.6	0.048	10.42	5.02	5.69	2.049×10^{-4}	0.1032	96.65	KB, MLP, (i)
XV-1	949.8	500	57.24	0.241	10.60	4.03	6.85	1.239×10^{-3}	0.1207	96.37	KB, MLP, (j)
XV-2	950.0	1000	118.72	0.116	18.15	7.50	11.51	1.030×10^{-3}	0.1169	94.34	KB, TLP, (j)
XV-3	950.1	1500	--	--	--	--	--	--	0.0959	85.44	KB, LP
XV-3(9/16")	950.2	1500	--	--	--	--	--	--	0.1571	92.54	KB, LP
XV-4(9/16")	949.9	2000	--	--	--	--	--	--	0.1320	83.54	KB, LP
XVI-1	850.0	500	89.83	0.153	0.766	0.620	0.147	1.637×10^{-5}	0.0834	99.28	KB, MLP, (k)
XVI-2	849.4	1000	196.0	0.070	1.148	0.841	0.310	1.607×10^{-5}	0.0767	98.29	KB, TLP, (k)
XVI-3	849.8	1500	330.4	0.042	1.752	1.287	0.471	1.432×10^{-5}	0.0695	97.33	KB, MLP, (k)
XVI-4	850.0	2000	537.3	0.026	2.651	1.923	0.742	1.398×10^{-5}	0.0578	94.82	KB, LP, (k)
XVII-1	899.8	500	54.26	0.254	2.04	1.52	0.53	9.768×10^{-5}	0.1327	98.85	KB, MLP, (l)
XVII-2	900.0	1000	111.9	0.123	3.06	2.06	1.02	9.156×10^{-5}	0.1284	98.06	KB, TLP, (l)
XVII-3	900.0	1500	186.9	0.074	4.35	2.78	1.61	8.710×10^{-5}	0.1169	98.75	KB, MLP, (l)
XVII-4	899.7	2000	279.6	0.049	6.06	4.00	2.15	7.746×10^{-5}	0.1054	95.26	KB, MLP, (l)
XVIII-2	899.8	1000	207.0	0.067	4.69	1.78	2.96	1.454×10^{-4}	0.0696	101.1	CP, MLP, (l), (m)
XIX-1	899.8	500	104.9	0.131	2.74	0.48	2.27	2.190×10^{-4}	0.0687	101.27	CP, MLP, (n)
XIX-2	900.1	1000	210.4	0.066	4.88	0.74	4.18	2.027×10^{-4}	0.0683	98.49	CP, MLP, (n)
XIX-3	900.2	1500	386.7	0.026	7.80	0.94	6.93	1.854×10^{-4}	0.0365	94.26	CP, MLP, (n)
XX-1	949.6	500	39.32	0.351	3.81	0.22	3.59	9.307×10^{-4}	0.1761	95.70	CP, MLP, (o)
XX-2	950.2	1000	80.91	0.170	8.29	0.31	8.01	1.031×10^{-3}	0.1703	97.90	CP, MLP, (o)
XX-3	950.2	1500	125.9	0.109	12.10	0.51	11.65	9.839×10^{-4}	0.1658	96.71	CP, MLP, (o)
XX-4	949.9	2000	180.6	0.076	15.43	0.73	14.81	8.863×10^{-4}	0.1557	96.29	CP, MLP, (o)
XXI-1	949.8	500	37.13	0.371	4.44	0.24	4.21	1.158×10^{-3}	0.1863	97.67	CP, MLP, (p)
XXII-1	950.0	500	44.54	0.310	5.50	0.39	5.13	1.182×10^{-3}	0.1554	98.22	CP, MLP, (q), (r)
XXII-2	949.5	1000	113.4	0.122	12.80	1.00	11.92	1.120×10^{-3}	0.1216	98.09	CP, MLP, (q), (r)
XXII-3	950.0	1500	201.9	0.068	18.40	1.35	17.28	0.941×10^{-3}	0.1033	96.35	CP, MLP, (r)
XXII-4	950.1	2000	--	--	16.90	1.43	15.69	--	0.0848	88.62	CP, LP, (r)

SUMMARY OF EXPERIMENTAL RESULTS--Continued

Run No.	Temp. °F	Press. psig	Average Residence Time ⟨τ⟩ (sec)	Average Velocity ⟨v⟩ (ft/sec)	Propylene Outlet %	Propylene Inlet %	Conv. %	Rate Constant k_c $(sec)^{-1}$	Dry Product Gas (SCFH)	Product Feed SCFH Ratio x100	Notes
XXIII-250	1100.1	250	15.38	0.896	70.40	3.14	69.44	7.705×10^{-2}	0.2072	96.39	CP, NLP, (s)
XXIV-1	824.9	500	112.2	0.123	2.49	0.25	2.24	2.028×10^{-4}	0.0682	99.43	CP, NLP, (t)
XXIV-2	824.9	1000	224.5	0.061	2.90	0.46	2.45	1.105×10^{-4}	0.0685	97.33	CP, TLP, (t)
XXV-1	825.0	500	109.1	0.126	1.45	0.11	1.34	1.238×10^{-4}	0.0701	94.49	CP, NLP, (u)
XXVI-1	899.8	500	61.8	0.223	4.45	0.60	3.85	6.812×10^{-4}	0.1165	101.24	CP, NLP, (v)
XXVI-2	900.5	1000	116.4	0.118	5.21	2.34	2.94	2.095×10^{-4}	0.1234	100.33	CP, NLP, (v)
XXVII-1	899.9	500	58.85	0.236	1.00	0.25	0.75	1.287×10^{-4}	0.1225	99.44	CP, NLP, (w)
XXVII-2	900.6	1000	118.6	0.116	2.04	0.54	1.51	1.281×10^{-4}	0.1212	98.01	CP, NLP, (w)

Footnote Comments on Experimental Results

CP - preheater constructed from coiled, stainless steel tube, 1/8" o.d. by 1/16" i.d. with 15'-7-3/8" length.

KB - preheating accomplished in four modified Kuentzel bombs connected in series.

NLP - no liquid product in receiver at conclusion of run.

TLP - trace of liquid product in receiver at conclusion of run.

LP - liquid product present in receiver at conclusion of run.

(a) - liquid product approximately 10 per cent by weight of feed on Run IV-2. Plugging occurred at reactor outlet at close of run. Decoked with compressed air at 1500 p.s.i. and 900°F. First decoking operation.

(c) - recycle valves were found to be leaking at the end of Run V, thus providing an explanation for the low recovery. The k_c values are calculated from product gas meter flow and hence are correct.

(d) - plugging at reactor outlet occurred when raising pressure to 750 p.s.i. after Run VIII-1. The obstruction was removed in approximately 10 minutes with compressed air at 2000 p.s.i. and 1025°F.

(e) - broke handle on preheater outlet sample valve on Run IX-2.

(f) - inlet composition was determined after runs by passing feed through the preheater alone, with reactor bypassed.

(g) - after Run XII and XIII the Kuentzel bomb preheaters were found partially plugged and were decoked. The decoking procedure activated the preheater to the extent that subsequent measured preheater outlet compositions could not be used to obtain the true reactor conversion.

(h) - chromatograms showed other products in addition to propylene and cyclopropane.

(i) - returned to use of sample connection at reactor inlet.

(j) - favorable comparison with Run I.

(k) - the calculated k_c values of Run XVI were found to be much lower than those for Run III. This discrepancy was later found to be the result of carbon accumulation in the reactor.

(l) - low k_c value was later found to be the result of carbon accumulation in the reactor.

(m) - returned to use of stainless steel coil as preheater.

(n) - after Run XVIII, for two hours air was passed through the reactor under 1500 p.s.i. pressure with temperature maintained between 900 and 1030°F. This operation was partially successful. The reactor inlet sample cooler was found plugged with fine carbon and replaced after Run XVIII.

(o) - Run XX was made after decoking for five hours at temperatures up to 1165°F. with compressed air under

a pressure of 1200 p.s.i. The k_c values are 8 to 20 per cent below those of Run I, indicating the presence of some remaining coke.

(p) - after Run XX, the reactor was decoked for an additional 5½ hours at temperatures up to 1200°F. with air at 1100 p.s.i. Excellent k_c check with Run I. Compressor failure prevented further runs.

(q) - The k_c values of Run I were reproduced at the 500 and 1000 p.s.i. levels.

(r) - preheater became partially plugged when shutting down after Run XXII. Preheater was cleared with air under 2300 p.s.i. pressure, while maintaining a temperature of 1100°F. Extremely fine carbon was blown from the preheater.

(s) - when raising pressure to 500 p.s.i., plugging started at reactor outlet. Decoked one hour with air at 1900 p.s.i. while temperature was between 900 and 1000°F.

(t) - chromatograms indicated catalytic reaction in both preheater and reactor. Pressure increased to 1400 p.s.i. on the pump discharge at the end of Run XXIV-2. Passed air through system for 1½ hours at pressure between 1300 and 1800 p.s.i. and temperature from 825 to 1000°F. The k_c values were much too high for thermal reaction alone. <u>These runs were the first to indicate a catalytic effect in the reactor</u>.

(u) - Run XXV-1 was made to see if the previous decoking operation had been successful in eliminating the unusual reactor behavior. It wasn't. Decoked again with reactor at 1120°F. and preheater at 980°F. Air pressure was maintained at 1000 to 1300 p.s.i. for 5 hours.

(v) - Run XXVI was made to determine if previous results at 900°F. could be reproduced after the prolonged decoking period. They weren't. On Run XXVI-1, k_c is 2.5 to 3.0 times too large. For Run XXVI-2, the k_c value is low. Chromatograms indicated large quantities of two light products eluted prior to propylene in the product sample.

(w) - the unit was run for three hours prior to these observations until an equilibrium condition appeared to exist. The k_c values were at first high and then low. The strange behavior starting with Run XXIV-1 was explained when the reactor was opened. The reactor lining was found to be collapsed for essentially the full tube length.

TABLE 13

SUMMARY OF RUNS USED IN ARRHENIUS CORRELATIONS

Figure	15	16	17	18	19
		Run Number			
Pressure(psi)	250	500	1000	1500	2000
	III-250	I-1	I-2	I-3	I-4
	V-250	II-1	II-2	II-3	II-4
	VII-250	III-1	III-3	III-3	III-4
	VIII-250	IV-1	V-2	VI-3	IX-4
	XI-250	V-1	VI-2	IX-3	X-4
	XXIII-250	VI-1	VII-2	X-3	XIV-4
		VII-1			
		IX-1	IX-2	XIV-3	
		X-1	X-2	XXII-3	
		XIV-1	XIV-2		
		XV-1	XXII-2		
		XXI-1			
		XXII-1			

APPENDIX H

SAMPLE DATA SHEETS AND CALCULATIONS

THERMAL ISOMERIZATION OF CYCLOPROPANE

Run Data Sheet No. 1

Date 6/12/64 Time (B) 6 45 PM

(E) _____

Run No. II-4

Conditions:

Reactor Outlet Pressure	2000 ± 10	psig	
Reactor Temp. (No. 7) (L & N 8662)	(a) 900.0 °F.	900.0	899.9 AVE.
	(b) 899.9 °F.	900.0	
	(c) 899.65 °F.		
Pump Discharge Pressure	2050	psig	
Fluidizing Air Rate	8.0	Rdg	
Propane Fuel Rate	9.0	Rdg (Glass)	
Pump Cylinder: Near	✓	Far _____	
Stroke Length	7/16	Inches	
Cyclopropane Storage: Pressure	180	psig	
Temp.	76	°F.	
Wet Test Meter Temperature	82	°F.	
Barometric Pressure	28.68	in. hg.	
Chilled Water Temperature	36	°F.	
Ambient Temperature	79.9	°F.	

Observation No.	Time (Minutes)	Cyclopropane Level (cm) (B)	(E).	diff.	Wet Gas Flow(CF) (Uncorrected)
A	5	55.5	23.9	31.6	0.530
B	5	55.3	24.4	30.9	0.516
C	5	55.1	23.7	31.4	0.525
D	5	55.0	23.8	31.2	0.522
E	5	54.8	23.2	31.6	0.533
			AVE.	31.3	MAX. DEV. 1.40%

NOTE: For Recorded Temperatures See Separate Strip Chart.

Remarks:

GOOD UNIFORM METER ROTATION

THERMAL ISOMERIZATION OF CYCLOPROPANE

Run Data Sheet No. 2

Run No. II-4

Auxiliary Readings:

Preheater Powerstat: Near 46 %
Far 46 %

Bayley Sand Bath Control:
Coarse 9.22 Rdg
Fine 2.0 Rdg

Reactor Outlet Heater 75 %

Reactor Inlet Heater 100 %

CHROMATOGRAPH*

Observation No.	Time for 50 ml Helium Flow (sec)	Cell Current (milliamps)	Bath Temp. °F.
A	60.2	10.04	143.1
B			
C			
D			
E			
F			

* Note - see separate chromatograms

LEGEND

T. C. No.	Description
1	Preheater Side Well
2	Sand Bath Center Well (6"Length)
3	Sand Bath Top Well (12" Length)
4	Preheater Outlet (IC)
5	Preheater Top Well
6	Reactor Outlet (IC)
7	Sand Bath Probe
8	Reactor Outlet (IC)

CALCULATION WORK SHEET NO. 1

Calculation of Corrected Wet Test Meter Flow Rates

Run No. II-4

(1) Wet Test Meter Temperature 82 °F.

(2) VP of Water @ WTM Temp. 1.1016 in. hg.

(3) Barometric Pressure 28.68 in. hg.

(4) Total Wet Gas (see each obs.) cu. ft.

(5) Observation Period (see each obs.) min.

(6) WTM Temp. Plus 459.69 541.69 °R

Dry Gas Volume

Fraction = (3) $\frac{28.68}{28.68}$ - (2) 1.1016 = (7) $\frac{27.578}{28.68}$ = 0.9616

Dry Gas (SCFM) = (4) ✓ x (7) $\frac{27.578}{5}$ x (3) $\frac{\times}{29.92}$ x $\frac{519.69}{541.69}$ (5) (6)

= (4) ✓ x (8) 0.1769

Observation No.		(9) SCFM	(9)/Liquid (SCFM)	Recovery %
A	(4) 0.530 x (8) 0.1769	0.0938	10.0946	99.15
B	(4) 0.516 x (8) ✓	0.0913	10.0925	98.70
C	(4) 0.525 x (8) ✓	0.0929	10.0940	98.83
D	(4) 0.522 x (8) ✓	0.0923	10.0934	98.82
E	(4) 0.533 x (8) ✓	0.0943	10.0946	99.68
F	(4) ____ x (8) ____	____	/	____
	AVE.	0.0929		99.04
	MAX. DEV.	1.72 %		

CALCULATION WORK SHEET No. 2

Calculation of Cyclopropane SCFM From Liquid Pumping Rate

Sight Glass Volume Per cm Lenght = 1.258 cc

Run No. II-4

(1) Cyclopropane Storage Temperature 76 °F.

(2) Cyclopropane Density 0.5987 gm/cc

(3) Liquid Pumped (level difference) (see each obs.) cm

(4) Observation Period (see each obs.) min

Weight Per cm = 1.258 x (2) 0.5987 = (5) 0.7532

Total Weight Pumped = (5) _____ x (3) _____ = (6) _____

$$SCFM = \frac{(6)}{(4)} \times \frac{1}{453.6} \times \frac{379.37}{42.078} = 0.01988 \times \frac{(6)}{(4)}$$

Observation No.	(3)	(3)x(5)	(4)	(6)/(4)	SCFM
A	31.6	23.80	5	4.760	0.0946
B	30.9	23.27	5	4.654	0.0925
C	31.4	23.65	5	4.730	0.0940
D	31.2	23.50	5	4.700	0.0934
E	31.6	23.80	5	4.760	0.0946
F					

CHROMATOGRAPH RESULTS

Date 6/12/64

Run II-4

Reactor Outlet

Observation	Peak Height Ratio =/Δ	Propylene %
A	0.1665	
B	0.1592	
C	0.1572	
D	0.1610	
E	0.1765	
Ave	0.1641	7.63

Preheater Outlet

B	0.0152	
E	0.0155	
Ave	0.01535	0.71

Net Reactor Conversion 6.92 %

Comparison of Standard Sample Checks With Calibration

Bomb No.	Propylene %	Peak Height Ratio =/Δ (or reciprocal when starred) Calibration	Check	No. Samples
1	93.81	0.0648*	0.0650*	1
2	82.73	0.2092*	0.2125*	3
3	73.08	0.3472*	0.3507*	3
4	59.33	0.5822*	0.5880*	2
5	36.75	0.8482	0.8424	2
7	21.51	0.4696	0.4725	2
8	12.58	0.2701	0.2692	3

Remarks:

k_c CALCULATION WORKSHEET

Run II-4 Date 6/12/64

$$k_c = \frac{Z_m R T F_o}{P V_R} \ln \frac{(Y_A)_I}{(Y_A)_o}$$

Pressure (P) 2014.7 psia V_R = 0.00883 cu ft

Temp (T) 1359.59 °R R = 10.73

Evaluate Z_m @ Arithmetic Average Composition

F_o = $\frac{0.0929}{(60)(379.37)}$ SCFM = 0.4081×10^{-5} moles/sec

CRITICAL PROPERTIES

	=	Δ
T_c(°R)	649.80	716.06
P_c(psia)	667.22	796.99

Ave. Propylene MF=(0.71 % in + 7.63 % out)/200 = (1) 0.0417

T_c(mix) = (1) 0.0417 (649.80) + {1.0 - (1)} 0.9583 (716.06)=
(2) 713.3 °R

P_c(mix)=(1) 0.0417 (667.22)+{1.0-(1)} 0.9583 (796.99)-(3) 791.58 psia

$p T_r = \frac{(T)\ 1359.59}{(T_c)\ 713.30} = 1.90$ Z_m = 0.942

$p P_r = \frac{(P)\ 2014.7}{(P_c)\ 791.58} = 2.545$

$$k_c = 12155.2 \frac{Z_m (0.942)\ T\ (1359.59)\ F_o (0.4081 \times 10^{-5}) \ln \frac{(Y_A)_I\ 0.9929}{(Y_A)_o\ 0.9237}}{P\ (2014.7)}$$

$$= (0.3153 \times 10^{-2}) \times \ln (1.0749)$$

$$k_c = 0.3153 \times 10^{-2} \times 0.0722 = 2.276 \times 10^{-4} \text{ sec}^{-1}$$

APPENDIX I

REACTION RATES NEAR EQUILIBRIUM

Any reaction rate may be expressed in the functional form

$$r = r(x_1, x_2 \cdots x_n; y_1, y_2 \cdots y_m) \qquad \text{I-1}$$

where x_n represents n thermodynamic variables; such as pressure, temperature and component activities; and y_m denotes nonthermodynamic variables; such as, catalyst properties, phenomenological quantities, etc. On the other hand, the free energy of reaction is a function of thermodynamic variables alone; that is

$$\Delta G_R = \Delta G_R(x_1, x_2 \cdots x_n) \qquad \text{I-2}$$

where $\Delta G_R = \sum_i \nu_i \bar{G}_i$ is the free energy change per mole of reactant ($\nu_R = 1$) and ν_i signifies the stoichiometric coefficient for component i in the reaction equation: negative for reactants and positive for products.

It is permissible to replace any arbitrary thermodynamic variable x_j in Equation I-1 with its value in terms of ΔG_R from Equation I-2 to obtain a rate expression of the form

$$r = f_j(x_1, x_2, \cdots x_{j-1}, x_{j+1} \cdots x_n; y_1, y_2 \cdots y_m; \Delta G_R) \qquad \text{I-3}$$

Since the choice of x_j is arbitrary, there are n possible equations like Equation I-3.

At equilibrium, r = 0 and $\Delta G_R = 0$; therefore,

$$f_j(x_1, x_2 \cdots x_{j-1}, x_{j+1}, \cdots x_n;\ y_1,\ y_2 \cdots y_m;\ 0) = 0 \qquad \text{I-4}$$

For each of the n equations in I-3, r can be expressed by Taylor's theorem as

$$r = \sum_{p=0}^{\infty} \left[\frac{1}{p!} \frac{\partial^p f_j}{\partial (\Delta G_R)^p} (x_1, x_2, \cdots x_{j-1}, x_{j+1}, \cdots x_n; y_1, y_2, \cdots y_m; \Delta G_R) \right]_{\Delta G_R = \Delta G_o} (\Delta G_R - \Delta G_o)^p \qquad \text{I-5}$$

Upon expanding Equation I-5 about $\Delta G_R = 0$ (at any one of the many possible states of equilibrium), one obtains

$$r = f_j(x_1, x_2 \cdots x_{j-1}, x_{j+1} \cdots x_n; y_1, y_2 \cdots y_n;\ 0) \cdot (\Delta G_R - 0)^0 \qquad \text{I-6}$$

$$+ \frac{1}{1!} \frac{\partial f_j}{\partial \Delta G_R} (x_1, x_2, \cdots x_{j-1}, x_{j+1}, \cdots x_n; y_1, y_2 \cdots y_m;\ 0) \cdot (\Delta G - 0)^1$$

$$+ \frac{1}{2!} \frac{\partial^2 f_j}{\partial (\Delta G_R)^2} (x_1, x_2, \cdots x_{j-1}, x_{j+1}, \cdots x_n; y_1, y_2, \cdots y_m;\ 0) \cdot (\Delta G_R - 0)^2$$

$$+ \text{ etc .}$$

The first term in Equation I-6 vanishes because of Equation I-4. For small values of ΔG_R near equilibrium, second order and higher terms in Equation I-6 may be neglected. Then the resulting rate expression near equilibrium is

$$r = \frac{\partial f_j}{\partial \Delta G_R} (x_1, x_2, \cdots x_{j-1}, x_{j+1} \cdots x_n; y_1, y_2, \cdots y_m;\ 0) \cdot \Delta G_R \qquad \text{I-7}$$

From Equation I-6, it is apparent that, for a given equilibrium condition, there can be only one Taylor series expansion of r in terms of ΔG_R; hence, in Equation I-7

$$\frac{\partial f_1}{\partial \Delta G_R} = \frac{\partial f_j}{\partial \Delta G_R} = \frac{\partial f_n}{\partial \Delta G_R} \equiv f' \qquad \text{I-8}$$

The relationship of Equation I-8 demonstrates that near a given equilibrium condition, the net rate of reaction is the same linear function of the free energy of reaction, regardless of which thermodynamic variable is changed. This result has been established by Manes, Hofer and Weller (56) in a different way. Prigogine, Outer and Herbo (64) have demonstrated the linear relationship between the reaction rate and free energy of reaction near equilibrium with variation in a single thermodynamic variable. However, Prigogine et al. did not arrive at the general result of Equation I-8. The present development is an extension of the Prigogine et al. treatment to obtain the general result. According to Bak (1, p. 7), the proportionality of reaction rate to the free energy change near equilibrium was first used by de Donder.

$$r = f' \cdot \Delta G_R \qquad \text{I-9}$$

In Equation I-9 it must be remembered that f' is a function of the particular equilibrium state chosen, and of the non-thermodynamic variables. Because of the latter, it is apparent that reaction rates can never be predicted from thermodynamics alone, even near equilibrium.

The second law of thermodynamics requires that f' always be of negative sign. This condition can be shown most readily by considerating a reaction under conditions comparable to those in the present investigation. Energy and entropy balances are written for a differential volume $A\Delta X$ of

tubular reactor with uniform cross-section A through which reactants pass in steady-state plug flow at constant temperature and pressure.

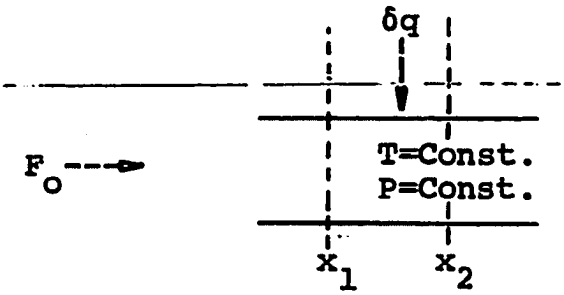

The energy balance in difference form is

$$H_I\Big]_{x_1} - H_o\Big]_{x_2} + \delta q_v \cdot A\Delta x = 0 \qquad \text{I-10}$$

where δq_v is quantity of heat transferred across the boundary per unit of volume. Similarly, the entropy balance for the differential volume is

$$S_I\Big]_{x_1} - S_o\Big]_{x_2} + \frac{\delta q_v}{T} \cdot A\Delta x + \frac{\delta S_p}{A\Delta x} \cdot A\Delta x = 0 \qquad \text{I-11}$$

Then upon multiplying Equation I-11 by T and subtracting from Equation I-10, one obtains

$$(H_I - TS_I)\Big]_{x_1} - (H_o - TS_o)\Big]_{x_2} - T\frac{\delta S_p}{\Delta x} \cdot \Delta x = 0 \qquad \text{I-12}$$

Since by definition G = H-TS, then Equation I-12 may be written as

$$G_o\Big]_{x_2} - G_I\Big]_{x_1} + T\frac{\delta S_p}{\Delta x} \cdot \Delta x = 0 \qquad \text{I-13}$$

On dividing Equation I-13 by Δx, and finding the limit as Δx approaches zero, the result is

$$\frac{dG}{dx} = -T\frac{dS_p}{dx} \qquad \text{I-14}$$

The free energy change is also given by the equation

$$dG = -SdT + vdp + \sum_i \mu_i dn_i \qquad \text{I-15}$$

which at constant temperature and pressure yields

$$dG = \sum_i \mu_i dn_i \qquad \text{I-16}$$

Substitution of Equation I-16 into Equation I-14 gives

$$\frac{dS_p}{dx} = -\frac{1}{T} \sum_i \mu_i \frac{dn_i}{dx} \qquad \text{I-17}$$

It is convenient to employ the degree of advancement variable defined by de Donder (63) as

$$\xi = \frac{n_i - n_i^o}{\nu_i} \qquad \text{I-18}$$

where ν_i is the stoichiometric coefficient as previously defined. Differentiation of Equation I-18 yields

$$d\xi = \frac{dn_i}{\nu_i} \qquad \text{I-19}$$

Then Equation I-17 transforms to

$$\frac{dS_p}{dx} = -\frac{1}{T} \frac{d\xi}{dx} \sum_i \nu_i \mu_i = \frac{-\Delta G_R}{T} \frac{d\xi}{dx} \qquad \text{I-20}$$

For a reaction which involves no change in the number of moles, and whose reactants and products form ideal solutions, as is the case for cyclopropane isomerization, the residence time is proportional to the reactor length at constant temperature and pressure; hence, the time variable t can be substituted for x in Equation I-20 to obtain a more conventional form of the entropy production equation. This substition in

effect is equivalent to a change of reference to follow a differential volume of reactant through the reactor. Equation I-10 then becomes

$$\frac{dS_p}{dt} = \frac{-\Delta G_R}{T}\frac{d\xi}{dt} \qquad \text{I-20}$$

By definition, the rate of reaction for any arbitrary reactant A is

$$r_A = -\frac{1}{V}\frac{dn_A}{dt} \qquad \text{I-21}$$

From Equation I-19 and the fact that the stoichiometric equation of the reaction can always be put into the form where $\nu_A = -1$, Equation I-21 becomes

$$r = \frac{1}{V}\frac{d\xi}{dt} \qquad \text{I-22}$$

Substitution for $d\xi/dt$ in Equation I-20 from Equation I-22 yields

$$\frac{1}{V}\frac{dS_p}{dt} = -r\cdot\frac{\Delta G_R}{T} \qquad \text{I-23}$$

Since the entropy production will always be positive, it is apparent that

$$-r\cdot\frac{\Delta G_R}{T} > 0 \qquad \text{I-24}$$

Thus, r and ΔG_R must always be of opposing sign. Then referring to Equation I-9, it is obvious that f' must be of negative sign to satisfy the second law of thermodynamics.